J Pharmacokinet Pharmacodyn (2015) 42:S11–S107
DOI 10.1007/s10928-015-9432-2

ABSTRACTS

Abstracts Accepted for American Conference on Pharmacometrics 2015 (ACoP6)

M-01

PMXstan: An R Library to Facilitate PKPD Modeling with Stan

Yuan Xiong*, David James, Fei He, Wenping Wang

Novartis Pharmaceuticals Corporation

Objectives: Using Bayesian approach to make statistical inferences is gaining popularity in recent years. Stan, a probabilistic programming language that implements efficient Hamiltonian Monte Carlo method, attracts more and more users, pharmacometricians in particular. Our objective is to provide a tool (PMXstan, an R library) to facilitate practical Bayesian PKPD modeling and simulation using Stan.
Methods: PMXstan, consisting of a set of R and C++ functions, addresses two hurdles that have largely limited broad applications of Stan in pharmacometrics: (1) a steep learning curve for pharmacometricians to write PKPD model-specific C++-like Stan code; (2) no general and efficient ODE solver that works seamlessly with the No-U-Turn Sampler (NUTS) to handle generic PKPD models, often expressed as differential equations.
Results: PMXstan helps pharmacometricians to focus more on PKPD model building. It automatically handles irrelevant technical details using a set of wrapper functions. With a few model specification statements defined by a user, PMXstan generates model-specific ready-to-run Stan source code, followed by data-conversion functions transferring a conventional NONMEM dataset into a data list readable by Stan. The Stan code, fully accessible and modifiable by the user, is then compiled and an executable sampler generated. After reading the data list and running the sampler, another set of functions provide options for convergence checks and model diagnostics.
Within PMXstan, closed-form solutions are provided for PK models when applicable. For a general PKPD model expressed as a set of ODEs, a NUTS compatible template LSODA solver will be called. This ODE-solver was tested to be stable and efficient for a broad range of PKPD models. Utility of PMXstan is illustrated by real project data and its performance is compared with other available tools.

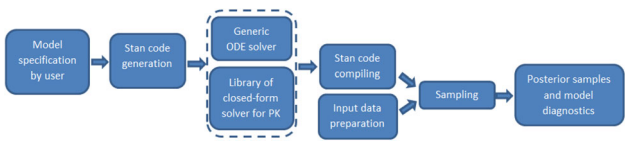

Flow chart of model specification, compilation, execution, and diagnostics by PMXstan

Conclusions: PMXstan frees users from extensive Stan coding, challenging to master by most pharmacometricians. It thus allows them to focus more on model building based on pharmacological understandings. Minimizing the possibility of errors, it provides a fully extensible and customizable platform that facilitates a practical Bayesian PKPD modeling approach.

M-02

Tafenoquine (TQ; SB252263) Population Pharmacokinetic (PK) Model and Efficacious Dose Simulation in *Plasmodium vivax* Malaria Subjects

David Tenero[1,*], Justin Green[2] Navin Goyal[1]

[1]GlaxoSmithKline, Clinical Pharmacology Modeling & Simulation, King of Prussia, PA; [2]GlaxoSmithKline, Clinical Development, Stockley Park, UK

Objectives: Develop a population PK model to support Phase III dose selection.
Methods: In Phase IIb study TAF112582**, subjects received single TQ doses of 50–600 mg. Five PK samples were obtained over 60 days (1067 samples in 223 subjects). A population PK model was developed (NONMEM v7.2). Bootstrap analysis and visual predictive check (VPC) were used for model qualification. Classification and regression tree analysis (CART; R v2.15.3) was used to estimate the probability of being relapse-free at 6 months.
Results: TQ concentration–time data were best described by a 2-compartment model with first-order absorption. Parameters were well defined with standard errors typically less than 15 %. Inter-individual variability was estimated on oral clearance (CL/F) and central volume of distribution (Vc/F) and was 32 and 39 %, respectively, while residual variability was 31 %. Model stability was confirmed by bootstrap analysis (<6 % failures) while VPC showed the model reliably described the observed data.
CL/F and Vc/F were influenced by gender and weight, respectively. However, no dose adjustment is deemed necessary since changes due to these covariates are considered minor and likely to be clinically insignificant.

CART analysis identified an AUC breakpoint of 56.4 μg h/mL as a predictor of malaria relapse (success rate 89 % ≥ 56.4 μg.h/mL versus 48 % < 56.4 μg h/mL). Clinical trial simulation (CTS) indicated that the 300 mg TQ dose would provide an AUC ≥56.4 μg h/mL in >90 % of subjects.

Conclusions: A population PK model was successfully developed for TQ after administration to malaria subjects. Although CL/F was influenced by gender, the magnitude of the change is unlikely to be clinically significant. CTS demonstrated that the 300 mg TQ dose would be expected to provide adequate exposure in >90 % of subjects and consequently lead to higher relapse-free rates at 6 months. This model based approach was critical in dose selection for Phase III studies.

[**Funded by GlaxoSmithKline as part of the tafenoquine co-development partnership with Medicines for Malaria Venture]

M-03

Systematic Comparison of Approaches to Handle Below Quantification Limit Data in Population Pharmacokinetic Analyses

L. Li*, C.S. Ernest II, J.Y. Chien

Eli Lilly and Company, Indianapolis, IN, USA

Objectives: The methods used to handle data below the quantification limit (BQL) in popPK analyses may have an impact on the robustness of parameter estimates. The objective of this work is to evaluate four commonly used methods for handling BQL data using established popPK models for two drugs with different sampling designs.

Methods: Four BQL methods were evaluated: discarding all BQL data (M1); estimating the likelihood that a BQL observation is less than the lower limit of quantitation (LLOQ) without (M3) or with (M4) the condition that all observations be positive; replacing the first BQL by LLOQ/2 and discarding the rest (M6). PopPK models for a long half-life and short half-life drug were used to simulate, using a selection of optimized sparse sampling designs and varying amounts of BQL data (10 to 45 %). Both FOCE and IMPMAP methods were evaluated. The comparisons were based on convergence as well as bias and precision of parameter estimates.

Results: Both models had >70 % successful convergence using M1 and M6 methods, regardless of % BQL in the datasets. The M3 and M4 methods had low rate of successful convergence for the more complex model using FOCE, but the robustness was recovered by using IMPMAP. The covariate identification capability was similar across all the methods for both models. Based on the Root Mean Squared Error (RMSE) of parameter estimates, M3 and M4 performed better than M1 and M6 methods.

Conclusions: The M3 and M4 methods demonstrated statistical advantages across all scenarios. The improvement was modest for low % BQL and the long half-life drug with a simple PK model. However, M3 or M4 is recommended for a complex PK model with high % BQL, using IMPMAP estimation method to improve the robustness of parameter estimations. A decision tree can be developed to aid the selection of BQL method.

M-04

Sequential Population PK-Viral Dynamic Modeling of TD-6450, a Next Generation Once Daily NS5A Inhibitor, following 3-Day Monotherapy in Patients with GT-1 HCV Infection

Aniruddha Amrite[1*], David Bourdet[1], Joe Budman[2], Philip Worboys[1]

[1]Clinical Pharmacology and DMPK, [2]Molecular and Cellular Biology, Theravance Biopharma US, Inc., South San Francisco, CA

Objectives: To investigate the PK-viral dynamic (VD) relationship for a next generation NS5A inhibitor in patients with GT-1 HCV infection following 3-day dosing with TD-6450.

Methods: A sequential PK-VD modeling approach was considered. The population PK (POP-PK) dataset consisted of two clinical studies: a SAD (0.5 to 500 mg QD)/MAD (60 to 240 mg QD) study in healthy subjects (N = 80) and a 3-day dosing (60 to 240 mg QD or 240 mg BID) study in HCV patients (N = 42). The effect of covariates on the PK parameters was evaluated. The individual post hoc PK parameters were retreived as the empirical Bayes estimates. These estimates for HCV GT-1 subjects (N = 35) were used in the PK-VD modeling. The viral load data were fitted to models described in the literature with modifications for direct acting antiviral agents and use of a sigmoidal concentration-inhibitory effect relationship.

Results: The POP-PK of TD-6450 is well described by a two compartment disposition model with transit compartments for absorption and time varying bioavailability. Covariate analysis indicated a significant positive effect of BMI on the peripheral volume of distribution. The initial bioavailability (F0) was ∼40 % lower and the transit time (MTT) ∼ 1 h faster in the fasted state as compared to the fed state. The population viral dynamics of HCV GT-1 patients are well described by a three compartmental model with uninfected hepatocytes, infected hepatocytes, and virus as the three compartments and with proliferation terms for the hepatocytes. TD-6450 inhibits the production of the virus in a concentration dependent manner with a sub-nanomolar population mean IC_{50}. The estimates of drug independent VD parameters were in agreement with the values reported in literature.

Conclusions: The Phase-1/1b PK and PK-VD relationships are well characterized using a POP-PK modeling approach. The models may be useful in exposure–response simulations and dose selection for future trials.

M-05

Fabry Disease Progression with and without Enzyme Replacement Therapy

Albina Nowak[1], Gilbert Koch[2*], Johannes van den Anker[2], Uyen Huynh-Do[3], Marc Pfister[2]

[1]Department of Internal Medicine, University Hospital Zurich, Switzerland; [2]Pediatric Pharmacology and Pharmacometrics Research Center, University Children's Hospital Basel, Switzerland; [3]Department of Nephrology, Hypertension and Clinical Pharmacology, Inselspital, University of Bern Medical School, Switzerland

Objectives: Fabry disease is a rare inherited lysosomal storage disease, where kidney complications are a common and serious manifestation. Enzyme replacement therapies (ERT) with agalsidase-α and -β were investigated for a therapeutic effect on renal function in Swiss adolescent and adult Fabry patients. A model to describe the time course of estimated glomerular filtration rate (eGFR) was developed.

Methods: Data from 52 patients (25 female, 27 male) with ERT with a total of 373 observations and data from 20 patients (all female) without ERT with 73 observations were available. Age ranged from 17 to 67 years. eGFR was computed with the chronic kidney disease epidemiology collaboration (CKD-EPI) formula [1]. Nonlinear mixed effect modeling was applied and covariates such as

age at baseline, gender as well as drug and dose effects were investigated.

Results: A linear relationship between age and eGFR described best the available data. Female Fabry patients without ERT appeared to have a slight decrease of eGFR, whereas eGFR appeared to stabilize or slightly increase with ERT. Male Fabry patients showed decreasing eGFR during ERT, which was comparable or greater than eGFR decrease in males prior to ERT and greater than eGFR decrease in females without ERT. There was no apparent effect of prescribed ERT doses on the eGFR slope. Age at baseline was included as a covariate of the eGFR intercept of the linear model.

Conclusions: Available data and performed modeling suggest a positive effect on kidney function (i.e. eGFR change over time) at licensed ERT doses in female but not in male adolescent and adult Fabry patients. Future investigations are warranted to investigate whether higher ERT doses are associated with improved kidney function in male Fabry patients.

References:

1. Levey AS et al. (2009) A new equation to estimate glomerular filtration rate. Ann Intern Med 150(9):604–12.

M-06

Population Physiologically-Based Pharmacokinetic Model Incorporating Lymphatic Uptake for a Subcutaneously Administered Pegylated Peptide

Elliot Offman*, Colin Phipps, Andrea N. Edginton

School of Pharmacy, University of Waterloo, Ontario, Canada

Objective: To develop a population physiologically-based pharmacokinetic (popPBPK) model to account for the inter-individual variability in the subcutaneous (SC) time course of a pegylated (PEG) peptide.

Methods: Observed human data for a SC administered linear PEG-40 conjugated peptide (approximately 40 kDa) was obtained for 20 healthy volunteers receiving escalating single doses (n = 4/dose level). The model, previously developed in primates and scaled to a virtual human [1] was comprised of 15 anatomical compartments each with a vascular and interstitial sub-compartment. Additionally, a lymph compartment with flow from each organ was included, with a unique lymphatic transit compartment (LTC) incorporated to address drainage from the SC administration site into the lymphatic system. Organ, blood and lymph masses were sampled from either normal or log-normal distributions. Blood flows were calculated for each organ based on mean organ perfusion/g of organ tissue and lymphatic flow as a fraction of blood flow. Distributions were also incorporated for hematocrit and renal filtration fraction to address inter-individual variability in renal clearance. Clearance was characterized by renal, at 0.1 % glomerular filtration rate, and non-renal clearance.

Volume of the LTC was estimated as a fraction of the SC injection volume (Vfrac) using maximum likelihood estimation (Phoenix NLME, FOCE-ELS). Simulations of virtual males (n = 1000) across 5 doses levels were performed in MATLAB and plotted using R. Sensitivity analysis was performed to identify uncertain parameters and evaluate distribution estimates.

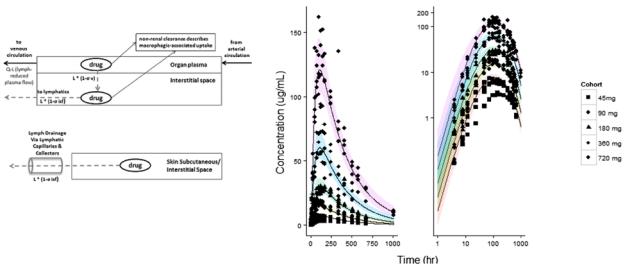

Fig. 1 *Left panel* depicts the sub-compartmental organ model and incorporation of LTC. *Right panel* presents observed (geometric symbols) vs. population predicted (5th–9th percentile, coloured ribbon) concentration vs. time profiles with linear and log–log axes

Results: Incorporation of a LTC resulted in similar line shape relative to observed data and incorporation of anthropometric variability accounted for individual differences in the absorption and elimination phases across all dose cohorts. Line shape was sensitive to Vfrac and vascular reflection coefficients, while Cmax and elimination were influenced by the distribution of blood volume and renal clearance, respectively.

Conclusion: Incorporation of a LTC combined with anthropometric variability accounted for the SC time-course in a population receiving a PEG-40 conjugated peptide.

References:

1. Offman, E., Edginton, AN. J Pharmacokinet Pharmacodyn, 42(2):135–150.

M-07

Population Pharmacokinetics of Mycophenolic Acid and its Glucuronide Metabolite in Lung Transplant Recipients with and without Cystic Fibrosis

Xiao-Xing Wang[1], Meihua R. Feng[1*], Tian Zheng, David E. Smith[1], Diane M. Cibrik[2], Jeong M. Park[1]

[1]College of Pharmacy, University of Michigan, Ann Arbor, Michigan 48,109, USA; [2]Department of Internal Medicine, School of Medicine, University of Michigan, Ann Arbor, Michigan 48109, USA

Objectives: The objective of this work was to characterize the population pharmacokinetics (PK) of mycophenolic acid (MPA), an immunosuppressant, and its glucuronide metabolite (MPAG) in adult lung transplant recipients with cystic fibrosis (CF) and without the disease (NCF) following repeated oral administration of the prodrug mycophenolate mofetil (MMF).

Methods: Three separate 12-h PK visits were conducted in CF and NCF lung transplant patients following repeated MMF treatment, with at least 2 weeks between the visits. A population PK model was developed, with simultaneously modeling of MPA and MPAG, using nonlinear mixed effects modeling and considering the contribution of physiological and pathological factors, and enterohepatic recirculation (EHC).

Results: Plasma MPA and MPAG concentration–time data after MMF oral administration were adequately described by a three-

compartment model, which included EHC. CF patients had elevated values for both the apparent total clearance of MPA (CL/F = 17.18 L/h) and apparent elimination clearance of MPAG (CL_M/F = 2.18 L/h) compared to NCF patients (CL/F = 9.98 L/h and CL_M/F = 1.22 L/h). The systemic appearance rate constant of MPA in CF patients (KA = 1.35 h^{-1}) was slower than that in NCF patients (KA = 2.90 h^{-1}).
Conclusions: The population PK model developed from our study successfully characterized the absorption, distribution, and elimination of MPA and its major metabolite MPAG in lung transplant recipients with or without CF. The decrease of MPA systemic appearance rate and increase of both CL/F and CL_M/F in CF patients suggests the importance of MPA therapeutic monitoring for this group.

M-08

Modeling and Simulation of Piperaquine (PQ) After Administration of Eurartesim® (PQ Tetraphosphate/Dihydroartemisinin)

Jean Lavigne[1*], Mary Lor[1], Silvia Pace[2]

[1]Celerion, Montreal, Canada; [2]Sigma-Tau, Rome, Italy

Objectives: Develop a population pharmacokinetic (PK) model for PQ by pooling data from 5 studies and applying it to predict PQ PK in pediatric patients (6–12 months) infected with *Plasmodium falciparum* malaria after administration of a new dispersible formulation.
Methods: Subjects/patients with at least one measurable PQ concentration were included in the analysis for a total of 207 PQ profiles, 4636 samples (4422 measurable samples). The MLEM algorithm in ADAPT5 [1] was used to estimate the population parameters. The M3 method from Beal [2] was used for concentrations below the limit of quantification. The Bayesian Information Criteria (BIC) was used for model discrimination and covariate inclusion/exclusion. Internal model validation was done with visual predictive check plots created with R [3] version 3.1.2.
Results: A three-compartment model with lag-time, zero-order absorption, and enterohepatic circulation was the structural model that best fitted the PQ data. Dose-corrected body weight improved the BIC. Inter-occasion variability on the bioavailability parameter for the first dose improved the model. Body weight (WGT), health status, food, formulation, crushed, and sex were covariates included in the final model. Two-hundred infants were simulated (gender balanced) receiving 80, 160, or 320 mg PQ, depending of their WGT, once a day for 3 consecutive days. WGT was simulated according to the WHO training [4]. Day 3 AUC, Cmax and Tmax were calculated.
Conclusions: Simulated results for the new dispersible formulation under fasted condition suggest that the geometric mean of PQ AUC and Cmax would be 11,322 ng/mL*h and 294 ng/mL, respectively, with a median Tmax of 5.48 h.

References:

1. D'Argenio, D.Z., A. Schumitzky and X. Wang. ADAPT 5 User's Guide: Pharmacokinetic/Pharmacodynamic Systems Analysis Software. Biomedical Simulations Resource, Los Angeles, 2009.
2. Beal SL. Ways to fit a PK model with some data below the quantification limit. Journal of Pharmacokinetics & Pharmacodynamics. 2001;28(5):481–504.
3. The R Project for Statistical Computing, R Manuals (http://www.r-project.org/)
4. Training Course on Child Growth Assessment—WHO—Module C: Interpreting Growth Indicators. http://www.who.int/childgrowth/training/module_c_interpreting_indicators.pdf

M-09

Time-to-event analysis of polatuzumab vedotin induced peripheral neuropathy to assist comparison of dosing regimen

Dan Lu[1*], Jin Yan Jin[1], Priya Agarwal[1], Chunze Li[1], Cheryl Jones[1], Yu-Waye Chu[1], Matts Kagedal[1], Sandhya Girish[1], William R. Gillespie[2]

[1]Genentech Inc.; [2]Metrum Research Group LLC

Objectives: Peripheral neuropathy (PN) has been frequently observed in clinical studies of polatuzumab vedotin (PoV), an antibody–drug-conjugate containing monomethyl auristatin E (MMAE). Conjugate exposure has a trend of correlation with PN incidence. To further quantify the correlation of exposure and treatment duration with the risk of developing clinically significant PN to assist comparison of dosing regimen, a time-to-event model was needed.
Methods: A base model was selected from a range of plausible models based on Akaike information criterion and graphical predictive checks, using Phase I/II data for PoV as a single agent or in combination with rituximab for treating Non-Hodgkin's lymphoma (N = 155, 0.1–2.4 mg/kg every-three-week). Effects of ~ 10 covariates (demographics and potential PN risk factors) were further explored on the base model.
Results: The final model (Figure 1) suggests PN onset is delayed relative to conjugate plasma concentrations; major factors associated with the PN risk included conjugate exposure and treatment duration. A trend of higher risk for higher body mass patients is observed. The model-predicted Grade ≥ 2 PN risk ratio for nominal dose of 2.4 mg/kg versus 1.8 mg/kg (every-three-week, 8 cycles) was 1.33 (90 % confidence interval [CI]: 1.25–1.49). However, when dose reductions were accounted (for 2.4 mg/kg), the risk ratio was 1.20 (90 % CI: 1.16-1.28); the corresponding model-predicted incidence of Grade 2 + PN events was 35.1 % (90 % CI: 26.2 %-41.7 %) and 28.9 % (90 % CI: 21.3 %-34.7 %) for 2.4 and 1.8 mg (every-three-week, 8 cycles), respectively.
Conclusions: The PN risk increases with conjugate exposure and treatment duration. At clinically relevant doses, 2.4 mg/kg confers a higher PN risk than 1.8 mg/kg. However, capping the treatment duration to 8 cycles may reduce PN risk compared to treatment until progression.

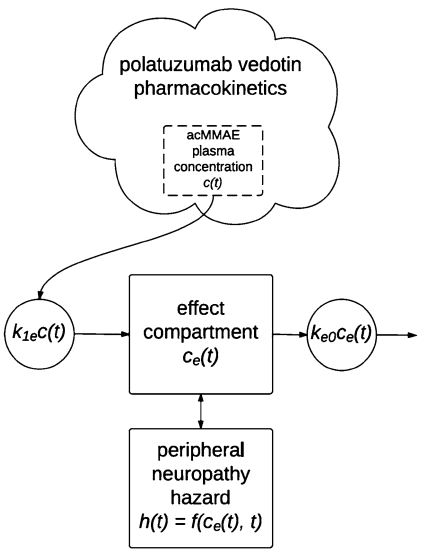

Fig. 1 The model structure

M-10

Population Pharmacokinetic Meta-Analysis of Ramucirumab in Cancer Patients

Lisa O'Brien[1*], Paul Westwood[2], Ling Gao[3], Michael Heathman[1]

[1]Eli Lilly and Company, [2]Indianapolis, IN; [2]Windlesham, UK; [3]Bridgewater, NJ

Objectives: Ramucirumab (Ram) is a monoclonal antibody that binds vascular endothelial growth factor receptor 2. The aims of this analysis were to characterize the pharmacokinetics (PK) of Ram in cancer patients, characterize the inter-patient variability (IIV), and investigate patient factors that influence Ram disposition.
Methods: The dataset consisted of 1639 patients with 6427 observations from 11 studies (Phase 1/1b, 2 and 3). Several disease states were represented: colorectal cancer (26.8 %), gastric cancer (24.4 %), non-small cell lung cancer (26.8 %), hepatocellular carcinoma (19.0 %), and other tumor types (3 %). Ram was administered as an IV infusion over 1 h, at either 8 mg/kg every 2 weeks or 10 mg/kg every 3 weeks. PK sampling varied across studies.
A pharmacostatistical base model was first developed to describe the concentration data. Demographics, cancer indication, dose, renal function, hepatic status, and other laboratory values were assessed as covariates using forward selection and backward elimination. Covariates were considered significant if they decreased IIV in the relevant parameter by $\geq$5 % and reduced the objective function by $\geq$6.635 ($p < 0.01$) in forward selection and $\geq$10.828 ($p < 0.001$) in backward elimination. The model was evaluated using bootstrap and visual predictive check. All analyses were performed using NONMEM 7.3.
Results: The PK of Ram were well characterized by a 2-compartment model with IIV estimated on all parameters and covariance between CL and V_1. A combined additive/proportional error model was used. No covariates were found to satisfy the predefined criteria, and no relationship was found between dose level and Ram PK. Mean (CV %) PK parameters derived from post hoc parameter estimates were: CL 0.0147 L/h (30.0 %), V_{ss} 5.38L (15.0 %), and terminal half-life 14.2 days (20.0 %).
Conclusions: The final model adequately described the time-concentration profile of Ram in patients with a range of cancer indications. The PK parameters were consistent with those obtained from non-compartmental analyses of Phase 1 and 2 studies, with the exception of half-life. Simulation using the model confirmed the appropriateness of weight-based dosing.

M-11

Assessment of Pembrolizumab (MK-3475) Dosing Strategy Based on Population Pharmacokinetics and Exposure–Response Models

Tomoko Freshwater[1*], Julie Stone[1], Rik de Greef[2], Anna Kondic[1], Dinesh P. De Alwis[1], Kapil Mayawala[1], Malidi Ahamadi[1], Claire Li[1], Manash S. Chatterjee[1], David C. Turner[1], Jeroen Elassaiss-Schaap[2], Mariëlle van Zutphen–van Geffen[2]

[1]Merck Research Laboratory, Merck & Co., Kenilworth, NJ, USA; [2]Quantitative Solutions B.V., Molenweg, Netherlands

Objectives: Most monoclonal antibodies (mAbs) have generally some contribution of body size to pharmacokinetic variability; therefore, dosing of mAbs is mostly based on body weight [1]; early pembrolizumab studies (pembrolizumab targets the programmed cell death 1 [PD-1] receptor) followed this approach. The dosing strategy of pembrolizumab was reassessed using population pharmacokinetics (PopPK) and exposure–response models to determine if weight-scaled dosing was necessary.
Methods: A PopPK model was fit to pooled data (KEYNOTE-001, 002 and 006). Model parameter estimation included power function exponents (α) describing the weight effect on CL and V. Predicted AUC distributions with fixed dosing were compared to the range of exposures from the pembrolizumab doses evaluated in early studies (2 mg/kg Q3W, 10 mg/kg Q3W/Q2W) to check whether fixed dosing would maintain exposures within the range of clinical experience. The safety profile has been similar and the efficacy near maximal across this entire dose range.
Results: CL and V were allometrically scaled by weight, with an estimated α of 0.578 [0.481, 0.666] and 0.492 [0.432, 0.553], respectively. The intermediate values of $\sim$0.5 estimated for the α between extremes of 0.0 (no relation to weight) and 1.0 (perfect weight scaled) suggest that the 2 dosing approaches would perform similar. Simulations of exposures at 200 mg Q3W indicate these to lie within the range of clinical experience associated with near maximal efficacy and good tolerability and to be close to those obtained with the 2 mg/kg Q3 W dose approved in several countries for melanoma, without substantive change in PK variability (Figure 1).

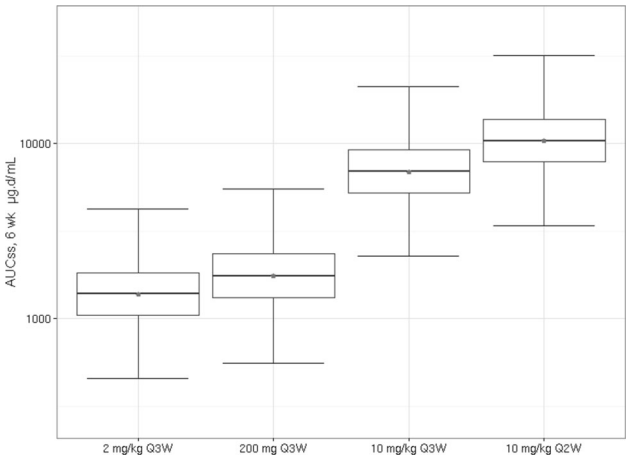

Fig. 1 The Distribution of Steady-State AUC Exposures Predicted by the Melanoma Population PK Model for a 2, 10 mg/kg dose and a 200 mg fixed dose administered every 3 weeks (Q3W) and 10 mg/kg every 2 weeks (Q2W) (Log scale)

Conclusions: Both weight-based as well as fixed-dose regimens would be appropriate for pembrolizumab. Doses of 200 mg and 2 mg/kg provide similar exposure distributions, with no advantage to either dosing approach.

Reference:

1. Bai et al. Clin Pharmacokinet. 2012;51(2):119–35.

M-12

Model-Based Approach for Dose Optimization of HSP90 Inhibitor Luminespib

Ying Hong[*], Hong Lu, Diep Le, Mikhail Akimov, Jeff Cramer

Novartis Pharmaceuticals Corporation, East Hanover, NJ

Objectives: To optimize the once weekly via 1-h intravenous infusion dosing regimens of luminespib in patients with advanced non-

small cell lung cancer (NSCLC) using a model-based approach. The hypothesis we proposed was that a longer infusion time at its current efficacious doses 40 mg/m^2 and above would likely improve the benefit and risk ratio of luminespib by blunting its C_{max} and prolonging its exposure in the systemic circulation.

Methods: The population PK analysis of luminespib was conducted in two-stages. First, the red blood cells (RBC)-plasma distribution model was developed to describe luminespib nonlinear capacity-limited specific binding and linear non-specific binding to RBC. Second, the systemic model parameters in plasma were estimated by fixing the apparent dissociation constant (k_d) to the value determined in the first stage. The relationship between the steady-state luminespib maximum blood concentration (C_{max}) and safety endpoints (G2+ diarrhea and G2+ eye disorders) were described by sigmoidal E_{max} logistic regression models. Model-based simulations were performed to determine the longer infusion dosing regimens for luminespib that could keep its C_{max} below the threshold level determined from the exposure-safety analyses.

Results: Luminespib PK in plasma was described by a linear three-compartment model with zero-order infusion. Luminespib PK in blood was nonlinear and was attributed to the concentration-dependent RBC binding. Luminespib C_{max} was found to be a significant predictor of G2+ diarrhea and eye disorders ($p < 0.001$). The C_{max} producing the 50 % maximum effect (EC_{50}) was 443 ng/mL for G2+ diarrhea, and 574 ng/mL for G2+ eye disorders. The model-based simulation indicated luminespib 1-h infusion at 40 mg/m^2 and above could produce $C_{max} > 443$ ng/mL in >90 % patients, while 4-h infusion at 40 and 54 mg/m^2 could cap C_{max} at 443 ng/mL in >80 % patients (Figure 1).

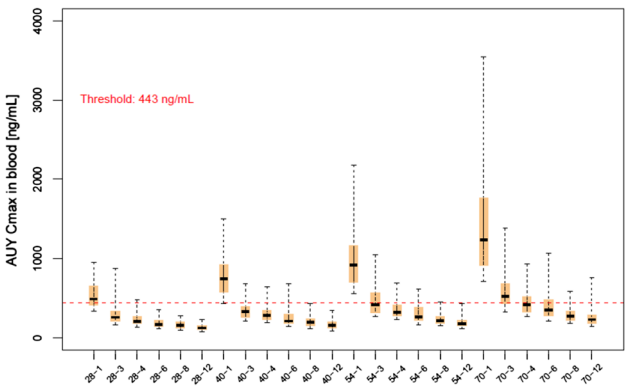

Fig. 1 Distribution of simulated luminespib blood C_{max} at series of dosing regimens (28, 40, 54, 70 mg/m^2 with the infusion time of 1, 3, 4, 6, 8, 12 h)

Conclusions: An integrated population PK model adequately described luminespib PK in blood and plasma. The higher luminespib C_{max} was associated with increased probability of G2+ diarrhea and eye disorders. The model-based approach was utilized to optimize luminespib dosing regimens that could keep drug exposure below the pre-determined threshold level.

References:

1. Snoeck E, et al. Br J Clin Pharmacol. 1996;42:605–613

M-13

Pharmacokinetics and Exposure–Response Relationships of Dasotraline in the Treatment of Attention-Deficit/Hyperactivity Disorder in Adults

Seth Hopkins[1]; Soujanya Sunkaraneni[1]; Estela Skende[1]; Jeremy Hing[2]; Julie Pasarell[2*]; Antony Loebel[1]; Kenneth S. Koblan[1]

[1]Sunovion Pharmaceuticals, Marlborough, MA; [2]Cognigen, Buffalo, NY

Objectives: To characterize the pharmacokinetic and pharmacodynamic data to explore the time–course and exposure–response relationships in Phase 2 to define dasotraline benefit-to-risk relationship in adult Attention Deficit Hyperactivity Disorder (ADHD) subjects. Simulations were performed to support Phase 3 study design and dose selection.

Methods: Dasotraline population PK were analyzed using data from 395 subjects after single/multiple doses from 0.2 to 36 mg (3 Phase 1 and Phase 2 studies). PK/PD models related individual dasotraline exposures to norepinephrine metabolite DHPG concentrations, ADHD RS-IV total scores, and time to study dropout using data from 330 ADHD subjects. Final models were validated using VPCs. Clinical trial simulation scenarios examined a range of doses and durations to predict: minimal effective dose, no effect dose, and optimal duration of treatment for the planned efficacy study and determine the likelihood of a positive trial outcome (statistically significant ADHD RS–IV response comparing dasotraline to placebo with clinically meaningful effect size).

Results: A one-compartment model with dual (linear plus nonlinear) elimination described dasotraline PK. In an ADHD population administered 4 or 8 mg/day, dasotraline was characterized by a mean apparent half-life of 47 h and steady-state by 10 days of dosing. The exposure–response model for DHPG was a power function of predicted concentrations indicating clinically significant NET inhibition. Dasotraline average concentrations (C_{av}) reduced ADHD RS-IV according to a sigmoid E_{max} time-course model. A Cox proportional hazard model related time-varying C_{av} to the log of the survival function for dropout. Clinical trial simulations predicted 4 mg/day minimum effective dose, 2 mg/day no effect dose, and a sufficient likelihood of success for 8 week trials with 200 subjects per group (Figure 1).

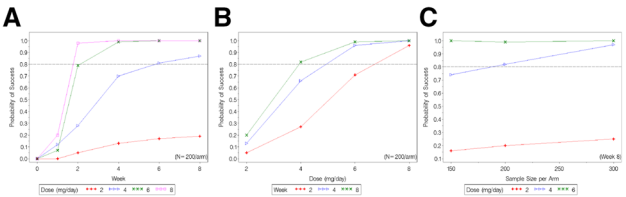

Fig. 1 Probabilities of Clinical Trial Success by Duration, Dose, and Sample Size

Conclusions: Modeling and simulations successfully related dasotraline PK to pharmacological activity via DHPG and ADHD RS-IV scores supporting the concept that maintaining constant, steady-state inhibition of both dopamine and norepinephrine transporters is a novel pharmacological approach to the management of ADHD symptoms.

M-14

CLIP: The Command-Line Interface to Phoenix NLME

Vince Perri, Michael Wilson, Vijay Ivaturi*

Center for Translational Medicine, School of Pharmacy, University of Maryland, Baltimore, Maryland

Objective: Phoenix NLME [1] is a module of the Phoenix platform that performs population PK/PD modeling and simulation. The main objective of this work is to develop a command-line alternative to the graphical interface of Phoenix NLME that fully harnesses the power of Phoenix NLME from the command line.
Methods: A Python [2] based command-line environment was developed that provides an easy-to-use toolkit for both novice and advanced users that controls the creation and execution of the Phoenix NLME's engine on a model file.
Results: CLIP supports modeling on a local system or computer clusters. CLIP can run, manage and edit models, interpret output, and create basic reports. It is easily extendible with custom scripts, and integrates smoothly with R. CLIP currently supports Phoenix NLME v1.4 and runs on Windows. The program has been able to accurately estimate models written in the Phoenix Modelling Language faster than its equivalent graphical operations and with equivalent accuracy. The method of stochastic simulation and estimation has also been implemented that indicates that the core of this program is extremely extensible, capable of performing non-trivial tasks with high performance and great ease.
Conclusion: CLIP is capable of not only duplicating the functionality of Phoenix NLME's graphical interface at a faster speed, but it is also capable of more intensive operations not practical to perform in a graphical windows environment. Future development will involve extending this product to a Linux architecture.

References:

1. http://www.certara.com/products/pkpd/phx-nlme/
2. https://www.python.org

M15

Prediction of Anthrax Toxin Protective Antigen Kinetics in Humans

A. Corey*

Parexel International

Objectives: Protective antigen (PA) kinetics are reported for animal inhalational anthrax models [1], but not for humans. Understanding PA kinetics explains efficacy of antibiotic or anti-toxin interventions for treatment of inhalational anthrax [2]. This analysis aimed to extrapolate human PA kinetics from relationships between animal characteristics or disease events and PA kinetic parameters.
Methods: A dataset was assembled of PA kinetic parameters, animal characteristics (weight, spore challenge duration and size) and disease events (time to first bacteremia, survival time) for *Bacillus anthracis* spore-challenged rabbits and monkeys. Relationships between PA kinetic parameters and animal characteristics or disease events were explored. The best relationship of a PA kinetic parameter to a predictor variable was selected to extrapolate that PA kinetic parameter in humans, using the predictor variable range in humans. Predicted human PA kinetics were compared to the chronology of human anthrax disease events to confirm that the PA kinetics/disease events concordance noted in animals was maintained for humans.
Results: As expected, time of bacteremia onset was good predictor ($r^2 = 0.84$) of λ (initial lag phase of the PA concentration–time profile). Survival time was not ideal, but was the best predictor for μ_m (rate constant for first rising phase of the PA profile) and A (magnitude of the plateau in the PA profile), with r^2 of 0.23 and 0.16, respectively. Survival time was a good predictor ($r^2 = 0.71$) for λ_2 (duration of the PA profile plateau). Since no relationships were evident for $\mu_{m,2}$ (rate constant for terminal rising phase) or N_0 (initial PA concentration), these PA kinetic parameters for humans were set to the monkey values. Table 1 summarizes the extrapolated human PA kinetics, with rabbit and monkey values for comparison.

Table 1 Extrapolated human PA kinetics

Species	N_0 (ng/ml)	λ (h)	μ_m (h^{-1})	A (unitless)	λ_2 (h)	$\mu_{m,2}$ (h^{-1})
Human						
Median	1.20	112	0.332	12.81	244	0.48
Minimum	0.98	89	0.198	11.65	202	0.14
Maximum	1.59	136	0.465	13.98	287	1.09
Rabbit						
Median	1.04	20	0.86	5.10	22	0.16
Minimum	0.14	17	0.44	1.98	22	0.08
Maximum	64.95	100	1.03	17.48	54	1.15
Monkey						
Median	1.20	36	0.56	4.88	71	0.48
Minimum	0.98	25	0.18	3.14	34	0.14
Maximum	1.59	123	1.15	10.49	203	1.09

Conclusions: Relationships between disease events and PA kinetics in animals allowed extrapolation of human PA kinetics, which reflect disease progression in humans as well as differences between animals and humans. Simulations using extrapolated human PA kinetics will allow evaluation of therapeutic interventions.

References:

1. Corey A, et al. Toxins, 5:120–38, 2013.
2. Corey A, et al. AAPS Journal. NBC Abstract T3185, 2013.

M-16

Combination of R "Shiny" and Application Programming Interface (API) to Create a Browser Based Visualization Tool for FDA Public Database

Ho-Pi Lin*, Sarah Dutcher, Andrew Babiskin, Jinzhong Liu, Xinyuan Zhang, Liang Zhao

Division of Quantitative Methods and Modeling, Office of Research and Standards, OGD, FDA, Silver Spring, Maryland, USA

Objectives: In June 2014, FDA launched OpenFDA, featuring an Application Programming Interface (API) which allows high-value, publically-available data to be accessed easily by software developers. Currently, the FDA Adverse Event Reporting system (FAERS), Recall Enterprise System (RES), and Standard Product Labels (SPL) are available for drug-related searches. The "Shiny" package by RStudio allows for the development of interactive web applications to visualize and summarize data. By combining "Shiny" and OpenFDA API, a web application aiming to facilitate visualization of FAERS data was developed. Upon submission of a drug name, the web application will use API to construct data set needed for further analysis.
Methods: Two R scripts (ui.R and server.R) were prepared allowing the end users to interact with FAERS and SPL data via the OpenFDA

API. Current output was designed to assist end users to identify generic drug products with high report frequencies indicating diminished drug effect.

Results: Upon user input into the web application (Fig. 1.1, web link available upon request), plots generated include: total FAERS report frequency stratified by drug-associated adverse events (Fig. 1.2), total FAERS report frequency stratified by associated application numbers (Fig. 1.3), and frequency of "Lack of effect" events stratified by drug application numbers (Fig. 1.4). Though FAERS data are not confirmatory and require further investigation, these visualizations can be used to generate hypotheses about potential signals for generic drug products.

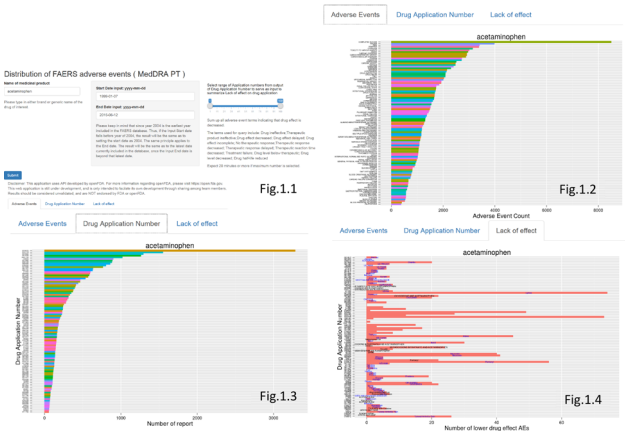

Fig. 1 Snapshots of the user interface

Conclusions: Combination of "Shiny" with OpenFDA API allows web application development to fit the needs of end users. To our knowledge, this is the first drug information-based and data query-based "Shiny" web application that will directly access public databases from OpenFDA. We believe building this web application can enhance real-time decision making and facilitate interactions across scientific disciplines and communities.

M-18

A Quantitative Systems Pharmacology Platform to Investigate the Impact of Cholesterol-Lowering Therapies on Lipid Profiles and Plaque Characteristics: Insights for the Clinical Application of PCSK9 Inhibitors

Derek W. Bartlett[1], Katherine Kudrycki[1], Ananth Kadambi[1], Christina M. Friedrich[1], Tu Nguyen[2], Karim Azer[2], Nassim Djebli[3], Britta Goebel[4], Alex Koszycki[2], Meera Varshneya[2], Poulabi Banerjee[5], Jeff Barrett[2], Jeffrey E. Ming[2], Michael J. Reed[1]*

[1]Rosa & Co, CA, USA; [2]Sanofi, NJ, USA; [3]Sanofi, France; [4]Sanofi, Germany; [5]Regeneron, NY, USA

Objectives: Reduction of low-density lipoprotein cholesterol (LDL-C) has been shown to lower morbidity and mortality from cardiovascular disease (CVD) when patients are treated with statins or ezetimibe plus statins. PCSK9 inhibitors, such as alirocumab, significantly reduce LDL-C and can enable patients not controlled on statins to reach LDL-C goals. Their impact on cardiovascular outcomes is under clinical investigation. Here, we describe the development of a PhysioPD platform to investigate mechanisms underlying LDL-C changes with therapy and their potential impact on atherosclerotic plaque dynamics.

Methods: The PhysioPD platform is a quantitative systems pharmacology model that incorporates cholesterol metabolism and transport including LDL receptor (LDLR) trafficking, reverse cholesterol transport (RCT), and SREBP regulation of cholesterol synthesis, LDLR expression, and PCSK9 expression. In the platform, mechanistic hypotheses linking plasma LDL-C to atherosclerotic lipid core deposition, fibrosis, and inflammation in a representative coronary plaque lesion are included. Simulated treatments include PCSK9 antibodies, statins, fibrates, and ezetimibe. The platform was developed and calibrated with published data in accordance with Rosa's Model Qualification Method.

Results: Simulated changes in lipid profiles following therapy were consistent with published clinical data, including the influence of concomitant therapies on LDL-C reduction by alirocumab. Platform research highlighted the impact of patient-specific factors, such as LDLR expression and RCT, on the dynamics of circulating LDL-C levels and potential changes in plaque size, composition, and stability.

Conclusions: A PhysioPD platform was developed to investigate the mechanisms through which cholesterol-lowering therapies affect lipid profiles and plaque characteristics. This platform, upon further development and qualification, may support dose optimization and clinical trial design for PCSK9 inhibitors and other lipid-modulating drugs and, in the future, help inform therapeutic management of patients with CVD.

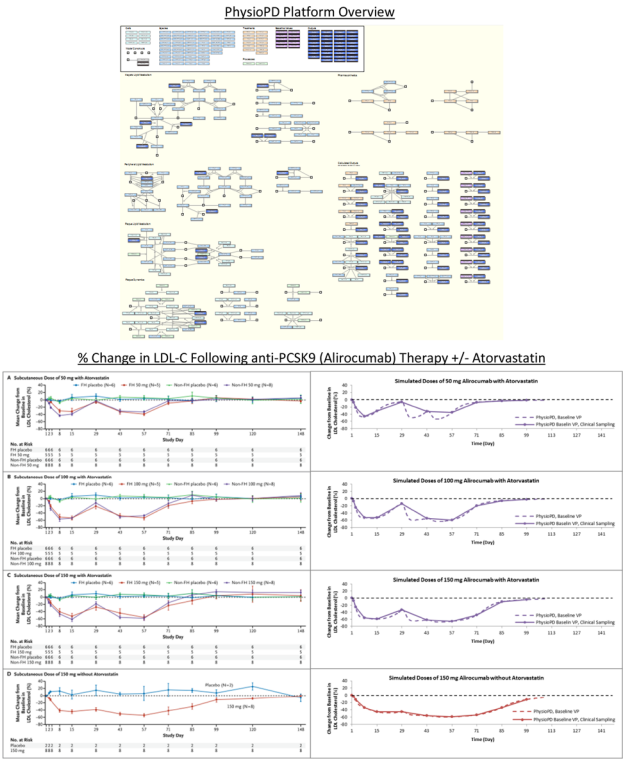

Fig. 1 PhysioPD platform overview and simulation examples. *Top* Graphical overview of the PhysioPD platform. *Bottom* PhysioPD simulations (*right*) with a representative Virtual Patient (VP) of multiple-dose alirocumab therapy (days 1, 29, 43) with or without atorvastatin compared to clinical data (*left*) published by Stein et al. NEJM. 2012; 366(12): 1108–1118

M-19

Modeling Complex PK Profiles of Long Acting Injectable Products Using a Convolution-Based Approach

Roberto Gomeni*, Françoise Bressolle

Pharmacometrica, La Fouillade, France

Objectives: The active pharmaceutical ingredient (API) in long acting injectable (LAI) products is usually encapsulated in microspheres (i.e., glycolide/lactide matrix) that extend the release of API into the systemic circulation, giving relatively long apparent half-lives and unique PK profiles. The PK profile of these products usually consists an initial release phase where APIs on the surface of the formulation ingredients are absorbed systemically, a lag phase with minimal API release, and a main release phase in which the ingredients in the formulation degrade allowing the API to be absorbed into the systemic circulation completely. The objective of this study was to apply a convolution-based methodology to characterize the PK profile of LAIs, to link in vivo release with in vitro dissolution data and finally to assist development of optimized LAI products.
Methods: Convolution-based methods are used to directly relate the time course of the plasma concentrations to the time course of the fraction of the dose released in vivo. A novel approach is proposed to implement joint models describing the time course of the in vivo drug release and the disposition and elimination processes of LAI products. The model describing the time course of the fraction of the dose released in vivo is implemented using the same models used to describe the in vitro dissolution profiles. This approach provide a modelling framework for linking the in vivo release with in vitro dissolution data, to assist development of optimized LAI products and to define new bioequivalence criteria for LAI formulations. The model has been implemented in NONMEM 7.3.
Results: The proposed methodology was successfully applied using single or dual Weibull in vivo release models for fitting the PK profiles of: a) four long-acting subcutaneous risperidone formulations, b) four long acting olanzapine microspheres formulations, and c) RISPERDA CONSTA® formulation.
Conclusions: A new modeling approach has been proposed to characterise the complex PK profiles of LAI products. The estimated in vivo release rate has been used to evaluate the in vitro/in vivo correlation and the define criteria for assessing comparative bioequivalence of LAI products.

M-20

Longitudinal Exposure–Response Relationship for Mirogabalin in Patients with Diabetic Peripheral Neuropathic Pain

Ophelia Yin[1*], Domenico Merante[2], Kenneth Truitt[1], Raymond Miller[1]

[1]Daiichi Sankyo Pharma Development, Edison, New Jersey, USA; [2]Daiichi Sankyo Development Ltd., Gerrards Cross, UK

Objectives: Mirogabalin (DS-5565) is a novel, preferentially selective α2δ-1 ligand characterized by high potency and selectivity for the α2δ subunit of voltage-sensitive calcium channel complexes in the central nervous system. The purpose of the analysis was to develop models to describe the potential relationships between mirogabalin exposure and clinical efficacy (average daily pain score, ADPS) and safety (incidence of somnolence or dizziness) outcome in a phase II dose-ranging study.
Methods: Patients with diabetic peripheral neuropathic pain were randomized to placebo, dose-ranging mirogabalin (5, 10, 15, 20, and 30 mg/day), or pregabalin (300 mg/day) for 5 weeks. Patients who received at least one dose of placebo or mirogabalin were included in the present analysis. Longitudinal ADPS (11-point Likert scale) was modeled using a proportional odds model, which included baseline pain scores, placebo and drug effect, and inter-individual random effects. The relationship between mirogabalin exposure and the incidence of somnolence or dizziness was analyzed using mixed effect logistic regression. Pharmacokinetic exposure at steady state, including AUC from time 0 to 24 h (AUC_{0-24}), average (C_{av}), maximum (C_{max}) and trough (C_{min}) concentration, were obtained for individual patients using population pharmacokinetic analysis, and then evaluated as potential significant predictors for the efficacy or safety endpoints.
Results: The final model for ADPS included a placebo time-course effect, and a drug effect that was described by an E_{max} relationship and driven by mirogabalin C_{av}. Model predicted changes in ADPS from baseline to week 5 are in good agreement with those observed (Table 1). Both mirogabalin C_{av} and C_{max} were found to be statistically significantly associated with the incidence of somnolence or dizziness.

Table 1 Observed versus model predicted mean change from baseline to week 5 in ADPS

Treatment group	Observed mean (min, max)	Model predicted mean (min, max)
Placebo (n = 99)	−1.93 (−9.57, 1.23)	−1.89 (−9.74, 1.05)
5 mg QD (n = 51)	−2.15 (−7.63, 1.29)	−2.13 (−7.19, 0.93)
10 mg QD (n = 53)	−2.40 (−7.14, 2.57)	−2.33 (−5.75, 1.66)
15 mg QD (n = 44)	−2.78 (−10.0, 1.52)	−2.53 (−7.46, 1.69)
10 mg BID (n = 46)	−2.87 (−10.0, 1.29)	−2.77 (−9.25, 0.47)
15 mg BID (n = 52)	−2.86 (−9.57, 1.33)	−2.99 (−9.01, 0.49)

Conclusions: The exposure–response models provided an appropriate description of the observed mirogabalin efficacy and adverse event profiles over time. The analysis results offer insights into the selection of mirogabalin doses in future phase III studies.

M-21

Nonlinear Mixed Effects Modeling of Disease Progression of Placebo Subjects from the Irbesartan Diabetic Nephropathy Trial

Phyllis Chan[1,*], Chunlin Chen[1], David Clawson[1], Holly Soares[1], Lara Pupim[1], Frank LaCreta[1], Malaz AbuTarif[1]

[1]Bristol-Myers Squibb, Princeton, NJ

Objectives: Diabetic nephropathy (DN) is the leading cause of end-stage renal disease, and a large heterogeneity is present in the patient population and in the rates of disease progression. The objective of this study was to develop a model to characterize the estimated glomerular filtration rate (eGFR) decline profile in DN patients, as well as to identify and estimate the contribution of baseline risk factors to the variability in rate of eGFR decline.
Methods: Longitudinal eGFR data from the placebo arm of the IDNT trial (n = 562) were used for analysis. Initial graphical analysis was performed to reveal the general profile of eGFR decline across the population strata. Base model building tested linear and asymptotic

models, as well as combinations of between and within subject variability distribution models. The full model was constructed using univariate screening ($p < 0.05$). The nonlinear mixed effect modeling approach was implemented using NONMEM and confidence intervals of parameter estimates were determined using bootstrapping.

Results: Repeated eGFR measurements of up to 48 months were adequately described by an exponential decline model, parameterized as the estimated baseline eGFR and rate constant of decline, with a lognormal distribution on the estimated baseline eGFR and Box-Cox transformation on the rate constant of decline. Within subject variability was described by an additive residual error model. Relative standard errors of the base model components were less than 20 %. Covariates included on the rate constant of decline in the full model are baseline urinary albumin-to-creatinine ratio, eGFR, age, hemoglobin, serum calcium, serum sodium, serum phosphorus, total cholesterol, race, and the number of anti-hypertensive drugs taken during the study.

Conclusions: Longitudinal eGFR profiles in DN patients were best described by an exponential decline model with baseline risk factors on the rate constant. The results of this disease progression modeling are currently being utlized as part of a model-based tool to assist with designing trials in progressive chronic kidney diseases.

M-22

Model-Based Meta-Analyses (MBMA) of DAS28 Reduction in Support of Rheumatoid Arthritis Development Programs

Yasong Lu*, Sun Ku Lee, Parul Gulati, Tarek Leil

Bristol-Myers Squibb, Princeton, NJ 08543

Objectives: Early development of RA drugs usually involves trials of ≥12 weeks with disease activity score, DAS28, as the efficacy endpoint. Questions facing RA early development include: (1) Can an efficacy-based decision for program advancement be made sooner than 12 weeks? (2) Can comparative efficacy of a novel RA treatment be evaluated against historical data of comparators? With the rich literature on DAS28 responses in RA patients, we employed MBMA of baseline-corrected DAS28 (ΔDAS28) to help address these questions.

Methods: Analyses were based on arm-level DAS28 records from a comprehensive database on RA trials published during 1994–2013. The analyses comprised of two parts. (I) Establishment of correlation between DAS28-ESR and DAS28-CRP. (II) MBMA of ΔDAS28. The model assumed ΔDAS28 to be a sum of placebo and drug effects. Each effect was described using a longitudinal Emax model, with baseline DAS28 as a covariate on the Emax. Each drug was modeled at the regulatory approved dose level. Simulations were conducted for arm-level ΔDAS28 for each drug at the corresponding dose.

Results: (I) The 193 paired records of DAS28-ESR and DAS28-CRP represented 7 distinct mechanisms with trial durations up to 52 weeks. The correlation, DAS28-CRP = 0.554 + 0.957 × DAS28-ESR, irrespective of mechanism and duration (Fig. 1A), supported the pooling of ΔDAS28-ESR and ΔDAS28-CRP for MBMA. (II) The MBMA included 127 trials of 7 drugs from 5 distinct mechanisms besides placebo, representing 17,381 patients, mostly incomplete responders to methotrexate with or without prior exposure to biologics. The time-course ΔDAS28 for each drug was adequately described by the model. The simulated arm-level mean ΔDAS28 for each drug is shown in Fig. 1B, C.

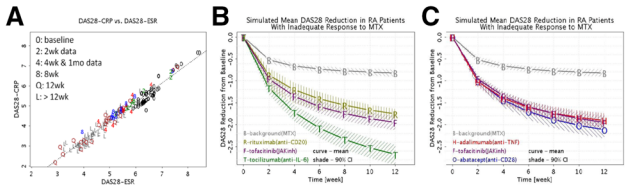

Fig. 1 Linear correlation between DAS28-CRP and DAS28-ESR in RA patients (**A**). Simulated arm-level mean ΔDAS28 profiles with treatment of various drugs in RA patients, who are incomplete responders to methotrexate (seperated into panels **B** and **C** for clarity)

Conclusions: The MBMA demonstrates that ΔDAS28 profiles for placebo and active drugs begin to separate at as early as 2 weeks of treatment, supporting the plausibility of early decision making based on data prior to 12 weeks. The simulated ΔDAS28 profiles provide a benchmark for evaluation of competitiveness of new anti-RA agents.

M-23

Development of a Physiologically Based Pharmacokinetic Model for Daclastavir and Prediction of Drug–Drug Interactions with P-gp and CYP3A4 Inhibitors

Qi Wang*, Ming Zheng, Tushar Garimella, Timothy Eley, Tarek Leil, Richard Bertz

Research and Development, Bristol-Myers-Squibb Co

Objectives: Daclastavir (DCV) is an inhibitor of the HCV NS5A replication complex approved in multiple countries including Japan and EU and is currently under review in the US. Objectives: 1) Develop a Physiologically Based Pharmacokinetic (PBPK) model to describe the clinical PK of DCV. 2) Use the PBPK model to identify the mechanism for the observed interactions between DCV and CYP3A4 and P-gp inhibitors.

Methods: The model was constructed based on in vitro and clinical data in Simcyp (v13r1). The model was verified with single and repeat dose PK study results, and drug–drug interaction results with midazolam, rifampicin, cyclosporine and ketoconazole. The prospective simulation was conducted with quinidine to examine the effect of P-gp inhibition on DCV PK.

Results: Simulated DCV AUC and Cmax after single and repeat dose were comparable to the observed data, with the AUC ratio of simulated/observed ranging from 0.9–1.3 to 0.8–1.5, and Cmax ratio ranging from 0.8–1.4 to 0.8–1.2, respectively. The simulated geometric mean ratio (GMR) for AUC of midazolam in presence/absence of DCV was similar to the observed GMR (0.90 and 0.88). The simulated GMR for AUC and Cmax of DCV in the presence/absence of rifampicin, cyclosporine, and ketoconazole were comparable to the observed GMR (Table 1). The GMR for AUC in the presence/absence of quinidine was predicted to be 1.05.

Results/Conclusions: A PBPK model for DCV was successfully developed and validated with various clinical study results. Simulations with CYP3A4 and P-gp inhibitors suggested that inhibition of CYP3A4-mediated DCV metabolism was the major mechanism for the observed DDI with ketoconazole. Concomitant administration of P-gp inhibitor alone isn't expected to cause clinically meaningful change of DCV PK. Underestimation of cyclosporine inhibition of CYP3A4 and other transporters may explain the under-prediction of DCV change by cyclosporine. Inability to incorporate P-gp induction in the current Simcyp module is the reason for under-prediction of rifampicin effect on DCV PK.

Table 1 Change of DCV PK Parameters in Presence of Perpetuator Drugs

Drug (perpetuator)	Inhibition Mechanism	AUC ratio (GMR)			Cmax Ratio (GMR)		
		Simulated	Observed	Simulated/observed	Simulated	Observed	Simulated/observed
Rifampicin	CYP3A4 and P-gp induction	0.40	0.212	1.89	0.83	0.438	1.89
Ketoconazole	Strong CYP3A4 and P-gp Inhibition	3.11	2.99	1.04	1.25	1.57	0.80
Cyclosporine	Weak CYP3A4, Strong P-gp inhibition	1.04	1.4	0.74	1.03	1.04	0.99
Quinidine	Strong P-gp inhibition	1.05	NA	NA	1.03	NA	NA

NA not available

M-24

Feedback Control Indirect Response Models

Yaping Zhang, David Z. D'Argenio*

Department of Biomedical Engineering, University of Southern California, Los Angeles, CA

Objectives: Most physiological processes are subject to feedback regulation. We hypothesize that PK/PD models that do not appropriately incorporate known autoregulatory mechanisms are incomplete representations of the drug-response relationship, and may lead to an underestimation of a drug's potency. In this study, a new general framework is introduced for modeling pharmacodynamic processes that are subject to autoregulation, which combines the widely used indirect response (IDR) model approach [1] with ideas from classical feedback control of engineered systems.
Methods: Proportional (P), integral (I), derivative (D) and linear combinations of these control terms are incorporated into IDR models to reflect the various feedback input signals, and the constants G_p, G_i, G_d are their respective gains reflecting their contributions to the control input (see Figure).

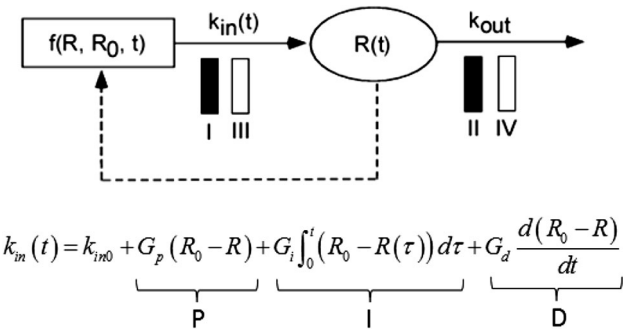

Fig. 1 Feedback control indirect response (FC IDR) model framework

Results: Model equations are derived and simulations are conducted to illustrate the framework of FC IDR models. It is demonstrated that ignoring the contributions of feedback control mechanisms in PD studies would lead to the underestimation of drug potency. Four examples [2–5] were selected from literature to illustrate the broad application of the FC IDR framework. The similarities and differences of this proposed framework and two less general approaches which also include feedback are further discussed.
Conclusions: The FC IDR modeling framework allows the drug's effects to be quantified independently of the autoregulatory mechanisms that also act on the effect variables. It tackles the difficulties long-recognized by systems physiologists in understanding the mechanisms of drug action that underlie processes subject to feedback regulation, and may provide a bridge for development of more mechanistic systems pharmacology models.

References:

1. Dayneka NL, et al. Journal of pharmacokinetics and biopharmaceutics. 1993;21:457–78.
2. Bundgaard C, et al. European journal of pharmaceutical sciences. 2006;29:394–404.
3. Mathot RA, et al. Clinical pharmacology and therapeutics 1999;66:140–51.
4. Agerso H, et al. Journal of clinical pharmacology 2001;41:163–9.
5. Jonkers R, et al. Clinical pharmacology and therapeutics 1987;42:627–33.

M-25

Mechanistic Modeling with DILIsym® Predicts Dose-Dependent Clincial Hepatotoxicity of AMG 009 That Involves Bile Acid (BA) Transporter Inhibition

Kyunghee Yang[1*], Jeffrey Woodhead[1], Ryan Morgan[2], Paul Watkins[1], Brett Howell[1], Scott Siler[1]

[1]The Hamner Institues for Drug Safety Sciences, Research Triangle Park, NC; [2]Amgen, Thousand Oaks, CA

Objectives: To predict the clinical hepatotoxicity of AMG 009 and species differences in AMG 009-mediated hepatotoxicity using DILIsym®, a mechanistic model of drug-induced liver injury
Methods: Inhibitory effects of AMG 009 for BA transporters were assessed using transporter-overexpressing vesicles and transfected cells. Hepatotoxicity responses to AMG 009 in humans and rats were simulated in DILIsym® using a PBPK model of AMG 009, BA homeostasis and toxicity sub-models [1,2], and in vitro BA transporter inhibition data. Previously constructed human and rat simulated populations (SimPops™) that incorporate variablity in BA disposition and mitochondrial function were employed for population analyses.
Results: AMG 009 was a mixed inhibitor of human BSEP ($K_i = 2.4$ μM;$\alpha = 2.4$), rat Bsep ($K_i = 5.6$ μM;$\alpha = 34$), and human MRP4 ($K_i = 12.9$ μM;$\alpha = 2.1$), and a weak inhibitor of human NTCP ($IC_{50} = 126.5$ μM) and rat Ntcp ($IC_{50} = 48.4$ μM). Employing only AMG 009-specific data, modeling of 100 mg AMG 009 bid for 14 days predicted serum ALT elevations > 3X upper limit of normal (ULN) in 17 % of the human SimPops™(Fig. 1A); this was similar to the clinically observed incidence of 12.5 % (1 out of 8). DILIsym® recapitulated the clinically observed ALT dynamics (e.g., delayed hepatotoxicity presentation, recovery after discontinuation) (Fig. 1A). Predicted incidence of Hy's Law cases (ALT > 3X ULN and bilirubin > 2X ULN) was 1.4 %, whereas no Hy's Law cases were observed among 8 individuals administered 100 mg. At 25 and

50 mg dosing, minimal toxicity was predicted (0 and 2 % of ALT > 3X ULN, respectively; no Hy's Law cases), consistent with the clinical data (Fig. 1B). Conversely, no hepatotoxicity was predicted in the rat SimPops^{TM} administered 1500 mg/kg/day AMG 009 for 1 month, consistent with the preclinical data.

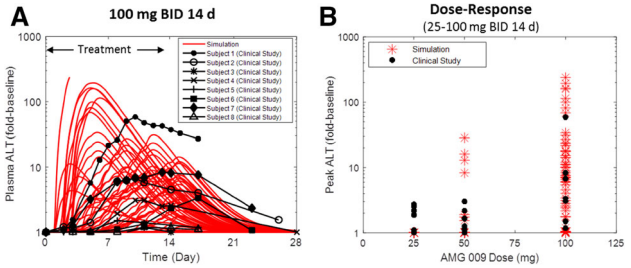

Fig. 1 **A** simulated and observed serum ALT profiles in humans administered 100 mg AMG 009 bid for 14 days. **B** Simulated and observed peak serum ALT in humans administred 25, 50, or 100 mg AMG 009 bid for 14 days

Conclusions: DILIsym® predicted dose-dependent, delayed AMG 009 hepatotoxicity in humans but no hepatotoxicity in rats, consistent with observed clinical and preclinical data. Mechanistic modeling is a useful approach to translate in vitro BA tranasporter inhibition data to clinical hepatotoxicity.

References:

1. Woodhead JL et al. CPT:PSP 3:e123, 2012
2. Woodhead JL et al. J Pharmacokinet Pharmacodyn 41:1(suppl) M-054, 2014

M-26

Evaluating the Efficiency of Payload Delivery by ADCs Using a Minimal PBPK Model

Linzhong Li*, Rachel Rose, Krishna Machavaram, Iain Gardner, Masoud Jamei

Certara, Sheffield, U.K

Objectives: Antibody drug conjugates (ADCs) aim to deliver a sufficient amount of payload (drug) into tumor cells whilst minimizing exposure of healthy tissues to the free payload. The amount of payload internalized into tumor cells depends on a number of factors including tumor capillary density, target antigen level, ADC internalization rate, target binding affinity, de-conjugation rate and extent of off-target binding. An integrated approach is needed to model the interplay of these multiple factors. For this purpose a minimal PBPK model was used to describe the disposition of ADCs in vivo and to evaluate the efficiency of payload delivery to a solid tumor.
Methods: A minimal PBPK model for monoclonal antibodies (mAb) [1] was adapted to describe each ADC species (defined by payload:mAb ratio) with payload release [2] leading to inter-conversion between ADC species (figure 1, upper panel). A tumor compartment was added to the model [3]. Target binding can occur at multiple sites and extended TMDD models allow multiple ADC species to compete for target binding. Payload is released following de-conjugation, target binding and internalization, and protein catabolism in tissue or plasma. The released payload (%ID) in the tumor is calculated.
Results: Both a high level of antigen with low internalization rate and a low level of antigen with high internalization rate can achieve a high payload delivery to the tumor (Figure 1(a)). For a given antigen level and internalization rate there is an optimal range of doses to achieve maximal efficiency of payload delivery (%ID). Figure 1(b) shows the impact of antigen level in normal tissue on the efficiency of payload delivery to the tumor compartment.
Conclusions: A mechanistic tumor model was incorporated into a minimal PBPK framework to model the efficiency of payload delivery to the tumor by ADCs.

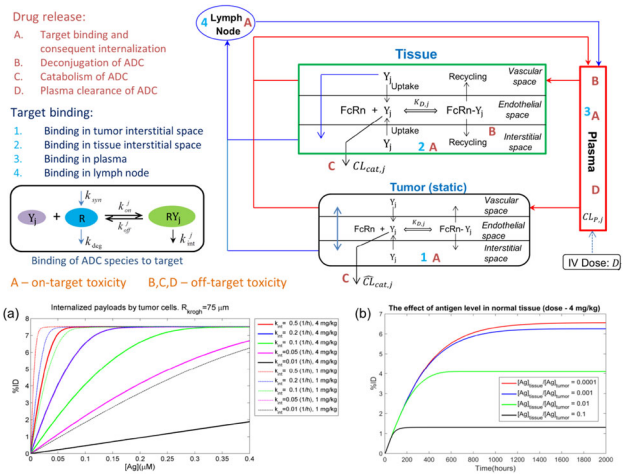

Fig. 1 A schematic representation of a minimal PBPK model for ADCs (upper panel) and the simulation results: (a) the percentage of injected dose (payload) internalized into tumor cells (%ID) for a range of antigen concentrations with different internalization rates; (b) the impact of antigen expression levels in normal tissues on %ID. Y_j—ADC species with DAR j

References:

1. Li et al. AAPS J. 2014; 16.
2. Gibiansky et al. J PK/PD 2014; 41.
3. Thurber et al. J Theor Biol. 2012; 314.

M-27

Development of a Quantitative Systems Pharmacology (QSP) Platform to Support Translational Research and Clinical Development in Immuno-Oncology

Brian J. Schmidt[1*], Derek W. Bartlett[2], Shruti Agrawal[1], Michael Reed[2], Maria Jure-Kunkel[1], Andres A. Gutierrez[1], Raphael A. Clynes[1], Bruce S. Fischer[1], Satyendra Surywanshi[1], Ananth Kadambi[2], Christina Friedrich[2], Katherine Kudrycki[2], Amit Roy[1], Tarek A. Leil[1]

[1]Bristol-Myers Squibb, Princeton, NJ; [2]Rosa & Co, San Carlos, CA

Objectives: Mechanistic models capable of integrating molecular, cellular, and tissue level datasets to provide research predictions of tumor response are well-positioned to play a central role in translational research and clinical development for the emerging immuno-oncology therapeutic paradigm. The availability of calibration and validation data from clinical trials from the first successful immuno-oncology therapies such as ipilimumab and nivolumab (including CA184004, MDX1106-03, CA209004, CA209009) facilitates comparison of simulated outcomes with clinical data. Our goal was to

develop a QSP platform to propose and analyze putative mechanisms of immuno-oncology agent efficacy.
Methods: A multidisciplinary team developed the biological scope of a mechanistic, ordinary differential equation-based simulation platform. The platform includes interactions of multiple immune cell types, cancer cells, soluble mediators, cell–cell contact, checkpoint engagement, as well as ipilimumab and nivolumab therapies within the microenvironment of a prototypical simulated lesion and their effect on tumor shrinkage.
Results: The platform was calibrated, taking into account antibody plasma concentrations, circulating absolute lymphocyte counts, trends in tumor cytokines, an IFN-γ gene expression signal, changes in tumor infiltrating lymphocytes, and lesion size data. In agreement with clinical observations, an enhancement in lesion response was observed with the combination therapy.
Conclusion: The platform recapitulates essential immune response pathways in a simulated lesion and exhibits qualitative agreement with patient response phenotypes to immuno-oncology agents. Having demonstrated proof-of-principle with a preliminary calibration, the platform will serve as a framework to facilitate biomarker identification, integrate additional therapeutic mechanisms, propose new combination strategies, and serve as a sub-model within a framework for the cancer-immunity cycle [1].
The results in this abstract were previously presented at the ASCPT 2015 Annual Meeting and published in the proceedings as abstract QP-32.

References:

1. D. S. Chen and I. Mellman (2013) Immunity 39(1):1–10.

M-28

Analyzing Patient-Reported Outcomes in Breast Cancer through Item-Response Theory Pharmacometric Modeling

Emilie Schindler[1*], Bei Wang[2], Bert Lum[2], Sandhya Girish[2], Jin Y. Jin[2], Lena E. Friberg[1], Mats O. Karlsson[1]

[1]Department of Pharmaceutical Biosciences, Uppsala University, Sweden; [2]Genentech Inc

Objectives: Patient-reported outcomes (PROs) provide valuable information on the subjective impact of a disease and treatment on patients. However, methodological challenges exist for interpreting PROs due to their multi-scale nature and frequent missing data. This analysis aims to describe Functional Assessment of Cancer Therapy-Breast (FACT-B) questionnaire data and investigate relationships to drug exposure in T-DM1 (ado-trastuzumab emtansine, Kadcyla) treated patients with HER2 + locally-advanced or metastatic breast cancer using item-response theory (IRT) based pharmacometric approaches [1].
Methods: Item-level FACT-B data (n = 2655) were available from 484 T-DM1-treated patients included in a phase 3 trial [2]. FACT-B contains 36 ordered categorical items divided into 5 subscales (physical, social, emotional and functional well-being, and breast-cancer specific). Each item was modeled using a proportional-odds model, where the probability of a score is described as a function of item-specific fixed effect parameters and a subject-specific random variable (WB_i) describing the underlying well-being. For each patient, one WB_i variable was estimated for each subscale. Correlations between the 5 subscales were estimated. WB_i are assumed to be standard normally distributed at baseline. The effect of time after first dose and TDM-1 AUC_{cycle1} [3] on WB_i parameters were investigated.
Results: A total of 180 item-specific parameters were estimated. Correlations between subscales exceeded 33 %. Well-being improved over time for all subscales except social well-being. However, well-being increased with increased AUC_{cycle1} for all subscales. Item-characteristic curves showed that items within the breast-cancer subscale may not relate to the same underlying variable. These items would benefit from reassignment to another subscale.
Conclusions: This work is the first attempt to our knowledge to use IRT-based modeling approach as a framework for analyzing PROs in oncology. The exploratory analysis showed positive relationships between time, drug exposure and FACT-B data. The developed model will be used to further evaluate time-varying exposure–response relationships for PROs.

References:

1. Ueckert et al. Pharm Res. 2014;31(8):2152–65.
2. Welslau et al. Cancer. 2014;120(5):642–51.
3. Lu et al. Cancer Chemother Pharmacol. 2014;74(2):399–410.

M-29

A Method to Evaluate Fetal Erythropoiesis from Postnatal Survival of Fetal RBCs

Denison J. Kuruvilla[1*], John A. Widness[2], Demet Nalbant[2], Robert L. Schmidt[2], Donald M. Mock[3] and Peter Veng-Pedersen[1]

[1]Department of Pharmaceutical Sciences and Experimental Therapeutics, University of Iowa, Iowa City, IA; [2]Department of Pediatrics, University of Iowa, Iowa City, IA; [3]Departments of Biochemistry & Molecular Biology and Pediatrics, University of Arkansas for Medical Sciences, Little Rock, AR

Objectives: To present a novel method that utilizes cord blood RBCs collected at birth to study both the non-steady state (non-SS) in utero RBC production and the changes in in utero RBC lifespan over time; and to apply this method to in vivo RBC disappearance curves of umbilical cord RBCs from critically ill very low birth weight (VLBW) preterm anemic infants tracked via a biotin label.
Methods: The mathematical model, which considers both changes in rate of erythropoiesis and RBC lifespan and which accurately accounts for the confounding effect of multiple phlebotomies, was developed and applied to survival curves for biotin labeled RBCs from ten VLBW infants. The infants were between 24 and 28 weeks gestation and was being cared for in the Neonatal Intensive Care Unit (NICU). It was assumed that the disposition of Hb/RBCs was lifespan based. The effect of changes in erythropoiesis rate and RBC lifespan on the RBC survival curves were investigated using model-based simulations.
Results: The estimated mean fetal RBC production rate scaled by body weight was 1.07×10^7 RBCs/day.g (CV = 47.75 %), and the mean RBC lifespan at birth was 52.1 days (CV = 10.8 %). The in utero RBC lifespan increased at a rate of 0.51 days per day of gestation (CV = 12.75 %).
Conclusion: Due to practical and ethical concerns with fetal blood sampling, there is very limited information available on the dynamic changes associated with in utero RBC production. This study introduces a novel method to utilize cord blood RBCs collected at the time of birth to look "backward in time" to evaluate fetal erythropoiesis. The proposed mathematical model and its implementation provides a flexible framework to study in utero non-SS fetal erythropoiesis in newborn infants.

M-30

An Approximation to the Solution of Systems of Nonlinear Ordinary Differential Equations in Pharmacokinetics-Pharmacodynamics

Stephen Duffull[1*], Gareth Hegarty[1,2]

[1]School of Pharmacy, University of Otago, Dunedin, New Zealand; [2]Department of Mathematics and Statistics, University of Otago, New Zealand

Objectives: PKPD models are often formulated as systems of ordinary differential equations (ODE). Nonlinearity in PKPD is not uncommon. Due to the nonlinearity it is not possible to solve these systems, except in the simplest cases, in closed algebraic form and iterative time-stepping algorithms are employed. These algorithms, e.g. the Runge–Kutta methods, although very effective general solutions may be slow, are prone to imprecision, provide solutions at discrete time points and require knowledge of the stiffness of the system. In this work we propose a rapid iterative solution that is exact to any arbitrary level of accuracy and is continuously differentiable over time.

Methods: If we have an ODE of the general form $dy/dt = f(t,y) + A(t,y)y$ with defined initial conditions, then this system can be linearized to a time-varying linear system by plugging in our previous value of $y\{n-1\}$ as the predictor of our updated value of $y\{n\}$, such that:

$$dy\{n\}/dt = f(t, y\{n-1\}) + A(t, y\{n-1\})y\{n\}$$

The system is now no longer nonlinear as the functions f and A do not depend on the current iteration of $y\{n\}$. The process is updated N times so that $y\{n-1\}$ converges to $y\{n\}$. The time-varying linear solution can now be solved using standard procedures such as quadrature.

This general method is applied to a first-order input Michaelis–Menten output model.

Results: The starting values for the first iteration of the linearization for the plug-in values of $y\{n-1\}$ were set to the initial condition ($y(0) = 0$) for all y. The linearized (time-varying) solution was then solved using Gauss–Legendre quadrature. It was found that 7 iterations of the linearization process resulted in a relative error of $1e{-}5$. The solution was shown to be convergent.

Conclusions: A method for solving nonlinear ODEs is presented and illustrated with a simple example. Because the solution depends continuously on time and analytical derivatives available the method is particularly amenable to estimation and optimisation problems.

M-31

Immuno-Viral Dynamics Modeling of Letermovir for Treatment of Human Cytomegalovirus (HCMV) Infection in Post-Transplant Settings

Eric G. Burroughs[1*], Chandni Valiathan[2], Kevin Dykstra[1], Cameron M. Douglas[2], William L. Marshall[2], Peter Lischka[3], and Carolyn R. Cho[2]

[1]qPharmetra, Andover, MA, USA; [2]Merck & Co. Inc., Kenilworth, NJ, USA; [3]AiCuris GmbH & Co. KG, Wuppertal, Germany

Objectives: Letermovir is a novel inhibitor of human cytomegalovirus (HCMV) being developed for HCMV prophylaxis in hematopoietic stem cell transplants (HSCT). A viral dynamics model that integrates viral replication, the immune response, and letermovir's hypothesized mechanism of action targeting the viral terminase complex has been developed from literature models and clinical and non-clinical letermovir data.

Methods: A published HCMV immuno-viral dynamics model [1] was modified to account for letermovir's hypothesized mechanism of action (see Figure). Clinical drug effect was translated from an Emax model of in vitro data from over 50 HCMV viral strains isolated from clinical samples. Data from literature and the development program informed virus and immune function parameter estimates and initial conditions. Letermovir population pharmacokinetics (PK) models generated PK profiles for dosing regimens of interest. Model qualification consisted of comparing viral load reduction and failure rate projections against outcomes from a Phase 2a preemptive treatment study [2] and a Phase 2b prophylaxis study [3].

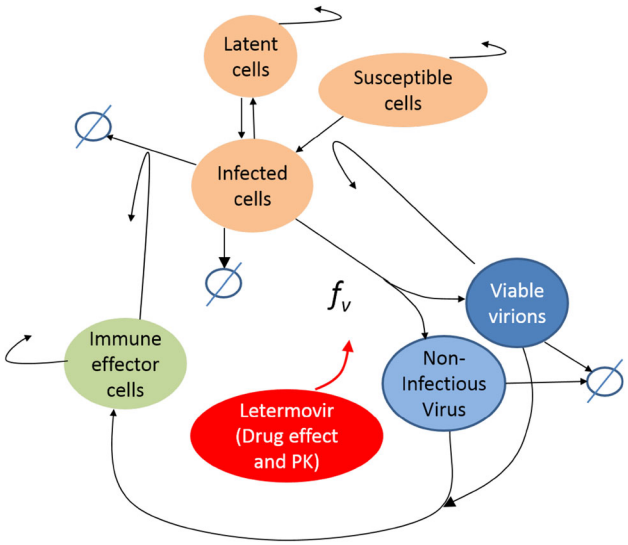

Fig. 1 Letermovir MOA-specific immuno-viral dynamics model schematic diagram for treatment of HCMV infection in post-transplant settings: compartments are indicated by *circles*, while *arrows* indicate processes. Infected cells arise from either reactivation of latently infected cells or through infection of susceptible cells by viable virions. The fraction, fV, of viable virions to non-infectious virus produced by infected cells is determined by letermovir exposure–response characteristics and dose regimen. Immune response enhances the clearance of infected cells from the system. The level of immune effector cells is suppressed by immunosuppressants but stimulated by both non-infectious virus and viable virions. Processes that are increasing or decreasing the values of the compartments are indicated with *directional arrows* while *arrows* that loop back towards a compartment indicate maintenance of cell/virion populations. Arrows directed toward null compartments, Ø, indicate clearance from the system

Results: A broad diversity of initial subject conditions coupled with limited subject-level observations, especially for the preemptive treatment study, limited quantitative qualification capabilities. Instead, subjects were stratified into scenarios (initial conditions and dosing regimens) representative of Phase 2a and 2b subjects. Simulations based on these representative scenarios using the final letermovir-specific integrated population PK and immuno-viral dynamics model were found to qualitatively reproduce observed clinical outcomes.

Conclusions: A letermovir-specific immuno-viral dynamics model was developed that qualitatively reproduces clinical outcomes. The model enables support of critical questions which may arise concerning HCMV infection in HSCT.

References:

1. Kepler, G. M et al. (2009). Mathematical and computer modelling, 49(7): 1653–1663.
2. Stoelben, S. et al. (2013). Transpl Int, 27: 77–86.
3. Chemaly, Roy R. et al. (2014). NEJM, 370:1781–1789.

M-32

Pharmacogenetic-Based Pharmacokinetic Modeling of Plasma and Intracellular Concentrations of Efavirenz on Adult Ethiopian HIV and TB/HIV Patients

Habtewold A[1,2,3], Aklillu E[2], Makonnen E[2], Amogne W[3], Yimer G[3], Aderaye G[3], Bertilsson L[2], Burhenne J[4], Owen JS[1*]

[1]Department of Pharmaceutical Sciences, School of Pharmacy, Union University, Jackson 38305, Tennessee (USA); [2]Division of Clinical Pharmacology, Department of Lab Medicine, Karolinska University Hospital, Huddinge, Stockholm (Sweden); [3]Department of Pharmacology, School of Medicine, Addis Ababa University (Ethiopia); [4]Department of Clinical Pharmacology & Pharmacoepidemiology, University of Heidelberg, Heidelberg, (Germany)

Objectives: As HIV replicates within immune cells, it is important to delineate the intracellular (IC) pharmacokinetic (PK) behavior of antiretroviral drugs like efavirenz (EFV). No previous study modeled PK of EFV in IC observations. Objective: To describe the population PK of plasma and IC EFV concentrations and explore covariates of PK.
Methods: From 313 patients, 1811 steady state plasma (n = 1132) and corresponding IC (n = 679) EFV concentrations were analyzed using LC/MS/MS after 600 mg per day. Baseline body weight and organ function values; age, sex, type of combination antiretroviral therapy and pharmacogenetic markers were explored as covariates. CYP2B6*6 alleles were included in the base model. PK parameters and random inter-individual variability (IIV) were estimated using NONMEM 7.1.
Results: One-, two- and three-compartment models with first-order absorption; lag-time or transit compartments were explored. A two-compartment model, plasma as central compartment (Vc/F = 93L; CV = 36 %) with first-order absorption and Alag and IC as peripheral compartment (Vp/F = 130L; CV = 65 %), described the data well (Figure 1). IC clearance followed a nonlinear transfer rate (CLp/F = 32L/h; Vmax = 25 μg/mL/h; Km = 4.1 μg/mL). The estimated CL/F for CYP2B6*1/*1, CYP2B6*1/*6 and CYP2B6*6/*6 were 18, 14 and 8.7 L/h, respectively. Covariate relationships on CL/F, Vc/F and Vmax were also explored using delta plots and added to the base model, when identified. Among the covariates identified, only CYP3A5*1 showed significant effect on CL/F (ΔOFV = 8.259, df = 1, α = 0.01), contributing for 1 % CL/F IIV.

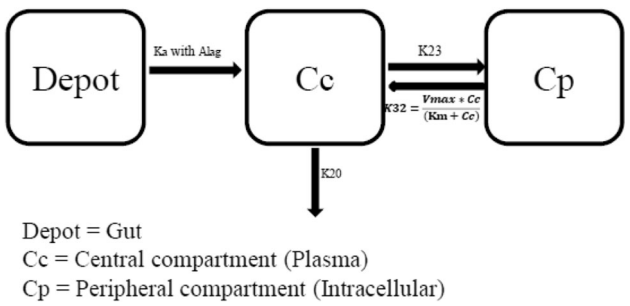

Fig. 1 Stuctural model

Conclusions: The present study revealed that EFV IC accumulated to higher concentrations than in plasma and was well described by zero-order transfer rate from peripheral cells to the plasma. Besides CYP2B6*6, CYP3A5*1 alleles minimally contribute for IIV of CL/F.

M-33

From Big Data to Smart Data. How Quantitative Systems Pharmacology Can Support CNS Pharmaceutical R&D

Hugo Geerts[1,2*], Athan Spiros[1]

[1]In Silico Biosciences, Berwyn, PA; [2]Perelman School of Medicine, University of Pennsylvania

Objectives: Traditional bio-informatics tools are very powerful in elucidating correlations or associations between data and certain clinical endophenotypes from large sets of data. However correlation is not identical to causation and many clinical development programs have failed to support the one gene-one protein-one disease hypothesis.
Mental Health issues, including Alzheimer's disease (AD) are rapidly becoming a major burden with only symptomatic treatments available and many more clinical trial failures. At the same time, extensive and longitudinal information of thousands of patients is currently being collected at a substantial cost.
Methods: In order to optimize the use of this information for developing succesfull therapeutic interventions, identifying protective lifestyles or defining subpopulations of patients that will respond to specific therapies, we need to convert this information into actionable knowledge. Quantitative Systems Pharmacology is a set of mechanism-based computer models of human brain cricuits (i.e. virtual human patients) with relevant and actionable predictive outcome for CNS R&D, especially in terms of clinical trial development in Neurology and Psychiatry. The model includes formalized representations of domain expertise in CNS (neurobiologists, neuropharmacologists, imagers and clinicians), has over 30 targets in addition to 5 common human genotypes (such as COMTVal158Met, the s/l 5-HTT, the D2DRTaq1A1 allele and CACNA1C genotype derived from human imaging studies) and has the complete pharmacology of all CNS active drugs, including PK profile and metabolites. It is essentially a form of Physiology-Based Pharmacodynamic Modeling.
Results: We will show examples where we correctly and blindly prospectively predicted an unexpected clinical outcome suggesting that our QSP platform captures better the human clinical environment than preclinical animal models. In addition, we will explore possible hypotheses why some clinical trials in AD and schizophrenia failed.
Conclusions: Running virtual patient trials in silico, i.e. identifying which comedications or genotypes influence the dose–response of a new investigative drug can improve clinical trial success.

M-34

Implementation of Non-linear Mixed Effect Modeling Approach in Allometric Scaling For Human Clearance Prediction

D. Zhang[1*], A. Ahmad[2], D. Boudinot[3]

[1]Merck & Co. Kenilworth NJ, USA, [2]Pfizer Inc. Cambridge, MA, USA, [3]Virginia Commonwealth University, VA, USA

Objective: Investigate the potential correlations between the allometric exponents from multiple-species AS method and the physiochemical properties, with an attempt to identify covariates that may explain the inter-drug variability in AS relationship, thus enabling individualization of AS for better human CL prediction.
Methods: After mining the scientific literature, a total of 251 literature reported drugs with intravenous pharmacokinetic parameter (CL) values in humans and rat or dog or monkey (at least three species including humans) were collected and were used as the MEM model dataset. The physicochemical and DMPK properties of each drug were estimated. The nonlinear MEM modeling approach with NONMEM was applied to the data to investigate the central tendency and distribution of allometric scaling (AS) coefficient and exponent. An investigation was conducted between the AS exponent and coefficient (CL at unit weight) with the physicochemical and DMPK properties of drugs to identify potential significant covariates.
Results: A nonlinear MEM AS model with additive residual error was developed. The estimated central tendency and distribution of AS exponent was consistent with literature reports strengthening the confidence of applying commonly accepted allometric exponents. Polar surface area (PSA) was identified as statistical significant covariate for AS coefficient by explanation of 5.7 % of inter-drug variability for AS coefficient from 104 to 98.3 %. However, compared to the 98.3 % remained un-explained inter-drug variability (IDV), this 5.7 % IDV finding may not have much practical usage.
Conclusion: By using MEM modeling for allometric scaling, the central tendency and distribution of AS exponent was systemically investigated and confirmed the empirical adopted value. Overall, with the largest data set reported in the allometric field of pharmacokinetics and the rigorous analyses on the correlations of the physiochemical properties and allometric relationship, this work showed little or no impact of physiochemical covariates on the allometric predictions of clearance.

M-35

Prediction of Pharmacokinetic Profiles of an Anti-TWEAK Monoclonal Antibody, BIIB023, in Pediatric patients with Lupus Nephritis

Xiao Hu[1*], Gerald Galluppi[1], Pratapa Prasad[1], Ivan Nestorov[1]

[1]Biogen, Cambridge, MA

Objectives: Our objective was to project BIIB023 pharmacokinetic (PK) profiles in pediatric subjects to support dose selection for a pediatric investigation plan (PIP), thereby, addressing the unmet medical needs in pediatric lupus nephritis (LN) patients. BIIB023, a monoclonal antibody against tumor-necrosis-factor-like-weak-inducer-of-apoptosis (TWEAK), is being developed to treat LN.
Methods: BIIB023 PK data was collected in two Phase 1 studies in healthy and rheumatic arthritis adults following IV infusion. A population PK model was built. Two virtual populations ranging from 5 to <12 years and ranging 12 to <18 years, respectively, were generated, using CDC smoothed growth curve. The simulated PK profiles and PK parameters following 6-month intravenous dose at 20 mg/kg monthly were compared between adults and pediatric subjects.
Results: The adult PK profiles were adequately fitted using a two-compartment model with both a linear elimination rate and a non-linear elimination rate. Significant covariates included body weight for clearance, and body weight and sex for volume of distribution. Renal function did not affect IgG PK under normal renal function, which may be different for LN patients. For the simulation, renal function was assumed to affect adults and children with LN similarly for BIIB023. The simulated BIIB023 PK profiles showed that the majority of the [5th, 95th] concentration intervals overlapped between pediatric subjects and adults. The median AUC_{tau} was 139, 166, and 174 mg/(mL h) for the 5 to <12 years age group, 12 to <18 years age group, and adults, respectively; the C_{max} was 447, 574, and 630 μg/mL, respectively, and the C_{trough} was 140, 144, and 142 μg/mL, respectively. Considering that the predicted C_{max} was smaller in pediatric subjects, as compared with adults, while the AUC_{tau} and C_{trough} were similar, the simulation results supported a proposed dosing regimen of 20 mg/kg in pediatric subjects of 5 to <18 years of age.
Conclusions: Simulation supported the proposed dose for LN patients of 5 through <18 years of age.

M-36

Exploration of Model-Based Bioequivalence (BE) Evaluation as an Alternative Approach for the Sparse Pharmacokinetic (PK) Sampling Design

Hyewon Kim[1*], Lanyan Fang[1], Stephanie Choi[1], Liang Zhao[1], Robert Lionberger[1]

[1]Office of Generic Drug, Center for Drug Evaluation and Research, Food and Drug Administration

Background: The current draft guidance for a sparse PK sampling scheme recommends bootstrapping concentrations to attain the mean concentration at each time point to derive the mean PK profile. However, the bootstrap-based evaluation method may be influenced by outliers and does not utilize all available information to accurately derive C_{max} and AUC_{tlast}. The purpose of this study was to explore the model-based bioequivalence evaluation as an alternative method to the current bootstrap-based method.
Methods: Ophthalmic products are a product category where a sparse PK sampling scheme is part of the bioequivalence evaluation. In a study to determine the effect of particle size and viscosity on ocular bioavailability, three formulations of budesonide suspension were dosed to both eyes of New Zealand white rabbits (n = 73). Each animal was euthanized at one of six time points and the aqueous humor samples were collected.
Bioequivalence was evaluated using four approaches: Method 1—Currently recommended evaluation approach (using arithmetic means), Method 2—Same as Method 1 but with geometric means, Method 3—Model based BE evaluation in which 500 BE studies (n = 24) with intensive PK profiles were simulated from the population PK model fitted to observations; and Method 4—Model based BE evaluation with bootstrap. Population PK model was fitted to each of 1000 bootstrapped datasets. BE standards were derived from the estimated typical PK parameters from each bootstrap dataset for BE evaluation.
Results: The currently BE evaluation method (Method 1) suggested that 3 formulations were not bioequivalent to each other. All other approaches concluded consistent results (Table 1). The model-based BE evaluation methods yielded narrower confidence interval that implied fewer subjects may be needed in the BE study than when other approaches are used. As a conclusion, the model-based BE evaluation approach may serve as an alternative method for evaluating studies using a sparse PK sampling design.

Table 1 90 % Prediction interval results for BE standards

	46C vs. 46A	47D vs. 46A	47D vs. 46C
C_{max} ratios			
Current BE (n = 50,000)	0.545, 1.614	0.112, 2.829	0.313, 2.428
Current BE with geometric mean (n = 50,000)	1.053, 1.704	0.463, 1.887	0.359, 1.356
Model-based BE method (n = 500)	1.260, 1.538	0.695, 0.852	0.498, 0.605
Model-based BE method with bootstrap (n = 1000)	1.169, 1.776	0.602, 0.963	0.432, 0.678
AUC_{tlast} ratios			
Current BE (n = 50,000)	0.423, 1.502	0.259, 1.013	0.463, 0.873
Current BE with geometric mean (n = 50,000)	0.756, 1.623	0.460, 0.989	0.473, 0.756
Model-based BE method (n = 500)	1.356, 1.508	0.771, 0.863	0.541, 0.600
Model-based BE method with bootstrap (n = 1000)	1.143, 1.829	0.652, 1.019	0.454, 0.727

M-37

Evaluation of the Expected Fisher Information Matrix without Linearization, in Nonlinear Mixed Effect Models for Discrete and Continuous Outcomes

Marie-Karelle Riviere, Sebastian Ueckert*, France Mentré

IAME, UMR 1137, INSERM and University Paris Diderot, Paris, France

Objectives: In recent years, estimation algorithms for NLMEMs have transitioned from linearization-based approaches towards higher-order methods. Optimal design, on the other hand, has mainly relied on first-order linearization (FO) to calculate the expected Fisher information matrix (FIM). Although efficient in general, FO precludes the application of optimal design with complex nonlinear models and in studies with discrete endpoints. The objective of this work was to apply integration algorithms, which have proven to be efficient for estimation, to evaluate the asymptotically exact FIM in NLMEM for both discrete and continuous outcomes.
Methods: For NLMEMs, the FIM has no analytical form as its calculation involves multiple integrations. We used either Adaptive Gaussian Quadrature (AGQ) or Markov Chain Monte Carlo (MCMC) to integrate the derivatives of the log-likelihood over the random effects, and Monte Carlo (MC) approximation to evaluate its expectation w.r.t. the observations. The proposed methods were implemented in R and used STAN for MCMC sampling. Evaluation was performed with models for continuous, binary, count and repeated time-to-event outcomes by comparing the FIM based relative standard errors (RSE) to the relative root mean square errors (RRMSE) from clinical trials simulation (performed using R & MONOLIX).
Results: AGQ and MCMC-based approaches showed good performance on scenarios for continuous and discrete outcomes with RSEs close to the RRMSEs obtained by simulations. RSE predicted by linearization gave close results for rich designs, but showed larger deviations for sparse designs and very non-linear models. We also compared time calculation of the FIM.
Conclusions: Two complementing methods for calculating the exact FIM were proposed and evaluated: AGQ as fast algorithm for simple discrete models, and MCMC suited even for large complex models where FO fails.

This work was supported by the IDEAL project.

The results in this abstract have been previously presented in part at PAGE 2015, Crete and published in the conference proceedings as abstract 3401.

M-38

Implementation of a highly nonlinear, multi-scaled and long-term HIV dynamic model with treatment interruptions and non-static BQL data for population analysis

Shuhua Hu*, Kevin Feng, Bob Leary, Mike Dunlavey, Bill Poland

Certara/Pharsight, Cary, NC

Objectives: The goal is to apply QRPEM estimation in Phoenix® NLME™ (Pharsight/Certara) to a highly nonlinear, multi-scaled and long-term HIV dynamic model [1] for population analysis with clinical data [1] including treatment interruptions, total CD4 + T-cells and non-static BQL viral load. A simpler model was considered in [2] for population analysis using SAEM and does not incorporate some important features including HIV-specific CD8 + T-cells and another possible source of latency. Here we do not try to compare QRPEM with methods used in other software but rather show the capability of QRPEM in implementing such a complex model.
Methods: Due to the complexity of the problem, this model cannot be directly implemented in Phoenix® NLME™. For example, model states may become unrealistically negative in numerically solving it due to round-off error caused by large-scale differences among model states and parameters. Moreover, ODE solvers often failed due to some unrealistic parameter values obtained during the optimization process. To alleviate the first difficulty, we converted the model by log-transformation of all model states and parameters. To avoid obtaining unrealistic parameter values, we imposed lower and upper bounds on posthoc parameters and modified Mu-model for QRPEM estimation. To incorporate treatment interruptions, we added treatment as a time-varying covariate using a linear-interpolation approach.
Results: Through proposed methods, we successfully implemented this model and obtained reasonable goodness of fit for all patients (Figure 1 shows fitting results for one patient).

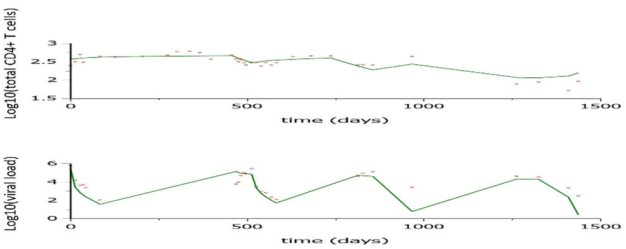

Fig. 1 Model fitting results for patient number 9 using QRPEM, where red circles are the data, and green solid line denotes the predicted model solution. (Upper panel): log10(total CD4 + T cells) versus time (days); (lower panel) log10(viral load) versus time (days)

Conclusions: Numerical results demonstrate the capability of QRPEM in analyzing a complex dynamic model with complicated data. In the future, we plan to investigate a hierarchical structure of this model or other disease models and then use these models to design adaptive dosing regimens via the Phoenix modeling language engine.

References:

1. H.T. Banks, et al., Journal of Biological Dynamics, 2 (2008), 357–385.
2. M. Lavielle, et al., Biometrics, 67 (2011), 250–259.

M-39

Ipilimumab Exposure–Response (E-R) Analysis of Overall Survival (OS) in Patients with Advanced Melanoma

Heather E. Vezina*, Yan Feng, Amit Roy

Bristol-Myers Squibb, Princeton, NJ, USA

Objectives: The human monoclonal antibody ipilimumab selectively binds CTLA-4 on a subset of T-cells, thereby augmenting anti-tumor immune response. Based on an earlier analysis, steady-state trough concentration (Cminss) was a significant predictor of OS in previously treated advanced (stage III/IV metastatic) melanoma patients [1]. Our objective was to describe the relationship between Cminss and OS in both previously treated, and chemotherapy naive advanced melanoma patients using a pooled analysis.
Methods: An E-R of OS analysis was performed with data from four Phase 2 ipilimumab monotherapy studies in previously treated advanced melanoma patients and one Phase 3 study of ipilimumab administered with dacarbazine in chemotherapy naive advanced melanoma patients (N = 1007, ipilimumab doses of 0.3, 3, and 10 mg/kg). The relationship between Cminss and OS was characterized using Cox proportional-hazards (CPH) models. A full CPH model was developed by incorporating all covariates of interest with appropriate functional forms into the base model.
Results: Figure 1 shows the estimated hazard ratios (95 % CI) for predictors in the CPH model. Notably, prior chemotherapy is not a predictor of OS. Higher Cminss is associated with a decrease in the risk of death. A poor ECOG performance score (ECOG > 0), high baseline lactate dehydrogenase (LDH), and advanced M-stage at study entry (M1C) increase the risk of death. There was also a significant interaction between Cminss and dacarbazine (hazard ratio 95 % CI does not include 1.0) suggesting a reduced ipilimumab effect in the presence of dacarbazine.

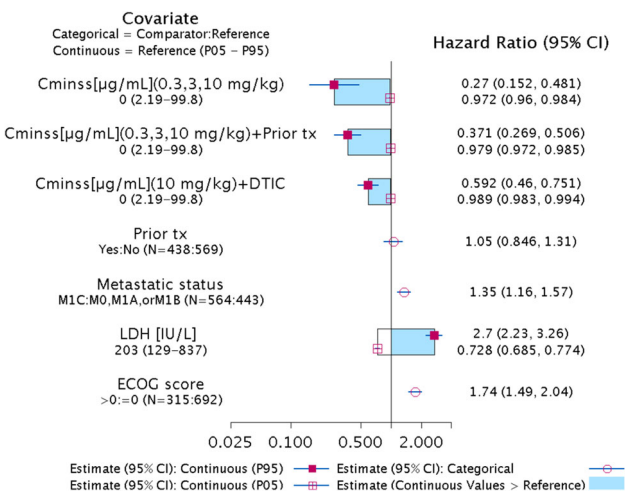

Fig. 1 Covariate Effects on the Hazard Ratio of OS (Full CPH Model)

Conclusions: The risk of death for previously treated and chemotherapy naive advanced melanoma patients decreased with increasing ipilimumab Cminss over the range of exposures achieved with the doses evaluated; however, concomitant dacarbazine administration reduced this benefit. The risk of death increased with high baseline LDH, and in patients with ECOG > 0 and M1C metastatic disease.

References:

1. Feng Y, Roy A, Masson E, et al. Clin Cancer Res. 2013;19(14):3977–86.

M-40

Translational Modeling of Regular Human Insulin Pharmacokinetics and Glucose Dynamics in Minipigs

Yanhui Lu[1*], Oskar Alskär[2], Mats O. Magnusson[2], Pavan Vaddady[1], Ester Carballo-Jane[1], Chandni Valiathan[1], Maria C. Kjellsson[2], Carolyn Cho[1], Sandra A.G. Visser[1]

[1]Merck & Co., Inc., Kenilworth, NJ USA; [2]Pharmetheus, Uppsala, Sweden

Objectives: Minipigs are used as an animal model for studying pharmacokinetics/pharmacodynamics (PK/PD) of insulins. A translational minipig PK/PD model for regular human insulin (RHI) is helpful to assess novel insulins in the early development phase. The overall aim of this project is to develop an integrated glucose-insulin model of RHI following intravenous (IV) and subcutaneous (SC) administration for translation from minipigs into humans.
Methods: Single IV or SC doses of RHI were administered in diabetes mellitus type I (T1DM) and non-diabetic minipigs in a dose range of 0.17–1.4 nmol/kg. Pre- and post-dose plasma insulin and glucose concentrations were measured up to 480 min. An integrated glucose-insulin model previously developed for IV RHI in minipigs was used as a starting point [1, 2]. First-, zero-order, and combined first- and zero-order absorption models were evaluated to characterize RHI absorption. A saturable insulin-dependent glucose clearance model based on the human model [3] was implemented, as opposed to the linear function in the previous IV model [2].
Results: A sequential zero- and first-order absorption model described the absorption of SC RHI the best. RHI absorption rate, elimination and bioavailability did not differ between non-diabetic and T1DM minipigs following SC administration. RHI-dependent glucose clearance was higher in non-diabetic than in T1DM minipigs independent of dose administration route. This updated model demonstrated improved predictions of the glucose disposal rate in humans compared to the previous IV model.
Conclusions: This translational integrated glucose-insulin model described insulin pharmacokinetics and glucose dynamics following IV and SC administration of RHI in T1DM and non-diabetic minipigs. The improved translational capability of the model on the insulin-glucose relationship from minipigs into humans will facilitate early phase development of novel insulins.

References:

1. Silber HE, et al. J. Clinical Pharmacol 2007; 47:1159–71.
2. Visser S, et al. PAGE 2015 Abstr 3490.
3. Fancourt, et al. ACOP 2015.

M-41

Population Pharmacokinetic Analysis of Once Daily Formulation of Tacrolimus in Kidney Transplantation Patients

Jangsoo Yoon[1], Su-jin Rhee[1], Seonghae Yoon[1], SoJeong Yi[1], SeungHwan Lee[1], Sang-il Min[2], Jongwon Ha[2], In-Jin Jang[1*]

[1]Department of Clinical Pharmacology and Therapeutics, Seoul National University College of Medicine and Hospital, Seoul, Korea; [2]Department of Surgery, Seoul National University College of Medicine and Hospital, Seoul, Korea

Objectives: Tacrolimus is a calcineurin inhibitor that is used to prevent graft rejection after kidney transplantation [1]. Advagraf®, a prolonged-release tacrolimus formulation, allows once-daily dosing to improve adherence [2]. The aim of this study was to develop a population pharmacokinetic (PK) model for Advagraf® in kidney transplantation patients.
Methods: A total of 272 tacrolimus whole blood concentrations from 25 patients (age 21–66 years, body weight (WT) 41.15–84.90 kg) who had received kidney transplantation in Seoul National University Hospital were analyzed to develop a population PK model using the nonlinear mixed-effects method using NONMEM (Version: 7.3). Subjects received dose-adjusted oral Advagraf® once-daily and blood samples were collected at steady-state. The first-order conditional estimation with interaction estimation method was implemented. The adequacy of model was evaluated using standard goodness-of-fit diagnostics and visual predictive checks.
Results: A two compartment linear PK model, first-order absorption with lag time best described the data. Covariate included in the final model was dose on relative bioavailability (F1). The mean population PK parameters (interindividual variability, CV %) of clearance, central volume of distribution, peripheral volume of distribution, intercompartmental clearance, absoprtion lag time and relative bioavailability were 27 L/h (7.4 %), 358 L (44.3 %), 527 L (0 fixed), 51.9 L/h (0 fixed), 0.443 h (0 fixed) and $((DOSE/10)^{-0.92})$ (21.5 %), respectively.
Conclusions: As the oral dose of Advagraf® increased, the relative bioavailability (F1) was decreased. This result implies that absorption of Advagraf® in kidney transplantation patients might be non-linear and should be considered when physician adjust dose of Advagraf®. The model-fitted parameter estimates may be applied to determine the optimal dosage regimens of Advagraf® in kidney transplantation patients.

References:

1. Ma, M.K., et al. Ren Fail. 35(7): 942–5, 2013
2. Kramer, B.K., et al. Am J Transplant: 10(12):2632–43, 2010

M-42

Mechanistic Population Pharmacokinetics Model of PF-00547659, a Full Human lgG2 anti-MAdCAM Monoclonal Antibody in Ulcerative Colitis Patients

Steven W. Martin[1*], Anne C Heatherington[2], Alaa Ahmad[2], Anasuya Hazra[3], Robert Clare[2], Fabio Cataldi[2] and Rujia Xie[4]

[1]Pharmacometrics Group, Pfizer, Cambridge MA; [2]PharmaTherapeutics Clinical R&D, Pfizer, Cambridge, MA; [3]Clinical Pharmacology, Pfizer, Groton, CT; [4]Pharmacometrics Group, Pfizer, China

Objectives: Characterize the pharmacokinetics (PK) of PF-00547659 in ulcerative colitis (UC) patients and identify clinical relevant covariates.
Methods: One phase 1/2a and 1 phase 2 studies with a total of 363 subjects with 2476 serum concentrations were included in the analysis. The Phase 1/2a study included single or multiple (MD) intravenous (IV) or subcutaneous (SC) dosing every 4 weeks up to 8 weeks with doses ranging from 0.03 to 10 mg/kg. The ongoing phase 2 study utilized MD SC dosing from 7.5 mg to 225 mg. The PK analysis was conducted using the nonlinear mixed-effects modeling.
Results: The PK of PF-00547659 in UC patients was best described by a two compartment model incorporating first-order SC absorption; with elimination combining linear and a nonlinear pathway binding to mucosal addressing cell adhesion molecule (MAdCAM) and subsequent internalization and elimination of the complex (termed target mediated drug disposition, TMDD[ref1]). Covariates identified were baseline body weight (BWT), baseline albumin (BALB), and baseline CRP (BCRP) on linear antibody clearance (CL), and BWT on central compartment volume (V1). For a typical patient (BWT of 73 kg, BALB of 3.9 g/dL and BCRP of 0.52 mg/dL), linear CL was estimated to be 8.43 mL/h (half-life = 21 days) with central and peripheral compartment volumes of 3.34L and 2.2L, respectively. The production, degradation rates (assumed same as complex) of MAdCAM, and Kd were 0.0706 nmol/h, 43.2 mL/h, and 0.396 nmol/L, respectively. TMDD was fully saturated at doses $\geq$75 mg/month.
Conclusions: The pharmacokinetics of PF-00547659 was typical of a monoclonal antibody with TMDD observed at low doses. PF-00547659 remained primarily within the vasculature near its target site. Following SC dosing of 22.5 mg every four weeks, the model predicted an average suppression of >90 % in free MAdCAM in UC patients.

References:

1. S.W.Martin, et al. (2009) AGA Digestive Disease Week, Chicago IL.

M-43

Population Pharmacokinetic Model (PopPK) for Dacomitinib and its Metabolite in Healthy Volunteers (HV) and Patients with Advanced Solid Tumors

Nagdeep Giri[1*], Richard Upton[3], Diane R. Mould[3], Carlo L. Bello[2], Michael A. Amantea[1]

Pfizer, San Diego, CA[1]; New York, NY[2]; Projections Research, Phoenixville, PA[3]

Objectives: Dacomitinib is a small molecule inhibitor of human EGFR family of kinases that is being developed for treatment of non-small cell lung cancer. Objective of this analysis is to develop an integrated and predictive PopPK model for dacomitinib and its metabolite using pooled data from patients and HV, and to identify potential covariates that may be important predictors of variability in dacomitinib disposition and elimination.
Methods: Data from 8 HV and 11 patient studies (n = 129 and 949) was used to develop final models for each of dacomitinib and metabolite. Oral or IV daily doses ranged from 0.5 to 60 mg. Fraction of dacomitinib clearance (CL) going for metabolite formation (FMET) was fixed at 0.3 based on prior data. Effect of food, gastric pH altering agents (PPIs), demographics, liver function, ECOG score, and EGFR/KRAS mutation status upon dacomitinib and metabolite were also examined. R and NONMEM (Ver. VII level 2) packages were used for graphical analyses and model-building.

Results: Final models that best described dacomitinib and metabolite disposition were a 2- and 1-compartment linear model, repectively; a transit compartment was necessary to account for slow oral absorption of dacomitinib. Table 1 provides parameter estimates and covariate effects upon dacomitinib. For dacomitinib, food influenced mean transit time (MTT) and bioavailability (F), CYP2D6 inhibition decreased CL, PPIs increased MTT and decreased F, body weight affected both CL and central volume, and ECOG score decreased CL. Modeling results were consistent with observed results from traditional evaluations for effect of food, PPI and drug interactions.

Table 1 Parameter values for final decormitinib model

Description	Unit	Pop value	se (%)	BSV (ratio)	se (%)	Etabar *p* value	Eta shrinkage (%)
Clearance	L/h	23.7	3.5	0.321	10.9	0.901	20152
Central volume	L	283	14	1.432	15.6	0.154	44.872
Inter-compartment clearance	L/h	101	5.6	0.543	38.6	0.974	58.926
Peripheral volume	L	1630	2.7				
Bioavailability (logit)		3.34	12.8	1.926*	11.1	0.532	46.116
Mean transit time	h	10.2	3.5				
Effect of FOOD on MTT		−0.279	0				
Effect of FOOD on LGT1		2.65	0				
Effect of CYP2D6 on CL		0.262	0				
Effect of PPI on LGT1		1.69	38				
Effect of PPI MTT		0.288	20.3				
Effect of WT on CL		0.632	11.1				
Effect of WT on V1		1.3	26.1				
Effect of ECOG 1 on CL		0.144	28.8				
Effect of ECOG 2 on CL		0.343	13.4				
Effect of ECOG 3 on CL		0.378	36				
Proportional residual error − Volunteers	Ratio	0.261	5.1				
Proportional residual error − Patients	Ratio	0.273	4.5				
Common additive residual error	ng/ml	0.66	21.2				

Conclusions: Predictive performance of final integrated model for dacomitinib and metabolite was found to be satisfactory using Visual Predictive Check plots of concentrations versus time for frequently used doses, and by plots of trough concentrations conditioned on key covariates. The model was therefore considered suitable for simulation of dacomitinib and metabolite exposure in clinical setting.

M-44

Quantitative Approach to Predicting Human Pharmacokinetics of Monoclonal Antibody (DSP-mAbX) from Preclinical Data

Kenta Kadotsuji[1*], Yuta Shibue[1], Jin Shimakura[2], Takao Watanabe[1], Masashi Yabuki[1]

[1]Preclinical Research Laboratories, [2]Research Planning & Intelligence, Sumitomo Dainippon Pharma Co., Ltd

Objectives: The objective of this study was to develop a mechanistic approach to predicting human pharmacokinetics from in vitro data and in vivo non-human primate PK data based on the construct of a target-mediated drug disposition (TMDD) model [1].
Methods: A fully human IgG monoclonal antibody (DSP-mAbX) directed against a membrane-bound target on lymphocytes was evaluated in this study. Free DSP-mAbX concentration in monkey plasma was measured using immunoassay. Free, bound and total antigen on lymphocytes of monkeys were measured using flow cytometry. Mechanistic parameters (kon and koff binding kinetics) were obtained using surface plasmon resonance. A two-compartment TMDD model was implemented to describe the nonlinear PK profiles observed in monkeys. Human PK was predicted using a hybrid approach: allometric scaling of PK parameters such as CL and V, and mechanistic parameters specific for human targets on lymphocytes. NONMEM® VII was used to develop the model. Model performances were evaluated through changes in objective function, goodness-of-fit plots and visual predictive check.
Results: The two-compartment TMDD model described the nonlinear single-dose and multiple-dose PK profiles of DSP-mAbX in cynomolgus monkeys and enabled estimation of antibody elimination, target turnover, and complex elimination such as internalization rate. Parameters were estimated with reasonable precisions, and the TMDD model was translated to human to predict efficacious dose and minimum anticipated biological effect level (MABEL) by incorporating information on mechanistic parameters in human.
Conclusions: The PK of DSP-mAbX, which is especially directed against membrane-bound targets, is greatly affected by the binding and target kinetics. Incorporating target kinetics into a mechanistic PK model to be used for interspecies scaling is a sensible approach for human PK prediction. Further strategies for improving model robustness and predicting human PK are discussed.

References:

1. Mager, D.E. & Jusko, W.J. General pharmacokinetic model for drugs exhibiting target-mediated drug disposition. J Pharmacokinet Pharmacodyn 28, 507–32 (2001).

M-45

Quantitative Assessment of the Exposure- Response Relationships of PF00547659, a Full Human IgG2 anti-MAdCAM Monoclonal Antibody, as Induction Therapy for Ulcerative Colitis in a Phase 2 Study

Anasuya Hazra[1*], Satoshi Shoji[2], Yoshiro Tomono[2], Alaa Ahmad[1], Arnab Mukherjee[1], Steven W. Martin[2], Anne Heatherington[1], Rujia Xie[2], Robert Clare[3], Fabio Cataldi[3]

[1]Clinical Pharmacology, [2]Global Pharmacometrics, [3]PharmaTherapeutics Clinical R&D, Pfizer Inc

Objectives: To characterize exposure–response (ERR) and dose response (DRR) relationship of PF-00547659 (PF) for various clinical efficacy endpoints in ulcerative colitis (UC) to inform Phase 3 dose selection.
Methods: This was a double-blind, randomized, placebo-controlled, parallel, dose-ranging, 12 week induction study in 357 subjects with moderate to severe UC, randomized to receive 3 subcutaneous (SC) doses 7.5, 22.5, 75 and 225 mg PF or placebo (1:1:1:1:1 ratio) at 0, 4 and 8 weeks followed by clinical efficacy measurement at Week 12. Logistic regression E_{max} models were used to link dose or population PK model derived individual PF concentrations (from 341 subjects) (C_{trough}) to WK12 probability of three important efficacy endpoints;

a) clinical remission (CRM), b) endoscopic improvement (EI), and c) clinical response (CRS). Clinical trial simulations (CTS) were performed to assess probability of success at various doses.

Results: Model predicted placebo adjusted median [90 % CI] estimates of efficacy endpoints

Dose (mg)	CRM (%)	EI (%)	CRS (%)
7.5	3.4 [0.4–10.3]	2.5 [0.23–11.6]	3.1 [<0.001–25.5]
22.5	11.3 [5.3–16.4]	14.1 [5.4–21.1]	20.2 [1.1–32.2]
75	12.0 [6.2–17]	16.1 [8.5–22.6]	23.5 [5.3–33.9]
225	12.2 [6.4–17.3]	16.4 [9–23.1]	24.6 [10.5–34.3]

EC_{50} (%RSE) values were 21.1 (147 %), 63.4 (154 %) and 121.5 (305 %) ng/ml, for CRM, EI and CRS, respectively. Baseline Mayo scores, baseline endoscopic subscores, body weight, baseline C-reactive protein and subject's experience with anti-TNF therapy were evaluated as covariates. CTS using parameters from ERR analyses of primary endpoint (CRM) and a potential co-primary endpoint (EI) suggest doses ≥22.5 mg Q4 W would potentially offer distinctive benefit over lower doses, and there is limited benefits of dosing over 75 mg Q4 W.

Conclusions: Characterization of DRR and ERR of PF enabled Phase 3 dose selection. Both DRR and ERR suggested PF induction doses ≥22.5 mg Q4 W may be appropriate to investigate for future confirmatory trials.

M-46

8-Year Disease Progression in Asymptomatic at Risk for Alzheimer Dementia (ARAD) Subjects from ADNI-1

Mahesh N. Samtani*, Nandini Raghavan, Gerald Novak, Vaibhav A. Narayan, Dai Wang, David Baker, Partha Nandy on behalf of ADNI

Janssen R&D, NJ, USA

Objectives: The Preclinical Alzheimer Cognitive Composite (PACC) has been proposed as an end-point to measure cognitive decline in ARAD subjects. PACC decline was explored in 3 observational studies and exhibited amyloid related decline across cohorts except ADNI-1 where trajectories converged at 3-years. This analysis aimed to understand the characteristics of the decline of the PACC in ADNI-1.

Methods: Data were obtained from ADNI database on April 29th, 2015. The observed mean PACC decline was assessed in ARAD amyloid positive vs negative subjects. A portion (77/122: 63 %) of these subjects volunteered to enroll in an extension phase beyond 3-years. PACC progression was assessed up to 8-years in extension subjects and additional analysis included comparison of extension and non-extension subjects; and analysis of sub-scale scores to understand the behavior of the composite.

Results: Amyloid negative subjects declined minimally in PACC over 8 years, while decline in amyloid positive subjects began after 3 years (Fig. 1). Over 3 years extension subjects declined less than non-extension subjects. Learning effects were seen for wordlist memory for 1 year and paragraph-recall for 3 years. The learning effect in paragraph-recall was probably related to multiple exposure of the same story. The executive function subscale exhibited high variability and relatively small longitudinal change. Finally, subjects correctly answered most test items on MMSE longitudinally and exhibited ceiling effects.

Conclusions: In ADNI-1, PACC exhibited ceiling and learning effects and may require longer follow-up in an intervention trial, however a PACC composed of alternative items may behave differently. The learning effect may be mitigated by using alternate equivalent forms of paragraph-recall, while the highly-variable subscales get down-weighted by their variability at baseline. This analysis is limited by small sample size and may represent atypically slower PACC progression since it is based on extension subjects who had less initial decline than non-extension subjects.

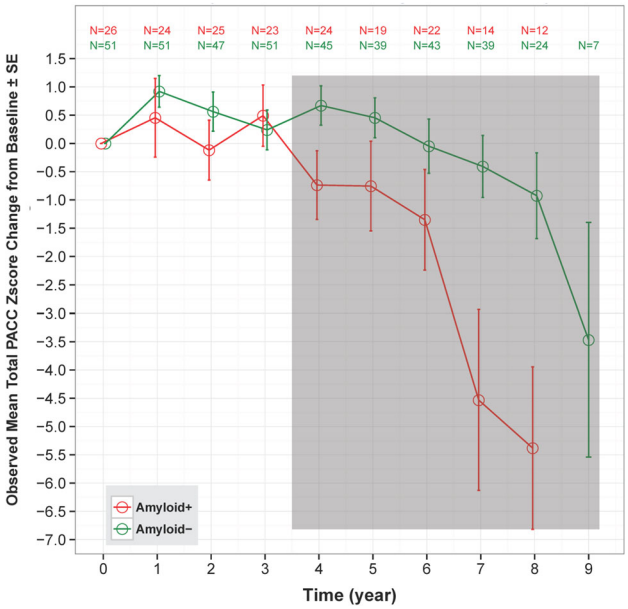

Fig. 1 PACC Total Z-score in ADNI-1 Extension Subjects: PACC Change from Baseline as a Function of Baseline Amyloid Status. Grey shaded area represents the extension phase on the study

M-47

Pharmacokinetic/pharmacodynamic (PK/PD) Characteristics of Veliparib with and without Temozolomide in Patients with Hematological Malignancies

Renu Singh[1*], Mathangi Gopalakrishnan[1], Brian F. Kiesel[2], Jacqueline M. Greer[3], Judith E. Karp[3], Ivana Gojo[3], Jogarao Gobburu[1], Michelle A. Rudek[3], Jan H. Beumer[2]

[1]University of Maryland, Baltimore, MD; [2]University of Pittsburgh Cancer Institute, Pittsburgh, PA; [3]The Kimmel Comprehensive Cancer Center at Johns Hopkins, Baltimore, MD

Objectives: Veliparib is an oral inhibitor of poly (ADP-ribose) (PAR) polymerase enzyme that is currently in development for the treatment of non-hematologic and hematologic malignancies. The objectives of

this analysis were a) to quantitatively describe the PK/PD characteristics of veliparib in patients with hematologic malignancies b) assess the sources of between subject variability and c) to explore the effect of temozolomide co-administration on PK/PD of veliparib.
Methods: Population pharmacokinetic analysis was performed using Phoenix® NLME with rich PK data from 37 subjects after oral administration of veliparib from a Phase I study with and without temozolomide. Final PK model with covariates was validated by visual and quantitative predictive checks. Preliminary PD analysis of PAR inhibition relative from baseline was performed to assess dose-efficacy relationship.
Results: A one-compartment model with first-order elimination and a sequential first order-zero order absorption model adequately described veliparib PK. Population mean apparent clearance (CL/F) and volume of distribution (V_d/F) were 14 L/h and 162 L, respectively. Veliparib clearance did not change after temozolomide administration. CLCR and body weight were found to be clinically significant covariates for veliparib disposition. PD analysis shows >60 % inhibition of PAR levels in peripheral blood mononuclear cells (PBMCs) at doses evaluated when compared to baseline values (Figure 1) and no statistically significant dose-dependent difference was observed.

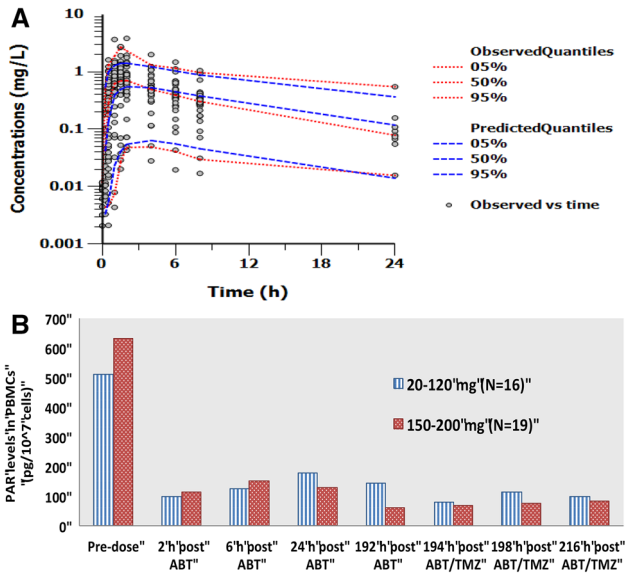

Fig. 1 **a** Visual predictive check for Day 1 data for the final PK model. *Circles* represent observations, and lines represent the 5th, 50th, and 95th percentiles of observed (*red*) and simulated (*blue*) data. **b** Mean PAR levels before and after veliparib (ABT) administration and with temozolomide (TMZ) addition at 20–120 mg (*blue*) and 150–200 mg (*red*) dose levels

Conclusions: The CL/F and V_d/F estimates of veliparib were similar to those reported in literature for non-hematological malignancies [1]. Dosage adjustment of veliparib may not be required when temozolomide is co-administered. Statistically significant inhibition of PAR levels was observed after administration of veliparib at all dose levels. The developed population PK model will be utilized for exposure-efficacy (PAR inhibition) and safety (neutrophil count) analysis of veliparib.

Reference:

1. Salem AH, et al. Clin Pharmacokinet. 2014, 53:479–88.

M-48

Quantitative Systems Modeling Provides Biological Plausibility for Potential Mechanisms of Tolvaptan-Induced Hepatotoxicity

Woodhead JL[1*], Brock W[2], Roth S[2], Brouwer KLR[3], Siler SQ[1], Church RC[1], Watkins PB[1], Shoaf SE[2], Howell BA[1], Shoda LKM[1]

[1]The Hamner Institutes for Health Sciences, RTP, NC; [2]Otsuka PDC, Rockville, MD; [3]University of North Carolina Eshelman School of Pharmacy, Chapel Hill, NC

Objectives: Tolvaptan and a major metabolite have been shown to inhibit bile acid transporters and mitochondrial respiration. We used systems modeling to test whether these mechanisms could account for hepatotoxicity observed in a clinical trial for autosomal-dominant polycystic kidney disease (ADPKD) but not observed in clinical trials for other tolvaptan indications.
Methods: Tolvaptan and metabolite pharmacokinetics, transporter inhibition constants, and quantitative assessments of mitochondrial respiration inhibition were entered into DILIsym®, a quantitative systems model of drug-induced liver injury [1, 2]. Toxicity was modeled in the DILIsym® baseline patient and in a simulated ADPKD patient population.
Results: No toxicity was predicted for a non-ADPKD population given a 60 mg dose of tolvaptan for 60 days. Clinically significant serum ALT elevations were predicted in 7.9 % of the simulated population given the highest dose used for ADPKD trials (120 mg/day for 180 days), similar to ADPKD trial observation (4.2 %). Simulations suggested that inhibition of both bile acid transporters and mitochondrial respiration are necessary to account for the observed hepatotoxicity. The most significant patient-specific risk factors predicted by DILIsym® include basal ETC flux, mitochondrial respiratory reserve capacity, and BSEP function (Table 1); exposure-related characteristics were less correlated (as measured by R-value) with susceptibility. DILIsym® has therefore suggested hypotheses for genetic or non-genetic biomarkers that may assist in risk management of tolvaptan hepatotoxicity.
Conclusion: DILIsym® recapitulated the observed hepatotoxicity by combining inhibition of bile acid transporters and mitochondrial respiration. Although other mechanisms may contribute, the identification of patient-specific risk factors suggests predictive biomarkers that can now be tested in archived urine and plasma samples.

Table 1 List of correlations (R-value) between hepatotoxicity endpoints and population-variable DILIsym® parameters

Parameter	Max ALT		Min ATP	
	P-value	R-value	P-value	R-value
Basal ETC flux	<0.0001	−0.323	<0.0001	0.373
Respiratory reserve scaling factor	<0.0001	−0.265	<0.0001	0.296
CDCA-amide canalicular Vmax	<0.0001	−0.511	<0.0001	0.549
Metabolite generation Vmax	0.0033	−0.194	0.0068	0.178
CDCA amidation Vmax	0.008	−0.175	0.0226	0.151

References:

1. Woodhead, J. L. et al. CPT Pharmacomet. Syst. Pharmacol. 3, e123 (2014).
2. Yang, Y. et al. Pharm Res. 32(6):1975–92 (2015).

M-49

Application of Complementary Statistical and Modeling Analyses to Identify Predictors of Sustained Virologic Response in Patients with Chronic Hepatitis C

April M. Barbour[1*], Khamir Mehta[1], Matthew L. Rizk[1], Hwa-ping Feng[1], Larissa Wenning[1], Barbara Haber[1]

[1]Merck & Co., Inc., Kenilworth, NJ

Objective: Identify predictors of sustained virologic response 12 weeks post-treatment (SVR12) in a phase II study in chronic HCV patients receiving grazoprevir/elbasvir (100 mg/50 mg) with sofosbuvir (400 mg) QD for various treatment durations, (i.e., 4, 6, 8, or 12 weeks), and quantify their impact on SVR12.
Methods: Two independent but complementary analyses, Random Forrest Classification Analysis (RFCA) using the package randomForest in Rv3.1.0 and logistic regression (LR) implemented in NONMEMv7.1.2, were used. A total of 27 factors, including patient specific covariates related to disease (e.g. baseline viral load (BVL)), general demographics (e.g. weight), plasma concentrations of each drug, and treatment duration were explored. Explored predictors for the LR model were selected based on initial data exploration and results from the RFCA. A preliminary population pharmacokinetic model was used to simulate elbasvir concentrations and compare the predicted probability of SVR12 between a 50 mg and 100 mg QD dose (in combination with 100 mg grazoprevir and 400 mg sofosbuvir).
Results: Duration of treatment followed by elbasvir concentrations were the most important predictors of SVR12 from RFCA and the only significant predictors during LR. While RFCA revealed BVL as an important predictor (although not as important as treatment duration), this was not confirmed with LR due to a coincidental study imbalance such that subjects with the least duration of treatment also had higher BVL. Simulations demonstrated 50 mg QD for 12 weeks achieves near maximal response and increasing the dose to 100 mg does not increase the predicted probability of SVR12, with 90 % CI of 98–100 % for both doses.
Conclusions: The combined approaches gave novel insights into the data and robustly identified predictors of SVR12, i.e. treatment duration and elbasvir concentrations. Through the unique advantages of each approach the synergistic benefit was highlighted as RFCA had a low computational time to evaluate a large number of potential predictors, including confounded variables, while LR had predictive ability.

M-50

The Robust Response of a Physiological Model of Granulopoiesis to PK Variability

Craig, M.[1,2*], González Sales, M.[1,3], Li, J.[1], Nekka, F.[1,4]

[1]Faculté de pharmacie, Université de Montréal, [2]Centre for Applied Mathematics in Biosciences and Medicine, [3]inVentiv Health Clinics, [4]NSERC Industrial Chair in Pharmacometrics, jointly supported by Novartis, Pfzier, and inVentiv Health Clinics

Objectives: The increasing use of mechanistic models in pharmacometrics raises numerous questions about their sensitivity to pharmacokinetic (PK) variability and the reliability of their predictions when considering patient populations as opposed to individual patients. We investigated the robustness of the predictions of a physiological model for neutrophil development with regards to PK variability.
Methods: We have previously determined optimal filgrastim dosing during 14-day cyclical chemotherapy treatment using our physiological model of granulopoiesis. This model was constructed using first principles and parameters were estimated from the literature. To investigate the sensitivity of the model's predictions, we incorporated previously published PopPK (both interindividual and interoccasion variability—IOV) models for both PM00104 and filgrastim. A variety of variability scenarios were simulated for respective cohorts of 500 in silico patients and several statistical measures were performed with reference to three crucial clinical endpoints, namely the time to the neutrophil nadir, the nadir value, and the area under the concentration-effect curve.
Results: In all five test scenarios, no statistically significant deviations from the reference case were found using three different statistical measures. The inclusion of IOV did not impact the predictions over three successive chemotherapy cycles.
Conclusions: Our results suggest that physiological models inherently incorporate variability by means of their rational construction. Accordingly, mechanistic models demonstrate robust predictions, which situates their utility in systems pharmacology and lends credence to efforts incorporating physiological accuracy into mathematical models for use in pharmacometrics.

References:

1. Craig, M., González Sales, M., Li, J., Nekka, F. (2015-under review). European Journal of Clinical Pharmacology, EJCL-S-15-00241.
2. Craig, M., Humphries, A.R., Bélair, J., Li, J., Nekka, F., Mackey, M.C. (2015-under review). Neutrophil dynamics during concurrent chemotherapy and G-CSF administration: Mathematical modelling guides dose optimisation to minimise neutropenia. Journal of Theoretical Biology, JTB-D-14-00842R2.

M-51

Mechanistic Model based Assessment of PK/PD Critical Success Factors (CSF) for Next-Generation Ultra-fast Acting Insulins

Karen Schneck*, Xiaosu Ma, Jennifer Leohr, Tong Shen and Jenny Chien

Eli Lilly and Company, Indianapolis, IN, USA

Objectives: Exogenously administered insulins aim to mimic the rapid onset of endogenous insulin response to hyperglycemia following meals. Subcutaneous fast-acting insulins are delayed by absorption-rate limited kinetics. To support the definition of "faster onset", mechanistic PK/PD model-based assessments were conducted to identify the CSF for faster onset of insulin action.
Methods: A population PK model with physiological components (NONMEM 7.3) and a mechanistic model of glucose-insulin dynamics were developed based on published fast-acting meal-time insulin data. Model components were introduced to allow simulations of hypothetical "faster acting" insulins following different mechanisms of subcutaneous absorption. Simulations and sensitivity analyses were implemented in R and Physiolab®. A comprehensive list of PK and glucodynamic parameters were derived from the simulated profiles to evaluate a critical success factor of ">20 % faster". Time related parameters (e.g., Tmax, Cmax, time to fraction of Tmax) and various fractional area-under-the-concentration (AUC) metrics were examined.
Results: Insulin plasma data were described by a two-compartment model. After subcutaneous administration, zero-order absorption commenced immediately and lasted for ~0.3 h, followed by first-

order absorption of the remaining fraction of dose (>90 %). A relationship between body weight and volume of distribution was the only significant covariate detected. To explore hypothetical ultra-rapid insulins, the fraction and duration parameters were allowed to vary systematically based on the mechanism of action. Simulations supported the selection of time to 50 % of Tmax and partial AUC in the first 15 to 30 min to represent the faster absorption.
The PD model-based simulation following meals with varying amounts of carbohydrate showed that the glucose AUC in the first 2 h was a sensitive and relevant parameter to represent "faster onset" of action for comparative evaluation.
Conclusions: The PK/PD models described the time-action profiles of fast-acting insulin well. Simulations provided sample size recommendations to meet CSF for next generation fast-acting insulins with 20 to 50 % faster absorption and onset of action.

M-52

Pooled Population Pharmacokinetic and Immunogenicity Analysis of Pembrolizumab Using Data from KEYNOTE-001, KEYNOTE-002 and KEYNOTE-006

Malidi Ahamadi[1]*, Claire Li[1], Tomoko Freshwater[1], Marianne van Vugt[2], Eric Mangin[1], Rik de Greef[2], Julie Stone[1], Anna Kondic[1]

[1]Merck Research Laboratory, Merck and Co., USA; [2]Quantitative solutions, Holland

Objectives: Pembrolizumab is a potent antibody against the cellular immune 'switch' programmed death receptor 1 (PD-1) that has shown robust antitumor activity in patients with advanced solid tumors. We characterized the pharmacokinetic (PK) properties of pembrolizumab and quantified the effect of intrinsic and extrinsic factors on exposure. To investigate the immunogenicity potential of pembrolizumab, the development of antidrug antibodies (ADA) response on efficacy or safety was established.
Methods: Pooled data from KEYNOTE-001 (NCT01295827), KEYNOTE-002 (NCT01704287) and KEENOTE-006 were used to characterize the pembrolizumab serum concentrations over time in patients with advanced or metastatic melanoma and non-small cell lung carcinoma. The relationships between PK parameters and various baseline covariates were examined. Simulations were performed to evaluate the magnitude of the exposure effects of any covariates included in the model in order to assess their clinical relevance.
Results: The pharmacokinetics of pembrolizumab in the 1 to 10 mg/kg dose range was described by a two-compartment pop-PK model with linear clearance from the central compartment. The PK profile of pembrolizumab indicated a low clearance (~ 0.2 L/day), limited volume of distribution (~7 L) and low variability (15–30 %), consistent with other monoclonal antibodies. The effect of age, sex, geographic location, baseline ECOG PS, eGFR, AST, bilirubin, albumin, glucocorticoid coadministration, tumor type and burden, and prior ipilimumab on pembrolizumab exposure is limited, as alterations of 20 % or less are predicted by the PopPK model. Thus, these marginal effects on exposure were clinically insignificant on PK properties of pembrolizumab. Of 392 patients evaluable for ADA, 1 (<1 %) developed confirmed treatment-emergent ADA with no impact on efficacy or safety.
Conclusions: There was no clinically meaningful effect of baseline clinical factors on pembrolizumab exposure. Pembrolizumab has limited potential to elicit the formation of ADA. These results support the use of the approved pembrolizumab dose of 2 mg/kg Q3 W.

M-53

Repolarisation Rate: An Integrative Biomarker of cCardiac Action Potential Repolarisation

Ben G Small[1,*], David Hollinshead[1], Masoud Jamei[1], Sebastian Polak[1,2]

[1]Simcyp (a Certara Company); [2]Unit of Pharmacoepidemiology and Pharmacoeconomics, Faculty of Pharmacy, Jagiellonian University Medical College, Poland

Objectives: The pro-arrythmic potential of NCE's continues to be an issue in drug development [1]. The aim was a preliminary evaluation of the utility of a novel biomarker (ReRa) summarising and discriminating the slope (ΔmV/Δms) between indices of phase II (APD_{50}) and phase III (APD_{90}) cardiac action potential repolarisation.
Methods: Simulation of an epoch (10,000 ms, sampled every 1 ms) of action potentials in both placebo and drug exposed conditions from a single female subject (34 years) was undertaken using the O'Hara-Rudy model [2] in the Cardiac Safety Simulator (CSS v2.0, Simcyp). Input parameters included in vitro measurements of the IC_{50} and n_H (μM) of 6 compounds (Figure) at hERG, Nav1.5, Cav1.2, I_{Ks} and I_{to} and the effective therapeutic plasma concentration (EPTC; μM) of these same compounds [3]. Extraction of the membrane potentials (mV) at which 50 ($V_{m,50}$) and 90 ($V_{m,90}$) % repolarisation occurred and the corresponding APD_x values allowed calculation of the slope between APD_{50} and APD_{90} and hence repolarisation rate (ReRa).

$$Repolarisation\ Rate(mV/ms) = \frac{V_{m,90} - V_{m,50}}{\Delta(APD_{90} - APD_{50})}$$

Results: ReRa separated bepridil (range −0.92 to −0.87) from dl-sotalol (−1.04 to −0.98), amiodarone (−1.06 to −1.01), astemizole (−1.07 to −1.02) and dofetilide (−1.07 to −1.02) (Figure). Additional ion channel affinities of bepridil beyond those specified for the other compounds shown here maybe an explantory variable.

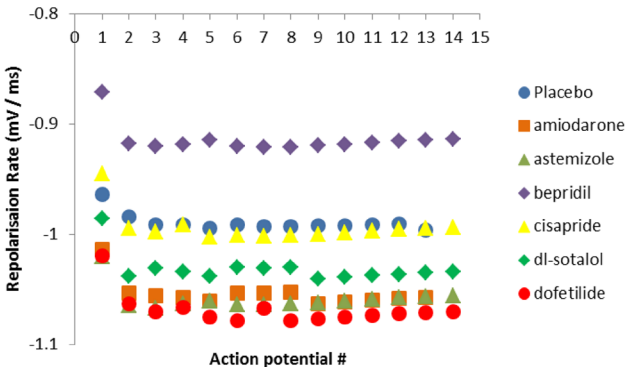

Fig. 1 ReRa discriminates between compounds that have different and known propensities to block physiological currents underlying conduction and repolarisation of the cardiac action potential

Conclusions: Future work will focus on extending this to other compound types and expand this method to understand whether this composite measure can capture inter-subject population variability. This biomarker may have utility as an 'early' indicator of pro-arrythmic potential.

References:

1. Polak S et al., (2015). AAPS J. doi:10.1208/s12248-015-9773-1.
2. O'Hara T et al., (2011). PLoS Comput Biol 7 (5):e1002061.
3. Okada J-i et al., (2015). Science Advances 1 (4).

M-54

Overestimation of Shape Parameter of Weibull Base Hazard in the Modeling of Time-To-Event Data

Sung Min Park, Seunghoon Han, Dong-Seok Yim*

Department of Clinical Pharmacology and Therapeutics, Seoul St. Mary's Hospital; PIPET (Pharmacometrics Institute for Practical Education and Training), College of Medicine, The Catholic University of Korea, Seoul, Korea

Objectives: Overestimation of maximum likelihood estimator (MLE) of the shape parameter in the analysis of time-varying hazard (Weibull) model is already reported for heavily-censored survival data [1]. Because the biased MLE has not been properly addressed in the biomedical modeling field, we performed a simulation study to explore its implication. Shape parameter overestimation initially found in the analysis of time to gastric re-bleeding data collected from emergency room motivated this simulation study.
Methods: Survival datasets with shape parameters from 0.2 to 0.8 were simulated (100 subjects per dataset) using cumulative hazard function in the MS-Excel. Weibull shape parameters and 95 % prediction intervals were estimated for the simulated datasets using R, SAS and NONMEM.
Results: MLEs of the shape parameter and its true values used for simulation (in parenthesis) were 0.5 (0.2), 0.78 (0.6), 0.94 (0.8), and 1.14 (1.0). Discrepancy between Kaplan–Meier plots of simulated survival data and 95 % prediction intervals calculated using the MLEs was obvious at the lowest simulated shape parameter (0.5). There was no difference among MLEs from R, SAS and NONMEM.
Conclusions: The MLE of the shape parameter when its true value was 0.5 or less was not appropriate to model time-to-event data with the Weibull-shpaped hazard. Currently, this bias does not seem to be avoidable by any popular software packages used among pharmacometricians.

References:

1. Mackisack, M. S. and Stillman, R. H. (1996). A cautionary tale about Weibull analysis. IEEE Trans. Reliability, 45, 244–248.

M-55

inVentR: The Pharmacometrician's Best Friend

Olivier Barrière[1*], Mario González-Sales[1,2], Pierre-Olivier Tremblay[1], Fahima Nekka[2], Mario Tanguay[1,2]

[1]Inventiv Health Clinical, Canada; [2]Université de Montréal, Canada

Objective: The pharmacometrician workflow has routine steps: (1) build the dataset, (2) explore the data, (3) model the data, (4) validate the model and (5) communicate the findings. The automation of these steps saves time, money, reduces errors and increases reproducibility. The objective of this work was to create a flexible and user-friendly tool to help the pharmacometrician in his daily tasks.
Methods: The inVentR package consists of a series of functions developed in R [1], for data assembling, input and output visualization, and model development. An important focus has been put on user friendliness, documentation, training examples, and extensibility.
Results: Using a specific function, NONMEM® formatted datasets can be generated from basic tabulated files. This function can handle PK and PD data, multiple analytes and responses, and also different types of administration routes including: bolus, infusion, and first and/or zero order absorption processes. An exhaustive list of functions is made available for plotting purposes. These functions use a friendly syntax with a high level of abstraction that allows vectorized input, such as multiple thetas or covariates, and return *ggplot* objects. This way, we take advantage of the modularity of *ggplot* to allow different layers to be combined or the plot to be faceted later. Moreover, there are specific functions dedicated to facilitating the modeling process and to increase reproducibility. These functions can, among others, provide reasonable initial estimates, summarize model parameters, duplicate a model updating the value of the parameters, and run NONMEM® from R. The inVentR package can be used to easily generate professional reports and informative outputs.
Conclusions: The inVentR package is a very flexible, powerful and efficient tool that helps the pharmacometrician through the complex model building process. inVentR is available as an open source package from the Comprehensive R Archive Network (CRAN).
A preliminary version of inVentR has been previously presented at PAGE, Hersonissos, Crete, 2–5 June 2015.

References:

1. R, http://cran.r-project.org.

M-56

Semi-Mechanistic Model to Predict In-Hospital Natural Weight Changes in Term Neonates

Mélanie Wilbaux[1*], Severin Kasser[2], Sven Wellmann[2], Chiara De Angelis[3], Hanna Rickenbacher[2], Noemi Klarer[2], Johannes N. Van Den Anker[1,4], Marc Pfister[1,5]

[1]Department of Paediatric Clinical Pharmacology, Paediatric Pharmacology and Pharmacometrics Research Center, University Children's Hospital Basel (UKBB), Basel, Switzerland.[2]Division of Neonatology, UKBB, Basel, Switzerland.[3] Department of Pediatrics, San Gerardo Hospital, Monza, Italy.[4]Division of Pediatric Clinical Pharmacology, Children's National Health System, Washington, DC, USA.[5]Quantitative Solutions LP, Menlo Park, CA, USA

Objectives: The magnitude of physiological weight loss within the first days of life varies strongly among newborns and can reach high amounts resulting in serious long term complications. The objectives of this study were to develop a semi-mechanistic model to characterize natural weight changes during the first week of life and to quantify effects of key covariates on model parameters.
Methods: Longitudinal weight data and individual characteristics from 1335 healthy term breast-feeding neonates up to 10 days of life were available. A semi-mechanistic model was developed to characterize weight changes during these first days of life. A population analysis was performed with NONMEM7.3. Model selection was based on statistical criteria, goodness-of-fit plots and simulations. Covariate testing was performed utilizing a standard stepwise forward–backward covariate model building approach (SCM).
Results: Weight changes by time were described as a balance between weight gain rate (KIN) and weight loss rate (KOUT); Fig. 1. KIN was modeled as an exponential function of time. KOUT was modeled with a saturable function to describe the initial loss of fluid followed by an exponential time-dependent increase. Gestational age had a positive effect on birth weight (WT0) and KIN. Gender was associated with WT0, with higher values in males. According to goodness-of-fit plots, weight changes were properly fitted. Visual predictive check demonstrated good predictive performance of the model; Fig. 1.

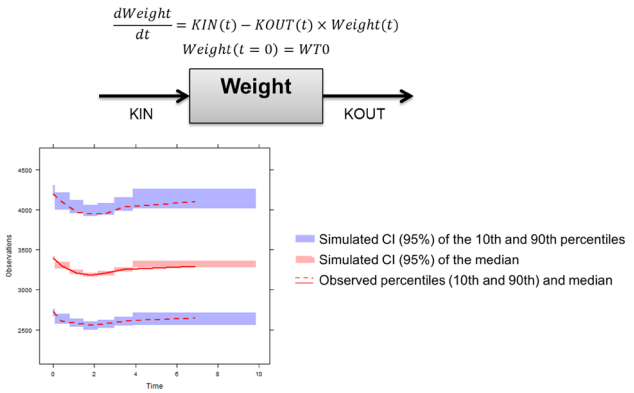

Fig. 1 Semi-mechanistic model

Conclusions: We provide the first model describing the pattern of physiological weight changes in healthy breastfed neonates in the first days of life. Such a model could be a useful tool for clinicians to early detect neonates at risk for high amount of weight loss and consecutive morbidities.

M-57

Leveraging Longitudinal Tumor Data for Prediction of Overall Survival from I-O therapy: A Proof of Concept with Quantitative Models and External Validation

Satyendra Suryawanshi[1*], CJ Godfrey[2], Amit Roy[1], Katy Simonsen[1], Jonathan French[2], Manish Gupta[1]

[1]Bristol-Myers Squibb, Princeton, USA; [2]Metrum Research Group, CT, USA

Objective: To identify and validate a summary measure of tumor-response (TM) that is predictive of clinical efficacy in patients with solid tumors treated with ipilimumab (IPI).
Methods: The estimation dataset included all available overall survival (OS) and longitudinal tumor data from 351 IPI treated advanced melanoma patients from 3 Phase 2 studies (CA184007, 008 and 022). The validation dataset included similar data from 395 IPI treated advanced melanoma patients from Phase 3 study (MDX01020). Previously-reported tumor growth dynamic model was used to derive following TMs for individual patients: Maximum predicted tumor shrinkage (TS_{max}), predicted tumor response at week 16 and week 8 (TS_{wk16} and TS_{wk8}), Tumor growth rate (TGR) and time to tumor growth (TTG) [1]. Each TM was tested as predictor of OS by a Cox Proportional Hazard model, after accounting for the effect of known prognostic factors. Cross validation and bootstrap-based VPC were performed to evaluate model performance, and determine order of TMs as a predictor of OS. External validation was performed to evaluate discrimination and calibration ability of final OS models for survival probability in different risk group based on weighted sum of prognostic variables.
Results: Individual tumor response data was best described using mono-exponential shrinkage and linear growth rate. TMs were incorporated as nonlinear predictors of log hazard for OS. TS_{max}, TS_{wk16} and TS_{wk8} were most favourable predictors of survival based on cross validation and VPC. TGR and TTG did not demonstrate satisfactory performance. Final OS models provided good discrimination between risk groups in new dataset when PIs were constrained to similar range as estimation data. Final OS models tended to over predict survival probability to a modest extent in the validation dataset.
Conclusions: This analysis provided robust evaluation of tumor response metrics as predictors of survival in patients receiving IPI I-O therapy.

References:

1. Feng Y et al., ASCO, 2014, Chicago, IL.

M-58

Characterization of the Pharmacokinetics and Exposure–Response Relationship for Nivolumab in Patients with Previously Treated or Untreated Advanced Melanoma

Gaurav Bajaj*, Manish Gupta, Yan Feng, Paul Statkevich, Amit Roy

Bristol-Myers Squibb, Princeton, NJ, USA

Background: Nivolumab is a fully human immunoglobulin-G4 (IgG4) monoclonal antibody (mAb) that selectively binds to programmed death-1 (PD-1) membrane receptor, to promote antitumor immune responses. Nivolumab, 3 mg/kg every 2-weeks (Q2W), is approved for treatment in patients with advanced melanoma who progressed post anti-CTLA-4 (aCTLA4) therapy. The purpose of this analysis is to assess relationship between nivolumab exposure and overall survival (OS) in both previously treated (PT) and untreated (UT) advanced melanoma (MEL) patients, after accounting for the potential effect of other covariates, to support the dose recommendation in both PT/UT MEL patients.
Methods: Nivolumab pharmacokinetics (PK) was characterized by a linear 2-compartment population PK (PPK) model with serum concentration data from 1087 patients with solid tumors. The exposure–response (E-R) analysis relating PPK model derived Cavgss to OS in PT/UT MEL patients (N = 399) was conducted by a Cox Proportional-Hazards model. The effect of covariates: prior-treatment, prior-aCTLA-4 treatment, sex, ECOG status, baseline body-weight (BBW), nivolumab clearance (CL), age, week-8 tumor-shrinkage (W8TS), tumor size, baseline lactate dehydrogenase (BLDH), were evaluated. M-stage, PD-L1, and BRAF-mutant status were also tested by sensitivity analyses. E-R model of OS was evaluated by visual predictive check comparing the 90 % model-predicted cumulative time-to-event distributions with the corresponding distribution determined by non-parametric Kaplan–Meier analysis.
Results: Nivolumab Cavgss produced by 1–10 mg/kg Q2 W was not a significant predictor of OS in PT/UT MEL patients after accounting for the potential effect of other covariates. The predictor variables with significant effect on OS in the full model were W8TS, CL, BLDH, BBW and age. BLDH and W8TS were the only significant predictors in sensitivity analyses when M-stage, BRAF-mutation, and PD-L1 status were included in the model.
Conclusion: The efficacy of nivolumab is similar over the range of exposure produced by 1–10 mg/kg Q2 W in patients with PT/UT MEL patients.

M-59

Comparison of Different Methods for Predicting Pharmacokinetics of Monoclonal Antibodies in Human

Renu Singh (Dhanikula)[1*], Maria Moreno[2] and Danica Stanimirovic[2]

[1]National Research Council of Canada, 6100 Royalmount Avenue, Montréal QC Canada H4P 2R2; [2]National Research Council of Canada, 1200 Montreal Road, Ottawa, Ontario K1A 0R6

Objectives: Prediction of human pharmacokinetics from pre-clinical species is a founding step in first -in-human (FIH) dose selection. Despite of several advances in understanding mAbs pharmacokinetics, reliable method for prediction of FIH dose remains to be established. This analysis compares different methods for predicting FIH dose for mAbs exhibiting non-linear pharmacokinetics in cynomologus monkeys.
Methods: Data of 5 mAbs exhibiting non-linear pharmacokinetics was used for this purpose. Three methods were evaluated for predicting human pharmacokinetic profile and FIH. The first method was based on allometric scaling of cynomolgus monkey pharmacokinetic data to estimate human parameters followed by simulation of human profile using two compartment model with a parallel linear and non-linear elimination from the central compartment. The second method was based on allometric scaling of cynomolgus monkey pharmacokinetic data to estimate human parameters followed by minimal physiologically-based pharmacokinetic (mPBPK) model to determine human pharmacokinetic profile. The third method used species time-in variant method to predict human pharmacokinetic profile followed by a two-compartment pharmacokinetic model with parallel linear and non-linear elimination from central compartment for simulations.
Results: Predictability of human peak serum concentration (Cmax) and area under serum concentration–time curve (AUC) for mAbs was concentration dependent. The predictive performance of all methods was found to be best at the target saturating concentrations, an increased difference between observed and predicted exposure was observed at low doses. However, an improvement in predictability of human exposure was seen with mPBPK modelling.
Conclusions: Allometric scaling in combination with mPBPK modelling as well as species time-in variant method predicted the human exposure better than allometric scaling alone. Additional evaluation with larger dataset of mAbs is ongoing and is considered imperative for understanding which method will improve certainty in prediction of human pharmacokinetic profile at low doses.

M-60

PKPD Modeling of Vilazodone (VLZ) in Adult Patients with Generalized Anxiety Disorder (GAD)

Tatiana Khariton[1], E Niclas Jonsson[2], Martin Bergstrand[2], Timothy J Carrothers[1*], Parviz Ghahramani[1]

[1]Forest Research Institute, Inc., an affiliate of Actavis, Inc., Jersey City, NJ; [2]Pharmetheus, Uppsala, Sweden

Objectives: To characterize the relationship between VLZ exposure, efficacy (Hamilton Anxiety Rating Scale total score [HAM-A]), and safety (changes in sexual functioning questionnaire total score [CSFQ])
Methods: The analysis was based on the data from three double-blind placebo-controlled Phase 3 studies in adult GAD patients. The data included patients from placebo and VLZ treatment arms (20 and 40 mg/day). A previously developed population PK model was used to predict individual exposure (AUC) for each patient. Non-linear mixed-effects models were developed to characterize the relationship between individually predicted exposure and the longitudinal placebo and vilazodone treatment response for HAM-A and CSFQ scores. Linear and Emax exposure–response relationships were investigated for both; covariate-parameter relationships were also explored. The dropout model was developed to improve the model selection and simulation based diagnostics.
Results: The final PKPD model for HAM-A was a linear model; it predicted higher reduction in HAM-A scores with higher VLZ-exposures (AUCss). The 20 and 40 mg/day treatment arms were predicted to result in a 0.91 and 1.48 point reduction in HAM-A score from placebo at day 56, respectively. The probability of dropout was developed iteratively and was found to be best modeled as a function of HAM-A score and treatment group; it was incorporated into simulation-based diagnostics for HAM-A and CSFQ scores. The CSFQ score was best explained by a step model, i.e. the VLZ-effect was higher compared to placebo (1.96-points for males and 0.97-points for females), independent of VLZ dose.
Conclusions: These data suggest a correlation between VLZ-exposures and changes in CSFQ and HAM-A scores; however, while the reductions in HAM-A scores (i.e., improvement in GAD symptoms) with higher VLZ-exposures were deemed to be clinically meaningful, the increase in CSFQ scores (i.e., worsening of the sexual function) for patients on VLZ treatment was not clinically meaningful and did not increase any further with higher exposure.

M-61

Characterizing Exposure–Response (E-R) Relationship of Safety for Nivolumab in Combination with Ipilimumab in Patients with Previously Untreated Advanced Melanoma

Xiaoning Wang*, Yan Feng, Paul Statkevich, and Amit Roy

Bristol-Myers Squibb, Princeton, NJ, USA

Objectives: Several immune-checkpoint inhibitors that modulate different pathways are approved as anti-cancer therapy including nivolumab and ipilimumab. In addition, nivolumab in combination with ipilimumab is currently being developed for the treatment of previously untreated advanced melanoma patients. The presented E-R analysis for safety was conducted to support justification of such combination dose regimen recommended for this patient population.
Methods: The analysis used data from multiple clinical studies in subjects with advanced melanoma and treated with monotherapies of both nivolumab (N = 718) and ipilimumab (N = 351) as well as the combination (N = 474). The relationship between time-averaged concentration at the 1st dosing interval (Cavg1) and adverse events leading to discontinuation or death (AE-DC/D) was characterized using a Cox proportional hazards (CPH) model. The model included appropriate functional forms of nivolumab and ipilimumab exposure effects on the hazard of AE-DC/D, as well as covariate effects of interest.
Results: There were 361 events of AE-DC/D, 7 of which were AEs leading to death. The risk of AE-DC/D increased with increasing Cavg1 of nivolumab and ipilimumab and both effects were statistically significant (hazard ratio 1.06 and 1.12, 95 % CI 1.04–1.08 and 1.10–1.14, for every 2.72-fold increase of nivolumab and ipilimumab Cavg1, respectively). There was no statistically significant interaction between the two exposure effects. Covariate analysis (Figure 1) showed that the hazard appeared to increase with increasing age and baseline LDH, but the following covariates did not appear to have a significant effect on the risk of AE-DC/D: body weight, ECOG status, line of therapy, M stage and PD-L1 status. Model evaluation by predictive check showed that the model can adequately describe the observed data.
Conclusions: Nivolumab given in combination with ipilimumab produced a greater increase in the risk of AE-DC/D relative to nivolumab or ipilimumab monotherapy. The exposure effects of nivolumab and ipilimumab appeared to be additive and not synergistic.

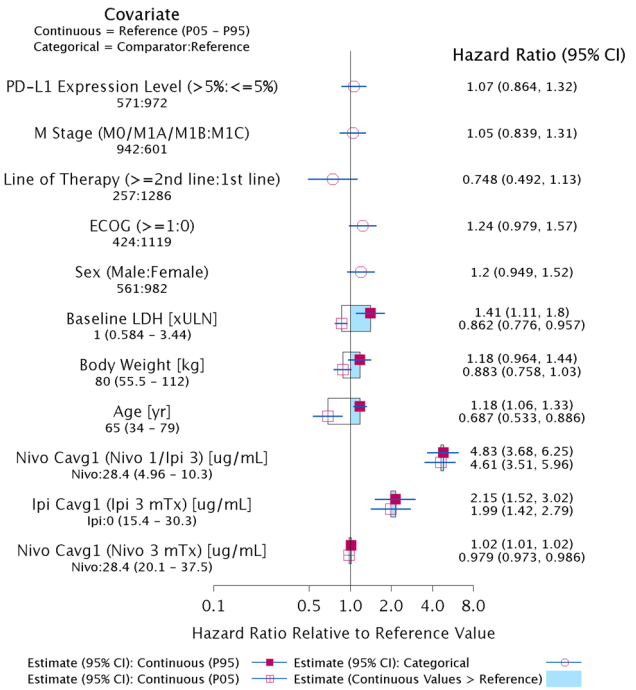

Fig. 1 Covariate Effects on the Hazard Ratio of AE-DC/D. Reference: median Cavg1 at nivolumab 3 mg/kg monotherapy

M-62

A PKPD Model Describing the Effect of Ixekizumab on Absolute Psoriasis Area and Severity Index (PASI) score in Patients with Moderate to Severe Plaque Psoriasis

Nieves Velez de Mendizabal[1], Michael Heathman[1], Choi Siak-Leng[2], Emmanuel Chigutsa[1], Laiyi Chua[2], Stuart Friedrich[1], Leijun Hu[1], Kimberley Jackson[3*]

[1]Eli Lilly and Company, Indianapolis, IN, USA; [2]Lilly-NUS Centre for Clinical Pharmacology, Singapore; [3]Eli Lilly and Company, Windlesham UK

Objectives: To describe and quantify the effect of ixekizumab on the absolute Psoriasis Area and Severity Index (PASI) score over time in patients with moderate to severe plaque psoriasis using a longitudinal PK/PD model.
Methods: Data from patients in a Phase 2 (N = 115) and a Phase 3 (N = 1247) study were included in this analysis. In the Phase 2 study, ixekizumab was administered subcutaneously (SC) at doses from 10 to 150 mg at weeks 0, 2, 4, 8, 12, and 16. In the Phase 3 study, ixekizumab 80 mg SC was dosed every 2 weeks (Q2W) or every four weeks (Q4W) during an induction period (weeks 0 to 12); and Q4 W or every 12 weeks (Q12W) during the maintenance period (weeks 12 to 60). A starting dose of 160 mg was administered at the beginning of this study. PASI score was modeled as a continuous covariate using an indirect response model. Drug and placebo effects were included in the model. All analyses were performed with the non-linear mixed-effect modeling software NONMEM® version 7.3.
Results: The PKPD model well describes the time course of PASI response. The model predicted that both doses of ixekizumab studied in Phase 3 resulted in significant improvements in PASI scores compared with the placebo group, and agreed with the observed data. Complete clearance of the disease (achievement of PASI100) was predicted for both Phase 3 doses in more than one-third of the treated patients by week 12 of treatment.
Conclusions: An indirect response model well described the time course of PASI score in patients with moderate to severe plaque psoriasis. This model could be adapted to describe PASI response for other treatments and for other indications e.g. Psoriatic Arthritis.

M-63

Mechanistic Predictions of Response to Combinations of Biologic Agents in a Quantitative Systems Pharmacology Model of Rheumatoid Arthritis

Craig J. Thalhauser[1*], Brian J. Schmidt[1], Marko Miladinov[2] and Tarek A. Leil[1]

[1]Quantitative Clinical Pharmacology, [2]Research Information Technology & Automation, Bristol-Myers Squibb, Princeton NJ 08543

Objectives: To evaluate the utlity of a fully calibrated rheumatoid arthritis (RA) virtual population, developed from a mechanistic model of the pathophysiology in an inflamed joint, to predict clinical responses in the population to combinations of approved biologic therapies.
Methods: The Entelos RA PhysioLab platform and a collection of 1200 valid virtual patients was employed in this simulation study. The virtual patients were calibrated to published clinical trial data for several clinically approved therapies along with background methotrexate (MTX). Combination therapy strategies were designed by applying sub-therapeutic doses of two biologics at standard dosing intervals also with background MTX. Clinical response in the form of ACR20, ACR50 and ACR70 was measured, and the responses to each biologic combination were compared to the full-strength clinical course of each parent therapy.
Results: The virtual population demonstrated good qualitative and quantitative calibration to the training data set by Fisher's composite goodness of fit metric. All tested combinations at sub-therapeutic doses were at least non-inferior to the more potent of their full strength parent compounds. Rituximab proved to be the best matching agent (Table 1). Greater degrees of improvement were observed for the ACR50 and ACR70 responses. Virtual patients who responded to a combination strategy while not responding to one or both of the parent strategies were analyzed and suggest domininat supportive interactions between adaptive and innate immune cells in the rheumatic joint.

Table 1 ACR response rates after 24 weeks of therapy

	Combinations			Full-strength Therapies		Parent
	ADA/RTX	ADA/TCZ	TCZ/RTX	ADA	RTX	TCZ
ACR20	79.5	67.1	71	59.5	60.5	59
ACR50	57.5	45.6	52.5	37.6	30.7	36.5
ACR70	36.7*	24	34.2*	20	14.3	18.4

* Super-additive response

Conclusions: Combinations of current biological therapies are an attractive means to intervene against multiple clinically validated

targets of RA simultaneously. This simulation study suggests that synergy between sub-therapeutic doses of these compounds potentially drives a stronger magnitude of response (ACR50 and ACR70 vs ACR20) in a diverse set of patients .

M-64

Model Qualification Approaches for Quantitative Systems Pharmacology and Mechanistic Physiological Models

Christina M. Friedrich[1*]

[1]Rosa & Co. San Carlos, CA

Objectives: Quantitative Systems Pharmacology (QSP) has emerged as a powerful approach in model-informed drug development. QSP is an umbrella term for mathematical modeling that considers drug MOA in the context of biological disease mechanisms to improve understanding of human biology and pharmacology. Specific QSP modeling methods vary, and there is currently no one unifying qualification method [1]. Several recent publications discuss QSP model qualification [2–4]. Mechanistic physiological models are one established QSP approach in which biological mechanisms and drug MOA are represented by appropriate equations (usually ordinary differential equations) and parameters. Whole-system behavior can then be simulated to gain insights into the connections between mechanisms and outcomes. Here, we compare and contrast newly proposed QSP qualification approaches with the Model Qualification Method (MQM, Figure 1) for Rosa's PhysioPD™ Research Platforms, first presented at ACoP 2011 [5].
Methods: Recent publications discussing QSP model qualification [2–4] were analyzed and compared with the MQM.
Results: The MQM comprises eight criteria addressing relevance, uncertainty, variability, and consistency with test data. QSP qualification approaches proposed recently share several themes with each other and the MQM, and add useful details and examples for addressing several of the MQM criteria. The MQM is broader and includes additional criteria, particularly regarding biological uncertainty, that are not addressed in other published approaches.
Conclusions: The MQM developed for mechanistic physiological models can serve as a framework for qualifying QSP models. Use of the MQM would complement and enhance other proposed approaches. The industry may be converging on a set of QSP qualification criteria.

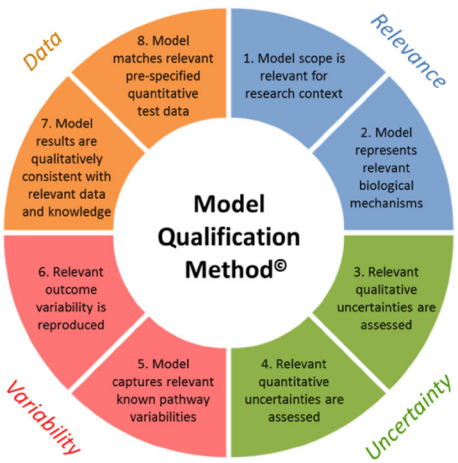

Fig. 1 Rosa's Model Qualification Method for mechanistic physiological models

References:

1. Jusko WJ. 2013. Journal of Pharmaceutical Sciences 102:2930–40.
2. Visser SA, de Alwis DP, et al. 2014. CPT: Pharmacometrics & Systems Pharmacology 3:e142.
3. Agoram B. 2014. CPT: Pharmacometrics & Systems Pharmacology 3:e101.
4. Howell BA, Yang Y, et al. J Pharmacokinet Pharmacodyn 39:527–41.
5. Friedrich C, Bosley J, Baillie R, Beaver R. 2011. ACoP. San Diego, CA.

M-65

Physiologically Based Pharmacokinetic Modeling of Rosuvastatin and Prediction of Transporter-Mediated Drug–Drug Interactions Involving Gemfibrozil

J.S. Macwan[1]*, V. Lukacova[1], G. Fraczkiewicz[1], M. B. Bolger[1], F. Akhlaghi[2], W. S. Woltosz[1]

[1]Simulations Plus, Inc. Lancaster, CA, USA; [2]University of Rhode Island, Kingston, RI, USA

Objectives: Rosuvastatin (Crestor®) may be coprescribed with gemfibrozil due to their complementary lipid-lowering effects. Rosuvastatin is a substrate of OATP1B1, OATP1B3, OATP2B1, NTCP and BCRP transporters. Gemfibrozil inhibits OATP1B1, which accounts for ~50 % of the active liver uptake clearance of rosuvastatin. Coadministration of statins and gemfibrozil is associated with an increased risk of myopathy and rare but life-threatening rhabdomyolysis. Patients with genetic polymorphisms of OATP1B1 may be at high risk of severe DDIs when rosuvastatin and gemfibrozil are coprescribed. The objective of this study was to develop a PBPK model of rosuvastatin and to predict tDDIs with gemfibrozil.
Methods: A mechanistic absorption/PBPK model for rosuvastatin was built in the GastroPlus™ 9.0 (Simulations Plus, Inc.). In vitro and clinical profiles were obtained from literature. The permeability-limited liver model included clearances involving sinusoidal uptake, passive diffusional, metabolic, and biliary mediated by canalicular efflux. BCRP-mediated intestinal efflux and EHC were incorporated in the model. The model was validated across several different dose levels following single and multiple oral administrations of rosuvastatin. OATP1B1 tDDIs were predicted through dynamic simulations using the validated PBPK models.
Results: The model adequately predicted hepatobiliary disposition of rosuvastatin. The predicted $AUC_{0\text{-}t}$, C_{max}, and t_{max} values were within 2-fold of the observed data of rosuvastatin. The predicted increase in $AUC_{0\text{-}t}$ and C_{max} of rosuvastatin in the presence of gemfibrozil was ~2-fold which was in close agreement with observed values [1].
Conclusions: The absorption and pharmacokinetics of rosuvastatin were accurately predicted using only in vitro data. The model successfully predicted tDDIs between rosuvastatin and gemfibrozil. This model can be extended for quantitative prediction of the impact of genetic polymorphisms and tDDIs by OATP and BCRP inhibitors. The proposed model can help to identify populations with increased risk of side effects and to optimize their dosing regimen for safe treatment with rosuvastatin.

References:

1. Schneck, et al. CPT. 2004;75(5):455–63

M-66

A General Method for Initialization of Steady-States in Complex PK/PD Systems

Lubna Abuqayyas[1], John Harrold[1*]

[1]Amgen Inc

Objective: Steady-states for systems are typically determined by analytical solutions. However, this is not always feasible for complex systems where manual adjustment of the steady state is common. This may impact the accuracy of the results. The objective is to develop a robust method to determine the steady-state synthesis rates of endogenous species in complex systems.
Methods: The concept of an integral controller (Figure 1) was adapted to determine the steady-state synthesis rates of non-zero quantities for two systems. The first system, one biomarker upstream of another, was selected to allow for comparison of analytical and numerical solutions explicitly. The second system is a complex physiologically-based pharmacokinetic (PBPK) model where the synthesis rate of endogenous Immunoglobulin-G (IgG) was determined to maintain IgG homeostasis. The proposed method was evaluated during parameter estimation (at each objective function call) as well during stochastic simulations (τ_I values ranging from $5e^{-9}$ to $5e^{-6}$/min). The accuracy of this method for both systems was evaluated by comparing the absolute relative error normalized to the specified physiological baseline value at t_{ss} (NARE).

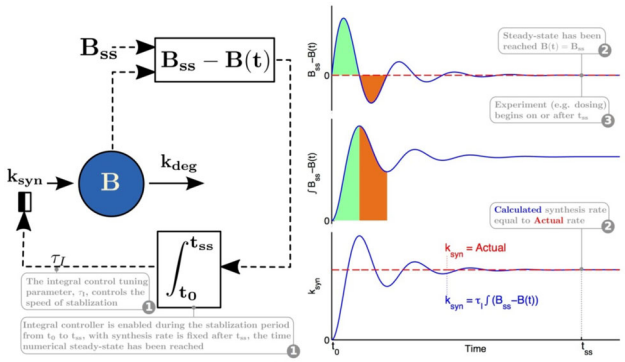

Fig. 1 Schematic showing the determination of the endogenous synthesis rate (k_{syn}) of a biomarker B in order to maintain the system at the homeostasis level B_{ss}

Results: The proposed method was able to bring both systems to the physiological steady-state levels. The parameter space explored for the PBPK model during an estimation exercise resulted in steady-state synthesis rates ranging from $9.7e^{-5}$ to $9.0e^{-4}$ nmol/min. Further, the PBPK system was able to be stabilized within 25 days over a large range of values of τ_I (valid for $5e^{-8}$ to $5e^{-6}$/min) resulting in steady-state synthesis rates of $9.5e^{-5}$ to $8.3e^{-4}$ nmol/min for the parameter sets considered. The lowest value of τ_I considered ($5e^{-9}$/min) required a greater stabilization time. For the first system the NARE was below 10^{-6} for both biomarkers at t_{ss}. For the PBPK system, the NARE was less than $8.02e^{-5}$ at 25 days, both during the parameter estimation exercise and for the stochastic simulations for the valid values of τ_I.
Conclusion: A numerical method has been adapted and tested for automating the determination of synthesis rates of endogenous species under homeostasis. This method is applicable to complex systems, such as PBPK and quantitative system pharmacological models, where analytical solutions are not practical.

M-67

In Vivo Mechanisms of Drug-load Release for Antibody Drug Conjugates and Their Relationships To Drug-Related Toxicity

Sihem Ait-Oudhia*

Center for Pharmacometrics and Systems Pharmacology, Orlando, FL. State University of New York at Buffalo, Buffalo, NY

Objectives: To develop a unified model describing the pharmacokinetics (PK) of trastuzumab emtansine (TDM1) and brenduximab vedutin (SGN35), and their myelosuppressive effects in mice.
Methods: TDM1 and SGN35 PK and their effects on platelets (PLT) and neutrophils (ANC) counts were assessed in balbc normal or human xenografted mice after single or repeated doses and compared to control groups. Total trastuzumab concentrations were measured while total plasma concentrations for SGN35, the payloads (DM1 and MMAE for TDM1 and SGN35), and the antibodies (trastuzumab and anti-CD30 for TDM1 and SGN35) were extracted from the literature [1, 2]. MONOLIX and Berkeley Madonna were used to model the data.
Results: Two-compartment models with linear elimination and deconjugation from the ADCs (kdec) described the PK of the 2 ADCs, and their respective payloads and monoclonal antibodies. Myelosuppression from both ADCs was captured with a series of five transit compartments representing cell proliferation and maturation in the bone marrow, and PLT or ANC in blood. A negative feedback loop accounted for the observed tolerance. TDM1 and SGN35 half-lives were estimated at 4.8 and 4.6 days and kdec were 0.46 and 0.12 h^{-1}. The lifespans for PLT under TDM1 and ANC under SGN35 were 3.73 and 4.72 days. Comparison of alternative model performance suggested that TDM1 and SGN35 myelosuppressions are caused by different mechanisms: ADC binding to FcgR for TDM1 and payload-driven toxicity for SGN35 due to high lipophilicity of MMAE. Model based-simulations suggested that a 6-fold increase and 70 % decrease in kdec of TDM1 and SGN35 would improve myelosuppression.

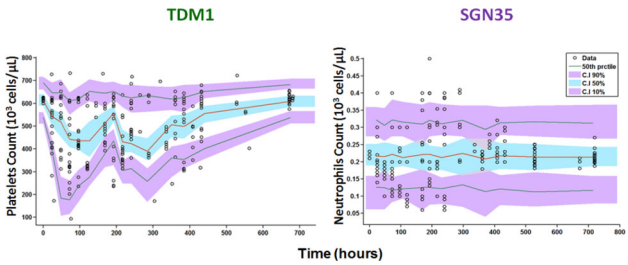

Fig. 1 Prediction-corrected visual predictive check plots

Conclusions: The proposed model successfully captured the PK and myelosuppressive effects of TDM1 and SGN35 and may serve as a general PK/PD platform for ADCs.

References:

1. Erickson, H.K., et al. Mol Cancer Ther, 2012. 11(5):1133–42.
2. Hamblett, K.J., et al. Clin Cancer Res, 2004. 10(20):7063–70.

M-68

Model-Based Analysis to Support Clinical Pharmacology Profiling of Elotuzumab in Patients with Multiple Myeloma

L. Gibiansky[1], C. Passey[2*], A. Roy[2], A. Bello[2], M. Gupta[2]

[1]QuantPharm LLC, [2]Bristol-Myers Squibb

Background: Elotuzumab (ELO) is a humanized anti-SLAM7 IgG1 monoclonal antibody under development for combination use with lenalidomide/dexamethasone (Len/Dex), and bortezomib/dexamethasone (Bor/Dex) for the treatment of relapsed or refractory multiple myeloma (MM). A model based analysis was conducted to support the clinical pharmacology profiling of ELO by characterizing ELO's PK and determining effect of covariates on PK and exposure parameters in MM patients.
Methods: The PK of ELO was described by a population pharmacokinetics (PPK) model, developed using 6958 serum concentration values from 375 MM patients receiving ELO at doses of 10 or 20 mg/kg in 4 clinical studies. The PPK model was estimated by nonlinear regression using the NONMEM software program and the Monte Carlo expectation–maximization (EM) method with importance sampling (IMPMAP). The impact of the following baseline covariates on PK was assessed: body weight, age, race, sex, renal function (as measured by eGFR), hepatic function, ECOG performance status, LDH, albumin, Len/Dex co-administration, serum M-Protein, and β_2-microglobulin. The final PPK model was developed by retaining covariates that improved the Bayesian Information Criterion (BIC). The final model was then evaluated and refined using data from another study of ELO in combination with Bor/Dex.
Results: ELO PK is characterized by a two compartment model with zero order IV infusion, parallel non-specific (linear) and Michaelis–Menten elimination from the central compartment, and additional target-mediated elimination from the peripheral compartment. Non-specific clearance of ELO (CL) increases with increasing body weight; body-weight based dosing of ELO results in uniform ELO exposures across body weight ranges. Co-administration of Len/Dex or Bor/Dex background therapy resulted in a decrease of ELO non-specific clearance by 35 and 50 %, respectively, relative to ELO monotherapy. Target-mediated elimination of ELO increases with increasing baseline serum M-protein, resulting in lower exposure in patients with high baseline serum M-protein concentrations. None of the other tested covariates had clinically relevant (<20 %) effects on elotuzumab CL.
Conclusion: This analysis indicated that ELO PK was non-linear.

M-69

Bayesian Fisher Information Matrix for Predicting Estimation Error and Shrinkage of Individual Parameters with Data Below the Quantification Limit

Thi Huyen Tram Nguyen[1], Thu Thuy Nguyen[1,2], France Mentré[1*]

[1]IAME-UMR 1137, INSERM and University Paris Diderot, Paris, France; [2] CEA, LIST, 91191, Gif-sur-Yvette, France

Objectives: In population approach, individual parameters are usually estimated as the maximum a posteriori (MAP). The standard errors (SE) and shrinkage of individual parameters, which depend on individual designs, proportion of data below the limit of quantification (LOQ) and the method for handling them, can be predicted from the Bayesian Fisher Information Matrix (BFIM) [1, 2]. Here, we developed a method to account for data below LOQ in BFIM and illustrated the use of BFIM to predict SE and shrinkage of individual parameters.
Methods: The contribution of data below LOQ in BFIM was calculated by deriving their log-likelihood, defined as the probability to be below LOQ [3]. We compared the predictions of BFIM with clinical trial simulation results, using a pharmacokinetic/viral kinetic model [4] and different designs. Next, we studied the influence of designs, interindividual variability (ω) and residual error (σ) on SE and shrinkage using BFIM or the individual Fisher information matrix (IFIM).
Results: The predictions of BFIM were close to clinical trial simulation results in absence or presence of data below LOQ. The predicted SE were lower with BFIM than IFIM. SE increased with sparse designs or increased variability; shrinkage increased with sparse designs and high σ but decreased as ω increased.
Conclusions: The shrinkage and SE of individual parameters estimated by MAP can be efficiently predicted from BFIM, which is available in the R-package PFIM4.0 [5] and PFIM Interface 4.0 (www.pfim.biostat.fr).
This work has been presented at PAGE 24, Greece (06/2015) and published in the conference proceedings as abstract 3516.

References:

1. Merlé et al. J Pharmacokinet Biopharm, 1995.
2. Combes et al. Pharm Res, 2012.
3. Boulanger et al. Journée Biopharmacie et Santé, 2012.
4. Nguyen et al. Clin Pharmacol Ther, 2014.
5. Mentré F et al. PAGE 23, 2014 Abstr 3032 [www.page-meeting.org/?abstract=3032]

M-70

Optimal Design for Informative Protocols in Xenograft Tumor Growth Inhibition Models

Giulia Lestini[1,2], France Mentré[1*], Paolo Magni[2]

[1]IAME, UMR 1137, INSERM, University Paris Diderot, Paris, France, [2]Dipartimento di Ingegneria Industriale e dell'Informazione, Università degli Studi di Pavia, Pavia, Italy

Objectives: Tumor size measurements in vivo xenograft experiments are usually taken only during treatment [1], preventing a correct identification of certain parameters of tumor growth inhibition models. Optimal design in the Simeoni model [2] was used to evaluate the importance of including measurements during the tumor regrowth phase in those studies.
Methods: Optimal design was performed for several xenograft experiments [2, 3] in treated and control arms, involving different drugs, schedules and cell lines. Sampling design was optimized, for each selected experiment, with or without the constraint of not sampling during tumor regrowth, that we defined as "short" and "long" studies, respectively. In the long study, measurements could be taken up to six grams of tumor weight, for ethical reasons, whereas in the short study the experiment was stopped two/three days after the end of treatment period. Design optimization was performed using the determinant of the Fisher information matrix in PFIM 4.0 [4]. Predicted Relative Standard Errors (RSE) were used to compare those scenarios.
Results: Predicted RSE obtained in long studies were better compared to those obtained in the short study of the corresponding experiments. Indeed, some optimal times were located in the regrowth phase, highlighting the importance of continuing the experiment also after the end of the treatment.
Conclusions: Based on results obtained here, making measurements during tumor regrowth should become a general rule for more informative preclinical studies in oncology.

This work was supported by the DDMoRe project (www.ddmore.eu).
The results in this abstract have been previously presented in part at PAGE 24, Crete, June 2015 and published in the conference proceedings as abstract 3431.

References:

1. Simeoni M, et al. Drug Discov Today Technol. (2013) 10(3):e365–72.
2. Simeoni M, et al. Cancer Res. (2004) 64(3):1094–101.
3. Simeoni M, et al. PAGE (2004) Abstr 496.
4. www.biostat.pfim.fr

T-01

A Compartmental Epidemic and Outcome Model Framework with User-Friendly Interactive Inputs and Dynamic Outputs

Xiaohua Gong[1,*], Yin Yin[2], Paul Mudd[3]

[1]Incyte Corporation, Wilmington, DE; [2]PAREXEL International, Durham, NC; [3]Roivant Sciences, Durham, NC

Objectives: To develop a user-friendly tool that identifies important factors, including the number of initial infected individuals, target population, target efficacy, and drug supply, that affect the death rate from an infectious disease outbreak.
Methods: A compartmental epidemic SEIR (susceptible-exposed-infectious-removed) model with medicine intervention and logistics was developed. Clinical outcomes (most importantly the death rate) and health economic measures (amount of medicine needed for treatment and/or prophylaxis) were primary endpoints. Medicine logistics were also incorporated into the modeling. Both the R/shiny technology and Excel Workbooks were adopted to develop two independ application implementing similar user-friendly applications.
Results: Two interactive tools were developed based on R/shiny and Excel, respectively, that both adopted a compartmental epidemic SEIR model allowed easy adjustment/tuning of model inputs and parameters, and to customize the visualization of model output. The advantage of Excel is its availability. However, the R/shiny solution has a built-in separation between the model developers/maintainers and the model users so that users don't need to have R on their computers. Multiple users can also access the R/shiny application simultaneously and each can explore a range of values for each factor and identify the most cost-effective way to control the death rate under the tested scenarios.
Conclusions: Interactive user-centric applications effectively demonstrated the impact of initial infected individual, target population, target efficacy, medicine intervention of treatment and/or prophylaxis, and drug supply on the clinical outcome (death rate) and health economics (demand for drug supply) from an infectious disease outbreak.

References:

1. Wu JT, "Modeling Interventions and logistics", 2010, http://sph.hku.hk/shortcourse/2010/1515 Day 1 JTW Modeling interventions and logistics.pdf (last accessed on 07Apr2015)
2. RStudio, Inc., "shiny: Easy Web Application in R", 2014, http://shiny.rstudio.com
3. Jenness SM, "SIR Model with Vital Dynamics", http://glimmer.rstudio.com/smjenness/SIR/ (last access on 07Apr2015)

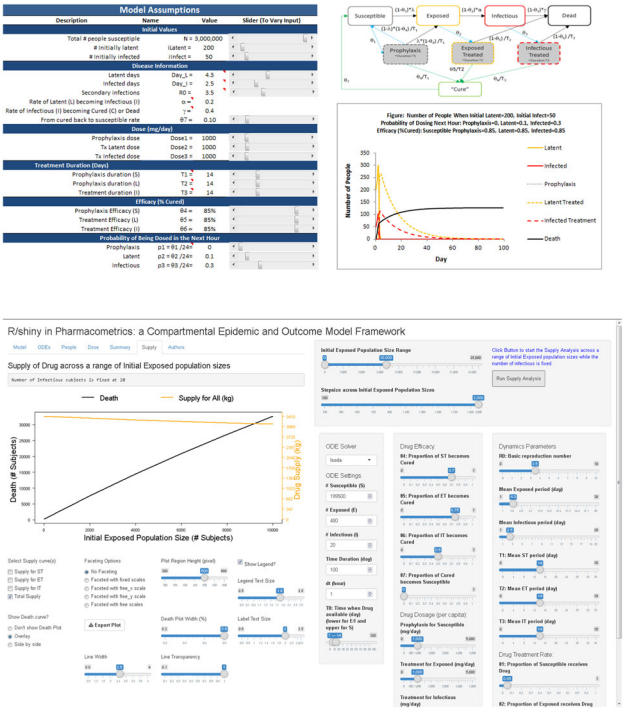

Fig. 1 Model diagram and application input/output interfaces

T-02

Non-Homogeneous Poisson Process (NHPP) Analysis of Time to First Flare for Canakinumab (CAN) Dose Justification in SJIA

Yuan Xiong*, William Ebling, Olivier Luttringer, Wenping Wang

Novartis Pharmaceuticals Corporation

Objectives: To provide dose justification argument for sBLA submission by: 1) exploring the relationship between SJIA flare reduction and CAN exposure with consideration of patient baseline characteristics; 2) predicting the effects of CAN dosing regimens at 1 to 6 mg/kg every 4 weeks on SJIA flare rates compared with placebo.
Methods: While traditional Cox regression model assumes proportional hazard, a model-based NHPP analysis was performed that naturally linked the time-changing plasma concentration of CAN to the time-changing flare hazard. The model considered treatments and multiple covariates, including baseline steroid dose, heterogeneity of the population with respect to disease severity, and declining CAN concentrations over time due to washout in patients on PBO who received CAN previously. The model was also used to explore the dose–response relationship between flare hazard and CAN dose based on 1000 simulated trials, each with 700 patients randomized to 1 of 7 treatment arms: PBO and 1 to 6 mg/kg (all administered every 4 weeks) of CAN.

Results: Based on the simulations, CAN at 4 mg/kg every 4 weeks reduces the probability of flare (90 % CI) over PBO by 39 % (28, 49 %) over 12 months, consistent with the clinical data observed. The predicted changes in flare probability are +13, +6, +2, −2, and −3 % for the 1 to 6 mg/kg every 4 weeks doses respectively, compared to 4 mg/kg. These results support 4 mg/kg every 4 weeks as the appropriate dose for preventing SJIA flare events. Doses greater than 4 mg/kg provide only marginal gain in flare reduction, while doses less than 4 mg/kg relatively increase the risk of experiencing a flare.

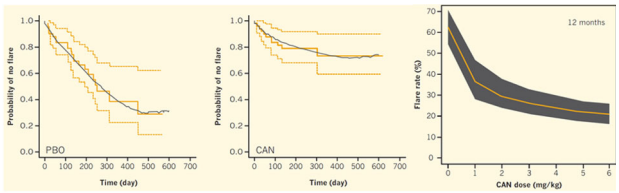

Fig. 1 **a** Observed K-M and point-wise median of simulated K-M curves of flaring for PBO and CAN. **b** Predicted flare rate by CAN doses at 12 months

Conclusions: A NHPP-based modeling approach was adopted and able to re-produce the observed Kaplan–Meier curves with fidelity. Inferences from the NHPP model include: 1) CAN can fully suppress flare hazard with high statistical significance; 2) CAN suppresses flare hazard in a concentration dependent manner; 3) a CAN dose-flare rate relationship sufficiently justifies the recommended CAN dose in SJIA.

T-03

A Mechanism-Based Translational Mathematical Model for Gastrointestinal Toxicity

Harish Shankaran[1*], Paul Jasper[2], Matthew Wagoner[1], John Tolsma[2], and Jay Mettetal[1]

[1]Drug Safety and Metabolism, AstraZeneca, Waltham, MA; [2]RES Group Inc, Needham, MA

Objectives: The gastrointestinal (GI) epithelium undergoes rapid cell proliferation and self-renewal, and is a frequent target for chemotherapy-induced toxicity. Our objective was to build a mechanism-based model that would enable the translation of preclinical GI histopathology data to predictions of GI damage in man.
Methods: We built a model for intestinal dynamics where the stem cells in the crypt divide to generate transit amplifying daughter cells (TADCs), which then undergo multiple rounds of division before differentiating into the enterocytes in the villi (Fig. 1A). We parameterized rodent and human versions of the model using literature data on cell numbers, division rates, and villus transit times. We used ordinal logistic regression to fit the model to Irinotecan rat histopathology data. Scores for crypt degeneration and villous atrophy were linked to SN38-induced stem cell and enterocyte decreases. Drug effect parameters obtained from these fits were combined with human PK and system parameters to predict clinical effects.
Results: We obtained good fits to rat data for Irinotecan (Fig. 1B). The EC50 values for SN38-induced stem cell killing, TADC killing and TADC cell cycle arrest were 0.54 μM, 4.3 μM and 0.19 μM, respectively indicating that the SN38 preferentially induces cell cycle arrest of TADCs. A key aspect captured by the model is the slower cell division and transit kinetics in humans that is predicted to contribute to slower recovery. Predictions for the time course of GI damage in humans (Fig. 1C) were in excellent agreement with data on the incidence of diarrhea [1].

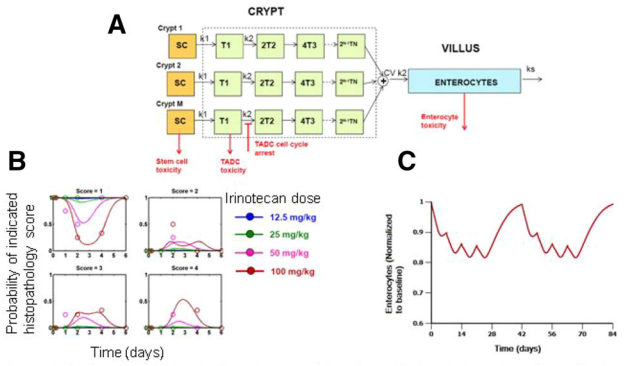

Fig. 1 **A** Schematic description of the model for intestinal cell dynamics. Drug effects are in *red*. **B** Model fits (*lines*) to experimental data on the fraction of rats exhibiting the indicated villous atrophy scores following treatment with the indicated doses of irinotecan. **C** Prediction for loss in enterocytes in humans for 125 mg/m^2/week Irinotecan, 4 weeks on and 2 weeks off

Conclusions: The model enables quantitative translation of preclinical data, and allows us to understand the mechanisms of drug-induced GI toxicity. We are validating the model with preclinical and clinical data for additional compounds. The model can be used to optimize doses and schedules for chemotherapeutic agents, and to assess the clinical GI risk for novel therapeutics based on preclinical data.

References:

1. Hecht, Oncology, v12, 1998

T-04

Pharmacokinetic-Pharmacodynamic (PK-PD) Modeling of Tolvaptan and Diuretic Use on Fluid and Electrolyte Balance in Healthy Subjects

Scott Van Wart[1*], Susan Shoaf[2], Suresh Mallikaarjun[2], and Donald Mager[1]

[1]SUNY-Buffalo, Buffalo, NY; [2]Otsuka, Rockville, MD

Objectives: To develop a PK-PD model characterizing the impact of the oral V_2R antagonist tolvaptan, furosemide and hydrochlorothizide (HCTZ) on fluid and electrolyte balance in healthy subjects.
Methods: Urine and electrolyte data were obtained from 101 subjects across 3 Phase 1 studies, including a crossover study (N = 12) in which tolvaptan or furosemide/HCTZ was given alone or in combination. A series of linked indirect response models were used to describe dietary intake and urinary elimination of water and electrolytes as well as their relative ECF:ICF distribution. Synchronized cosine functions for dietary intake and renal elimination were used to characterize transient system changes in the absence of treatment. A population PK model for tolvaptan [1] was used to predict plasma tolvaptan concentrations to drive inhibition of the fractional tubular water reabsorption (FR_W). Furosemide and HCTZ PK models [2, 3] were employed to predict the urinary diuretic excretion rates used to drive inhibition of fractional tubular Na^+ reabsorption (FR_{Na}).

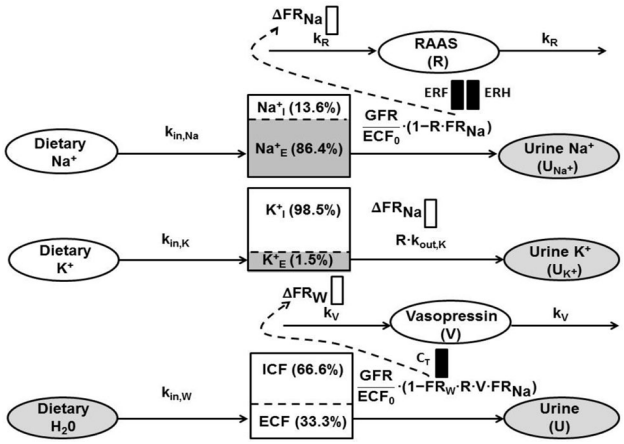

Results: Maximal tolvaptan-induced inhibition of FR_W was 7.65 % (vasopressin produces ~10 % of water reabsorption in the collecting ducts). Tolvaptan-induced inhibition of FR_W was used to stimulate relative vasopressin activity to reduce the extent of diuresis upon repeated dosing. The maximal furosemide-induced inhibition of FR_{Na} was 18.3 % (Na^+-K^+-Cl^- transporter produces ~20 % of Na^+ reabsorption in the ascending limb of the loop of Henle) and for HCTZ was 2.51 % (Na^+-Cl^- symporter produces ~3.5 to 5 % of Na^+ reabsorption in the proximal tubule). Diuretic-induced changes in FR_{Na} were used to drive secondary effects such as diuresis, kaliuresis and the stimulation of relative RAAS activity causing feedback modulation.

Conclusions: A physiologically relevant PK-PD model was constructed to characterize fluid and electrolyte balance, which can be adjusted to account for pathophysiological factors explaining differences in response for fluid overload patients.

References:

1. Van Wart et al. Biopharm Drug Dispos. 2013;34(6):336–47.
2. Van Wart et al. Biopharm Drug Dispos. 2014;35(2):119-33.
3. Van Wart et al. Biopharm Drug Dispos. 2013;34(9):527–39.

T-05

Enhancing Clinical Utility of Model-based Pharmacokinetic Profiles of Subcutaneous Insulin Through Interactive Visualization

Karen Schneck[1*], Lai San Tham[2], Ali Ertekin[3], Jesus Reviriego[4]

[1]Eli Lilly and Company, Indianapolis, IN, USA; [2]Lilly-NUS Center for Clinical Pharmacology Pte Ltd, Singapore; [3]Eli Lilly and Company, Turkey; [4]Eli Lilly and Company, Spain

Objectives: Optimal insulin therapy in diabetics delivers higher insulin concentration when glucose is elevated around mealtimes and lower insulin concentration between meals and during nighttime. The goal was to integrate pharmacokinetic (PK) models of insulin formulations with diverse onset and duration of action characteristics to enable simulation of insulin concentration–time profiles following subcutaneous administration of insulin. An interactive tool was applied to provide easily accessible visualization.

Methods: A PK model was developed using clinical studies with healthy volunteers or diabetics and implemented in a nonlinear mixed effects modeling program (NONMEM 7.3). The model was parameterized to reflect the absorption of rapid-, short-, and long-acting formulations, including insulin lispro, regular insulin, insulin isophane (NPH), and pre-mixed preparations (NPH with regular insulin (Mix 70/30), and lispro protamine with insulin lispro (Mix 50/50, Mix 75/25)). Influences on the concentration–time profile, including weight-based dosing, the effect of body weight (WT) on volume of distribution, and time of insulin administration relative to meal were incorporated into the model. Simulations were generated using differential equations solved in R and accessed through a customized web browser interface built with the Shiny package [1].

Results: The interactive tool displayed predicted insulin concentration–time profiles that reacted to changing user specified values for model variables such as formulation, dose, daily administration frequency, WT, concomitant insulin therapy, observation period, and number of doses. PK profiles were simulated for typical insulin regimens, single and multiple doses, and weight distributions representative of Asian and Western populations.

Fig. 1 Customized web browser interface for insulin PK simulation

Conclusions: Modeling enabled informative visualization of the concentration–time profiles of multiple insulin formulations. A customized web browser interface tool was an efficient way to quickly convey and interactively explore many insulin PK simulations.

References:

1. Wojciechowski J, Hopkins A, Upton R. Interactive Pharmacometric Applications Using R and the Shiny Package. CPT: PSP. 2015;4(3).

T-06

Systems Pharmacology Modeling and Analysis of Therapeutic Antibodies Antagonizing IL13-Mediated Disease Signaling

Seung-Wook Chung[1*], John Burke[2], Louise-Kelly Modis[2], Raj Nagaraja[1], Lee Frego[1], Kathy Last-Barney[1], Simon Roberts[1]

[1]Immune Modulation and NBE Discovery; [2]Immunology and Respiratory Diseases, Boehringer Ingelheim, Ridgefield, CT 06877, USA

Objectives: To provide a predictive tool of therapeutic monoclonal antibody (mAb) antagonizing interleukin 13 (IL13), which is known to be pathogenic in several immune diseases including asthma, and

thus to facilitate the discovery of an efficacious IL13-antagonist biologics in IL13-mediated diseases

Methods: A systems pharmacology model of anti-IL13 mAbs was developed based on consensus knowledge about the IL13 biology and non-clinical and clinical data reported in the literature. The model was trained with published clinical PK and PD data sets for IMA-026 and IMA-638 [1], and further validated using clinical PD data for GSK679586 [2].

Results: The model was used to characterize and compare a posteriori two distinct mechanisms of action (MOAs) of IL13 mAbs developed by multiple companies: MOA1 (which prevents IL13 signaling by blocking the heterotrimerization of IL13Rα1:IL13:IL4R, but still allowing binding to IL13Rα2, a decoy receptor) *vs* MOA2 (which prevents binding to both IL13Rα1 and IL13Rα2). Simulation analysis reveals that under the identical in silico conditions, MOA1-type mAb may exhibit more effective and sustained blockade of the the ligand-receptor oligomer having signaling capability, resulting in a lower efficacious dose, than MOA2-type mAb. The model also predicts that a subcutaneous dose of 0.4–2.1 mg/kg Q4 W in humans will be required for a MOA1-type mAb like lebrikizumab to achieve ≥95–99 % blockade of IL13-driven receptor oligomerization in blood. This predicted dose range is comparable with 37.5–250 mg of lebrikizumab that has demonstrated clinical benefits in the subsets of asthmatic patients.

Conclusions: Our mechanistic PK-PD model of IL13 provides a novel, quantitative insight into the therapeutic strategies of IL13 antagonism for patients in IL13-mediated immune diseases. We believe that our framework model can also serve as a preclinical candidate selection tool by providing key therapeutic property guidance, especially for combination therapy strategies associated with IL13.

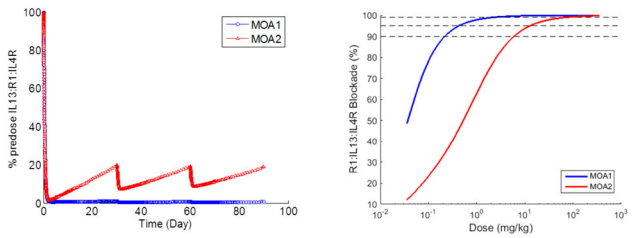

Fig. 1 **A** In silico comparision MOA1 (*blue*) and MOA2 (*red*) with respect to the heterotrimerization of IL-13, IL13Rα1 (denoted as R1) and IL4R, which is known to trigger IL-13-mediated disease signaling. **B** Human dose projections of two mAbs (MOA1 and MOA2; with binding affinity of 10 pM, bioavailability of 70 %, half-life of 20 days) at Q4 W s.c. dosing up to 12 weeks

References:

1. Kasaian (2011) J Immunol 187, 561–569
2. Hodsman (2012) Br J Clin Pharmacol 75, 118128

T-07

Uncompetitive and Competitive Drug–Drug Interaction with Target-Mediated Drug Disposition

Johannes Schropp[1*], Gilbert Koch[2]

[1]Department of Mathematics and Statistics, University of Konstanz, Germany; [2]Pediatric Pharmacology and Pharmacometrics Research Center, University Children's Hospital Basel, Switzerland

Objectives: To extend competitive and uncompetitive drug–drug interaction (DDI) with target-mediated drug disposition (TMDD), to investigate quasi equilibrium (QE) [1] and quasi steady state (QSS) [2] approximations in order to reduce model parameters, and to implement the resulting models in standard PKPD software without solving any additional equation systems.

Methods: Competitive and uncompetitive DDI was framed into the TMDD setting, i.e. internalization rates for the complexes, and production and degeneration rates for the target (i.e. receptors) were included. Typically, to reduce the number of parameters, the TMDD system is reformulated in total concentrations and receptor variables, and QE or QSS approximations are applied. In contrast to single TMDD, the challenge is to solve a system of nonlinear equations to obtain the original free drug concentrations, as already mentioned in [3] for competitive TMDD with QE. We present a general transformation resulting in ordinary differential equations for free drug concentrations and receptor variables.

Results: For DDI TMDD implementation of the QE or QSS approach an additional transformation to free drug concentrations is performed which avoids solving of arising equation systems. Further it turned out, that the QSS approach for uncompetitive TMDD seems to be an inadequate tool since not all binding rates could be eliminated.

Conclusion: Competitive and uncompetitive DDI was presented in the TMDD framework, QE approximation was applied to reduce the number of parameters, and a straightforward implementation for standard PKPD software like NONMEM or ADAPT 5 was presented.

References:

1. Mager DE, Jusko WJ (2001) General pharmacokinetic model for drugs exhibiting target-mediated drug disposition. J Pharmacokinet Pharmacodyn 28(6):507–32
2. Gibiansky L, Gibiansky E, Kakkar T, Ma P (2009) Approximations of the target-mediated drug disposition model and identifiability of model parameters. J Pharmacokinet Pharmacodyn 35(5):573–91
3. Yan X, Chen Y, Krzyzanski W (2012) Methods to solving rapid binding target-mediated drug disposition model for two drugs competing for the same receptor. J Pharmacokinet Pharmacodyn 39(5):543–60

T-08

Population Pharmacokinetics of Morphine in Patients with Non-Alcoholic Steatohepatitis (NASH) and Healthy Adults

Vadryn Pierre[1], Curtis K. Johnston[1,2], Brian Ferslew[1], Kim L.R. Brouwer[1], Daniel Gonzalez[1*]

[1]Division of Pharmacotherapy and Experimental Therapeutics, UNC Eshelman School of Pharmacy, Chapel Hill, North Carolina; [2]Metrum Research Group LLC, Tariffville, Connecticut

Objectives: Altered expression and function of hepatic transporters in NASH patients may affect the pharmacokinetics (PK), efficacy, and toxicity of drugs [1]. A population PK model was developed to assess differences in morphine and morphine-3-glucuronide (M3G) disposition in NASH patients and healthy volunteers.

Methods: A total of 267 serum and 42 urine samples from 21 volunteers (14-healthy; 7-NASH) were analyzed using NONMEM 7.3. Two- and three-compartment linear mammillary models were evaluated for morphine and one- and two-compartments for M3G [2]. Morphine clearance (CL_M) and volume of distribution were allometrically scaled using total body weight. Morphine serum

concentrations below the limit of quantification were fitted using the M3 method. NASH status, Fibroscan® score, AUC and fasting C_{max} of total serum bile acids were tested as covariates to explain inter-individual variability in CL_M, M3G clearance (CL_{M3G}) and volume of distribution (V_{M3G}) using stepwise covariate modeling with PsN (Perl-speaks–NONMEM). Goodness-of-fit plots, parameter plausibility and residual squared errors, and numerical and visual predictive checks (VPC) were used as criteria to evaluate model performance.

Results: A three-compartment model best described morphine disposition with a liver transit compartment accounting for the delay in M3G appearance in serum. M3G was best described by mono-exponential kinetics. Use of NASH status on CL_{M3G} and V_{M3G} resulted in a 10- and 8-point drop in the objective function value, respectively. The model predicted a 28 % and 22 % decrease in CL_{M3G} and V_{M3G}, respectively, for NASH patients compared to healthy volunteers. VPC plots indicate adequate fit for morphine and M3G (Figure 1).

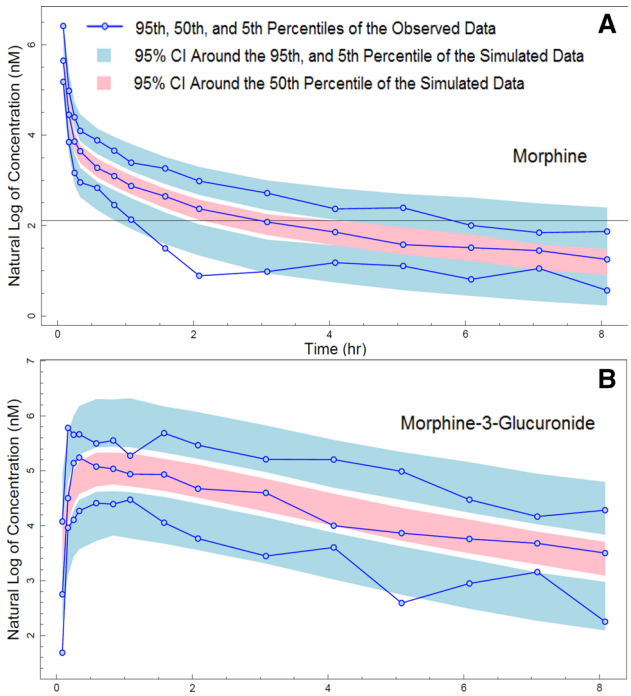

Fig. 1 **A** VPC of morphine in serum with a horizontal reference line representing LLOQ of 8.24 nM for the assay. **B** VPC of M3G in serum. Blue and pink shades represent the model predicted confidence interval around the 95th, 5th and 5th percentiles of the observed data

Conclusions: NASH status was the most significant predictor of differences in M3G exposure, which reflects altered transporter expression and function in this disease state. The final covariate model predicts higher AUC and C_{max} of M3G, for NASH patients compared to healthy volunteers.

Supported by NIH R01GM041935

References:

1. Ferslew CPT.97:419 (2015).
2. Lötsch CPT.72:151 (2002).

T-09

Simulation-Based Assessment of Insulin Lispro Dose Titration Algorithms Using a Model of Glucose-Insulin-Glucagon Dynamics

Xiaosu Ma[1*], Jenny Y Chien[1], Jennal Johnson[1], James Malone[1], Vikram Sinha[2]

[1]Eli Lilly and Company, Indianapolis, IN; [2]Food and Drug Administration, Silver Spring, MD

Objective: Evaluate glycemic outcome in patients with type 2 diabetes mellitus (T2DM) treated with insulin lispro (L) following various dose titration algorithms using a glucose-insulin-glucagon (GIG) model [1].

Methods: The GIG model included L and Glargine (G), and effect of Metformin (MET) on glucodynamics. It was used to simulate various dosing algorithms for patients administering basal G and pre-prandial L. The pharmacokinetics (PK) of both insulins was described by a one-compartment model with first-order absorption. The effect of MET on inhibition of glucose production was modeled as an effect compartment. The model was prospectively used to simulate the condition and design of the AUTONOMY study [2]: patients initiating with a single breakfast injection of L, with dose adjusted based on pre-lunch glucose from the previous day (Q1D) or 3-days until reaching glucose target. Lunch and dinner doses were titrated sequentially following the same algorithm. Treatment with G and MET only and two reference comparator algorithms [3] were also evaluated. Simulated 7-points self-monitoring of blood glucose (SMBG) was used to predict hypoglycemia rate. Endpoint HbA1c was predicted using a time-course model based on average daily glucose.

Results: Approximately 250 T2DM patients were simulated for each arm. HbA1c, fasting glucose, hypoglycemia rate and percent patients achieving HbA1c target (<7.0 %) were simulated and compared with study outcome. HbA1c was predicted to achieve approximately 1.1 % reduction from baseline using the Q1D algorithms compared to other algorithms (Figure 1).

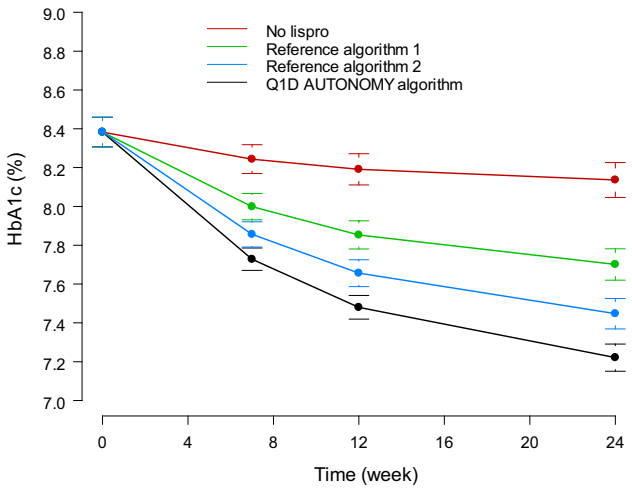

Fig. 1 Predicted HbA1c during 24-week treatment

Conclusions: Model-based simulation is an efficient approach to evaluate the impact of dosing algorithms on glycemic control in treatment of diabetes. The model predicted the results of the clinical trial and further supported the effectiveness of the recommended L self-titration algorithms.

References:

1. Schneck K et al. J. Pharmacokinet. Pharmacodyn. 2013, 40:67–80.
2. Edelman SV et al. Diabetes Care. 2014, 37(8):2132–40.
3. Abrahamson MJ et al. Ann. Med 2012, 44:836–46.

T-10

Web Accessible Population Pharmacokinetics Service—Hemophilia (WAPPS-Hemo): A Service for Bayesian Post Hoc Estimation

Alanna McEneny-King[1], Andrea Edginton[1*], Gary Foster[2], Alfonso Iorio[3] on behalf of WAPPS program investigators

[1]School of Pharmacy, University of Waterloo, Canada; [2]Clinical Epidemiology & Biostatistics, McMaster University, Canada; [3]Health Information Research Unit (HIRU), McMaster University

Objective: Tailoring prophylaxis to individual patient characteristics has been shown to effectively increase therapeutic benefit of hemophilia A and B treatment [1]. This project aims to develop a web-accessible service to assess clinically relevant PK of factor VIII and IX through: a) input of patient data, b) automatic estimation of PK parameters, c) expert validation of the estimation process and d) reporting of time to re-infusion (Figure).

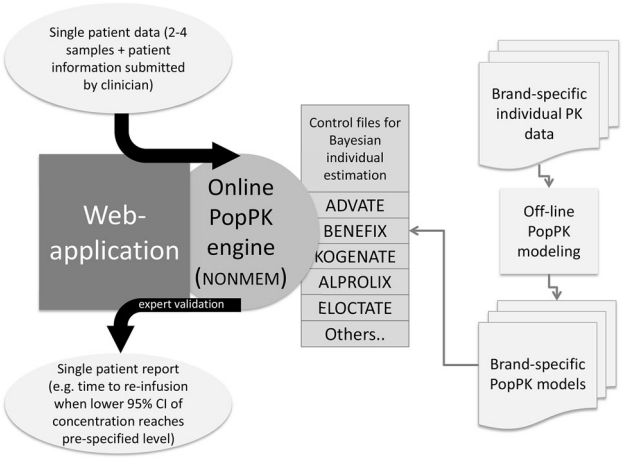

Methods: Clinical centres are recruited and must agree to provide at least 5 sets of patient data in the development and testing phase and in return are WAPPS co-investigators with full access to the database. Brand-specific PopPK models are developed using NONMEM/PDx-POP. Structural models and parameterization are based on data obtained from sponsors and literature information. Website development is on the IIS and dot.net platform with an MS SQL server for database management and an https:\\ protocol.
Results: Twenty-two centres from 14 countries are currently in the registration process. Data has been received for >700 subjects for model development (10 molecules, 6 sponsors). An additional 250 subjects from clinical sites make up the validation dataset. Eight population models are in the process of precision evaluation with limited samples, retrospective validation with an external dataset and within-patient prospective validation. The program website is live (www.wapps-hemo.org) and the application website is in beta testing.
Conclusions: This project will increase the evidence base used to treat hemophilia patients as the system progressively accrues individual PK data. The interconnection of a Bayesian engine, PopPK routines and smart end user interface will constitute an innovative blend of different high tech approaches to the care of this rare disorder. Funding: Baxter Canadian Hemophilia Epidemiological Research Program of the Canadian Hemophilia Society to *AI*.

References:

1. Iorio et al. 2011. Cochrane Database of Systematic Reviews (Online) 9

T-11

Quantitative Characterization of the Effects of Acute Radiation (AR) and Treatment with Filgrastim (Neupogen) on Absolute Neutrophil Counts (ANC) and Overall Survival (OS) in Non-Human Primates (NHP)

John Harrold[1], Per Olsson Gisleskog[2], Isabelle Delor[2], Philippe Jacqmin[2], Juan Jose Perez-Ruixo[3], Sameer Doshi[1], Bing-Bing Yang[1], Andrew Chow[1], Murad Melhem[1*]

[1]Amgen Inc.; [2]SGS Exprimo NV; [3]Janssen

Objectives: Develop a population model quantifying the myelosuppressive effect of AR exposure on ANC time-course in NHPs, and establishing the relationship between ANC time-course and OS in NHPs following AR exposure, in the presence or absence of treatment with filgrastim a recombinant granulocyte colony-stimulating factor.
Methods: Modeling was performed using data in adult rhesus macaques (weight 4–6.5 kg) that were exposed to 750 cGy of whole body irradiation [1]. NHPs were either given placebo or subcutaneous 10 μg/kg of filgrastim daily beginning one day after irradiation. ANC levels were measured at baseline and every 1–2 days for 60 days after irradiation. The time to death or last observation was collected for OS analysis. Population pharmacodynamic modeling of ANC response and OS following irradiation with or without filgrastim treatment was performed.
Results: The granulopoiesis model consisted of three components: (1) a catenary model of synthesis, proliferation and maturation of neutrophils from stem cells; (2) K-PD model of radiation injury (duration 10 days) [2]; and (3) a pharmacodynamics-mediated drug disposition model of filgrastim. Receptor occupancy was used to drive efficacy of both stem cell production (STIM = 4.5) and maturation (STIM = 2.2). OS was described using a survival model with time varying hazard, relating log hazard to a Box-Cox transformation of ANC, delayed through an effect compartment. The ANC timecourse (neutropenia depth and duration) was found to explain 76 % (95 % CI 41–97 %) of the survival benefit from filgrastim treatment (OS = 79.2 %) over placebo (OS = 40.9 %)
Conclusions: The granulopoiesis model adequately captured the ANC time-course after irradiation with and without filgrastim treatment. The OS model confirmed that NHP OS depends on the duration and depth of neutropenia and that ANC is a valid surrogate to predict OS in NHPs receiving irradiation.

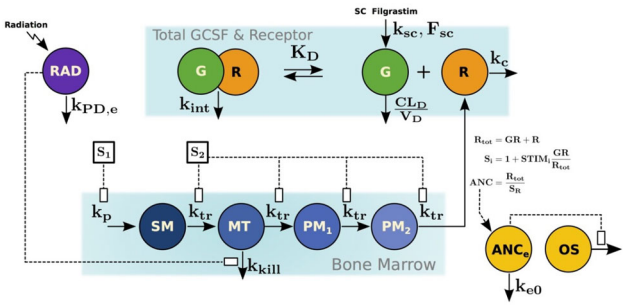

References:

1. Farese et al. Radiation Research, 179(1), 89–100.
2. Jacqmin et al. JPKPD 34(1), 57–85.

T-12

Development of a Joint PKPD Model of the Hyperinsulinemic Glucose Clamp

Craig Fancourt*, Chandni Valiathan, Dan Tatosian, Carolyn Cho, Sandra A.G. Visser

Merck & Co., Inc., Kenilworth, NJ USA

Objectives: The hyperinsulinemic glucose clamp is an experimental platform to measure insulin sensitivity by infusing exogenous insulin and glucose to measure insulin effect on whole-body glucose disposal rate (GDR) during homeostasis. We developed a pharmacokinetic (PK) - pharmacodynamic (PD) model of the hyperinsulinemic clamp that is physiologically plausible and can fit clinical data.
Methods: The PK model consisted of saturable binding of insulin to the insulin receptor, expressed as target-mediated drug disposition, which at steady-state results in Michaelis–Menten saturable clearance, plus a non-specific linear first-order clearance. The PD model consisted of (1) non-insulin mediated glucose disposal (constant glucose clearance); (2) non-linear and saturable insulin mediated glucose uptake (an insulin Emax model with Hill coefficient); and (3) glucose auto-inhibition of glucose uptake (a glucose Emax model, which modulates the sum of (1) and (2)).
This PKPD model was simultaneously fitted to data from [1], which studied 22 healthy male subjects at four porcine insulin infusion rates (0, 20, 60, 400 mU/min/m^2) and four glucose clamp levels (90, 160, 250, 400 mg/dL), using non-linear least-squares on log-transformed steady state insulin concentrations and GDR measurements.
Results: The model fit (Figure) was good and all parameters could be estimated. For the PK model, non-specific insulin clearance was 5.1 mL/kg/min, maximum IR clearance was 11.2 mL/kg/min, and Kd of insulin for its receptor was 716 pM. For the PD model, maximum non-insulin mediated clearance was 2.8 mL/kg/min, maximum insulin-mediated clearance was 11.1 mL/kg/min, insulin concentration at half-maximal GDR was 552 pM with a Hill coefficient of 2.0, and glucose concentration at half-maximal GDR was 353 mg/dL.

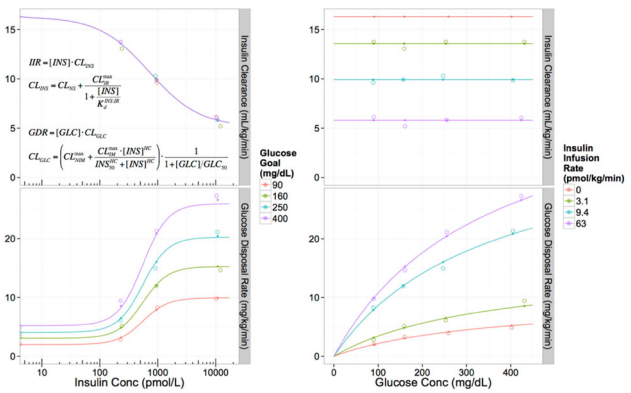

Fig. 1 PK (top) and PD (bottom) model fit to clinical clamp data. Open circles are data, closed circles are model predictions at measured values, and lines are model predictions at nominal values

Conclusions: A joint PKPD mechanistic model can describe and explain insulin PK and action during the hyperinsulinemic clamp. This model was successfully applied to investigate differences in PKPD between healthy and T1DM subjects [2].

References:

1. Yki-Järvinen et al., J. of Clinical Investigation 79.6(1987):1713.
2. Burrows et al. ACOP 2015.

T-13

Relationship Between Eslicarbazepine Exposure and Efficacy of Eslicarbazepine Acetate Adjunctive Therapy

Harvey, Jay[1*]; Andermann, Eva[2,3]; Chung, Steve[4]; Trinka, Eugen[5]; Cendes, Fernando[6]; Passarell, Julie[7]; Fiedler-Kelly, Jill[7]; Ludwig, Elizabeth[7]; Sunkaraneni, Soujanya[8]; Sousa, Rui[9]; Rocha, Francisco[9]; Blum, David[8]

[1]Texas Epilepsy Group, Dallas, TX; [2]Montreal Neurological Institute and Hospital, Montreal, QC, Canada; [3]McGill University, Montreal, QC, Canada; [4]St. Joseph's Hospital and Medical Center, Phoenix, AZ; [5]Paracelsus Medical University, Salzburg, Austria; [6]Universidade Estadual de Campinas, Campinas, Brazil; [7]Cognigen Corporation, Buffalo, NY; [8]Sunovion Pharmaceuticals Inc., Marlborough, MA; [9]BIAL – Portela & Ca, S.A., São Mamede do Coronado, Portugal

Objectives: Data from three randomized controlled trials demonstrated eslicarbazepine acetate (ESL) effectiveness as adjunctive therapy for partial-onset seizures, and were used to examine relationships between eslicarbazepine (primary active metabolite) exposure and efficacy endpoints.
Methods: Trials comprised 8-week baseline/14-week double-blind periods (titration and maintenance). ESL doses were 400–1200 mg QD. Developed models described relationships between eslicarbazepine exposure and: standardized seizure frequency (SSF; seizure frequency per 4 wks); probability of response (PR; $\leq$50 % reduction in SSF from baseline), and weekly seizure frequency over time. Individual eslicarbazepine exposures were calculated using a previously developed population pharmacokinetic model.
Results: Data were from 1150 patients: 80 % Caucasian, 53 % male, median age 37 years, 48.3 % received baseline concomitant carbamazepine. SSF was highly variable at baseline. Predicted SSF decreased with increasing ESL dose (400 mg, 5.4; 800 mg, 4.6; 1200 mg, 4.3; placebo, 6.5), with smaller reduction (E_{max}; Table 1) with concomitant baseline carbamazepine use, and in Western Europe (WE) patients. Predicted PR was lower for WE versus non-WE patients [PR ranges for 400–1200 mg doses were 0.18–0.26 (placebo 0.12) versus 0.3–0.4 (placebo 0.21), respectively]. Maximum reduction (E_{max}) in weekly seizure frequency from baseline with ESL was 56 %, where 39 % of the effect was contributed by time and 61 % was related to eslicarbazepine average steady-state concentration (C_{av-ss}). Estimated eslicarbazepine EC_{50} (half-maximal effective concentration) of 9.4 μg/mL is similar to the median C_{av-ss} with ESL 800 mg QD.

Table 1 Parameter estimates and standard errors for the final model describing standardized seizure frequency

Parameter	Final parameter estimate Typical value (% RSE)
Baseline SSF (per 4 weeks)[a]	2.19 (1.3)
Effect of Western European region	0.228 (30.6)
Effect of Latin American region	0.310 (18.4)
Effect of North American region	0.46 (15.3)
Age effect (slope)	−0.00922 (18.3)
Constant placebo effect	−0.276 (13.1)
Emax at baseline SSF of 2.4	−0.822 (13.9)
Effect of baseline CBZ use on Emax	0.150 (37.5)
Effect of Western European region on Emax	0.242 (27.9)
EC50 (ng/mL)	3530 (51.0)
Additive RV[b]	0.0255 (58.0)

CBZ carbamazepine; EC_{50} half maximal effective concentration; *Emax* maximum pharmacologic effect, *RV* residual variability, *RSE* relative standard error, *SSF* standardized seizure frequency

[a] Eastern Europe and "Rest of World" combined was the reference region

[b] The estimate presented is a variance. The RV is described by a SD of 0.16 seizures

Conclusions: The predicted exposure-SSF relationship was shallow; only slight improvements in seizure control are expected at higher concentrations of eslicarbazepine, and therefore routine monitoring of plasma concentrations is not required.

The results in this abstract have been previously presented in part at the American Epilepsy Society Annual Meeting, December 2014, Seattle, WA and published in the proceedings as abstract #1.319.

T-14

A Method for Simulating Dopamine Agonist Self-Administration with a Receptor-Based Mechanism

Alexander C. Ross*, Andrew B. Norman

Department of Pharmacology, University of Cincinnati College of Medicine

Objectives: Rats trained to self-administer dopamine receptor agonists do so with a regularity predicted by $T = \ln(1 + D_U/D_{ST})/k$, where T is the inter-injection interval, D_U is the agonist unit dose, k is the first-order agonist elimination rate constant, and D_{ST} is the minimum level of agonist maintained in the body[1]. Herein is detailed a method for simulating self-administration behavior with a PK/PD model, as well as simulations that better reproduce self-administration behavior qualitatively and quantitatively[2]

Methods: MATLAB Simbiology was used to construct a two-compartment PK/PD model, where the brain compartment contains a steady-state receptor population that mediates a response in the form of an agonist dosing event. If the concentration of agonist-receptor complexes is above a concentration corresponding to priming threshold—the minimum concentration required to induce agonist self-administration events—and below a concentration corresponding to D_{ST}, then agonist self-administration events will occur at short and defined intervals. Agonist-receptor binding proceeds according to the law of mass action, elimination and inter-compartmental distribution are assumed to conform to first-order kinetics, and the model can be exported as a set of ordinary differential equations.

Results: The model reproduced observations made with rats self-administering dopamine receptor agonists including a proportional (but non-linear) relationship between the dose and inter-event intervals. D_{ST} and T are now quantitatively similar to data from rats. Antagonist-induced acceleration of self-administration results from an increase in D_{ST} and the consequent increase in the rate of agonist elimination.

Conclusions: Several fundamental features of drug self-administration behavior can be explained by PK/PD interactions, which provides opportunities for pharmacometrics to advance the understanding of addictive behavior. This in silico approach provides a useful tool for exploring the contributions of specific pharmacological parameters to addictive behavior.

References:

1. Tsibulsky, V. L. & Norman, A. B. Brain research 839, 85–93 (1999).
2. Ross, A.C., Tsibulsky, V.L., & Norman, A.B. J Pharmacokinet Pharmacodyn 41, S77 (2014).

T-15

Population Pharmacokinetic Model for Oral Endoxifen in Patients with Breast or Gynecologic Cancers

Andrew Ralya[1], Richard C. Brundage[2], Renee M. McGovern[1], Matthew P. Goetz[1], Shivaani Kummar[3], Alice P. Chen[4], Joel M. Reid[1*]

[1]Mayo Clinic, Rochester, MN; [2]University of Minnesota, Minneapolis, MN; [3]Stanford University, Stanford, CA; [4]National Cancer Institute, Bethesda, MD

Objectives: To develop a population pharmacokinetic (PK) model to describe variability in the pharmacokinetics of oral endoxifen, evaluate PK linearity over dose and time, and to guide dosing and future trial design.

Methods: Two Phase-I dose-escalation trials (NCT01273168, NCT01327781) were conducted in breast or gynecologic cancer patients receiving flat oral doses of 20–300 mg (Z)-endoxifen HCl daily, on 28-day cycles. Intensive sampling occurred on days 1 and 28, and troughs on days 7 and 14. 1087 cycle-1 concentrations in 63 patients (median weight 68.9 kg) were available. Numerical values were retained for concentrations below the lower limit of quantification (10 samples), and values below the limit of detection were entered as concentration zero (4 of these 10 samples). Nonlinear mixed-effects modeling was performed using NONMEM and Pirana software. The model was evaluated with goodness-of-fit plots and visual predictive check.

Results: A 2-compartment model with first-order elimination, first-order absorption, and an absorption lag adequately described the data; a combined proportional and additive residual error was used. The typical (% RSE) oral apparent clearance (CL/F), apparent volume of central compartment (V2/F), apparent volume of peripheral compartment (V3/F), apparent intercompartmental clearance (Q/F), absorption rate constant (k_a), and absorption lag time were 4.63 L/h (5 %), 253 L (7 %), 88.1 L (19 %), 15.1 L/h (32 %), 0.984 h^{-1} (14 %), and 0.418 h (3 %), respectively. Between subject variability

(% RSE) for CL/F, V2/F, V3/F and k_a were 39 % (9 %), 37 % (15 %), 48 % (24 %) and 99 % (13 %), respectively. BSV on Q/F could not be estimated. All shrinkages were below 10 %, except 53 % on V3/F. GOF and VPC plots were deemed to be adequate.
Conclusions: A population pharmacokinetic model was identified that demonstrated endoxifen PK parameters were linear in the dosing range of 20–300 mg, and were unchanged over 28 days of dosing.

T-16

Simulated Implications of Predicted PA Kinetics in Humans for Treatment of Inhalational Anthrax

A. Corey*

Parexel International

Objectives: Extrapolated protective antigen (PA) kinetics in humans (see companion abstract) allow exploration of inhalational anthrax treatment options. These simulations assessed activity of 40 mg/kg intravenous raxibacumab given alone or with antibiotic after human *Bacillus anthracis* spore exposure.
Methods: Human raxibacumab concentration–time profiles were simulated using an existing model for healthy subjects [1]. Since raxibacumab clearance increases in anthrax-infected animals, additional human raxibacumab profiles were simulated with increased clearance. PA concentration–time profile simulations in humans used extrapolated PA kinetic parameters. PA profiles were simulated with and without antibiotic induced PA clearance, representing antibiotic-sensitive and -resistant infections, respectively. Dosing times assessed ranged from 0 to 336 h post spore exposure. Plots of simulated median and 90 % prediction interval (PI) raxibacumab and PA profiles were examined. Raxibacumab levels equimolar to or greater than concurrent PA levels were considered protective [2].
Results: For simulated antibiotic–resistant strains, raxibacumab administered at the time of spore exposure protected ≥95 % of subjects for nearly 6 days. Antibiotic killing of bacteria eliminates PA production, allowing PA clearance. Antibiotic treatment within 4 days after spore exposure should prevent toxemia, while later intervention allows toxemia to develop. Concurrent raxibacumab given before 7 days post spore exposure would protect ≥90 % of subjects. Raxibacumab administered ≥7 days post exposure would result in some subjects not having adequate protection against the toxin, despite eradication of bacteria by concurrently administered antibiotic (Figure 1). Treatment delay to ≥ 9 days post exposure results in ≥ 50 % of subjects having raxibacumab levels inadequate to neutralize concurrent toxin levels.

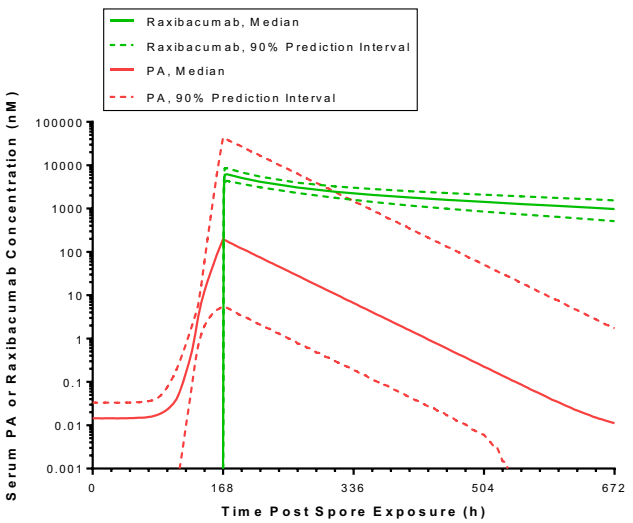

Fig. 1 Simulated human raxibacumab and PA Profiles with Raxibacumab/Antibiotic Treatment at 168 h Post Spore Exposure

Conclusions: These simulations support combined raxibacumab/antibiotic use as soon as possible after spore exposure, given the expected uncertainty about elapsed time since spore exposure, rapid progression of toxemia, lack of widely available PA assays, and uncertainty about accrued tissue damage from unneutralized toxin exposure.

References:

1. Corey A, et al. AAPS Journal. NBC Abstract T2080, 2009.
2. Corey A, et al. AAPS Journal. NBC Abstract T3185, 2013.

T-17

Effect of Clinical Study Design on Estimation of Pharmacokinetic Parameters in Pediatric Populations Using Pharmacokinetic Parameters from Adult Populations as Bayesian Priors: Application to Target Mediated Drug Disposition Models (TMDD)

Girish Bende[1], Joel S. Owen[1], Juan Jose Pérez-Ruixo[2], and Sameer Doshi[3*]

[1]School of Pharmacy, Union University, Jackson, TN, USA; [2]Janssen Research & Development, Beerse, Belgium; [3]Amgen Inc., One Amgen Center, Thousand Oaks, CA, USA

Objective: To assess the accuracy and precision of clearance estimates obtained from sparse pediatric data using adult population pharmacokinetic parameters as Bayesian priors and to evaluate the frequency of Type 1 and Type 2 errors.
Methods: Pediatric population data were allometrically simulated using Michaelis–Menten (MM) simplification of target mediated disposition model with known proportional differences (True-$\Delta = 0.6\times$, $0.8\times$, $1.0\times$, $1.2\times$, $1.4\times$) between adult and pediatric clearance parameters. In total, 25 scenarios were comprised of different numbers of patients (n = 3 to 15) and samples (2 to 10 per subject) at five dose levels per subject with concentrations spanning the nonlinear region. Clearance parameters and estimates of differences in linear (Δ-CLL) and non-linear (Δ-CLN) clearance s were assessed from simulated data. Accuracy and precision were calculated as mean prediction error (MPE) and root mean square error (RMSE).
Results: The accuracy and precision of estimates of Δ-CLL and Δ-CLN were high (MPE < 25 %; RMSE < 0.3) for all studied scenarios and conditions (True-Δ). The precision of both parameters increased with increases in sample size and number. However, an increase in the number of samples did not substantially alter the accuracy in the estimation of Δ-CLL and Δ-CLN. Across scenarios, Δ-CLN estimates were more accurate and precise than Δ-CLL estimates. Type II error was near zero in cases Δ = 0.6 and 1.4, and greatest in sparsest data.
Conclusions: Despite sparse sampling and limited subjects, clearance parameters in pediatric populations can be estimated with reasonable accuracy and precision by leveraging adult data as Bayesian priors. Results demonstrate pediatric studies can be suitably designed using this approach in order to minimize the number of subjects and samples without compromising power to discriminate pediatric from adult clearances when differences exist.

T-18

Prediction of Human Immunogenicity for a Biotherapeutic Candidate Using a Mechanistic Model of the Immune System

Lora Hamuro[1,*], Craig J. Thalhauser[2*], Akbar Nayeem[3], Giri S. Tirucherai[4], Renuka Pillutla[1], Binodh DeSilva[1], and Tarek Leil[2]

[*]Co-contributors, [1]Bioanalytical Sciences, [2]Quantitative Clinical Pharmacology, [3]Molecular Discovery Technologies, [4]Clinical Pharmacology and Pharmacometrics, Bristol-Myers Squibb, Princeton NJ 08543

Objectives: To evaluate utlity of a semi-mechanistic model of the humoral immune system to predict the anti-drug antibody (ADA) response for a biotherapeutic in early clinical development
Methods: A model was developed using a modified form of a published mechanistic model of the humoral immune response [1]. PK/PD parameter estimates and ADA were obtained from a single ascending dose (SAD) trial for the biotherapeutic agent. Other modifications included target-mediated drug disposition (TMDD), candidate-specific MHCII binding affinities, and refined MHCII allele frequencies in the target population. MatLab was used for modeling and simulations. 100 trial simulations of each dose were performed and the distribution of predicted ADA positive subjects compared to clinical data.
Results: An antigenic peptide with predicted high binding affinity to MHCII alleles was identified and used in the model to predict ADA development in the SAD population. The observed ADA incidence was within the model predicted distribution of ADA-positive subjects for all dose groups except the lowest dose (Figure 1). Predictions showed a trend for increasing ADA frequency with dose, but still allowed for dose-independent ADA responses observed in the SAD trial. The model predicted that ADAs would not have a meaningful impact on the PK/PD after single dose administration, consistent with clinical observations.

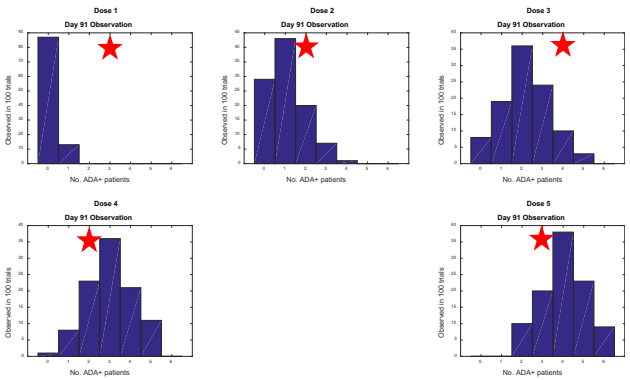

Fig. 1 Observed ADA Incidence (red star) versus Model Predicted for 5 Dose Levels

Conclusions: Immunogenicity is multi-factorial and includes both patient and product-specific factors. It was demonstrated that potential antigenic sequences when incorporated in a semi-mechanistic model of the immune system can be useful in predicting clinical ADA responses. Future efforts will focus on multiple dosing to evaluate model utility to predict effects of ADA formation on PK/PD after long-term dosing and to aid in design of future clinical trials.

References:

1. Chen, X., T. P. Hickling and P. Vicini (2014). CPT Pharmacometrics Syst Pharmacol 3: e133.

T-19

Exposure–Response of Idelalisib, a Novel PI3 Kδ Inhibitor, in the Combination Therapy of Chronic Lymphocytic Leukemia

Feng Jin*, Huafeng Zhou, Xiaoming Li, Terry Newcomb, and Srini Ramanathan

Gilead Sciences, Inc, Foster City, CA 94404

Objectives: Idelalisib is a potent PI3 Kδ inhibitor that is approved in combination with rituximab in relapsed CLL and as monotherapy in refractory FL and SLL. The relationships between idelalisib and GS-563117 (the major inactive metabolite) plasma exposures vs its efficacy/safety in the treatment for patients with CLL were evaluated.
Methods: Idelalisib and GS-563117 plasma exposures were generated using population pharmacokinetic (PK) models previously established for idelalisib and GS-563117 based on data from several phase 1/2 clinical studies. The relationships between idelalisib and GS-563117 exposures from an efficacy/safety dose ranging study (101–02; 50 mg to 350 mg BID, 150 mg and 300 mg QD), a Phase 2 study (101–07), and a Phase 3 study (GS-US-312-0116) were determined. Efficacy endpoints included best overall response rate (BOR), duration of response (DOR), progression free survival (PFS), sum of products of the greatest perpendicular diameters (SPD) of index lesions, and lymph node response (LNR) and safety endpoints included neutropenia, diarrhea, skin rash, infection, and aspartate aminotransferase (AST) or alanine aminotransferase (ALT) elevation.
Results: Over a wide dose/exposure range in dose-ranging study 101–02, median SPD response increased with idelalisib exposure (C_{trough}) quartiles, reaching a plateau at the 3rd quartile (Q3: range ~295–437 ng/mL), which encompassed the median C_{trough} (349 ng/mL) at 150 mg BID, supporting the selection of 150 mg BID for further development. In study 101–07 and GS-US-312-0116, where idelalisib was evaluated as a combination therapy (with anti-CD20 agents rituximab or ofatumumab) in subjects with relapsed CLL, no relationship was observed between idelalisib exposure vs. any of the efficacy or safety endpoints evaluated based on analyses including logistic regression and Cox regression, indicating the absence of exposure-efficacy/safety relationships at 150 mg BID.
Conclusions: There were no exposure–response relationships observed for efficacy or safety endpoints at idelalisib 150 mg BID supporting this dose to be used in combination therapy in the treatment of CLL patients.

T-20

The Impact of Ribavirin Plasma and Cellular Pharmacokinetics and Host Genetics on Anemia and Antiviral Response to Hepatitis C Treatment

Liviawati S Wu[1*], Leah C Jimmerson[2], Christine E MacBrayne[2], Jennifer J Kiser[2], David Z D'Argenio[1]

[1]University of Southern California, Biomedical Engineering, Los Angeles, CA; [2]University of Colorado Skaggs School of Pharmacy and Pharmaceutical Sciences, Department of Pharmaceutical Sciences, Aurora, CO

Objectives: To develop a model relating ribavirin systemic and intracellular exposure [1] to toxicity (anemia) and drug response (viral load) as a basis for guiding a more precise treatment of HCV with ribavirin.

Methods: The study [1] enrolled 36 subjects: 18 received pegylated interferon alfa (Peg-IFN α) and ribavirin, 18 received Peg-IFN α, ribavirin, and telaprevir. The model framework consisted of a systemic pharmacokinetic model of ribavirin, a cellular phosphorylation model in peripheral blood mononuclear cells (PBMC) and red blood cells (RBC), a ribavirin-induced anemia (toxicity) model and a viral dynamic (efficacy) model. Potential covariates considered were the effect of telaprevir use, age, weight, sex, creatinine clearance, and inosine triphosphatase (ITPA) and interferon lambda 3 (IL28B) genetics. The analysis was performed using the maximum likelihood, expectation maximization (MLEM) algorithm in ADAPT 5.
Results: Ribavirin-induced anemia was described by an indirect response model with ribavirin triphosphate exposure in RBC stimulating the loss rate of RBC. The feedback effect of endogenous erythropoietin was included through regulation of the RBC production rate ($R_{in} \cdot [Hb_0/Hb]^{\gamma}$). Individuals receiving telaprevir, with wild-type ITPA genetics and IL28B CC genotype were most likely to experience anemia. The 2-equation viral dynamic model [2] was improved by incorporating the better treatment efficacy associated with the co-administration of telaprevir and IL28B CC genotype.

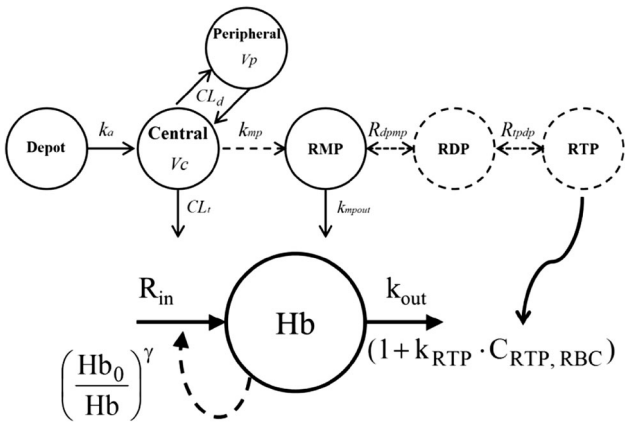

Conclusions: We have utilized quantitative systems modeling approaches to link ribavirin exposure to hemoglobin reduction and viral response, as well as the influence of pharmacogenetic and clinically relevant covariates on these processes. Simulations showed the utility of this model framework to investigate alternative treatment strategies to minimize the incidence of anemia associated with ribavirin treatment.

References:

1. Wu LS, et al. Antimicrob Agents Chemother. 59(4):2179-2188, 2015.
2. Neumann AU, et al. Science 282:103–107, 1998.

T-21

Population Pharmacokinetics of Tarolimus in Pediatric Renal Transplant Recipients on Two Different Formulations—Twice-daily Prograf® and Once-daily Advagraf®

SoJeong Yi[1], Hyeong-Seok Lim[2], Seonghae Yoon[1], Seol Ju Moon[1], Sang-il Min[3], Jongwon Ha[3], In-Jin Jang[1*]

[1]Department of Clinical Pharmacology and Therapeutics, Seoul National University College of Medicine and Hospital; [2]Department of Clinical Pharmacology and Therapeutics, Asan Medical Center, Seoul, South Korea; [3]Department of Surgery, Seoul National University College of Medicine and Hospital, Seoul, South Korea

Objectives: To evaluate the population pharmacokinetics of tacrolimus for both once-daily (Advagraf®) and twice-daily (Prograf®) formulations in pediatric renal transplant recipients
Methods: Thirty-eight children (age 7.0–16.3 years) in stable status after renal transplant took Prograf twice-daily until day 7 after study participation and from day 8 to 14 the tacrolimus regimen was converted to Advagraf once-daily on a 1:1 ratio for their total daily dose. From day 15 to 28, the dose of Advagraf was titrated based on the trough concentration. Concentration–time profiles were obtained for 24 h after dosing at day 7, 14, and 28. Population pharmacokinetic parameters were estimated using NONMEM (ver. 7.3) and the influence of covariates on pharmacokinetics were examined for *CYP3A5* genotype, demographics and clinical laboratory results. The adequacy of model was evaluated using standard goodness-of-fit diagnostics and visual predictive checks.
Results: Tacrolimus pharmacokinetics was best described by a two-compartment model with mixed first- and zero-order absorption kinetics for both formulations. The relative bioavailability of Advagraf to Prograf was 0.705, and the pharmacokinetic parameters of Advagraf including absorption rate constant, apparent clearance and apparent volume of distribution were significantly different from those of Prograf. The apparent clearance in CYP3A5 non-expressers (with *3/*3 genotype) were 24.6 and 29.1 % lower for Prograf and Advagraf, respectively, than those of CYP3A5 expressers (with *1/*1 or *1/*3 genotype). Due to circadian variation in twice-daily regimen, the rate constant on evening dose was smaller than that on morning dose (0.687 vs. 2.08 h^{-1}).
Conclusions: The conversion to once-daily Advagraf from twice-daily Prograf requires 30 % higher daily dose and once-daily regimen can reduce the circadian variation of absorption. Dose-adjustment according to *CYP3A5* genotype will be needed on both formulations.

T-22

tVPC: A User-Friendly Matlab-based Tool for the Evaluation and Simulation of Systems Pharmacology Models

Konstantinos Biliouris[1], Marc Lavielle[2], Mirjam N. Trame[1*]

[1]Center for Pharmacometrics and Systems Pharmacology, Department of Pharmaceutics, University of Florida, Orlando, FL; [2]Inria Saclay, POPIX team, Saclay, France

Objectives: Quantitative Systems Pharmacology (QSP) models are progressively entering the arena of contemporary pharmacology [1]. The efficient implementation and evaluation of complex QSP models necessitates the development of flexible computational tools that are built into QSP mainstream software. The objective of this work was to advance a recently developed tool, MatVPC, which was originally built for the automatic construction of Visual Predictive Checks (VPCs) and Quantified VPCs (QVPCs) of complex QSP models [2].
Methods: Two key options were added in MatVPC using Matlab 2013a: (i) conducting Monte Carlo simulations of the model and (ii) generating prediction-corrected VPCs (pcVPCs). In contrast to VPCs, Monte Carlo simulations provide the entire profile of the dependent and independent variable, plotted without the observations and usually without accounting for residual unexplained variability. pcVPCs are advanced VPCs wherein the biased originating from binning across different independent variables is removed [3].
Results: Two pharmacokinetic models were implemented in MatVPC to illustrate the new features. Monte Carlo simulations of these models were carried out and pcVPC plots were generated. The

pcVPCs were validated against pcVPCs constructed with the gold standard tools in pharmacometrics community [4], PsN/Xpose (with NONMEM) and Monolix.
Conclusions: MatVPC is continuously advanced and constitutes a useful addition to the toolboxes exploited by quantitative pharmacologists. MatVPC is publicly available at https://sourceforge.net/projects/matvpc/.

References:

1. Visser SAG et al., CPT: pharmacometrics & systems pharmacology (2014), 3(10): 1–10.
2. Biliouris K, Lavielle M, Trame MN, "MatVPC: A User-friendly Matlab Tool for the Automatic Construction of Visual Predictive Checks and Quantified Visual Predictive Checks", PAGE Meeting, Greece, 2015.
3. Bergstrand M, Hooker AC, Wallin JE & Karlsson MO (2011), The AAPS journal, 13(2), 143–151.
4. Vlasakakis G et al., CPT:pharmacometrics & systems pharmacology (2013), 2.5:e40.

T-23

Assessment of Partial AUC Requirement for Bioequivalence Evaluation of Methylphenidate Hydrochloride Extended-Release Oral Suspension

Nan Zheng*, Lanyan (Lucy) Fang

Office of Generic Drugs, U.S. Food and Drug Administration

Objectives: Quillivant XR (methylphenidate hydrochloride [MPH] extended-release oral suspension) is a modified-release formulation designed for a rapid initial drug release followed by a sustained drug release throughout the day. This work evaluates whether partial AUC would offer additional assurance in bioequivalence evaluation of generic products that reference Quillivant XR.
Method: We conducted sensitivity analysis on the pharmacokinetics/pharmacodynamics (PK/PD) model developed by the reference product sponsor. We evaluated the sensitivity of PK (Cmax, AUC0-t, AUC0-3, AUC3-7, AUC7-12 and AUC3-24) and PD (Effmax, AUEC0-t, AUEC0-3, AUEC3-7, AUEC7-12 and AUEC3-24) endpoints in response to formulation changes. With the formulation-specific model parameters varied for the test formulation, we calculated the test-to-reference ratios of these PK and PD parameters in a typical study subject, and calculated the chances of passing when bioequivalence testing was based on Cmax, AUC0-t, AUC0-3, AUC3-7, AUC7-12 and AUC3-24, in simulated single-dose, 2-sequence, 2-treatment bioequivalence studies.
Results: A one-compartment model with linear elimination and a parallel, zero order and first order absorption as well as a direct effect Emax model was used to describe PK/PD profile after Quillicant XR administration. Dose level, fraction of total dose, lag time and absorption rate for the first order absorption, lag time and duration for the zero order absorption, were identified as the formulation-specific model parameters. PK endpoints are in general more sensitive than PD endpoints to changes in formulation-specific model parameters. For example, values of all PK endpoints increase proportionally with dose while PD endpoints exhibit less than dose proportional increase. AUC0-3 and AUC7-12 are more sensitive than AUC0-t to changes in most of formulation-specific model parameters.
Conclusions: Because rapid onset and sustained exposure up to 12 h are important to achieve desirable therapeutic outcome for Quillivant XR and because partial AUCs are more sensitive to formulation-specific parameter changes than the conventional metrics of Cmax and AUC, we recommend using partial AUCs in bioequivalence evaluation of generic MPH extended-release oral suspension.

References:

1. http://www.regulations.gov/#!documentDetail;D=FDA-2014-P-1269-0001.

T-24

Quantitative Model Diagrams (QMD): A New Perspective in Model Evaluation

Benjamin Guiastrennec[1*], Ron J. Keizer[2] and Mats O. Karlsson[1]

[1]Department of Pharmaceutical Biosciences, Uppsala University, Uppsala, Sweden; [2]Insight$_{RX}$, San Francisco, CA, USA

Objectives: To facilitate model communication and evaluation through intuitive visual representation of their structure, parameter values and uncertainty.
Methods: An open source R package (R 3.2.0) was developed for the translation of model structure from NONMEM output and scaling of parameters into diagrams, using the packages DiagrammeR [1] and GraphViz [2] for plotting. QMD were generated by scaling the compartment size to the distribution volume and arrow width to the corresponding clearance or rate constant. When available, parameter uncertainty could be visualized using color-coded compartments and arrows.
Results: Diagrams for the standard NONMEM model library (ADVAN 1–4 and 11–12) have been fully automated. Differential equation-based models have been implemented to require minimal or no user input. To illustrate the use of QMD in Pharmacometrics, three example models of various complexities were selected, including a 2-compartment model with first order absorption [3], a Markov model [4] and a physiologically-based pharmacokinetic model [5].
Conclusion: QMD effectively summarized the information on model structure, compartment volume, clearance and rate constant, along with their uncertainty within a single intuitive graph. Informative representation of pharmacometric models was demonstrated to be applicable for a range of model structure and complexity and may improve model communication within and outside of the pharmacometric community.

References:

1. Sveidqvist et al. R package version 0.7. (2015).
2. Graphviz. [www.graphviz.org].
3. Dorlo et al. AAC, 52:8, 2855–2860. (2008).
4. Lacroix et al. CPT, 86:4, 387–395. (2009).
5. Björkman. BJCP, 59:6, 691–704. (2004).

T-25

Aqueous Humor VEGF Suppression and Clinical Efficacy of VEGF-targeting Biologics in Age-related Macular Degeneration

Songmao Zheng, Weirong Wang*

Biologics Clinical Pharmacology, Janssen R&D, 1400 McKean Road, Spring House, PA 19438

Objectives: Biologics targeting vascular endothelial growth factor (VEGF) are highly effective for age-related macular degeneration (AMD) treatment. The efficacy of anti-VEGF biologics is determined by ocular drug exposure and their ability to neutralize VEGF in the vitreous and aqueous humor. This study aims to identify the relationship between local VEGF suppression and clinical efficacy of biologics targeting VEGF.
Methods: A target-mediated drug disposition (TMDD)-based pharmacokinetic/target engagement (PK/TE) model was developed using literature data. Clinical data of ranibizumab PK and VEGF in the aqueous humor, as well as preclinical PK data of ranibizumab and aflibercept in the vitreous and/or aqueous humor, were used. Model fitting and simulations were conducted using NONMEM® V7.2.0.
Results: The PK of ranibizumab in human aqueous humor was described by a one compartment model. The degradation rate constant of VEGF in human aqueous humor was estimated using VEGF baseline and suppression data post ranibizumab intravitreal injection in three clinical studies. Clinically, ranibizumab dosed at 0.5 mg Q4W showed similar efficacy (i.e. visual acuity) when compared with aflibercept dosed at 2 mg Q4W (3 doses) + Q8W. Interestingly, our PK/TE model predicted similar magnitude of VEGF lowering following 0.5 mg Q4W ranibizumab and 2 mg Q8W aflibercept. In addition, it had been shown that aflibercept dosed at 2 mg Q4W is no more efficacious than 0.5 mg Q4W, while 2 mg Q12W is less efficacious. Based on these findings, the PK/TE model was able to identify the levels of VEGF suppression associated with compromised efficacy, and where further suppression of VEGF had no additional benefit.
Conclusions: A mechanism-based PK/TE model that integrated drug PK, target-binding affinity and target kinetics was developed to benchmark the desired local target suppression and clinical efficacy. Such modeling approach can be used to determine dosing regimens for new investigational biologics with similar mechanism of action.

T-26

Comparative Evaluation of Bias and Precision in Compartmental Models of Enterohepatic Circulation

Malek F. Okour*, Richard C. Brundage

Experimental and Clinical Pharmacology, University of Minnesota

Objectives: Enterohepatic circulation (EHC) of drugs can be described as a distribution process in which a fraction of conjugated drug is excreted in bile and transported to the gut, undergoes deconjugation by the gut flora, and then get reabsorbed back to the systemic circulation. The presence of EHC results in changes in the pharmacokinetic profile of the drug. The pharmacokinetic evaluation of drugs exhibiting EHC has been variable in the literature and frequently considers EHC as an elimination process rather than distribution. The objective of this analysis was to evaluate pharmacokinetic bias and precision of several compartmental models used to analyze simulated data from a drug undergoing EHC.
Methods: Stochastic simulation and estimation was implemented using NONMEM and PsN. An oral dosing depot with 1-compartment disposition and semi-mechanistic EHC model that included a gallbladder and continuous bile flow was used to simulate 250 datasets of 50 subjects; samples were obtained at times 0.5, 1, 2, 4, 6, 8, 10, 12, 16, and 24 h. Patients were assumed to have food intake at times 1,4 and 10 h that stimulated gallbladder contraction. The percentage of the drug undergoing EHC (PCT) was 40 %. Data analytic models included 1-compartment, 2-compartment, and several plausible EHC-based models with and without a gallbladder, continuous bile flow, and inclusion of 0, 1, 2 or 3 meals. Comparisons of OFV, CL, PCT, BSV, and RUV estimates across models were based on bias and precision.
Results: As expected, the simulation model produced the lowest OFV and smallest bias and imprecision. Inclusion of a gallbladder compartment also provided similar results, but ignoring meals in the model to stimulate gallbladder contractions generally increased bias. Not including a continuous bile flow in the model substantially increased bias in PCT. Both 1- and 2-compartment models produced results with more bias.
Conclusion: This study suggests that when modeling a drug undergoing EHC, it may be important to include a gallbladder compartment, continuous bile flow, and feeding times to minimize bias in parameter estimates.

T-27

Interpretation of Drug–Drug Interaction Study Results of Long Elimination Half-Life Drugs: Comparison of Conventional Bioequivalence Test Anda Model-Based Approach

Dooyeon Jang[1,2*], Sunil Youn[1,2], Gab-jin Park[1,2], Wan-Su Park[1,2], Taegon Hong[1,2], Jongtae Lee[1,2], Seunghoon Han[1,2], Dong-Seok Yim[1,2]

[1]Department of Clinical Pharmacology and Therapeutics, Seoul St. Mary's Hospital, Seoul, Korea; [2]PIPET (Pharmacometrics Institute of Practical Education and Training), College of Medicine, the Catholic University of Korea, Seoul, Korea

Objectives: For drugs with long elimination half-lives, multiple dosing drug–drug interaction (DDI) studies are challenging in the aspect of time, budget, and ethics from long-term administration of drugs to healthy subejcts. Despite multiple dosing, steady state may not be accomplished, and conventional non-compartmental analysis (NCA) at this situation may give biased bioequivalence (BE) test results. Thus, we tried a a mixed-effects model-based BE test with simulated data to compare its performance with the conventional BE test.
Methods: We used data from a healthy subjects DDI study (amlodipine for 8 days and then amlodipine and drug X for the next 10 days). Full pharmacokinetic (PK) sampling for amlodipine was performed on day 8 and 18. and a amlodipine population PK model developed using the PK data of day 8 (NONMEM, Ver. 7.2) was used to simulate the amlodipine $C_{max,ss}$ and $AUC_{\tau,ss}$ for day 18. The conventional BE test results (day 8 versus day 18) were compared with the BE test results on simulated data (day 18 simulated versus day 18 observed).
Results: Plasma concentration–time profiles of amlodipine were best described by a two-compartment model with first-order kinetics. The geometric mean ratios (GMR) and their 90 % confidence intervals (CI) of the conventional method were 1.187 (1.135–1.239) for C_{max} and 1.187(1.135–1.242) for AUC. The GMR for modeling based method were 0.997 (0.978–1.016) for C_{max} and 0.973 (0.962–0.983) for AUC, that clarified the PK of amlodipine did not change by DDI.
Conclusions: The PK analysis method using modeling and simulation enabled us to distinguish between the effect of DDI and the effect of drug accumulation. Likewise, the proposed method may be useful to evaluate DDI of drugs with long elimination half-lives that may not reach steady-state within the study periods.

References:

1. Gobburu, J. V & Marroum, P. J. Utilisation of pharmacokinetic-pharmacodynamic modelling and simulation in regulatory decision-making. Clin. Pharmacokinet. 40, 883–892 (2001).

T-28

Semi-Mechanistic Model to Characterize Effects of Gastric Emptying on Glucose Absorption in Obese and Non-Obese Adults

Mélanie Wilbaux[1*], Bettina Woelnerhanssen[2], Christoph Beglinger[2], Anne Christin Meyer-Gerspach[2], Johannes N. Van Den Anker[1,3], Marc Pfister[1,4]

[1]Department of Paediatric Clinical Pharmacology, Paediatric Pharmacology and Pharmacometrics Research Center, University Children's Hospital Basel (UKBB), Basel, Switzerland.[2]Division of Gastroenterology and Hepatology, University Hospital of Basel, Basel, Switzerland. [3]Division of Pediatric Clinical Pharmacology, Children's National Health System, Washington, DC, USA.[4]Quantitative Solutions LP, Menlo Park, CA, USA

Objectives: To develop a semi-mechanistic model that can be used to characterize and compare effects of gastric emptying on glucose absorption jointly in obese and non-obese healthy adults.
Methods: Glucose, insulin and gastric emptying data from 36 obese and 24 non-obese healthy adults were available. Oral glucose tolerance tests (OGTTs) were performed in each study subject with 10, 25 or 75 g of glucose. Blood samples and gastric emptying rates were collected at different time-points until 180 min. A semi-mechanistic model was developed to characterize gastric emptying effects on glucose absorption. A population analysis was performed using NONMEM7.3.
Results: Glucose kinetics after OGTTs was characterized by a one-compartment model. The complex absorption profile of glucose was adequately described using individual gastric emptying profiles as time-varying covariate on glucose absorption rate. Observed insulin profiles affected both glucose production and clearance. Differences between obese and non-obese subjects were identified: (i) faster glucose absorption rate in obese subjects ($Ka_{Obese} = 10*Ka_{Non\text{-}obese}$), (ii) different gastric emptying effect on glucose absorption and (iii) different insulin effect on glucose clearance, linear effect in non-obese and saturable effect in obese subjects. According to goodness-of-fit plots, glucose absorption and kinetics was properly fitted in both obese and non-obese healthy adults. Visual predictive check demonstrated good predictive performance of the developed model; Fig. 1.

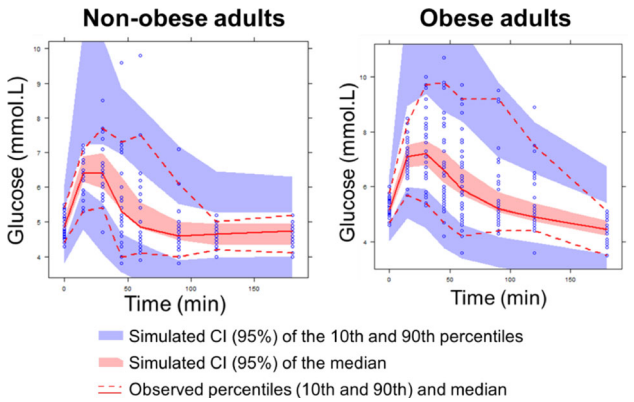

Fig. 1 Visual predictive check

Conclusion: This is the first semi-mechanistic model that characterizes interactions between gastric emptying, glucose absorption and glycemic control in both non-obese and obese adults. Such model can be applied to investigate effects of bariatric surgery on glucose kinetics, identify differences in glucose absorption between adults and pediatrics and quantify drug effects on gastric emptying and glucose absorption.

T-29

Towards Improving In Vitro–In Vivo Toxicity Extrapolation Using Multi-Scale Modeling: A Proof of Concept on Paracetamol Hepatotoxicity

Geraldine Celliere[1*], Noemie Boissier[1], Ahmed Ghallab[2], Reham Hassan[2], Amnah Othman[2], Seddik Hammad[2], Jan Hengstler[2], Dirk Drasdo[1]

[1]INRIA, Paris-Rocquencourt, France; [2]IfADo, Dortmund, Germany

Background: *In vivo* tests for toxicity assessment of drugs are increasingly replaced by in vitro approaches. However, the translation of in vitro results to in vivo conclusions is challenging and currently relies on PBPK/PD models. Yet, by considering the ADME processes within homogeneous compartments, classical PBPK/PD models do not properly represent some differences between the in vitro and in vivo situations that may be critical.
Objectives: We propose to take into account additional aspects, in particular (i) spatial inhomogeneities within organs [1], (ii) expression level differences of metabolic enzymes between cells in vivo and in vitro, and (iii) the possible influence of the time-dependent concentration experienced by the cells. We used paracetamol toxicity in mice as prototypical example.
Methods: Toxicity of paracetamol was determined experimentally by measuring the fraction of dead cells in vitro for several concentrations and in vivo for several doses. The in vitro–in vivo differences were explored using a multi-scale model that represents (i) each individual cell in a monolayer or liver lobule architecture, (ii) the intracellular metabolism of paracetamol in each cell, and (iii) paracetamol transport within the blood vessel network in vivo.

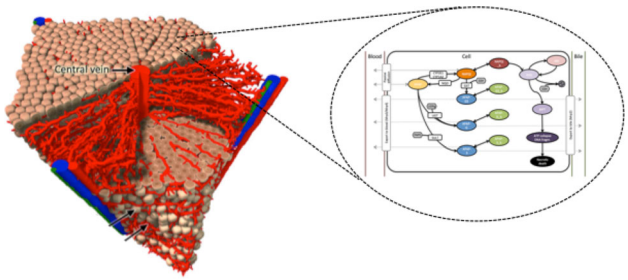

Fig. 1 A multi-scale model is developed to understand differences in paracetamol toxicity between in vitro and in vivo. In addiction to a PBPK module, the model comprises a spatial description of a liver lobule with blood flow and individual cells, and a metabolic model from drug entry to necrosis within each cell

Results: To compare the in vitro and in vivo toxicity, we first used a classical PBPK model to convert the in vivo dose-toxicity relationship into a concentration-toxicity relationship. Results show cells in vivo to be more susceptible to paracetamol than in vitro. Preliminary simulations indicate that the difference might be due to a down-regulation of CYP enzymes in vitro or to hypoxia due to liver congestion in vivo.
Conclusions: For paracetamol, simulations results of models refined beyond classical PBPK/PD show a better extrapolation of toxicity from in vitro to in vivo. Further simulations are being performed to better characterize the improvement obtained using the multi-scale model.

References:

1. Wambaugh, J., & Shah, I. (2010). PLoS Computational Biology, 6(4).

T-31

Delay Differential Equation Solver in ADAPT 5

Gilbert Koch[1,2*], Wojciech Krzyzanski[12] David Z. D'Argenio[3]

[1]Pediatric Pharmacology and Pharmacometrics Research Center, University Children's Hospital Basel, Basel, Switzerland; [2]Department of Pharmaceutical Sciences, University at Buffalo, Buffalo, NY, USA; [3]Department of Biomedical Engineering, University of Southern California, Los Angeles, CA, USA

Objectives: Delay differential equations (DDEs) are an important tool to model delays in biological systems, and become increasingly relevant in pharmacokinetics/pharmacodynamics (PK/PD) modeling [1] In contrast to ordinary differential equations, in DDEs the derivative of the states depends on both the current and past times. To efficiently solve DDEs, we extended the PK/PD software ADAPT 5 [2] with a DDE solver.
Methods: RADAR5 is the state-of-the-art DDE solver that can detect and solve stiff problems with state dependent delays [3]. RADAR5 subroutines were included in ADAPT 5 and its modeling language was expanded to account for additional DDE features such as delayed states and user defined history of the states. The DDE implementation was validated against published PK/PD models involving delays.
Results: PK/PD models in DDE formulation for cell maturation, infectious diseases, rheumatoid arthritis, and oncology were implemented in the extended ADAPT 5 software and applied to fit data. Model solutions were compared to the simulated results obtained by the DDE solver dde23 from MATLAB [4]. The PK/PD model library of ADAPT 5 was extended with examples of DDE based models from the above areas to demonstrate new DDE features.
Conclusions: RADAR5 allows applications of DDE based PK/PD models using ADAPT 5 algorithms that yield identical results with well-established DDE solvers.

References:

1. Koch G, Krzyzanski W, Perez-Ruixo JJ, Schropp J (2014) Modeling of delays in PKPD: classical approaches and a tutorial for delay differential equations. J Pharmacokinet Pharmacodyn 41(4):291–318.
2. D'Argenio DZ, Schumitzky A, Wang X (2009) ADAPT 5 User's Guide: Pharmacokinetic/Pharmacodynamic Systems Analysis Software. Biomedical Simulations Resource, Los Angeles.
3. Guglielmi N, Hairer E (2007), Stiff delay equations. Scholarpedia, 2(11):2850.
4. MATLAB Release (2014b) The MathWorks, Inc. MathWorks, Natick.

T-32

Dose-Exposure Simulation for Optimal Piperacillin-Tazobactam Strategy in Infants and Young Children

Céline Thibault[1], Nastya Kassir[3], Catherine Litalien[1,2], Julie Autmizguine[1,2*]

[1]Department of Pediatrics, CHU Ste-Justine, [2]Departement of Pharmacology, Université de Montréal, [3]Pharsight-A Certara Company, Montreal, Quebec, Canada

Objectives: To determine the optimal piperacillin-tazobactam dosing strategy in infants and children 2 months to 6 years to treat bacteria with increasing minimal inhibitory concentration (MIC).

Methods: Age and weight were simulated for 1000 infants and children based on WHO growth charts adapted for Canada. *Post-hoc* PK parameter estimates were generated using published clearance and volume of distribution data, assuming an inter-individual variability of 50 %. For different dosing regimens (0.5 to 4 h-infusion) and age groups, we estimated the probability of pharmacodynamics target attainment (PTA) over a range of MICs (4-128 mg/L). The pharmacodynamic target was defined as having the free piperacillin concentration above the MIC for ≥50 % of the dosing interval (50 % $fT > MIC$). A PTA ≥ 90 % at each MIC was defined as optimal.
Results: For MIC of 16 mg/L, the optimal dosing regimens were 80 mg/kg (4 h-infusion) every 8 h for infants 2 to <6 months and 130 mg/kg (4 h-infusion) every 8 h for children 6 months to 6 years (Table). Shorter infusions (0.5–2 h) failed to achieve PTA in all age groups and for all dosing regimens. None of the regimens were optimal at MICs >16 mg/L.

Table Probability of target attainment at minimal inhibitory concentration of 16 mg/L

Age	Piperacillin dosing Regimen	PTA (%) 0.5 h-infusion	PTA (%) 4 h-infusion
2 to <6 months	80 mg q 8 h	52	96
6 to <9 months	130 mg q 8 h	60	100
9 to <24 months	130 mg q 8 h	22	98
2 to 6 years	130 mg q 8 h	18	96

PTA probability of target attainment

Conclusion: Extended infusion of piperacillin-tazobactam dosing regimens were required to achieve optimal PTA at MIC of 16 mg/L in infants and children. Prospective clinical trials are necessary to validate the dosing regimens suggested in this study.

T-33

Improved Confidence Intervals and P-Values by Sampling from the Normalized Likelihood

Sebastian Ueckert[1,2*], Marie-Karelle Riviere[1], France Mentré[1]

[1]IAME, UMR 1137, INSERM and University Paris Diderot, Paris, France; [2]Pharmacometrics Research Group, Department of Pharmaceutical Biosciences, Uppsala University, Uppsala, Sweden

Objectives: Asymptotic theory-based statistics such as confidence intervals (CI) and p-values (PVAL) are the basis for most model-driven decisions in drug development. For small sample sizes these approximations do not hold and resampling methods are employed. Sampling from the normalized likelihood function represents an alternative, which with the development of Hamiltonian Monte-Carlo (HMC) methods becomes computationally attractive. The objective of this work was to compare HMC-based calculation of CI and PVAL with existing approaches.
Methods: A simulation study using a one-compartment model and different study sizes was used to evaluate the performance of HMC-based sampling from the normalized likelihood to calculate CI and PVAL.
CI: evaluation was based on runtime, median CI and coverage, and in comparison to CI obtained via covariance matrix (COV), log-likelihood profiling (LLP) and non-parametric bootstrap (BOOT).

PVAL: evaluation was based on runtime, type-I error and power, and in comparison to PVAL obtained via Wald test (WALD), log-likelihood ratio test (LRT) and permutation test (PERM).

The HMC-based methods were implemented using STAN with improper priors for sampling. Asymptotic theory and resampling-based results were obtained in NONMEM 7.3.

Results: The simulations showed good agreement between approaches for large sample sizes and increasing differences for smaller sample sizes. In contrast to most other methods, HMC showed nominal coverage and type-I error at all study sizes. In terms of computation time the HMC-based methods were between 10 and 60 times faster than resampling methods.

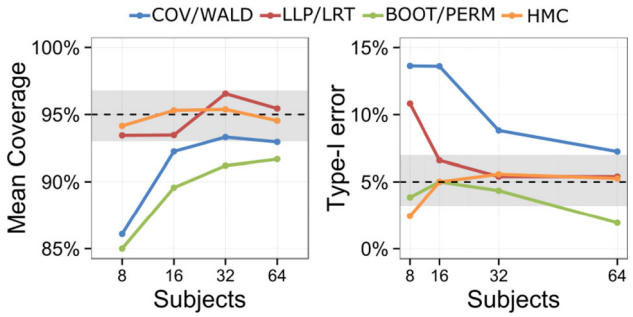

Fig. 1 Coverage (mean over all parameters) and type-I error from the simulation study for all investigated methods

Conclusions: CI and PVAL through sampling from the normalized likelihood using HMC yielded results with good theoretical properties at a drastically shorter runtime than resampling methods.

This work was supported by the DDMoRe project.

The results in this abstract have been previously presented in part at PAGE 2015, Crete and published in the conference proceedings as abstract 3632.

T-34

Handling Underlying Discrete Variables with Mixed Hidden Markov Models in NONMEM

Elodie L. Plan[1*], Joakim Nyberg[1], Robert J. Bauer[2], Mats O. Karlsson[1]

[1]Pharmacometrics Research Group, Department of Pharmaceutical Biosciences, Uppsala University, Sweden; [2]Pharmacometrics, R&D, ICON Development Solutions, MD, USA

Objectives: Unobserved phenomena/covariates are commonly not included in models, though many may be of great importance, hence ignoring them may cause a bias in estimates, e.g., masking effect of rescue medication in pain trials. Besides, latent variable models that represent the underlying disease have become an interest, due to their attractive drug effect characterization properties. Mixed Hidden Markov models (MHMM), capable of handling Markov chains of unobserved states and previously proposed [1], require maximum likelihood estimation (MLE) computation summing over all previous conditions.

The objectives of this work were to explore various MHMM implementations in NONMEM and to expand the investigation of the benefits of this methodology.

Methods: MHMM methodology was implemented in NONMEM7.3 with an initial stationary distribution and a scaling of the forward probabilities. A subroutine involving the Viterbi algorithm was used to evaluate the most likely hidden states chain during post hoc analysis.

First, 100 copies of a hypothetical trial (60 HIV + patients randomized to placebo or treatment with 60 observations each) were simulated and re-estimated with different models and MLE methods.

Second, an extension to a multivariate MHMM was developed (2 theoretical types of COPD records −1 measurement, 1 patient reported outcome- linked to presence or absence of relapse).

Results: MHMM can be implemented in NONMEM for systems involving 2 or more hidden states, discrete or continuous "open" observations and 1 or multiple variables. EM-methods, when applied to MHMMs, seem to be equally or more precise and accurate for fixed –not random– effects as well as faster than Laplace. In the 2 examples, MHMMs led to higher power to detect a drug effect, which was estimated closer to its true value compared to non-Markovian model (NMM).

Conclusions: MHMM offer possibilities of better understanding and modeling of underlying data in numerous applications.

Reference:

1. Delattre M, et al. JPKPD (2012).

The results in this abstract have been previously presented in part at PAGE24 (2015) and published in the conference proceedings as abstract 3625.

T-35

Mathematical Optimization of Combination Therapy for Chronic Myeloid Leukemia (CML)

Helen Moore[1*], Lewis Strauss[2], Urszula Ledzewicz[3]

[1]Bristol-Myers Squibb, Princeton, NJ, USA; [2]Bristol-Myers Squibb, Wallingford, CT, USA; [3]Southern Illinois University Edwardsville, Edwardsville, IL, USA

Objective: To use mathematical modeling and control theory to predict optimal dosing regimens for patients with chronic myeloid leukemia (CML).

Methods: A semi-mechanistic ODE model for in-host CML-immune dynamics was developed starting from a previous model [1]. The leukemic cells were further differentiated into quiescent and proliferating sub-types. Imatinib, dasatinib, and nivolumab were incorporated into the model. Some parameter estimates were obtained from literature or in vitro experiments. Others were obtained by fitting data from the randomized Phase 3 DASISION trial [2] using nonlinear mixed effects modeling in Phoenix NLME (1.3, Pharsight). Treatment constraints and an objective functional incorporating leukemic cell populations and toxicity from therapeutic agents were specified, starting from previous work [3, 4]. The objective functional was minimized using TOMLAB packages (BASE 8.0, SNOPT 8.0, and PROPT, Tomlab Optimization) with MATLAB (R2015a, Mathworks).

Results: A combination therapy regimen predicted to achieve optimal clinical outcomes was computed, given the specified constraints and the goals quantified in the objective functional. The full mathematical system and quantitative constraints will be shown, along with graphical representations of optimal regimens (including which drugs, doses, and timing) in different settings.

Conclusion: Control theory applied to a mathematical model of CML-immune dynamics can predict regimens expected to achieve optimal outcomes. Such regimens can help inform trial design or can be tested experimentally themselves. They can also provide a

benchmark for predictive comparison with other regimens of interest. This semi-mechanistic model is flexible enough to use in optimizing other therapies in the future.

References:

1. Moore and Li. A mathematical model for chronic myelogenous leukemia (CML) and T cell interaction. J Theor Bio (2004) 227:513–523.
2. Kantarjian, Shah, Hochhaus, et al. Dasatinib versus Imatinib in Newly Diagnosed Chronic-Phase Chronic Myeloid Leukemia. NEJM (2010) 362:2260–2270.
3. Nanda, Moore, and Lenhart. Optimal control of treatment in a mathematical model of chronic myelogenous leukemia. Math Biosci (2007) 210:143–156.
4. Schättler and Ledzewicz (2015). Optimal Control for Mathematical Models of Cancer Therapies. Springer Publishing Co., New York, USA.

T-36

Impact of Age on Population Parameter Estimates and Pediatric Prediction Performances of Monoclonal Antibody Clearance: A Simulation Study

Koichiro Yoneyama[1*], Yoshimasa Ishida[1], Tomohisa Saito[1], Satofumi Iida[1], Takehiko Kawanishi[1]

[1]Translational Clinical Research Science & Strategy Dept., Chugai Pharmaceutical Co., Ltd., Tokyo, Japan

Objectives: To explore the impact of the contribution of age to analysis datasets and estimation models on population parameter estimates (PPE) and pediatric prediction performances (PPP) of monoclonal antibody clearance (mAb CL) by a stochastic simulation and estimation approach.
Methods: Individual mAb CL data were simulated using a log-normal distribution model into which an allometric exponent (ALM) of 0.75 on body weight (BW) and an age-dependent maturation (MAT) submodel were incorporated according to Robbie et al. [1]. No target-mediated CL was assumed. Several datasets of CL were generated with different combination of subject's age categories (neonates/infants, children, adolescents and adults), and then analyzed by the true model and an alternative model without MAT. PPE were compared in terms of the analyzed dataset and applied model. PPP were evaluated by visual predictive checks. All analyses were conducted using NONMEM 7.2.0.
Results: When a dataset included all four age categories, all parameters of the true model were accurately estimated. The alternative model estimated ALM as approximately 0.94. Involving children's data in datasets enabled an accurate estimation of all parameters of the true model. With only adult data, the population mean, between-subject variability and ALM were comparable to the true values in both cases where estimated by the true and alternative models.
Conclusions: PPE of mAb CL are affected by the contribution of age to analysis datasets and estimation models. Children are a highly informative population to characterize mAb CL over age and BW. For pediatric predictions based on adult data, a simple approach assuming BW-proportional CL regardless of age (fixing ALM to 1 without MAT) may be useful. To be more accurate, it is recommended to fix ALM to 0.75 without MAT in adult population pharmacokinetic modeling, and then add the MAT submodel to the CL in pediatric simulations.

References:

1. Robbie GJ, et al. Antimicrob Agents Chemother. 2012;56(9): 4927–36.

T-37

Population Pharmacokinetics of Voriconazole in Healthy Korean Male with Various CYP2C19 Genotypes

Seol Ju Moon[1], Jangsoo Yoon[1], Jaeseong Oh[1], SeungHwan Lee[1], Kyung-Sang Yu[1*]

[1]Department of Clinical Pharmacology and Therapeutics, Seoul National University College of Medicine and Hospital, Seoul, Korea

Objectives: Voriconazole is a first line therapy for invasive fungal infections. Due to its highly variable and nonlinear pharmacokinetic(PK) characteristics, it is difficult to maintain voriconazole concentration in the therapuetic range. The objective of this study was to develop a population PK model of voriconazole in healthy Korean males with various CYP2C19 genotypes to aid personalized therapy of voriconazole.
Methods: Plasma voriconazole concentration—time data in one phase I study were used in population analysis. Subjects whose CYP2C19 genotypes were already known received a single intravenous dose of voriconazole and serial blood samples were collected for 24 h post-dose. The population PK model was developed using a nonlinear mixed-effects method (NONMEM®, Version:7.3). The first-order conditional estimation with interaction estimation method was implemented and model qualification was performed by bootstrapping and visual predictive checks(VPCs).
Results: A total of 650 voriconazole plasma concentrations from 49 healthy male volunteers with different CYP2C19 genotypes (EM: *CYP2C19**1/*1, N = 19; IM: *CYP2C19**1/*2, *1/*3, *2/*1, N = 21; PM: *CYP2C19**2/*2, *2/*3, *3/*3, N = 9) were included in the population PK analysis. A two-compartment nonlinear elimination model with combined error was chosen as the final PK model. The mean population maximum enzyme activity (V_{max}) was 36.9 mg/h and substrate concentration at which the reaction rate is half of V_{max} (K_m) was derived by the following equation: $K_m = TVK_m \cdot (age/26)$ mg/L where the TVK_m is 0.468, 0.742 and 2.43 for CYP2C19 EM, IM and PM, respectively. The mean population central volume of distribution (V1) was $48.2 \cdot (age/26)^{-0.759}$ L and peripheral volume of distribution was 127 L. Model evaluation by bootstrapping and VPCs suggested that the proposed model was adequate and robust with good precision.
Conclusions: The final population PK model adequately described the interindividual variability of plasma voriconazole concentrations among the subjects with different CYP2C19 genotypes. The model-fitted parameter estimates may be applied to develop the personalized therapy of voriconazole.

T-38

How Quantitative Modeling of a Biomarker was Leveraged in Understanding Pharmacodynamic Recovery: An Illustration using Changes in Natural Killer Cells with Tofacitinib

Manisha Lamba[1*], Matthew M Hutmacher[2], Samuel Zwillich[1], Sriram Krishnsawami[1]

[1*]Clinical Pharmacology, Pfizer, Groton, CT; [2]Ann Arbor Pharmacometrics Group, Ann Arbor, MI

Objectives: Tofacitinib is an oral Janus kinase (JAK) inhibitor for the treatment of rheumatoid arthritis (RA). JAK1 and JAK3 play key roles in lymphocyte development and homeostasis. The objective was to characterize the dose–response (DR) and time course of changes in Natural Killer (NK) cell counts in tofacitinib-treated RA patients.
Methods: Data were pooled from 3 parallel group, double-blind, placebo-controlled, Phase 2 studies. Patients received monotherapy (i.e. without background methotrexate [MTX]) in 2 studies, while the third study included background MTX. On-treatment data were collected at weeks 1, 2, 4 and 6 in the 6-week study following administration of placebo; 5, 15 and 30 mg BID tofacitinib; while baseline and 24-week data were collected in the other two studies evaluating placebo; 1, 3, 5, 10 and 15 mg BID doses. A square-root transformation was applied to the data and the model to correct the skewness in the NK cell counts. A drug-mediated inhibition of NK cell-synthesis was fitted within a longitudinal, nonlinear, mixed-effects model.
Results: The pooled DR comprised of 928 patients. NK cells showed dose-dependent decline with tofacitinib treatment, beginning at 2 weeks. NK cells were estimated to achieve nadir (steady-state) in 8–10 weeks after initiation of therapy. The estimated decreases in NK cells were 36 and 47 % for 5 and 10 mg BID doses, respectively. Based on the estimated elimination rate of NK cell counts (half life $\sim$14 days), NK cells counts were predicted to return to within 10 % of baseline within 4 weeks after cessation of therapy for both the 5 and 10 mg BID doses.
Conclusion: Application of model-based analyses on data pooled across studies with different durations, doses, and background treatments helped to quantity the degree of recovery of a relevant pharmacodynamic measure. The model-based findings from this analysis were incorporated into the prescribing information.

T-39

A Distributed Delay Approach for Modeling Delayed Outcomes in Pharmacokinetics and Pharmacodynamics Studies

Shuhua Hu*, Kevin Feng, Bob Leary, Mike Dunlavey

Certara/Pharsight, Cary, NC

Objectives: A distributed delay approach is used to model delayed outcomes, and it is conceptually similar to lifetime models [1] with each individual assumed to have its own lifespan. The goal is to demonstrate that this approach is general enough to incorporate many models as special cases including transit compartment models and models for describing double-peak phenomenon in pharmacokinetics.
Methods: Let k_{in} denote the inflow of signals to a terminating compartment, and $\mathfrak{T}$ be a random variable representing delay time with probability density function (PDF) G. Then the delayed signal is $x(t) = \int_0^\infty G(\tau)k_{in}(t-\tau)d\tau$. If $\mathfrak{T}$ denotes the absorption delay, then x is the input function feeding into the central compartment. While if $\mathfrak{T}$ represents the delay time for the observed drug effect, then x denotes the delayed drug effect.
Results: Let $\Gamma(t; v, k_a)$ denote the PDF of a gamma distribution with shape parameter v and rate k_a. We demonstrated that if $G(t) = \Gamma(t; v, k_a)$ with v being an integer, then the delayed signal reduces to a transit compartment model with v compartments. For impulsive inflow $k_{in}(t) = \sum_{i=1}^{m} D_i\delta(t-t_i)$ with multiple doses D_i's administered in a sequence of time points $t_i, i = 1, 2, \ldots, m$, we found $x(t) = \sum_{i=1}^{m} D_i G(t-t_i)$. This is the input function considered in [2, 3] feeding into the central compartment with $G(t) = \Gamma(t; v, k_a)$. We further showed that the distributed delay approach includes the two methods [4] for modeling double-peak phenomenon as special cases. Figure 1 illustrates good model fitting results for two example individuals [4] using FOCE-ELS in Phoenix® NLME™ (Pharsight/Certara).

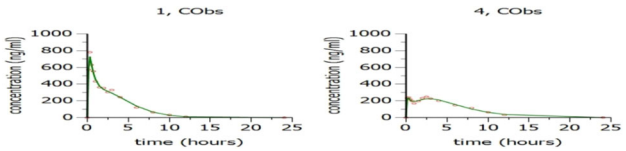

Fig. 1 Model fitting results for two individuals, where red circle denotes observations and green solid line represents predicated model solution

Conclusions: The distributed delay approach provides a more general and flexible way to model delayed outcomes including absorption, distribution, PK/PD link, drug response etc., and hence can capture more complex features.

References:

1. G. Koch, etc. J. Pharmacokinet Pharmacodyn (2014) 41:291–318.
2. R.M. Savic, etc., Journal of Pharmacokinetics and Pharmacodynamics (2007) 34:711–726.
3. J. Shen, etc., J Pharmacokinetics Pharmacodynamics (2012) 39:251–262.
4. K.R. Godfrey, etc., Computer Methods and Programs in Biomedicine, (2011) 104:62–69.

T-40

Real-Time Pharmacokinetic Analysis

Eric A. Sherer[1*], George W. Carpenter III[1], Katie A. Evans[1], Holly E. Grigsby[1], D. Patrick O'Neal[1]

[1]Louisiana Tech University, Ruston, LA

Objectives: We previously developed a photoplesthmograph (PPG) device which – operating on the same principles as a pulse oximeter—noninvasively measures the concentration of optically active materials in the bloodstream [1]. The objective of this study was to demonstrate the use of the real-time PPG concentration measurements for continuously updating individual pharmacokinetic parameter estimates during injection to make real-time predictions of individual exposure to indocyanine green (ICG).
Methods: In a secondary analysis of ICG injected into the tail of BALB/c mice, a population pharmacokinetic model was calibrated, using WinBUGS, to PPG data from 14 mice: 4, 6 and 4 mice received a low, medium, and high dose, respectively. Mice were injected at a constant rate until the desired ICG concentration was achieved with the PPG measuring the concentration every 5 s until the concentration returned to baseline. For validation, the individual predictions of exposure were made for 8 mice (2 low, 3 medium, and 3 large doses) where the posterior distributions from the population pharmacokinetic model were the prior parameter distributions and the individual pharmacokinetic parameter distributions—and corresponding exposure predictions—were updated in a Bayesian manner with each PPG measurement.
Results: The average absolute percent error between the individual predicted exposure and the actual exposure continuously decreased (31.7, 23.6, 14.2, 11.1, 9.8, and 9.4 %) every minute during the injection (see Figure).

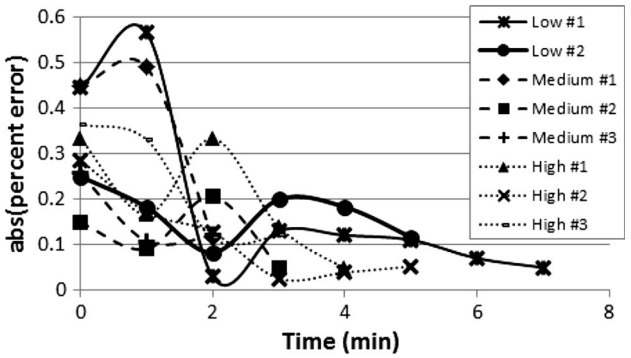

Fig. 1 Absolute value of the percent error between the individual predicted exposure (AUC) and the actual exposure for each of the 8 validation mice. Model-predictors were made after every PPG measurement (every 5 s) during the injection of ICG

In a simulation, 9.5 min of PPG measurements were required for 90 % confidence in the individual exposure prediction being within 10 % of the actual exposure.

Conclusions: The real-time concentration measurement capabilities of the PPG enable individual predictions of exposure while a drug is being injected. For ICG, if the injection rate provides 9.5 min of data, the exposure can be predicted to within 10 % and these model predictions could then be used to adjust the injection to ensure that the desired exposure is achieved.

References:

1. Michalak GJ, et al., Journal of Biomedical Optics, 18, 2010.

T-41

Evaluating the Performance of Different Expectation Maximization Algorithms in Handling Complex Pharmacometric Models

Xiaoxi Liu[1,2], Yuhuan Wang[1], Eyob Adane[3], Markos Leggas[1*]

[1]Pharmaceutical Sciences, College of Pharmacy, University of Kentucky, Lexington KY; [2]Division of Clinical Pharmacology, University of Utah, Salt Lake City UT; [3]Pharmacy Practice, Raabe College of Pharmacy, Ohio Northern University, Ada OH

Objectives: To evaluate and compare the performance of current-generation expectation maximization (EM) algorithms in modeling complex population pharmacokinetic (popPK) problems.

Methods: Data set (observation number 1000–2000, subject number 100–200) was simulated based on published/unpublished PK data of a novel anti-cancer drug DB-67. Three different popPK models were selected for algorithm evaluation: a one-compartment model, a four-compartment 'metabolite' model and a physiologically-based pharmacokinetic (PBPK) model. Evaluated algorithms included IMP (NONMEM 7.3, PDxPop and PsN/Pirana), QRPEM (Phoenix 6.4 NLME 1.3), SAEM (Monolix 4.3) and FOCE (NONMEM, as a benchmark). R packages (3.2.0, Rstudio) were used for data simulation, statistical analysis and diagnostic plotting. Evaluation criteria include estimation accuracy, computer time, model stability, noise during convergence and ease of use.

Results: For the one-compartment model, all algorithms converged with accurate parameter estimates. Comparatively, the computer time of EM algorithms was significantly longer (6 to 60 times that of FOCE). For the four-compartment model, only the EM algorithms converged, of which IMP and QRPEM were the most accurate. For the PBPK model, only IMP and QRPEM converged with accurate parameter estimates, but the IMP algorithm required twice the computer time of QRPEM. Reduction of Monte Carlo noise was limited in QRPEM due to the cap of the number of iterations in the current software package. Overall, the QRPEM implementation was preferred in terms of ease of use, accuracy, and time to convergence.

Conclusion: Considering the tradeoff between computer time and estimation accuracy, our results indicate FOCE is the most efficient algorithm for simple mammillary models. As expected, the advantages of using more advanced EM algorithms become significant when model complexity increases. Selection of EM version should be based on users' familiarity with the software settings and method optimization difficulty, which may vary considerably depending on the choice of software packages.

Reference:

1. Pharm Res. 2012 Jul;29(7):1722–36.

T-42

Exposure–Response Analsysis of Efficacy and Safety Endpoints for Crizotinib in the Treatment of Patients with ALK-Positive Non-Small Cell Lung Cancer (NSCLC)

Dana Nickens[1*], Weiwei Tan[2]

[1*]Pharmacometrics, Pfizer, La Jolla CA; [2]Clinical Pharmacology, Pfizer, La Jolla CA

Objectives: Evaluate the exposure–response relationship of crizotinib for efficacy and safety endpoints in patients with ALK-positive advanced NSCLC using data from the randomized phase 3 trial PROFILE-1007 and the single-arm phase 2 trial PROFILE-1005.

Methods: PROFILE-1007 had 174 patients and PROFILE-1005 included 934 patients. All patients from both studies received crizotinib 250 mg BID orally on a continuous basis. Efficacy endpoints, Objective-Response Rate (ORR) and Progression-free Survival (PFS), were analyzed separately for each trial. Safety endpoints, analyszed with pooled data from both studies, included on-treatment adverse events or lab abnormalities of interest: Pneumonitis (Grade $\geq$ 1), ALT Elevation (baseline Grade $\leq$ 2 to $\geq$ 3 post-baseline), Neutropenia (baseline Grade $\leq$ 2 to $\geq$ 3 post-baseline), Fatigue (Grade $\geq$ 2), Vision Disorder (Grade $\geq$ 1), Renal Cyst (Grade $\geq$ 1), Diarrhea (Grade $\geq$ 2) and Vomiting (Grade $\geq$ 2). A modeling approach to control for potential baseline confounders was used; confounders were included as main effects and potential effect-modifiers (interactions between covariates and exposure). Logistic regression was used for binary endpoints (ORR, safety endpoints); proportional-hazards regression was used for PFS. Exposure was the predicted average steady-state concentration for crizotinib based on the steady-state clearance for each patient estimated from the population PK model and average total daily dose (log-transformed).

Results: *Efficacy*—There were statistically significant exposure–response relationships for ORR and PFS, with higher exposure being associated with higher ORR and longer PFS in PROFILE-1005. The exposure–response relationship in PROFILE-1007 showed similar trends seen with PROFILE-1005; however, this relationship was not statistically significant. ECOG performance status was the only statistically significant effect modifier of the exposure–response relationship for PFS. *Combined Safety*—exposure–response analyses revealed a statistically significant relationship for neutropenia and renal cyst with increasing crizotinib exposure resulting in higher

incidence rates. Safety event rates were generally low (< 20 %) even at higher drug exposures.
Conclusions: Results from exposure–response analyses of PROFILE-1005 and -1007 support a favorable benefit/risk assessment at the approved 250 mg BID dosing regimen for ALK-positive advanced NSCLC patients.

T-43

The Effect of Poor Compliance on the Pharmacokinetics of Valproic Acid in Children with Epilepsy Using Monte Carlo Simulation

Chen-yu Wang[1], Jun-jie Ding[2], Zheng Jiao[1]*

[1*]Huashan Hospital of Fudan University, Shanghai,China;
[2]Children's Hospital of Fudan University, Shanghai, China

Objective: To investigate the effects of delayed and missed dose-s(poor compliance) on the pharmacokinetics of valproic acid(VPA) in epileptic children using Monte Carlo simulation.
Methods: VPA time-concentration profiles in various scenarios are generated on epileptic children using Monte Carlo simulation, based on five published population pharmacokinetic studies [1–5]. The scenarios include patients given multiple doses of VPA that ranged from 120 mg to 500 mg every 12 h or 500 mg and 750 mg once a day. The therapeutic range of VPA for each scenario is estimated to assess the effects of delayed or missed doses and to design corresponding rescue regimens.
Results: The risk for a sub-therapeutic range of VPA increase in a dose-dependent manner in both one and two times daily regimens when delayed or missed doses occurred. The effects of poor compliance are less prominent on the lower daily doses compared with those on the higher daily doses. The dose recommendations, in the event of poor compliance, are time related and dose dependent (Table 1).
Conclusion: Children with epilepsy should take the delayed doses as soon as possible when the delay occured, and partial missed doses may should be taken at the next scheduled time.

Table 1 Dosing recommendations for epileptic children with 8–30 kg body weight according to delayed or missed doses on valproic acid every 12 h or once daily regimens

Dosage	Scenarios	Dosing recommendation
100–300 mg (Syrup) q12 h	One dose was delayed up to 4 h	Take one dose immediately
	One dose was delayed 4–8 h	Take two-thirds of dose immediately
	One dose was delayed 8–12 h	Take half dose immediately
	Missed one dose	Take one and a half dose at the next scheduled time
	Missed two consecutive dose	Take two doses at the next scheduled time
500 mg (Tablets) q12 h	One dose was delayed up to 4 h	Take 500 mg immediately
	One dose was delayed 4–12 h	Take 250 mg immediately
	Missed one dose	Take 750 mg at the next scheduled time
	Missed two consecutive dose	Take 1000 mg at the next scheduled time
500 mg (Tablets) qd	One dose was delayed up to 4 h	Take 500 mg immediately
	One dose was delayed 4–24 h	Take 250 mg immediately
	Missed one dose	Take 750 mg at the next scheduled time
750 mg (Tablets) qd	One dose was delayed up to 4 h	Take 750 mg immediately
	One dose was delayed 4–12 h	Take 500 mg immediately
	One dose was delayed 12–24 h	Take 250 mg immediately
	Missed one dose	Take 1000 mg at the next scheduled time

References:

1. Ding JJ, et al. A population pharmacokinetic model of valproic acid in pediatric patients with epilepsy: a non-linear pharmacokinetic model based on protein-binding saturation. Clin Pharmacokinet. 2015;54(3):305–17.
2. Jiang DC, et al. Population pharmacokinetics of valproate in Chinese children with epilepsy. Acta Pharmacol Sin. 2007;28(10): 1677–84.
3. Correa T, et al. Population pharmacokinetics of valproate in Mexican children with epilepsy. Biopharm Drug Dispos. 2008;29(9):511–20.
4. Serrano BB, et al. Valproate population pharmacokinetics in children. J Clin Pharm Ther. 1999;24(1): 73–80.
5. Jason HW, er al. Population Pharmacokinetics of Valproic Acid in Pediatric Patients With Epilepsy: Considerations for Dosing Spinal Muscular Atrophy Patients. J Clin Pharmacol. 2012; 52(11): 1676–1688.

T-44

Towards Patient Stratification in Systemic Lupus Erythematosus using a Systems Pharmacology Approach

José David Gómez-Mantilla[1], Itziar Irurzun-Arana[1], Leire Ruiz-Cerdá[1], Ignacio González-Garcia[1], Chuanpu Hu[2], Honghui Zhou[2], An Vermeulen[3], Iñaki F. Trocóniz[1]*

[1]Pharmacometrics & Systems Pharmacology, University of Navarra, Pamplona, Spain; [2]Model Based Drug Development, Janssen Research and Development, Spring House, USA; [3]Janssen Research and Development, a division of Janssen Pharmaceutica NV, Beerse Belgium

Objectives: (1) Provide a Systems Pharmacology approach able to identify plausible altered pathways of the immune response that may explain the different and heterogeneous alterations in Systemic lupus erythematosus (SLE) patients, (2) classify patients according to their alterations, and (3) identify possible therapies for each patient subpopulation.

Methods: The immune response after production of autoantigens was modeled by Boolean networks [1, 2]. Networks were built focusing on the components of the immune response that have been reported to be altered in SLE patients. Simulations were performed perturbing the network in order to identify which nodes, if perturbed may trigger alterations similar to those observed in SLE patients. Clustering analysis was performed to group the network nodes according to the alterations these nodes may trigger. Simulations and analyses were performed in R.

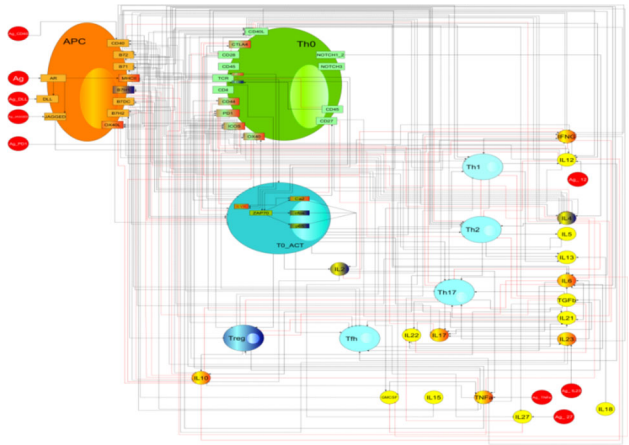

Fig. 3 Antigen Presentation Network in SL

Results: Different SLE manifestations were linked to different altered pathways of the immune response or initial conditions able to trigger the development of "Lupus like" manifestations. Virtual patients were clustered into different categories according to their manifestations. Group-specific therapies were identified able to reduce the disease alterations for different subpopulations. No single treatment was able to reduce the manifestations in all patient subpopulations.
Conclusions: Heterogeneity of SLE manifestations can be modeled by different underlying altered pathways of the immune system. Patients can be classified into different categories according to their alterations and optimal treatments can be identified for each patient subpopulation.

References:

1. Thakar J, Pilione M, Kirimanjeswara G, Harvill ET, Albert R (2007) Modeling systems-level regulation of host immune responses. PLoS Comput Biol 3: e109.
2. Saadatpour A, Albert R (2013) Boolean modeling of biological regulatory networks: a methodology tutorial. Methods 62: 3–12.

T-45

Estimating Parameters by Optimization Algorithms in a Simple PK Model with Bifurcations

Prakash Packirisamy[1], Rukmini Kumar[1*]

[1]Vantage Research, Chennai, India

Objectives: Estimating parameters for Ordinary Differential Equation models can be challenging, especially for systems with complex bifurcation structures [1]. Even simple compartmental PK models can display complex behavior including multiple steady-states and chaos. Knowledge of the model's bifurcation structure and prior information about range of parameters based on knowledge of physiology, can together be used in Bayesian algorithms.
Methods: A pharmacokinetic model with three ODEs was taken to be the exemplar system for estimating the parameters. The equations of the PK model are given below.

$$\frac{dI_{sc}}{dt} = D_0(t) - k_a I_{sc} \quad (1)$$

$$\frac{dI_{fsc}}{dt} = k_a I_{sc} - k_{abs} I_{fsc} \quad (2)$$

$$\frac{dI_p}{dt} = k_{abs} I_{fsc} - k_d I_p \quad (3)$$

This is a model of injectable subcutaneous long-acting insulin phamacokinetics [2]. Data is available for Ip, plasma concentration of injectable insulin at some doses. Parameters of the model are to be estimated for further predictions. A systematic analysis of the model's steady-states in parameter ranges of interest was carried out (Fig. 1 shows chaotic behavior with k_a). Functional minimization [3], global search and Bayesian optimization algorithms were used to estimate model parameters. Initial hypotheses of parameter ranges were determined based on expected behavior and knowledge of the physical range of parameters in the Bayesian case.

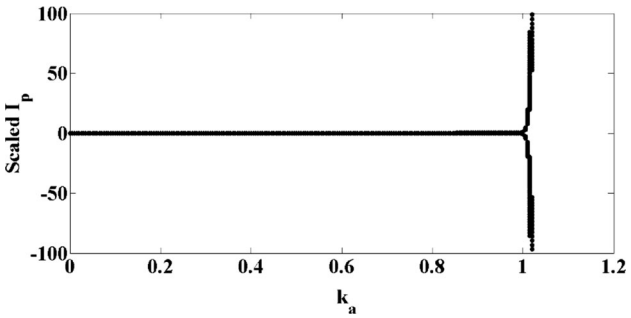

Fig. 4 Bifurcation plot with varying Ka

Results: It was found that functional minimization algorithms got trapped in multimodal minimas and global search algorithms with only very specific initial guess estimated the parameters appropriately. The prior information from bifurcation analyses and the physically feasible range for parameters as the initial guess provided a good estimate in the Bayesian algorithm. As further data is available, they can be systematically added to the algorithm, even if prior hypotheses are innacurate.
Conclusions: From functional minimization to global search algorithms, every algorithm has limitations. A simple Bayesian algorithm was found to estimate the parameters, much better than other algorithms in this case.

References:

1. Yuri A. Kuznetsov. (1998). Elements of Applied Bifurcation Theory.
2. Li J, Johnson JD. Mathematical models of subcutaneous injection of insulin analogues: a mini-review. (2009).
3. Mathworks. (2011).

T-46

Pharmacometric Markup Language (PharmML) & Standardised Output (SO) - Encoding Standards for Exchange of Models and Results in Pharmacometrics and Quantitative Systems Pharmacology

Maciej J Swat[1*], Nadia Terranova[2], on behalf of all DDMoRe contributors

[1]EMBL-EBI, Hinxton, UK; [2]Merck Institute for Pharmacometrics, Merck Serono S.A., Switzerland

Objectives: The definition and implementation of formats enabling a reliable exchange of pharmacometric models across software tools is one of the key goals for efficient collaborative drug and disease modelling and simulation research. PharmML, one of the key DDMoRe interoperability platform elements [1], has been designed to play the role of the exchange medium for mathematical and statistical models [2]. Similarly, SO has been developed as a complementary element, for storing typical output produced in a pharmacometric workflow.

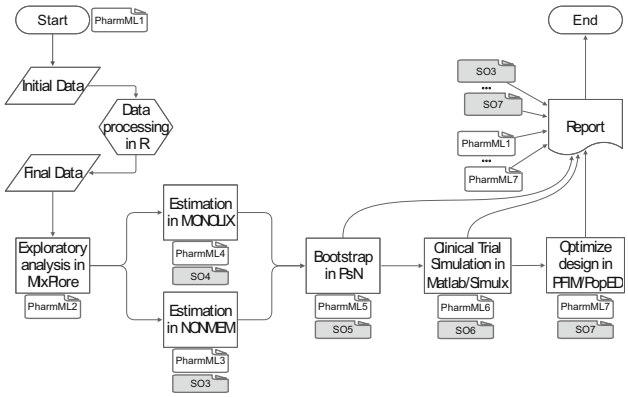

Fig. 1 Effective workflow support—the key benefit coming from PharmML and SO usage

Methods: The development of PharmML & SO is based on requirements provided by the DDMoRe community, including academic and EFPIA partners, and on use cases for estimation, simulations and optimal design tasks.

Results: PharmML supports MLE and Bayesian methods for non-linear fixed effect models, used in analysis of continuous and discrete longitudinal population data by accounting for the definition of

1. Structural model as a system of ODEs, DDEs or algebraic equations.
2. Parameter and variability models with structures allowing for the implementation of arbitrary parameter types, including discrete and continuous covariates.
3. Observation model supporting untransformed/transformed continuous, categorical, count or time-to-event data.
4. Trial design model as explicit specification of trials used for simulation and optimal design tasks.

SO, designed to be a tool-independent storage format aims at:

1. Providing a flexible structure for typical results produced in Pharmacometrics workflows, including estimation, optimal design and clinical trial simulation tasks;
2. Enabling effective data flow across tasks;
3. Facilitating information retrieval for post-processing and reporting.

Conclusions: PharmML and SO offer means to encode and exchange pharmacometric models and according results across tasks and tools, thus, extending the workflow capabilities.

References:

1. DDMoRe project, www.ddmore.eu
2. Swat, M.J., et al. (2015). Pharmacometrics Markup Language (PharmML) – Opening New Perspectives for Model Exchange in Drug Development, CPT:PSP. Published online on 29 May 2015.

T-47

Predicting Reductions in Chronic Obstructive Pulmonary Disease (COPD) Exacerbations from FEV_1 – A Model-Based Meta-Analysis of Literature Data from Controlled Randomized Clinical Trials

Jakob Ribbing[1,2*], Julia Korell[2], Frank Cerasoli[1], Peter A Milligan[1], Steven W Martin[1], Mats O Karlsson[2]

[1]Pfizer LTD; [2] Uppsala University

Objectives: To describe the relationship between forced expiratory volume in one second (FEV_1) and annual rate of moderate-severe exacerbations (ER) utilizing summary-level, literature data.
Shorter duration Phase 2 studies assess FEV_1 whereas Phase 3 chronic maintenance studies assess the registerable endpoint (prevention of COPD exacerbations).
Methods: Data was extracted from 29 randomized trials (80 treatment arms), of 43,472 patients. As predictors of ER, model-predicted trough FEV_1 [1] at baseline and week 12, as well as covariates, were investigated using NONMEM. Placebo ER was a function of covariates and interstudy variability. The ER ratio (treatment vs. placebo) was described by separate functions for FEV_1 efficacy ($\Delta\Delta FEV_1$) from direct bronchodilators (long-acting; LABD) and anti-inflammatory (AI) agents. Outcomes were derived as point estimate [95 % Confidence interval] vs placebo/reference arm.
Results: The final model predicted that placebo ER increased with a) disease severity (FEV_1 %Predicted), b) fraction of (ICS experienced) patients required to wash out from ICS ($ICS_{washout}$), and c) inclusion criteria requiring a history of exacerbations.
The log(ER-ratio) (treated vs untreated), was described by separate linear-slopes for LABD and AI $\Delta\Delta FEV_1$, and in addition for %$ICS_{washout}$; by a $\Delta\Delta FEV_{1AI}$-E_{max} model. The model predicted that for log(ER-ratio) <-0.2 (>18 % ER reduction), LABDs must achieve at least a $\Delta\Delta FEV_1$ 122 mL [114–132 mL] improvement (over placebo/reference). For a scenario with 62 % $ICS_{washout}$, an AI treatment (ICS/PDE4i) must achieve at least a $\Delta\Delta FEV_1$ 45 mL [17–79 mL] improvement, for log(ER-ratio) <-0.2.
Conclusions: The investigated AIs have modest efficacy on FEV_1, but if patients are washed out from ICS, these treatments achieve reductions in ER comparable to the new-generation LABD. The outcomes from this analysis may be applied while designing Phase 3 efficacy studies, pharmaco-economic outcomes studies, and quantifying comparative effectiveness of available treatments.

Reference:

1. Application of a model based longitudinal network meta-analysis of FEV1 in COPD trials in clinical drug development. [www.page-meeting.org/?abstract=3095].

T-48

Implementing FDA Specifications in R for Submission of Analysis Datasets

Timothy Bergsma[1*], Scott Pivirotto[2]

[1]Certara, Cary, NC, USA; [2]Metrum Research Group LLC, Tariffville, CT, USA

Objectives: Pharmacometric analysis datasets are subject to considerable formatting requirements for submission to the FDA [1, 2]. Our objective was to create a utility in the R programming language [3] to generate an integrated deliverable conforming to FDA guidance.
Methods: We developed a function *define* [4] that processes a list of file paths. Files are copied to a user-identified output directory or subdirectories. Files in CSV format are converted to SAS TRANSPORT format by means of the R package SASxport [5]. Text files are copied verbatim, appending the TXT extension as necessary.
The file *define.pdf,* created in the top directory, includes a table of contents with external hyperlinks to the archived files and internal hyperlinks to data definition tables. Column definitions are read from metadata files as per *specification* in metrumrg version 5.57 [6]. Rendering requires Latex and metrumrg utilities.
Results: The *define* utility was tested in a production envrironment. Resulting directory structure and *define.pdf* were satisfactory. Names and labels were automatically coordinated among transport files, tables of contents, and definition tables. The process was fast and accurate, with each discretionary value (e.g. dataset name) supplied only once.
Conclusions: Use of the *define* function allowed rapid, accurate preparation of a submission-ready directory containing archived pharmacometric analysis datasets and coordinated documentation.

References:

1. U.S. Food and Drug Administration (2012). Study Data Specifications. Version 2.0. http://tinyurl.com/nqcp7u3.
2. U.S. Food and Drug Administration (2014). Portable Document Format (PDF) Specifications. http://tinyurl.com/onocmc5.
3. R Core Team (2014). R: A language and environment for statistical computing. R Foundation for Statistical Computing, Vienna, Austria. http://www.R-project.org.
4. https://github.com/bergsmat/define.
5. Warnes G. SASxport: Read and Write SAS XPORT Files (2014). R package version 1.5.0. http://cran.r-project.org/src/contrib/Archive/SASxport/.
6. Bergsma TT, Knebel W, Fisher J, Gillespie WR, Riggs MM, Gibiansky L and Gastonguay MR (2013). Facilitating pharmacometric workflow with the metrumrg package for R. Computer Methods and Programs in Biomedicine 109 (1):77–85. http://www.cmpbjournal.com/article/S0169-2607(12)00191-5/abstract.

T-49

PK-PD Analysis of PASI with Data at Boundary: BI 655066 an Anti-IL-23A mAb for the Treatment of Psoriasis

Bojan Lalovic[1*], James Rogers[2], Jonathan French[2], Mary Flack[1]

Boehringer Ingelheim, Ridgefield, CT and Metrum Research Group, Tariffville, CT

Objectives: Psoriasis is a chronic, immunologically-mediated, inflammatory disease with scaly, erythematous, indurated skin of the scalp, trunk and limbs represented by an area severity index (PASI). This analysis describes longitudinal PASI scores from two studies (n = 156) combining data from a single and ongoing multiple dose administrations of IL-23 antagonist BI 655066 with data at the boundary to estimate PASI response rates.
Methods: A two compartment model adequately described the PK of BI 655066; individual level parameters were the input for an indirect response PK-PD model (IRM) of PASI scores. Drug concentrations were assumed to inhibit the formation of psoriatic lesions (kin) [1, 2]. PASI scores were normalized to a zero-to-one scale and modeled using an augmented beta distribution [3, 4]. This distribution was parameterized with three location parameters (the probability of a lower and upper boundary score and the conditional mean given that one is not on the boundary), functionally related to each other via logit link functions. Model performance was assessed using residuals, visual and numeric predictive checks (fraction of observations at boundary).
Results: The model adequately describes the observed PASI time course and proportion of subjects across three (or fewer) administered doses of BI 655066 in patients completing at least 24 weeks of treatment. Predictive checks of the observed and predicted PASI scores and derived change from baseline or PASI rates indicate an acceptable performance of the model.
Conclusions: The augmented beta regression approach implemented in NONMEM appears to be a viable approach for the analysis of PASI data from early studies, capturing the distributional properties of PASI scores.

References:

1. Zhu Y et al. J Clin Pharmacol 2009;49(2):162–175.
2. Zhou H, et al. J Clin Pharmacol 2010;50:257–267.
3. Xu S et al. J Pharmacokinet Pharmacodyn. 2013;40:537–544.
4. Rogers et al. J Pharmacokinet Pharmacodyn (2012) 39:479–498.

T-50

Modeling the Effect of Levetiracetam on Daily and Aggregated Seizure Counts in Adults and Children

Rik Schoemaker[1*], Armel Stockis[2]

[1]SGS Exprimo NV, Mechelen, Belgium; [2]UCB Pharma, Braine L'Alleud, Belgium

Objectives: To determine the exposure–response (PK/PD) relationship between levetiracetam concentration and seizure counts in the adjunctive treatment of epileptic seizures in both pediatric and adult subjects. Potential differences in this relationship between adults and children may be used to scale effects from adults to children for a drug with a similar primary mechanism of action.
Methods: A combined adult/pediatric PK/PD model was developed in analogy to a model developed for brivaracetam [1] with a similar primary mechanism of action, that described seizure counts using a negative binomial distribution, and using a mixture model to separate a 'placebo like' and a 'responder' sub-population, using material in part presented previously [2]. For the pediatric subjects, daily seizure count diaries were available, and for the adults, aggregated seizure counts were recorded over between visit (4 weekly) periods. The daily seizure counts for pediatric subjects were described taking previous day seizure frequencies into account, and using inter-individual variability on over-dispersion. For the aggregated adult seizure counts this level of detail was lost and therefore not incorporated. Visual predictive checks (VPCs) were used to ascertain the ability of the adult/pediatric PK/PD model to adequately simulate trial outcome using percentage change in seizure frequency from baseline, and

fraction of subjects with ≥50 % decrease in seizure frequency. Modelling was performed using NONMEM 7.2.

Results: The combined adult/pediatric PK/PD model was able to describe both the adult and the pediatric data using the same drug effect population parameters, and using a model structure very similar to the existing adult PK/PD brivaracetam model [1]. 32.6 % of subjects were estimated to be in the 'mixture model responders' subpopulation. VPCs illustrated that the adult/pediatric PK/PD model was capable of simulating the observed trial outcomes for both groups (Figure 1).

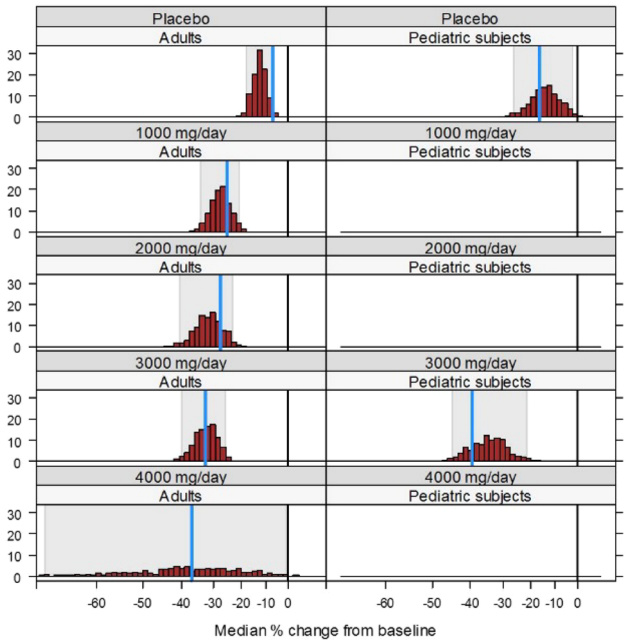

Fig. 1 VPC for the combined adult/pediatric PK/PD model by dose and adults and pediatric subjects for median % change from baseline. Histograms provide the distribution of outcomes for 500 simulated studies, the blue vertical line displays the result for the observed data, and gray areas encompass 95 % of simulated study outcomes. The 3000 mg/day dose identifier for pediatric subjects indicates the active treatment arm where the 60 mg/kg maintenance dose corresponds to 3000 mg/day for adult subjects

Conclusions: The combined adult/pediatric PK/PD model showed that no scaling was needed for drug related PD parameters between adults and children.

References:

1. PAGE 24 (2015) [www.page-meeting.org/?abstract=3559].
2. PAGE 17 (2008) [www.page-meeting.org/?abstract=1403].

T-51

Simple, Automatic Noncompartmental Analysis: The PKNCA R Package

William S. Denney[1*], Sridhar Duvvuri[1], Clare Buckeridge[1]

[1]Clinical Pharmacology, Pfizer, Cambridge, Massachusetts

Objective: Noncompartmental analysis (NCA) of pharmacokinetic (PK) data has typically been the realm of specialized software that does not integrate easily with data workflows. The goal of this project was to build an NCA analysis engine in R that can perform required calculations, plotting, and summarization.

Methods: Standard methods for NCA were implemented with the algorithms in Gabrielsson and Weiner [1]. For each subject in each period, the tool automatically determines the NCA parameters appropriate for calculation based on concentration–time and dosing data.

The information used for automatic determination of the correct parameters include selections based on route of administration, single or multiple dosing, the dosing interval (if multiple dosing), and if steady-state has been achieved. The NCA calculated during any given interval including C_{max}, T_{max}, AUC and AUMC with linear or linear-up/log-down integration, $t_{1/2}$, T_{ss} (time to steady-state) with either a monoexponential rise or the stepwise linear method [2], CL or CL/F, V_{ss}, T_{last}, C_{last}, and interpolated or extrapolated concentrations.

All settings, data cleaning, and summarization functions can be customized by the NCA analyst. Also, a NONMEM-ready dataset can be easily created after loading the data.

Results: The PKNCA R package has been integrated into an internal tool used for rapid, automated data analysis of Phase 1 studies, AMP (Automated Monitoring of Phase 1). Calculation results are identical when compared with validated internal and external software. The integration of NCA calculations into the dose-escalation study monitoring workflow has improved speed and reproducibility of the data for review.

Conclusions: The PKNCA R package was developed and will be made available to the public on CRAN. The package targets 100 % test coverage of the code, and as open source in R is easily integrated in almost any workflow.

References:

1. Gabrielsson J, Weiner D (2006). Pharmacokinetic & Pharmacodynamic Data Analysis: Concepts and Applications, Fourth Edition. Stockholm, Sweden: Swedish Pharmaceutical Press.
2. Panebianco DL, Maes A. Estimating time to steady state using the effective rate of drug accumulation. Pharm Stat. (2011) 10(1):27–33.

T-52

Facilitating Exposure–Response Analysis of Cardiovascular Safety Markers in Early-Phase Clinical Studies with the cardioModel Package for R

Daniela J Conrado[1*], Gregory J Hather, Danny Chen[1], William S Denney[1]

[1]Clinical Pharmacology, Pfizer Inc., Cambridge, MA; *Current address: Metrum Research Group, Wellesley, MA

Objectives: Exposure–response (ER) analysis of QT interval in single ascending dose (SAD) and/or multiple ascending dose (MAD) phase 1 study has been recently proposed as alternative to the thorough QT study [1]. A variety of ER models have been published describing drug effect on QT interval and other surrogates of cardiovascular (CV) safety. Therefore, we created the cardioModel R package to automatically evaluate models for assessing phase 1 CV safety data and identify the best fit ER model.

Methods: The selection of baseline and drug effect model structures included in the R package cardioModel was based on single- or multi-study ER or pharmacokinetic-pharmacodynamic (PK-PD) analyses on QT interval, BP, HR or pulse rate (PR) published in the scientific literature before August 2013 (searching Pubmed, OVID MEDLINE,

and Embase). Additionally, an unstructured baseline model (i.e., estimation of a baseline value at each study nominal time after the first drug dosing) was also included based on our previous work [2].
Results: cardioModel includes >90 mixed-effects model structures describing the relationship between drug concentration and QT interval, HR/PR and BP. Given an ER dataset, the tool fits each model structure to the observed data. The output includes all the tested models (ranked by the Akaike's Information Criterion), per-model parameter estimates, and a test for anticlockwise hysteresis (drug effect delay) to evaluate appropriateness of a direct-link ER analysis.
Conclusions: We propose that the cardioModel suite of models provide a unique opportunity to estimate and predict drug effects on CV safety markers for a small phase 1 study in a standardized and simplified manner. The cardioModel package will be made available to the public via the Comprehensive R Archive Network (CRAN).

References:

1. Darpo B et al. Clin Pharmacol Ther 2015; 97:326–35.
2. Conrado DJ, Chen D, Denney WS. Clin Pharmacol Ther 2014; 95: S18–19.

T-53

Model-Based Pooled Analysis of Exposure and Safety of Pembrolizumab with Advanced Melanoma and Non-Small Cell Lung Carcinoma (NSCLC)

Malidi Ahamadi[1]*, Claire Li[1], Jeroen Elassaiss-Schaap[2], Rik de Greef[2], Anna Kondic[1]

[1]Merck Research Laboratory, Merck and Co., USA; [2]Quantitative solutions, Holland

Objectives: Pembrolizumab, a humanized monoclonal IgG4 antibody against PD-1 that elicits T-cell–mediated antitumor activity, is approved in several countries for the treatment of advanced melanoma. The objective of this model-based analysis was to characterize exposure–response relationships for pembrolizumab with respect to safety in patients with melanoma and non-small cell lung carcinoma (NSCLC) treated in KEYNOTE-001, KEYNOTE-002 and KEYNOTE-006. We also sought to estimate the impact of potential predictors on the frequency of adverse events (AEs).
Methods: Data from 1720 patients who received pembrolizumab 2 or 10 mg/kg every 3 weeks (Q3W) or 10 mg/kg Q2 W were pooled. Exposure was defined as the area under the serum concentration curve over 6 weeks (AUCss-6wk) to account for the different dosing frequencies. Safety was assessed based on the incidence of AEs of special interest (AEOSIs) related to pembrolizumab's immune-mediated mechanism of action. Exposure–response relationship of pembrolizumab for safety was investigated using a non-linear mixed effects modeling approach.
Results: A two-compartment population PK model with linear clearance from the central compartment described pembrolizumab concentration. The PK profile of pembrolizumab indicated a low clearance ($\sim$0.2 L/day), limited volume of distribution ($\sim$7 L) and low variability (15–30 %), consistent with other monoclonal antibodies. A flat relationship for the occurrence of adverse event of special interest (AEOSIs) in this population was also suggested by logistic regression. Among the investigated covariates, duration of treatment was found to be a significant predictor for the occurrence of AEOSIs.
Conclusions: Pembrolizumab exhibits no exposure–response relationships for safety over the clinically tested dose range in melanoma and NSCLC patients, suggesting that no significant clinical benefit would be observed at higher dose levels. These results support the use of the approved pembrolizumab dose of 2 mg/kg Q3 W.

T-54

Enterohepatic Recirculation and Gender Differences of Roxithromycin in Humans Assessed via Population Pharmacokinetics

Soyoung Shin[2], Jürgen B. Bulitta[1,3,*], Martina Kinzig[1], Christoph Stelzer[1], Sven Hüttner[1], Tae Hwan Kim[4], Beom Soo Shin[5], Fritz Sörgel[1]

[1]IBMP - Institute for Biomedical and Pharmaceutical Research, Nürnberg-Heroldsberg, Germany; [2]Department of Pharmacy, Wonkwang University, Iksan, Korea; [3]College of Pharmacy, University of Florida, Orlando, FL, USA; [4]School of Pharmacy, Sungkyunkwan University, Suwon, Korea; [5]College of Pharmacy, Catholic University of Daegu, Gyeongsan, Korea

Objectives: Macrolide antibiotics undergo extensive enterohepatic recirculation (EHC) which affects their pharmacokinetics (PK). However, we are not aware of PK models to describe EHC for macrolides or for any other antibiotic. The aim of this study was to characterize the population PK and EHC of roxithromycin, a macrolide antibiotic, in humans over a range of doses and to assess potential gender differences.
Methods: We characterized the plasma concentration time profiles for roxithromycin given as a single oral dose of 50 mg (oral suspension), 150 or 300 mg (film-coated tablets) in healthy volunteers (in total: $n = 112$). Roxithromycin plasma concentrations were determined by LC–MS/MS and simultaneously modeled using the S-ADAPT software.
Results: The model contained compartments for undissolved drug, gut, liver, hepatocytes, and bile, as well as the central and peripheral compartment. A bile-flow turnover model described a pulsatile release of drug from bile into gut. The model provided reasonably precise and unbiased curve fits. Transfer of drug from the hepatocyte into bile was described by Michaelis–Menten kinetics. Females had a 17 % smaller maximum transfer rate compared to males ($p < 0.05$) leading to more extensive metabolism in females. This explained why females had a higher apparent total clearance compared to males (i.e. 27 % higher when clearance was expressed as L/h and 49 % higher when it was expressed as L/h/kg) based on non-compartmental methods.
Conclusions: The developed model for EHC excellently described the time-course of roxithromycin plasma concentrations. The significantly higher clearances in females compared to males were well explained by a slower transfer of drug from hepatocytes into bile in agreement with previous literature reports on gender difference in P-glycoprotein.

T-55

Development of a Quantitative Systems Pharmacology (QSP) Platform to Support Translational Research and Clinical Development of Affinity Drug Conjugates (ADCs)

Brian J. Schmidt*, Heather E. Vezina, Manish Gupta, Tarek A. Leil

Bristol-Myers Squibb, Princeton, NJ, USA

Objectives: ADCs used in oncology combine the antigen targeting capability of proteins (e.g. antibodies, adnectins) with the potency of small molecule cytotoxic drugs (i.e. payload) and hold promise for a

potentially improved therapeutic index versus traditional chemotherapy. However, there are a number of factors that govern whether administered ADCs can effectively reduce tumor burden. The objective of this analysis was to develop a computational ADC platform that mechanistically integrates relevant biological, biophysical, and chemical data to facilitate translational research and guide clinical dose selection.

Methods: Mechanistic processes of interest for drug discovery, bioanalytical [1], and clinical development were implemented in the QSP modeling framework. A mini-model that accounts for each conjugated active drug-to-antibody ratio (DAR) species was developed to improve interpretation of preclinical ADC plasma pharmacokinetic data from ligand binding assays (LBAs). A QSP platform was developed that included the impact of capillary and lesion pore sizes, interstitial and vascular tumor volumes, ADC bivalency, antigen expression and shedding, ADC internalization, endosomal processing, payload export, cellular target binding, and tumor growth. The platform was used to analyze preclinical data on initial DAR distribution, in vivo deconjugation and deactivation of payload, in vitro fluorophore-labeled antibody internalization, murine xenograft growth, and 89Zr-immuno-positron emission tomography (PET) xenograft uptake.

Results: Analysis of preclinical LBA data indicated sensitivity to average DAR and estimated deconjugation and deactivation rates. The platform enabled quantitative tuning of processes governing antibody uptake into the tumor and compared tradeoffs in characteristics such as pore structure, interstitial volume fraction, and label loss to interpret the observed PET signal from tracer retention in xenografts.

Conclusion: The ADC QSP platform successfully integrated quantitative preclinical information from mechanistic pathways. The platform will serve as a framework for preclinical and clinical data interpretation, and has the potential to predict efficacious intratumoral ADC concentrations, guide dose selection, and support clinical development programs.

References:

1. H. Myler, et al. (2015). Bioanalysis (in press).

T-56

Exposure–Response (E-R) Analysis of Progression Free Survival (PFS) for Nivolumab in Combination with Ipilimumab in Patients with Previously Untreated Advanced Melanoma

Yan Feng*, Xiaoning Wang, Paul Statkevich, Amit Roy

Bristol-Myers Squibb, Princeton, NJ, USA

Objectives: Nivolumab and ipilimumab as monotherapy (mTx) have demonstrated improved survival in previously untreated advanced melanoma (MEL) patients. Our objective was to characterize the E-R relationship of PFS in MEL patients treated with nivolumab and ipilimumab in combination.

Methods: The E-R of PFS analysis was performed with data from 927 patients in a 3-arm Phase 3 study: 3 mg/kg nivolumab mTx every 2 weeks (Q2W), 3 mg/kg ipilimumab mTx Q3 W (4-doses) and 1 mg/kg nivolumab and 3 mg/kg ipilimumab in combination (4-doses Q3 W, followed by 3 mg/kg nivolumab Q2W). The relationship between nivolumab and ipilimumab exposure (Cavg1, time-averaged concentration over the 1st dosing interval) and PFS was characterized using a Cox proportional hazards (CPH) model. A full CPH model was developed by incorporating all covariates of interest with appropriate functional forms into the base model.

Results: Cavg1 of nivolumab mTx and ipilimumab mTx were not significant predictors of PFS (hazard ratio 95 % CI includes 1.0) after accounting for all other covariates effect, indicating a plateau in the E-R at the mTx doses. There was a significant interaction between Cavg1 of nivolumab and ipilimumab given in combination suggesting a synergistic effect, resulting in a lower hazard of PFS. Covariate analysis (Figure 1) showed that PFS improves in PD-L1 positive, male subjects with lower LDH, higher body weight and higher tumor shrinkage at week 12 (TS-WK12).

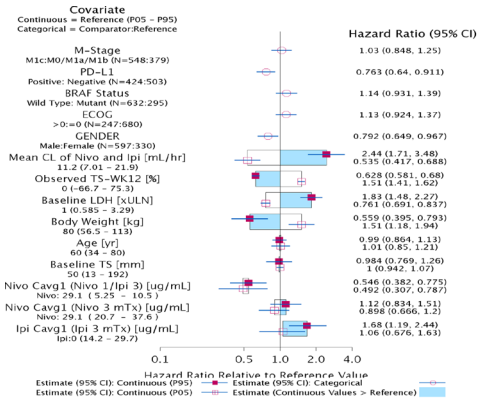

* Note: Reference subject is in the nivolumab mTx arm (reference nivolumab Cavg1 is median of 3 mg/kg Q2W, and ipilimumab Cavg1=0)

Fig. 1 Covariate Effects on the Hazard Ratio for the Multivariate CPH Model. Reference subject is in the nivolumab mTx arm (reference nivolumab Cavg1 is median of 3 mg/kg Q2W, and ipilimumab Cavg1 = 0)

Conclusions: The relationship of E-R is flat in the nivolumab 1 mg/kg and ipilimumab 3 mg/kg combination group as well as the 3 mg/kg nivolumab and ipilimumab mTx groups. Interaction of nivolumab and Cavg1 of ipilimumab was identified as a significant predictor of PFS, suggested the synergistic effect in the combination therapy.

T-57

Enhancing the Utility of Systems Pharmacology Modeling in Pharmaceutical R&D: Lessons from the development of a PCSK9 Inhibitor Model

Karim Azer[1*], Jeffrey E. Ming[1], Tu Nguyen[1], Alex Koszycki[1], Meera Varshneya[1], Britta Goebel[2], Nassim Djebli[3], Poulabi Banerjee[4], Derek W. Bartlett[5], Mike Reed[5], Benedetto Piccoli[6], Sean McQuade[6], Edouard Ribes[7], Jeffrey Barrett[1]

[1]Sanofi, Bridgewater, NJ, USA; [2]Sanofi, Frankfurt am Main, Germany; [3]Sanofi, Montpellier, France; [4]Regeneron, Tarrytown, NY; [5]Rosa & Co., San Carlos, CA; [6]Rutgers University, Newark, NJ, USA; [7]Sanofi, Paris, France

Objectives: We describe a methodology for using a quantitative systems pharmacology (QSP) model to describe variability in response to treatment. An interactive visualization environment that facilitates QSP simulations is presented. The methodologies are illustrated using a QSP platform, designed to support development of alirocumab, an anti-PCSK9 antibody.

Methods: We highlight the biology incorporated in a QSP platform to address mechanistic scenarios of interest to PCSK9 inhibitors. A methodology has been developed for using this QSP model to perform virtual population simulations and represent variability in treatment

response. This is based on flux balance analysis and control theory approaches, and was developed for translating pre-defined patient phenotypes into virtual populations. An overall framework for simulation and visualization of QSP results is presented.

Results: A QSP platform integrating peripheral and liver cholesterol metabolism, PCSK9 function, and currently available lipid-lowering therapies (statins, fibrates, and ezetemibe) is utilized to simulate effects of PCSK9 inhibition and combination therapies on lipids. A randomly generated virtual population (e.g. statin responder/non-responder) is used to simulate population response to a therapy, or how changes in a metabolite impact lipid levels, carrier proteins (e.g. ApoB), or PCSK9 levels (Figure). Finally, we present novel web-based visualization tools for interacting with QSP models and visualizing simulations of clinical scenarios.

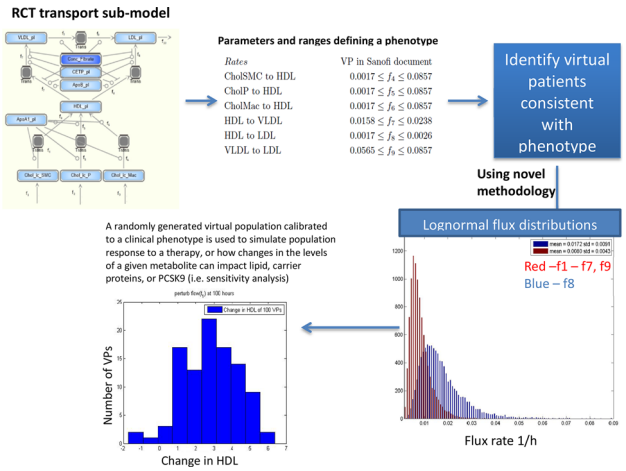

Fig. 1 Methodology for virtual popoulation creation and simulation

Conclusions: A QSP framework developed to explain variability in treatment response, and to facilitate QSP simulation capabilities was applied to a PCSK9 inhibitor. This framework can be adapted across disease areas, strengthening utility of QSP modeling for linking mechanisms to endpoints, addressing mechanistic questions pertinent to drug development, and bringing this field closer towards predictive science.

References:

1. McAuley, et al. BMC Systems Biology. 6:130, 2012.

T-58

Population Pharmacokinetics of Sorafenib in Acute Myelogenous/B-Type Leukemia Patients

Tao Liu[1], Philip Sabato[1], Vijay Ivaturi[1*], Jacqueline M. Greer[2], Keith W. Pratz[2], B. Douglas Smith[2], Michelle A. Rudek[2]

[1]Center for Translational Medicine, University of Maryland Baltimore [2]The Sindey Kimmel Comprehensive Cancer Center at Johns Hopkins, Baltimore, MD

Objectives: To characterize the pharmacokinetics of sorafenib administered using an intermittent dosing regimen, given cyclically to improve the safety and efficacy of patients with Acute Myelogenous Leukemia (AML).

Methods: Data from 15 patients with leukemia given 400 mg or 600 mg BID oral administration of sorafenib were analyzed using QRPEM algorithm in Phoenix NLME v1.4. Different absorption models were evaluated. Body weight, age, gender, prior therapy and baseline disease status were explored as potential covariates. Bound and unbound plasma concentration were modeled simultaneously using an unbound fraction parameter.

Results: A one-compartment model with transit absorption compartment and enterohepatic re-circulation successfully described the PK profile in leukemia patients. A transit absorption model performed better than a standard lag time model. Body weight was modeled as covariate on both volume of distribution and clearance using an Allometric scaling approach. The pharmacokinetic model parameter estimates for a 70 kg patient were CL/F = 6.4 L/h, V/F = 166 L and Mean Transit Time (MTT) = 1 h. The estimated unbound fraction was 1.8 %. No other covariates contributed to the pharmacokinetic variability.

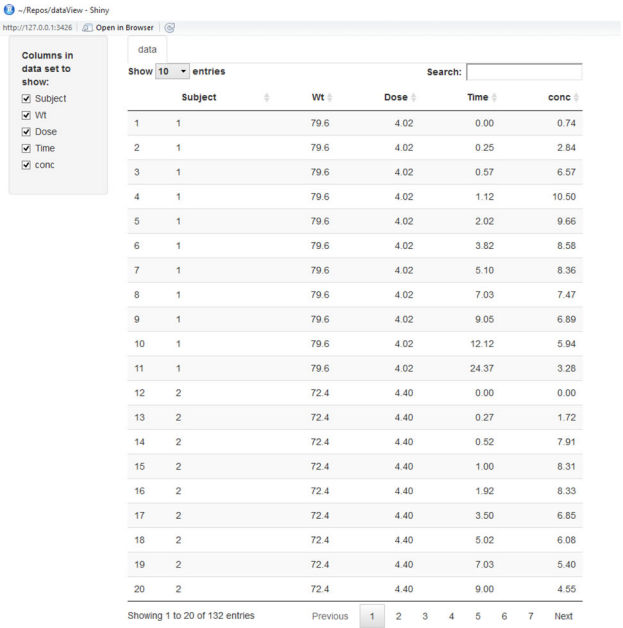

Fig. 1 Example dataview shiny application for viewing data currently available in Rstudio session

Conclusions: The estimated pharmacokinetic parameters for patients in AML were consistent with those previously published in solid tumor patients and existing knowledge in sorafenib pharmacokinetics. These results will be used to understand the relation between exposure and safety in this new intermittent cyclic regimen in AML patients.

Reference:

1. Jain L, et al. Br J Clin Pharmacol 72:2;294–305.
2. Villarroel MC, et al. Invest New Drugs 30:6;2096–102.

T-59

Extending Rstudio's Functionality to Accelerate Modeler Workflows via Shiny Applications

Devin Pastoor[1*]

[1]Center for Translational Medicine, School of Pharmacy, University of Maryland

Objectives: The Rstudio IDE [1] has become a staple in most R user's workflows. It provides information regarding your active

evironment, includes key functionality such as syntax highlighting, code completion, and plot rendering, and is available on all platforms, including server environments. There are, however, a number of limitations, such as only being available in one window at a time, locking into specific layouts, and only running one R process at a time. The objectives of this work were to demonstrate how Shiny [2] can be used to extend Rstudio's functionality and provide a conceptual framework for R users to come up with their own custom applications.

Methods: Shiny applications were developed to illustrate how two specific limitations can be overcome with minimal effort: (1) the single Rstudio window, and (2) running long scripts prevents concurrent analysis.

Results: To address the single window limitation, a shiny app was developed to extend the *View* function by sending the data to a separate shiny process that captures the new data and renders it as an interactive table, complete with sorting and filtering capabilities. For long running scripts, a multi-functional app was developed, that allowed the user to either select and run a script independently of Rstudio without having to resort to the command line directly, or to work with Rstudio to capture a 'snapshot' of the Rstudio environment directly before the long running process is exceuted, and execute the remainder in the separate process.

Conclusions: Both Shiny applications were developed to solve limitations of the Rstudio platform. The dataView application allow users to separate viewing output and code, rather than having to tab back-and-forth. This is especially beneficial for users with multiple monitors as they can spread their workflow across both. The script execution application gives users uncomfortable with sourcing scripts directly from the command-line an easier way of not consuming their primary Rstudio process, as well as offers a method for directly communicating with Rstudio rather than separating the analysis into separate scripts entirely.

References:

1. "RStudio, new open-source IDE for R | RStudio Blog". Blog.rstudio.org. Retrieved 2015-05-29.
2. Winston Chang, Joe Cheng, JJ Allaire, Yihui Xie and Jonathan McPherson (2015). shiny: Web. Application Framework for R. R package version 0.12.1. http://CRAN.R-project.org/package=shiny.

T-60

Population PK/PD from a Phase I Study of the Single-Agent PARP Inhibitor, Veliparib, in Patients with PARP Sensitive Tumor Types or *BRCA 1/2* –Mutated Cancer

Sharon Karan[1*], Christie Scheuerell[1], Brian F. Kiesel[2], Jiuping Ji[3], Shannon Puhalla[2], Jan H. Beumer[2], Mathangi Gopalakrishnan[1] and Joga Gobburu[1]

[1]Univeristy of Maryland, School of Pharmacy, Pharmacometrics; [2]University of Pittsburgh Cancer Institute; [3]National Cancer Institute

Objective: Poly ADP ribose polymerase (PARP) is activated during DNA damage response and repair. In-vitro studies have shown that inhibitors of PARP are cytotoxic in cell-lines deficient for *BRCA1*/2. The PARP inhibitor, veliparib, was studied as a single-agent in known *BRCA1/2* mutated tumors. The objectives of these analyses were to characterize veliparib population PK/PD by assessing typical parameter values, random and residual variabilities, covariate effects and determine if PARP is inhibited through PAR measurements.

Methods: The study enrolled 73 cancer patients who received twice daily doses of veliparib for 28 day cycles between 50 and 500 mg. PK was assessed during Cycle 1 and PBMCs were collected to measure PARP activity through Cycle 4. The PK/PD analysis used nonlinear mixed-effects modeling utlizing Pharsight Phoenix® NLME and employing FOCE for final runs. Model adequacy and complexity were guided by goodness-of-fit criteria including visual inspections of diagnostic plots, successful minimumization routine convergence, parameter estimates plausibility, correlations between model estimation errors and AIC minimum objective values.

Results: Veliparib pharmacokinetics were best described using a proportional error one-compartment model. Multiple first-order error models were assessed; however, initial absorption and maximum concentrations were not adequately characterized. Numerous individual patient profiles appeared to display zero order kinetics despite oral dosing. A mixed order (first-order – zero order) absorption model with Tlag adequately described veliparib absorption. Weight and creatinine clearance covariates were incorporated into the model to explain variability. PAR measurements were integrated by applying a limited proportional error inhibition PD model as shown in the following equation:

$$E(t) = \frac{(1 - E_{\max}) * C}{C + \mathrm{EC}_{50}}$$

E(t) is the veliparib effect on the PD response at time t
E_{max} is the maximum veliparib effect
C is the predicted veliparib concentration
EC_{50} is the veliparib concentration that produces half of the maximum effect

Conclusion: The PK/PD relationships show exposure–response correlations after veliparib administration. PAR expression diminished after multiple doses of veliparib, suggesting an alteration in PARP mechanism regulating cellular tumor repair. This model has been used to provide insight into the PK/PD relationships and could be utilized in simulating estimates for purposes of dose optimization or predicting response.

T-61

Population Pharmacokinetic (PPK) Modeling of Vilazodone in Adolescent Patients with Major Depressive Disorder (MDD)

Tatiana Khariton[1], E Niclas Jonsson[2], Martin Bergstrand[2], Timothy J Carrothers[1*], Parviz Ghahramani[1]

[1]Forest Research Institute, Inc., an affiliate of Actavis, Inc., Jersey City, NJ; [2]Pharmetheus, Uppsala, Sweden

Objectives: To confirm the doses for adolescent patients (12–17 years) with MDD and to recommend doses for younger children (7–11 years) to be used in the forthcoming efficacy and safety study in pediatric patients 7–17 years of age. To determine the additional number of serially sampled subjects, if any, needed to meet FDA requirements for PK parameter precision.

Methods: The vilazodone PPK model previously developed for adult patients was applied to the interim data collected from adolescent patients in an ongoing double-blind placebo-controlled efficacy/safety study in pediatric patients with MDD. To stabilize the parameter estimation, the PK parameter estimates from an adult PPK model and their corresponding uncertainties were used as informative priors.

Results: The PPK model for adolescents was developed using the interim data from 26 patients with rich and 59 patients with sparse sampling. The adult PPK model provided an adequate structural fit for the adolescent data. Pediatric doses of 15 and 30 mg/day for 7–17 years olds were predicted to result in exposures that were within 25 % of the adult median exposures following doses of 20 and 40 mg/day. For 40 mg/day, the median adult AUCss was estimated to be 1281 ng h/L, as compared to 1413 and 1127 ng*h/L for 7–11 and 12–17 years olds, respectively. The power analysis found that the rich PK samples already collected in 12–17 year olds provided adequate precision and that further rich PK sampling in younger patients was not neccessary.

Conclusions: The interim adolescent data was successfully modeled using a parameter prior approach; CL/F and Vc/F were estimated with high precision. Reducting the adult dose by 25 % was found to be adequate for 7–17 year olds. The completed study is expected to meet FDA's precision requirement with high power (95 % CIs for CL/F and V/F to be within 0.6–1.4 of the geometric mean).

T-62

GGplot-Shiny: A Shiny App That Facilitates Data Manipulation And Exploration

Mohamad-Samer Mouksassi[1*], Devin Pastoor[2]

[1]Certara/Pharsight, Princeton, NJ; [2]University of Maryland, Baltimore

Objectives: The objectives of developing this Shiny application were twofold: (1) to develop an application that enables non-R users to manipulate their data and to produce rich graphics using modern R packages ggplot2 and dplyr. and (2) to provide a reference extensible application that demonstrates many of the elements required for future applications in our field.
Methods: The shiny application framework was used to provide a graphical front-end as outlined in Figure 1. The dplyr library was used to control the data used to render plots and provide basic data manipulation capabilities such as filtering, recoding a continuous variable into categorical and splitting into groups. To create the plots the ggplot2 library was used, with customizations, such as adding smoother lines, median, mean, prediction intervals with the possibility to add a group and a color by group by interacting with the User Interface elements. The UI inputs translate into appropriate mapping to geoms behind the scenes and no knowledge of ggplot2 or dplyr syntax is assumed.

Fig. 1 The GGplot-shiny app User Interface rendered on a Smartphone. Scan the QR code to launch the app on your phone or computer

Results: The resulting application allows users to quickly and easily create professional quality plots. Key components of the data analysis workflow, including data input, manipulation and visualization were demonstrated and code open sourced on github to allow others to leverage those components in future apps [1]. The app was deployed using ISOP shinyapps.io account and can be accessed [2].
Conclusions: It was demonstrated that a traditional analysis workflow in R using packages such as ggplot2 and dplyr can be translated to a visual tool that non-R and R users alike can use. Due to the modular design many components of the app can be seamlessly integrated into new applications.

References:

1. https://github.com/isop-phmx/GGplot-Shiny.
2. https://isop.shinyapps.io/GGplot-Shiny.

T-63

SASR (Survival Analysis using "Shiny" R): A Browser Based Survival Analysis Visualization Tool using R "Shiny"

Jinzhong Liu[1*], Brian Corrigan[2], David Flockhart[1] and Liang Zhao[3]

[1]Division of Clinical Pharmacology, Indiana University School of Medicine, Indianapolis, IN; [2]Pfizer Inc., Groton, CT; [3]Division of Quantitative Methods and Modeling, Office of Research and Standards, Office of Generic Drugs, US Food and Drug Administration, Silver Spring, MD

Objectives: A browser based app named "SASR" (Survival Analysis using "Shiny" R) was developed using R packages "shiny" and "survival" to allow interactive web based modeling of survival analysis.
Methods: "Shiny", a free R package for developing interactive web apps, has been used for data visualization, summarization and communication. To date, few "Shiny" apps have been created to visualize survival analysis modeling. Two R scripts (ui.R and server.R) were programmed to allow reactive interactions between modeling inputs and result outputs. R package "survival" was used to conduct survival analysis in "SASR". "SASR" was placed on an external R server allowing public access: https://jzliu.shinyapps.io/SASR/.
Results: Figure 1 shows the use interface of "SASR". Any typical survival data file in a csv (comma separated values) format can be uploaded in the "Data File" tab on the web page. In the "Log-rank Test" tab, summary of log-rank test can be obtained. Once end users select variables for survival time and survival event (e.g. "0" indicates a censored event and "1" indicates an observed event), plot and summary of Kaplan–Meier estimation can be viewed or downloaded in the "Kaplan–Meier Plot" tab. In the "Cox model" and "Parametric model" tabs, Cox survival model and parametric survival (accelerated failure time) model can be conducted after selecting independent variables. In addition, for a data file containing a variable of drug exposure, "SASR" can divide drug exposure into 4 quartiles and perform Kaplan–Meier estimation stratified by drug exposure quartiles.

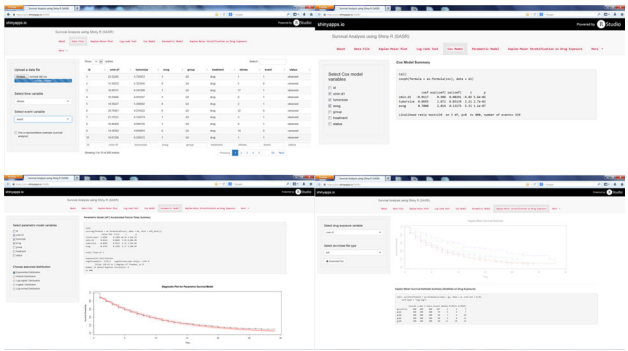

Fig. 1 Snapshots of the user interface of "SASR"

Conclusions: "SASR" is a "Shiny" based interactive web app performing survival analysis, which offers a free, effective and reusable way for sharing modeling results with both R and non-R users.

T-64

The Effect of Body Weight on Necitumumab Pharmacokinetics and Pharmacodynamics in Patients with Squamous Non-Small Cell Lung Cancer: Dosing Implications

Emmanuel Chigutsa[1*], Amanda Long[1], Michael Heathman[1], Johan Wallin[1]

[1]Global PKPD and Pharmacometrics, Eli Lilly and Company

Objectives: Necitumumab is a monoclonal antibody being investigated for the treatment of squamous non-small cell lung cancer. Having characterized the exposure–response relationship, we sought to determine patient factors that could potentially influence the pharmacokinetics and pharmacodynamics of necitumumab and investigate their impact on dosing recommendations.
Methods: A 2-compartment model with parallel first order and mixed order elimination was used to describe the pharmacokinetics of necitumumab in patients, when administered as 800 mg on day 1 and day 8 of a 21 day cycle. Body weight was positively correlated with both clearances and volumes of distribution. The pharmacodynamic model involved a simultaneous fit of tumor size and overall survival data. Tumor size dynamics were modeled as zero order growth with first order shrinkage due to drug effect. Dynamic tumor size was then applied as a predictor of hazard for overall survival in a time to event model. Monte-Carlo simulations were then carried out to compare flat dosing, weight-based, and BSA-based dosing in terms of variability in both exposure and efficacy in the study population.
Results: Allometric scaling with estimated exponents of 0.77 and 0.50 for clearances and volumes, respectively, adequately characterized the influence of body weight on necitumumab pharmacokinetics. The simulations revealed that no significant reduction in inter-patient variability of drug exposure would be obtained by weight-based (mg/kg) or BSA-based (mg/m^2) dosing compared to a flat dose. Furthermore, the simulated median survival time stratified by drug exposure quartiles was similar across all 3 dosing regimens (flat dose, weight based and BSA-based).
Conclusion: A flat dose was effective and achieved adequate drug exposure in the vast majority of patients (99.6 %). No improvement in efficacy can be expected with individualized dosing based on body size metrics.

T-65

Latent Variable Approach to Assess the Time-Varying Effect of Immunogenicity on the Pharmacokinetics of Elotuzumab in Patients with Multiple Myeloma

C. Passey[1*], L. Gibiansky[2], A. Roy[1], A. Bello[1], M. Gupta[1]

[1]Bristol-Myers Squibb, [2]QuantPharm LLC

Background: Elotuzumab (ELO) is a humanized anti-SLAM7 IgG1 monoclonal antibody, under development for multiple myeloma. A model based analysis was conducted to evaluate the impact of immunogenicity on the PK of ELO.
Methods: ELO PK was characterized by a two compartment model with parallel linear and Michaelis–Menten elimination from the central compartment, and additional target-mediated elimination from the peripheral compartment. Population Pharmacokinetic (PPK) model was developed using the Monte Carlo EM method with importance sampling in NONMEM. The final PPK model was then used to evaluate an ad-hoc effect of immunogenicity on the linear clearance (CL) of ELO. Specifically, a latent variable ρ was introduced, equal to zero at time zero and at time points where ADAs were not detected and equal to one at time points where ADAs were detected. At time points between ADA measurements, a sigmoid function with estimated onset and offset times was used to interpolate ρ as a function of time.
Results: Population PK analysis indicated that CL and V_C were independent of ADA status; however, target-mediated elimination was increased (V_{MAX} was higher and K_M was lower) in ADA-positive patients; V_{MAX} increased with increasing baseline M-protein. In majority of ADA positive patients, ADAs occurred early on in treatment, was transient and resulted in corresponding transient increases in CL. CL appeared to return to baseline values at later timepoints when ADAs were no longer detected. The increase in ELO CL due to immunogenicity at times when ADA were detected was 110 % (95 % CI 55.8–218 %), and variability of this increase was very large (CV = 215 %). However, model-based simulations indicated lower ELO exposures in ADA-positive patients than in ADA-negative subjects, which may not be due to a direct causal relationship, but could be associated with higher baseline serum M-protein in ADA-positive patients.
Conclusion: The relationship between ELO immunogenicity and PK appears to be confounded by the influence of baseline M-protein concentration.

T-66

Population Pharmacokinetics of ABT-493 in HCV Genotype 1 Infected Subjects with or without Cirrhosis in Three-Day Monotherapy Study

Chih-Wei Lin*, Aksana Kaefer Jones, Wei Liu, Sandeep Dutta

Clinical Pharmacology and Pharmacometrics, AbbVie

Objectives: ABT-493, an HCV nonstructural protein 3/4 A (NS3/4A) protease inhibitor discovered by AbbVie and Enanta, is under clinical development to be coadministered with ABT-530, a NS5A inhibitor, against HCV virus across genotypes 1 to 6. The objective of this analysis was to characterize population pharmacokinetics of ABT-493 in HCV genotype 1-infected subjects with or without cirrhosis in a three-day monotherapy study.
Methods: Population pharmacokinetic analysis was performed using data from 44 HCV infected subjects who received ABT-493 doses ranging from 100 to 700 mg QD (100, 200 (including cirrhotics), 300,

400, or 700 mg QD) following 3 day monotherapy. Population pharmacokinetic model was built using nonlinear mixed-effects modeling approach in NONMEM 7.3. Model evaluation and validation techniques were used to assess adequacy and robustness of the pharmacokinetic models.

Results: The observed pharmacokinetic profiles of ABT-493 exhibited delayed absorption and bi-phasic disposition. The delayed absorption was well described by a transit absorption model, and the bi-phasic disposition was well described by a two-compartment disposition model. The estimated mean transit time in absorption was 2.7 h. The estimated apparent clearance (CL/F) and apparent volume of distribution (V/F) were 29 L/h and 31 L, respectively. The concentration–time profiles of ABT-493 were adequately described by the final pharmacokinetic model as shown in Figure. Estimated relative bioavailability of ABT-493 increases with dose as the ABT-493 exposures increases in a higher than dose-proportional manner. Approximately 4.2-fold higher exposures of ABT-493 were observed in cirrhotic population compared to non-cirrhotic population.

Conclusions: The developed population pharmacokinetic model well described the concentration time profiles and variability of ABT-493 across wide ranges of ABT-493 doses in HCV infected subjects with or without cirrhosis. This population pharmacokinetic model can be used to conduct simulations to support selection of doses that achieve target exposures and to evaluate exposure–response relationships to inform combination therapy strategies.

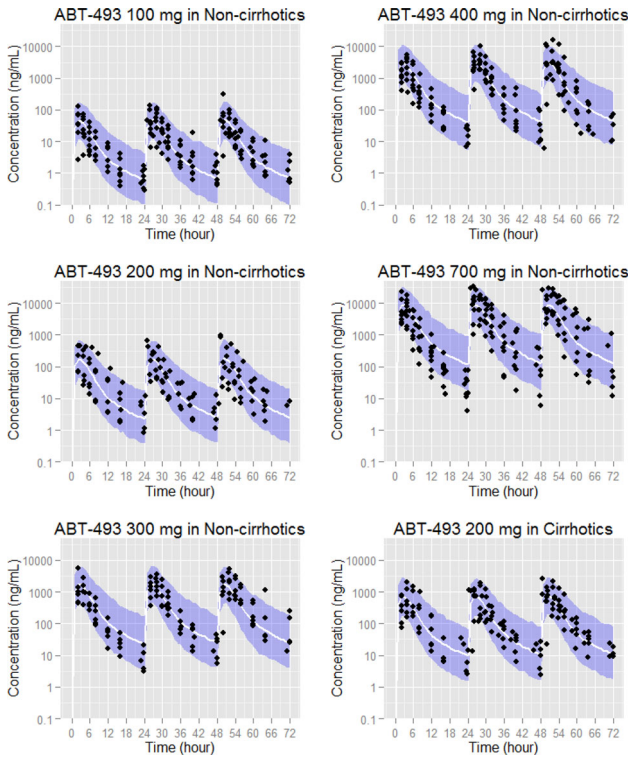

Fig. 1 Visual Predicted Check for ABT-493 population PK model

T-67

Trends in the Application of Pharmacometric Modeling and Simulation in the Development of Orphan Drugs in the 21st Century

Janelle Hajjar[1,2*], Jeannine Fisher[3], Marc Gastonguay[1,2,3]

[1]Metrum Institute, Augusta, ME, [2]University of Connecticut, Storrs, CT, [3]Metrum Research Group LLC, Tariffville, CT

Objectives: This investigation evaluates trends in the application of mathematical modeling and simulation (M&S) to support U.S. regulatory filings of drugs approved for treatment of orphan indications in the last 15 years.

Methods: The FDA orphan drug approvals website [1] was searched for all approved orphan drugs from January 1, 2000 to June 5, 2015. The resulting list of drugs was then searched in the FDA database [2]. From the Review documents for each drug, the *Clinical Pharmacology and Biopharmaceutics Review* document was examined. If this document was not available, the *Summary Review, Medical Review* and/or *Statistical Review* were examined instead. For drugs that had been approved for other non-orphan indications, only the M&S activities directly related to the orphan indication were considered.

Results: In the studied period of time, 297 drugs were approved for orphan indications. 143 of those approvals were included the analysis subset. Of this subset, 24 approvals (17 %) did not include any pharmacometric M&S in the review documents. The remaining filings included the following M&S methods: pop-pkpd, which included any population pharmacokinetic/pharmacodynamic or pharmacokinetic or pharmacodynamic M&S (75 %); pbpk, physiologically-based pharmacokinetic M&S (8 %); exposure–response M&S (15 %); mechanistic M&S (0.7 %); and systems pharmacology M&S (0.7 %).

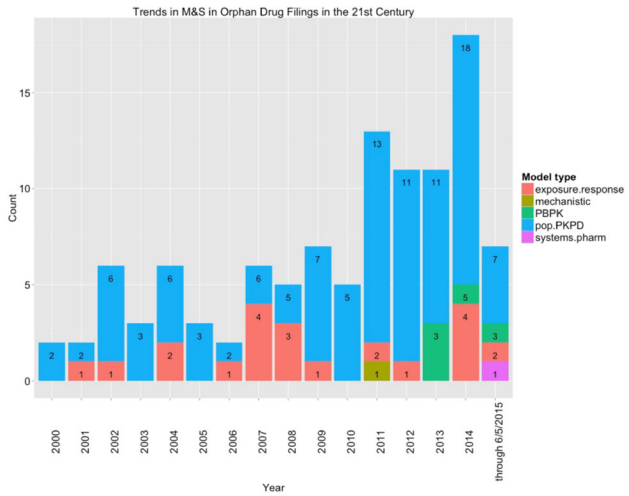

Fig. 1 Trends in M&S in orphan drugfilings in the 21st century

Conclusions: This investigation reveals an overall increasing trend in the use of M&S in orphan drug approval over the last 15 years. Although the pop-pkpd methodology is most common, a variety of M&S methods have been applied in more recent years. This analysis only reflects M&S in regulatory filings, and does not necessarily reflect the application of M&S for internal drug development decision-making.

References:

1. Search Orphan Drug Designations and Approvals. FDA Developing Products for Rare Diseases & Conditions. http://www.accessdata.fda.gov/scripts/opdlisting/oopd/.
2. Drugs@FDA. FDA Approved Drug Products. http://www.accessdata.fda.gov/scripts/cder/drugsatfda/index.cfm.
3. Lesko, L. Quantitative Analysis to Guide Orphan Drug Development. Clin.Pharmacol.Ther. 92, 258–261 (2012).

4. Gastonguay, M. Rare Disease Day 2014: Orphan Drug Trial Design and Analysis. Metrum Minutes (2014). http://metrumrg.com/blog/2014/02/28/rddorphan.html.

T-68

Letermovir Exposure is Similar in HSCT Patients and Healthy Volunteers

M. Prohn[2], D. Zhang[1*], T. Kerbusch[3], W. L. Marshall[1], K. Dykstra[2], C. R. Cho[1]

[1]Merck & Co., Kenilworth NJ, USA; [2]qPharmetra LLC, Cary, NC, USA, [3]Quantitative Solutions B.V., Oss, The Netherlands

Objectives: Letermovir is a potent, well-tolerated, inhibitor of the cytomegalovirus (CMV) terminase complex that is being developed for the prophylaxis of CMV infection in hematopoietic stem cell transplant (HSCT) patients. In a Phase 2b trial (AIC246-01-II-02) Letermovir was administered orally for 84 days at 60, 120 or 240 mg QD. Although letermovir pharmacokinetics (PK) following multiple doses in patients was similar to that in healthy volunteers (HV), PK following single dose administration was not previously reconciled with multiple dosing. This analysis aims to evaluate PK differences between patients and HV, leveraging the updated Phase 1 population PK model that describes PK non-linearities and putative induction.
Methods: The analysis included 1041 PK samples from 83 patients collected at predose, 0.5–1, 1–3, 3–5 and 8–10 h postdose on day 8 or 15 plus weekly trough samples. Modeling was performed using NONMEM 7.3 with stepwise-covariate modeling (PsN 4.2.0). Simulations were performed to confirm the previously selected Phase 3 dosing regimen.
Results: The final PK model was a 2-compartment model with nonlinear clearance, first-order absorption with lag-time, inter-individual variability on several parameters and inter-occasion variability on the relative bioavailability. Induction and nonlinear distribution could not be estimated in Phase 2 due to sparse PK sampling. Nonetheless, the model offered novel insight: differences in single dose PK in HV could be attributed to putative induction (increase) of clearance. Simulations also confirmed that 92 % of patients reach the target exposure after administration of the Phase 3 dose, 480 mg letermovir QD.
Conclusions: The model bridges single and multiple dose letermovir administration which has not been previously described. This model provides insight which may be required to address critical questions such as the impact of intrinsic and extrinsic factors on letermovir exposure in patients, and will serve as the basis for the analysis of Phase 3 data.

T-69

Phxnlme: An R Package that Faciliates Pharmacometrics Workflow of Phoenix NLME Analyses

Chay Ngee Lim[1*], Shuang Liang[1], Kevin Feng[2], Jason Chittenden[2,3], Ana Henry[2], Samer Mouksassi[2], Angela Birnbaum[1]

[1]Dept of Experiment & Clinical Pharmacology, University of Minnesota, Minneapolis, MN; [2]Certara/Pharsight, Princeton, NJ; [3]qPharmetra LLC, Andover MA

Objectives: Visualization, modeling, simulation, and reporting are integral parts of the pharmacometrics workflow. Currently, tools such as *Xpose* [1], *metrumrg* [2] and *saemix* [3] provide population model building support by faciliating this process, for NONMEM and Monolix respectively, via an R interface. The goal of this project was to build a comprehensive and flexible platform for the implementation of Phoenix NLME modeling, performance of model diagnostics, visualization and simulations, through development of an R package, *Phxnlme*.
Methods: *Phxnlme* is developed in R, and utilizes other R packages such as *ggplot2* and *lattice* for static graphics and *manipulate* for interactive graphics.
Results: The R package, *Phxnlme* offers (1) access to several Maximum Likelihood engines to perform individual, population, and pooled data analyses using Phoenix NLME, (2) a flexible and efficient R class for storage and retrieval of Phoenix NLME output, (3) plotting functions that allow easy generation and customization of various diagnostic and exploratory plots such as observations versus predictions, correlation, residuals, parameter distribution, forest plots, and individual and dynamic individual fits, and (4) capability to execute nonparametric bootstraps and simulation, as well as generate summary statistics of the bootstraps and visual predictive checks with stratification up to three covariates.
Conclusions: *Phxnlme* is an open source package that provides users with the ability to readily implement models, simulation and bootstrap on the Phoenix NLME engine, and generate high-quality and easily customizable graphs that are currently unavailable on the Phoenix NLME graphical interface. *Phxnlme* will be made freely available for download at http://cran.r-project.org/web/packages/Phxnlme/index.html.

References:

1. http://cran.r-project.org/web/packages/xpose4/xpose4.pdf.
2. Bergsma et al., 2012 doi:10.1016/j.cmpb.2012.08.009.
3. http://cran.r-project.org/web/packages/saemix/saemix.pdf.

T-70

Comparative Population Pharmacokinetics of Ofloxacin, Ciprofloxacin, Levofloxacin, and Moxifloxacin using Bioequivalence Study Data

Bo-Hyung Kim[1], Do-Hyun Kim[2], Sung-Vin Yim[1], Kyung-tae Lee[2], Eun Kyoung Chung[2*]

[1]Department of Clinical Pharmacology and Therapeutics, College of Medicine; [2]Department of Pharmacy, College of Pharmacy, Kyung Hee University

Objectives: To compare the pharmacokinetics of ofloxacin, ciprofloxacin, levofloxacin, and moxifloxacin by developing the population pharmacokinetic models using bioequivalence study data.
Methods: Data obtained from previous bioequivalence studies were used to develop the population pharmacokinetic models; 516 plasma drug concentration–time data (observations) from 23 subjects for ciprofloxacin, 572 observations from 24 subjects for levofloxacin, 976 observations from 38 subjects for moxifloxacin, and 1592 observations from 72 subjects for ofloxacin were included for this pharmacokinetic analysis. All study participants received oral formulations. Models were developed separately for each drug. One- and two-compartment models with first-order absorption and first-order linear elimination were evaluated for potential structural models. For stochastic error models, exponential inter-individual error model and combinational, proportional, and additive residual error models were evaluated.
Results: Plasma drug concentration–time data for all drugs were best described by a two-compartment model with first-order absorption and first-order elimination. Model-derived pharmacokinetic

parameters include apparent systemic clearance (CL/F), apparent volume of distribution in the central compartment (V2/F), apparent volume of distribution in the peripheral compartment (V3/F), apparent inter-compartmental flow (Q/F), and absorption rate constant (Ka). CL/F was substantially larger for ciprofloxacin compared to levofloxacin, moxifloxacin, and ofloxacin (typical value [%CV]; 27.9 [21.2 %] L/h vs. 8.63 [31.6 %], 9.03 [15.1 %], and 9.96 [19.4 %] L/h). Volumes of distribution ([V2+V3]/F) were relatively comparable among tested drugs. The final models supported the correlation between CL/F and V2/F for levofloxacin and moxifloxacin and CL/F and V3/F for ofloxacin, but for ciprofloxacin, no correlation between any pharmacokinetic parameters was supported by the final model.
Conclusions: Data from bioequivalence study were successfully used to develop population pharmacokinetic models for pharmacokinetic comparison of individual drugs in the same class. Different physiologic disposition pathways of our tested drugs appear to account for the observed pharmacokinetic differences between ciprofloxacin, levofloxacin, moxifloxacin, and ofloxacin.

W-01

Model Based Meta Analysis to Characterize the Dose-Efficacy Profile of Recombinant FSH for Controlled Ovarian Stimulation

Da Zhang*, Barbara J., Stegmann, Stefan, Zajic, Ferdous Gheyas, Yanfen, Guan, Pravin R Jadhav

Merck and Co., Whitehouse Station NJ

Objective: In order to support dose selection of recombinant follicle-stimulating hormone (recFSH) in future studies, a model-based meta-analysis of available clinical outcome data was conducted to characterize the dose-efficacy relationship of recFSH in subjects undergoing controlled ovarian stimulation (COS).
Methods: A comprehensive database of summary level clinical outcomes for recFSH was constructed from publicly available sources and Merck-conducted clinical study results. A systemic search of electronic sources such as journal articles, conference reports and abstracts through PubMed, EMBASE, and regulatory agency websites was conducted. Additionally, internal reports from Merck clinical studies from 1984 until 2014 for randomized controlled trials investigating different doses of recFSH in COS were included. From these sources, oocyte retrievals, corresponding recFSH doses with demographic information, e.g. age and body weight were extracted. Data were analyzed by graphical evaluation followed by model based meta analysis. Multiple structural models were explored to describe the dose-efficacy relationship and covariate effects were tested. R-3.1.2 was used for data programming and modeling.
Results: A database of 19 randomized controlled trials, 31 arms in adult women aged from 18 to 42 years old representing a total of 4471 subjects treated with recFSH dosing from 100 to 300 IU was assembled. Oocyte retrieval was modeled as a function of recFSH doses. The relationship between recFSH dose and oocyte retrieval was assumed to be a sigmoid E_{max} model with Hill coefficient. This was based on model selection crtieria as well as previous modeling experience with individual level data:

$$N_{ooc} = \frac{(E_{max} \cdot dose^{n})}{dose^{n} + ED_{50}^{n}}$$

As shown in Table 1, a shallow dose response for recFSH at doses >150 IU was identified. Age or body weight was not found to be significant covariate as only summary level information rather than individual level data were available.

Table 1 Simulated RecFSH dose–response at clinical relevant doses based on the model based meta analysis

recFSH dose	100 IU	150 IU	200 IU	250 IU	300 IU
Predicted mean oocytescount (95 % CI)	7.16 (4.7–8.3)	9.99 (8.8–10.7)	10.6 (9.7–11.3)	10.83 (9.9–11.5)	10.94 (9.9–11.7)

10,000 simulations conducted incorporating parameter uncertainty

Conclusions: A shallow dose–response relationship of recFSH for COS was established by leveraging internal and external data. Modeling results suggest that a plateau in response was achieved around a dose of 150 IU. RecFSH doses of >150 IU are expected to result in similar outcome for oocyte retrieval. This work demonstrates the value of model-based meta-analysis in integrating available literature evidence to support dose selection of recFSH.

W-02

Utilizing Modeling and Simulation to Inform Dose Selection, Titration Algorithms, and Trial Design of Oral Testosterone (T) Products for Testosterone Replacement therapy (TRT) in Hypogonadal Men

Chao Liu, Jeffry Florian, Yaning Wang, Myong-Jin Kim, Edward D. Bashaw, Vikram Sinha, Dhananjay Marathe*

Office of Clinical Pharmacology, OTS/CDER/FDA

Objectives: The key primary efficacy and safety regulatory endpoints for T trials are ≥75 % subjects with T Cavg within 300–1000 ng/dL; ≤15 and 0 % subjects with T Cmax > 1500 and >2500 ng/dL respectively. With these criteria multiple intramuscular injection and transdermal products have been approved for TRT in hypogonadal men. However, there are currently no approved oral testosterone products in USA. Oral T products may have potential challenges in simultaneously achieving both endpoints due to PK characteristics of high peak-to-trough ratios along with possibly substantial inter- and intra-subject/inter-occasion variability. These factors put the onus on appropriate selection of dosing regimen and titration algorithm to successfully design trials. Here, we evaluate how various product PK profiles can influence design decisions for dose, regimen (QD/BID/TID) and titration algorithm for pivotal phase 3 trials.
Methods: A linear one-compartment population PK model with oral administration and a negative feedback for suppression of endogenous testosterone was built (NONMEM v7.3) and used for clinical trial simulations (R v3.1.2). Different magnitudes of inter-occasion variability (0 to 100 %) and clearance-volume of distribution combinations that would support QD or BID dosing were simulated. Also, various titration algorithms were considered and the resulting Cavg and Cmax were compared with regulatory endpoints.
Results: The simulations showed that with high inter-occasion variability (≥45 %) there is minimal chance of achieving both regulatory endpoints with QD or BID dosing irrespective of choice of titration algorithm, but with smaller inter-occasion variability (≤20 %), the regimen was able to achieve the endpoints. In situations involving high intra-subject variability, more frequent dosing

may be needed to satisfy both endpoints rather than relying on a titration algorithm.
Conclusions: Understanding the magnitude of variability (intra- and inter-subject) is key to the successful trial design of oral T products. Simulations, combined with collected intensive PK and assessment of product variability, can help with arriving at important trial design elements for reasonable chance of success of pivotal trial or go/no-go decision.

W-03

Population Pharmacokinetics and Pharmacodynamics of an Oral Glucagon Receptor Antagonist (LY2409021) in Patients with Type 2 Diabetes Mellitus

Emmanuel Chigutsa[1], Cheng Cai Tang[2], Parag Garhyan[1]

[1]Global PKPD and Pharmacometrics, Eli Lilly and Company, Indianapolis, IN; [2]Eli Lilly and Company, Singapore

Objectives: LY2409021 is being investigated for the treatment of type 2 diabetes mellitus (T2DM). The objectives of the analyses were to describe the population pharmacokinetics (PK) of LY2409021, evaluate the factors influencing its PK, and quantify the exposure–response relationships for efficacy (fasting plasma glucose [FPG] and glycosylated hemoglobin [HbA1c]).
Methods: Data from a total of 373 healthy subjects and patients with T2DM (7 studies) were combined to develop the population PK model and investigate the effect of predefined covariates. Pharmacodynamic data (FPG and HbA1c) were available from a 24 week phase 2 dose ranging study (N = 264). This PK model was used to predict LY2409021 concentration in a PKPD model to describe the relationship between concentration, FPG and HbA1c simultaneously. All modeling was performed using NONMEM 7.3.0.
Results: A one-compartment model with first order absorption and elimination adequately described the pharmacokinetics of LY2409021. Body weight was the only significant predictor of clearance and volume. A linked indirect response model was used to describe the time course of FPG and HbA1c simultaneously. LY2409021 decreased FPG, with an EC_{50} of 1186 ng/ml. Formation of HbA1c was linked to FPG through an indirect response model. The glucose-lowering effect of LY2409021 was constrained such that the HbA1c could not be reduced below a physiological threshold, estimated to be 5.7 %. A time-dependent placebo effect on FPG and HbA1c was also included in the model.
Conclusions: A 20 mg dose resulted in average steady state concentrations approximately 2-fold higher than EC_{50} whilst the 10 mg dose resulted in exposure around the EC_{50}. Simulations revealed mean reduction in HbA1c of 0.9–1.4 % for doses between 10 and 20 mg and 0.1 % for placebo after 26 weeks of treatment from a baseline of 8.0 %. Therefore daily doses of 10 mg to 20 mg of LY2409021 would be effective in achieving clinically significant FPG and HbA1c reductions in patients with T2DM.

W-04

PBPK Modeling to Guide Experimental Design in Drug Development

Kristin Dickschen[1*], Juergen Jaeger[1], Meike Hutt[2], Nadine Pollak[2], Martin Siegemund[2], Oliver Seifert[2], Roland Kontermann[2], Klaus Pfizenmaier[2], Michael Block[1]

[1]Bayer Technology Services GmbH, Computational Systems Biology, Leverkusen, Germany; [2]Institute of Cell Biology and Immunology, University of Stuttgart, Stuttgart, Germany

Objectives: One targetable hallmark of cancer is resisting cell death [1]. Here, targeting the death receptor (DR) with tumor necrosis factor (TNF)-related apoptosis inducing ligands (TRAIL) represents a promising approach [2, 3]. Physiologically-based pharmacokinetic and pharmacodynamic (PBPK/PD) modelling provides a powerful tool to guide further experiments and assess risks for clinical development. We here present a detailed example.
Methods: A PBPK/PD model of cetuximab was established in mice, xenografts, and patients and a PBPK model for TRAIL fusion proteins in mice. PBPK models were developed using PK-Sim® and MoBi®. Processes included are target expression, binding, receptor dynamics, and internalization [4]. A PD model was integrated to represent tumor growth. Using cetuximab as a benchmark a rationale for further development of TRAIL fusion proteins was developed.
Results: The cetuximab model describes plasma PK in mice, xenografts, and patients and tumor PK and tumor growth in xenografts. The TRAIL model describes plasma PK in mice. The impact of changes in PK on tumor growth is investigated by an analysis of e.g. binding to EGFR, DR5, and FcRn. These results are used to inform future experiments, e.g. sampling times in xenografts.

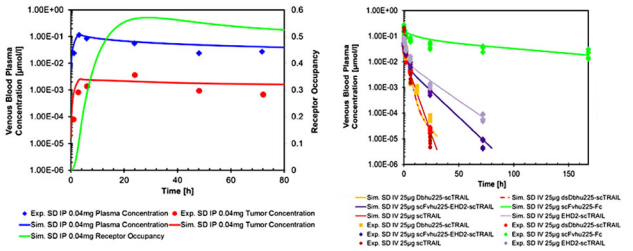

Fig. 1 Plasma and tumour PK of cetuximab in GEO xenograft following i.p. dosing [5] and realated receptor occupancy are shown on the left handed side. Plasma PK for several TRAIL fusion proteins are presented on the right handed side

Conclusions: PBPK/PD model-guided development of a compound enables for early potential and risk assessment of a compound. The presented example shows how such modelling approaches provide a consistent picture of the available biological knowledge of a new compound and a rationale for next steps in development with guidance from simulations.

References:

1. Hanahan, Weinberg. Cell. 2011. 144 (5): 646–674.
2. Schneider et al. Cell Death Dis. 2010. 1:e68.
3. Siegemund et al. Cell Death Dis. 2012. 3 (4): e295.
4. Garg, Balthasar. J Pharmacokinet Pharmacodyn. 2007. 34 (5): 687–709.
5. Luo et al. Cancer Chemo Pharmacol. 2005. 56: 455- 464.

Some parts of the results in this abstract have been previously presented in part at PAGE meeting 2015 in Crete and published in the conference proceedings as abstract III-01.

W-05

Model Based and Model Independent Evaluations of Steady-State Volume of Distribution (Vdss) of Two-Compartment Pharmacokinetic Models with Parallel First-Order and Michaelis–Menten Eliminations

Xiaotian Wu[1], Fahima Nekka[1,2] and Jun Li[1,2*]

[1]Faculté de Pharmacie, Université de Montréal, Québec, Canada; [2]Centre de recherches mathématiques, Université de Montréal, Québec, Canada

Objectives: Steady-state volume of distribution (V_{dss}) is an important parameter in pharmacokinetics. Its current evaluation is mainly through noncompartmental analysis (NCA). However, for those drugs exhibiting parallel first-order and Michaelis–Menten eliminations, the appropriateness of the non-compartmental version $V_{dss,nca}$ has been questioned. In this study, we aim to elucidate the suitability of $V_{dss,nca}$ and propose a reliable strategy for V_{dss} estimation.
Methods: Two-compartment models are investigated. While the first-order elimination can occur either from the central compartment (M_1) or the peripheral compartment (M_2), Michaelis–Menten elimination takes place at the central compartment for both models. The identifiability and indistinguishability of the two models are mathematically addressed. Closed form solutions of $V_{dss,nca}$, $V_{dss,M1}$ and $V_{dss,M2}$ are derived and compared. Moreover, the significance of the findings is validated for typical drugs: *G-CSF*, *rHuEpo, 5-MeO-DMT*.
Results: We show that M_1 and M_2 are indistinguishable in the sense that they can give rise to identical PK profiles for the same dose input, but $V_{dss,M1}$ and $V_{dss,M2}$ can largely differ. Moreover, we proved that

$$V_{dss,nca} < V_{dss,M1} < V_{dss,M2}$$

For more general situations, V_{dss} is lower and upper bounded by $V_{dss,M1}$ and $V_{dss,M2}$.
Conclusions: NCA underestimates V_{dss} when elimination is no more completely constrained to the central compartment, with an additional nonlinear elimination. In this situation, V_{dss} should be model dependent.

Reference:

1. Yates JW and Arundel PA. 2008. J Pharm Sci 97(1):111–122.

W-06

Pharmacokinetic-Pharmacodynamic (PK-PD) Model for Tolvaptan in Patients with Hypervolemic Hyponatremia

Scott Van Wart[1*], Susan Shoaf[2], Suresh Mallikaarjun[2], and Donald Mager[1]

[1]SUNY-Buffalo, Buffalo, NY; [2]Otsuka, Rockville, MD

Objectives: To develop a PK-PD model and evaluate the impact of the V_2R antagonist tolvaptan on correcting serum [Na^+] in patients with hypervolemic hyponatremia.
Methods: Urine and electrolyte data were obtained from 5 clinical trials (621 CHF and 39 cirrhotic patients). A PK-PD model developed in healthy subjects (ACoP6 abstract) describing dietary intake and urinary elimination of total body water (TBW) and electrolytes as well as their relative ECF:ICF distribution was modified. Initial TBW was calculated using fat free mass and hyponatremia severity. The relative ECF:ICF distribution of TBW was altered to account for ECF volume expansion. A population PK model for tolvaptan [1] was used to predict plasma tolvaptan concentrations to drive inhibition of the fractional tubular water reabsorption (FR_W). For patients concurrently receiving furosemide, a population PK model [2] plus patient-specific CLcr estimates were used to predict the urinary furosemide excretion rates to drive inhibition of fractional tubular Na^+ reabsorption (FR_{NA}). Monte Carlo simulation (MCS) with adaptive feedback control was performed to assess recommended tolvaptan dosing guidelines.

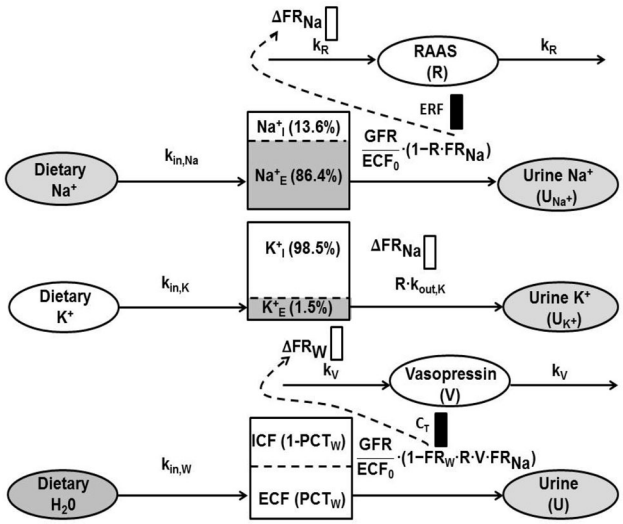

Results: Maximal tolvaptan-induced inhibition of FR_W was lower in cirrhotic patients (5.75 %) than CHF patients (8.39 %). Cirrhotic (EC_{50} = 222 ng/mL) and NYHA Class 3/4 CHF (EC_{50} = 257 ng/mL) patients were also less sensitive to tolvaptan than NYHA Class 1/2 CHF patients (EC_{50} = 108 ng/mL). Maximal furosemide-induced inhibition of FR_{Na} was only 1.24 % suggesting diuretic resistance. MCS predicted the magnitude of the daily change in serum [Na^+] and TBW, the percentage of patients who achieve overly rapid correction or conversely required dose titration to expediate correction of serum [Na^+], and the expected duration of tolvaptan therapy.
Conclusions: A physiologically relevant PK-PD model characterizing fluid and electrolyte balance in patients with hypervolemic hyponatremia enabled assessment of the ability of tolvaptan to provide a safe and effective reduction in ECF volume and correction of serum [Na^+].

References:

1. Van Wart et al. Biopharm Drug Dispos. 2013;34(6):336–47.
2. Van Wart et al. Biopharm Drug Dispos. 2014;35(2):119–33.

W-07

A Disease Progression Model of Castrate Resistant Prostate Cancer (CRPC) Using Prostate Specific Antigen (PSA)

Elizabeth Gray[1§], Tu H. Mai[1§], Manish R. Sharma[1*]

[§]co-primary authors; [1]University of Chicago

Objectives: Drug development for CRPC would be enhanced by an early endpoint that can distinguish the effectiveness of different therapies and correlate with survival. We aimed to develop a disease progression model for CRPC using longitudinal PSA data that could be used to compare the power of various early PSA-based endpoints to identify the most effective therapies.
Methods: We identified 1758 patients with CRPC who were treated with prednisone with or without docetaxel or mitoxantrone and had adequate longitudinal PSA data available from 6 clinical trials on ProjectDataSphere (www.projectdatasphere.org). 80 % of the data were used to fit a nonlinear mixed effects model in NONMEM, while

the remaining 20 % of the data were used to test the model by simulating and comparing predicted vs. observed results.
Results: Of several base models evaluated, a previously reported model (Stein WD, et al. Clin Cancer Res 2011; 17: 907–17) had the best fit: $PSA(t) = BSL * (e^{(-d*t)} + e^{(g*t)} - 1)$, where *BSL* is the estimated baseline PSA, *d* is the rate of decrease in PSA, and *g* is the PSA growth rate. We included a dropout hazard component in our model to account for the substantial amount of early dropout. Significant covariates included: ECOG performance status and baseline hemoglobin on *BSL*; prior docetaxel on *BSL*, baseline hazard for dropout and *g*; and treatment on *d*. Compared with *d*, empirical Bayes estimates for *g* are more strongly correlated with survival.

Parameter	Population Estimate	Half-life (days)	Correlation with time to death
d (prednisone)	0.0034	204	0.18
d (mitoxantrone plus prednisone)	0.0052	133	0.21
d (docetaxel plus prednisone)	0.0105	66	0.11
		Doubling time (days)	
g (prior docetaxel)	0.0031	225	−0.41
g (no prior docetaxel)	0.0008	856	−0.36

Conclusion: We developed a disease progression model of CRPC using PSA. Simulations will be used to explore the power of various early PSA-based endpoints to identify the most effective therapies, in order to support faster and better drug development decisions.

W-08

Pharmacodynamic Model of Vorinostat Effects in Multiple Myeloma Cells and Xenografts

Charvi Nanavati, Donald E. Mager*

Universityat Buffalo, SUNY, Buffalo, NY, USA

Objectives: To develop a mechanistic pharmacodynamic model to characterize vorinostat effects in multiple myeloma cells and apply the model as a translational platform to link exposure–response relationships in murine tumor xenografts.
Methods: Relative expressions of p21, pNFκB, Bcl-xL and cleaved PARP were measured using immunoblotting in U266 myeloma cells exposed to vorinostat (2 and 5 μM) for up to 48 h. Cellular proliferation was measured using WST-1 reagent up to 96 h. Vorinostat concentrations were measured in cell culture media by LC/MS/MS up to 120 h. Turnover models were applied to describe protein dynamics that linked to cellular proliferation. Pharmacokinetic and tumor growth data in murine xenografts were extracted from literature [1,2]. The cellular model structure and parameters were fixed for scaling the cellular system to describe tumor dynamics. All modeling was conducted using a naïve pooled approach with maximum likelihood estimation in ADAPT 5.
Results: *In vitro* and in vivo vorinostat pharmacokinetics were described using a biexponential function and a standard two-compartment model. The final cellular model (Fig. 1) consisted of indirect effects on Bcl-xL, indirect effects with a transit compartment on p21, pNFκB and cleaved PARP, an exponential growth rate constant for cellular proliferation, and a first-order rate constant for cell death. pNFκB and cleaved PARP stimulated production and degradation of Bcl-xL. Cell growth was inhibited by p21, and cell death was regulated by the relative ratio of cleaved PARP (pro-apoptotic) and Bcl-xL (anti-apoptotic). All parameters were estimated with reasonable precision. Tumor dynamics were well described by fixing biomarker signaling components from the cellular model and estimating the tumor growth rate and cell death parameters only.

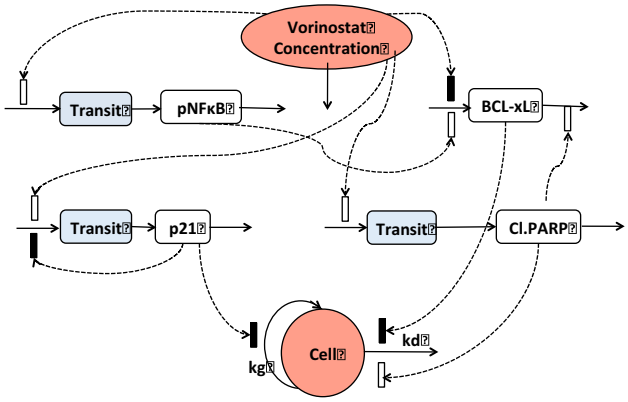

Fig. 1 Pharmacodynamic Model of Vorinostat in U266 cells

Conclusions: Vorinostat exposure–response relationships were successfully described by a mechanism-based pharmacodynamic model in U266 cells. The model was scaled to xenografts and can potentially serve as a translational platform for designing vorinostat combination treatments.

References:

1. Yeo et al. Biomed. Chromatogr., 21: 184–189 (2007).
2. Campbell et al. Eur J Haematol., 84: 201–211 (2009).

W-09

Target-Mediated Drug Disposition (TMDD) Equations and Approximations for Systems with 1:2 and 2:1 Drug-Target Binding Stoichiometry

Leonid Gibiansky*, Ekaterina Gibiansky

QuantPharm LLC, North Potomac, MD, USA

Background: TMDD equations were initially written and are used assuming 1:1 stoichiometry of drug-target binding even though many biological systems do not conform to this assumption. Specifically, this assumption is violated for monoclonal antibodies that have two identical binding sites. Although standard TMDD equations provide excellent fit of the observed data, it is of interest to derive equations and approximations that assume true binding stoichiometry.
Objectives: To derive TMDD model and its approximations for biological systems with 2:1 and 1:2 stoichiometry of drug-target binding.
Methods: TMDD equations for systems with 2:1 and 1:2 drug-target binding were formulated. Equations for total drug and total target

concentrations were then derived. Quasi-steady-state (QSS) conditions for two drug-target complexes were used to derive explicit relations that express concentrations of the free drug, the free target, and drug-target complexes via total drug and total target concentrations. These expressions together with differential equations for the total drug and total target concentrations constitute the QSS approximations of the corresponding TMDD systems. QSS systems with zero internalization rate or zero dissociation rate correspond to quasi-equilibrium (QE) or irreversible binding (IB) approximations of the TMDD equations. Michaelis–Menten (MM) approximations were derived assuming that concentrations of the drug-target complexes are much lower than concentrations of the free drug. To check the validity of the derived equations, concentration–time profiles from the full TMDD models and the corresponding QSS approximations were simulated for several dosing regimens.

Results: Simulations demonstrated a good agreement between exact and approximate equations, with some deviations at low concentrations. In addition to predictions of free and total, drug and target concentrations, new approximations predicted concentrations of two drug-target complexes with different stoichiometry.

Conclusions: QSS, QE, IB, and MM approximations of the TMDD models with 1:2 and 2:1 binding were derived. They can be used to provide a more detailed and precise description of the TMDD systems with 1:2 and 2:1 binding stoichiometry than those of the standard TMDD model.

$$C = C_{tot}\frac{(K_D + K_{IB})(K_D + K_{IB}/2) + K_{IB}R/2}{(K_D + K_{IB} + R)(K_D + K_{IB}/2 + R)}; \quad K_D = \frac{k_{off}}{k_{on}}; \quad K_{IB} = \frac{k_{int}}{k_{on}};$$

$$RC = C_{tot}\frac{R(2K_D + K_{IB})}{(K_D + K_{IB} + R)(K_D + K_{IB}/2 + R)}; \quad C_{tot} = C + RC + R_2C;$$

$$R_2C = C_{tot}\frac{R^2}{(K_D + K_{IB} + R)(K_D + K_{IB}/2 + R)}; \quad R_{tot} = R + RC + 2R_2C.$$

$$R = \frac{1}{2}\left[-(2C_{tot} + K_D + K_{IB} - R_{tot}) + \sqrt{(2C_{tot} + K_D + K_{IB} - R_{tot})^2 + 4(K_D + K_{IB})R_{tot}}\right]$$

$$\frac{dA_d}{dt} = -k_a A_d;$$

$$\frac{dC_{tot}}{dt} = \frac{In(t) + F_{SC}k_a A_d + k_{tp}A_T}{V_c} - (k_{el} + k_{pt})C - k_{int}C_{tot}\frac{R\cdot(2K_D + K_{IB} + R)}{(K_D + K_{IB} + R)(K_D + K_{IB}/2 + R)};$$

$$\frac{dA_T}{dt} = k_{pt}C\cdot V_c - k_{tp}A_T;$$

$$\frac{dR_{tot}}{dt} = k_{syn} - k_{deg}R_{tot} - (k_{int} - k_{deg})\cdot C_{tot}\cdot\frac{2R}{K_D + K_{IB} + R};$$

$$A_d(0) = D_1; \quad C_{tot}(0) = D_2/V_c; \quad A_T(0) = 0; \quad R_{tot}(0) = k_{syn}/k_{deg}.$$

Fig. 1 QSS Approximation of the TMDD equations for a drug with two binding sites

W-10

Population Pharmacokinetic/Pharmacodynamic Modeling of a Next Generation Recombinant Human Factor VIIa (LR769) to Derive the Dose to be Studied in Phase 3

Jules Heuberger[1], Johan Frieling[2], Matthijs Moerland[1], Joannes Reijers[1], Koos Burggraaf[1], Cornelis Kluft[3], Jean-Francois Schved[4], Jasper Stevens[1*]

[1]CHDR, The Netherlands; [2]LFB USA, USA; [3]GBS, Netherlands; [4]CHU Montpellier, France

Objectives: To develop a population PK-PD model characterizing Factor VIIa concentration-effect relationship for Thrombin Generation Assay with platelets (AUC of peak, TGTp_AUC), activated partial thromboplastin time (aPTT), thromboelastography (MCF: maximum clot firmness) and Prothrombin fragments 1 + 2 (F1 + 2). This model was then used to optimize a treatment regimen that is expected to be effective in treating and preventing bleedings in hemophilia A/B patients with inhibitors.

Methods: Data ater administration of 25, 75 and 225 μg/kg LR769 to 15 hemophilia A/B patients from a randomized, open label multiple dose cross-over study was used to develop a PK/PD model. FVIIa activity was assessed by modified STACLOT rTF assay. The identified population PK-PD models were used to simulate the response-curves as a function of Factor VIIa activity with different dosing regimens.

Results: A two-compartment model for bolus IV administration was selected for the pharmacokinetics of FVIIa, with lean body mass (LBM) as a covariate on Vd and inter-individual variability on the elimination rate constant. Using the PK model as a driving factor, four PD models were developed for different PD measurements. A sigmoidal maximal effect model was identified for TGTp_AUC, MCF, F1 + 2 (increasing with increasing FVIIa) and aPTT (decreasing with increasing FVIIa) with the latter two having a gamma fixed at 1. Also, the effect in F1 + 2 showed a delayed effect, which was modelled using an effect compartment. Several dose regimens were simulated and evaluated for desired effects.

Conclusions: Based on these results, LR769 showed dose responsiveness and two dosing regimens were chosen to be studied in the Phase 3 study: 75 μg/kg every 3 h and 225 μg/kg, if needed followed 9 h later by 75 μg/kg were deemed to have the most optimal effect-profile. Preliminary results of the ongoing Phase 3 study indicate these doses may be effective and safe.

W-11

Model-Based Meta-Analysis to Develop a Vitamin D Parent-Metabolite Population-Pharmacokinetic Model

Ocampo-Pelland AS[1,3*], Gastonguay MR[1,2,3], French JL[2,3], Riggs MM[2]

[1]Biomedical Engineering, University of Connecticut, USA; [2]Metrum Research Group, LLC; [3]Metrum Institute, Tariffville, Connecticut, USA

Objectives: Association of Vitamin D (D3 & D2) and its 25OHD metabolite (25OHD3 & 25OHD2) exposure with various diseases is an active research area [1]. Clinical studies variations, including dosing regimen, assays, demographics, and control of endogenous D3 production, lead to uncertain and conflicting exposure-related associations. Dose-equivalency of D3 and D2 is also under debate. Population PK (PPK) models were developed to predict D and 25OHD to provide comparisons of D3 and D2 exposures and an added understanding of variability related to dose, baseline and assay type.

Methods: Public-source PK data pertaining to D and 25OHD in healthy or osteoporotic populations, including 74 studies representing 5684 individuals (40 individual-level and 140 group-level units), were selected using specified search criteria in PUBMED. Data included IV, oral, single and multiple dose: dose ranges for D3 (400–100,000 IU/d), D2 (400–100000 IU/d) and 25OHD3 (15–1000 μg/day). Nonlinear mixed effects models were developed simultaneously for D and 25OHD PK (NONMEM v7.2). Model development explored 1- and 2-compartment models with linear (CL)

or nonlinear clearance (CLNL). Unit-level random effects and residual errors were weighted by arm sample size.

Results: D2 and D3 parent and metabolite were each described by 2-compartment models with numerous shared estimates (Figure 1). D3 CLNL resulted in inverse 25OHD3 relationships with dose and baseline; D2 did not exhibit nonlinearity. Quadrupling D3 dose (400 to 2000 IU/d, 25OHD3 baseline = 40 nmol/L) resulted in only a 1.3 fold 25OHD3 increase. Precision and bias differences for 25OHD3 competitive protein binding assay and chemiluminescence suggested that assay be considered when comparing these with RIA or HPLC–MS.

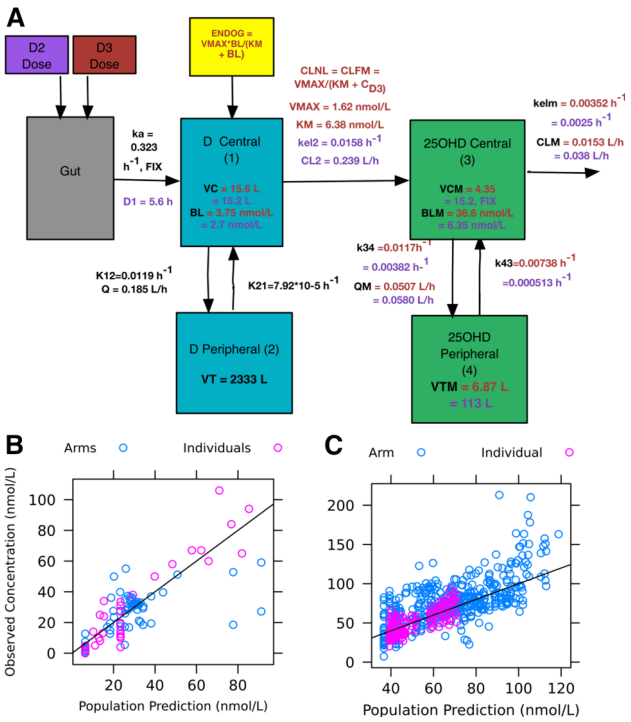

Fig. 1 **a** Comparatmental model for D (D2 and D3) and 25OHD (25OHD2 and 25OHD3) with parameter values (*red* = D3, *purple* = D2, *black* = shared). **b** Diagnostic plot for 25OHD2 and **c** 25OHD3. *ENDOG* endogenous D3 production, *BL* baseline concentration

Conclusions: D3 and 25OHD3 PK modeling suggested that CLNL was important when considering these exposure comparisons across studies and dosing regimens. Notable D2/D3 differences included CLNL for parent D3 and higher (nearly doubled) estimated D2 metabolite CL.

References:

1. Hagenau, R et al. Osteoporos. Int. 20, 133–140, 2009

W-12

Population Pharmacokinetics and Exposure–Response Analysis of Entospletinib, a Selective Spleen Tyrosine Kinase Inhibitor

Shringi Sharma[1*], Feng Jin[1], Jing He[1], Michelle Robeson[1], Esteban Abella[1], Jeff P. Sharman[2,3], Srini Ramanathan[1]

[1]Gilead Sciences, Foster City, CA; [2]Willamette Valley Cancer Institute and Research Center, Eugene, OR; [3]US Oncology Research, The Woodlands, TX

Objectives: Entospletinib (ENTO) is an orally bioavailable, selective, reversible, small molecule spleen tyrosine kinase inhibitor. ENTO is currently in a Phase 2 clinical trial in patients with relapsed or refractory CLL/NHL. The objective was to develop a population pharmacokinetic model for ENTO and investigate the exposure-efficacy relationship.

Methods: In healthy volunteers (N = 96, HV), ENTO (25 mg to 1200 mg) was orally administered as single or multiple (once daily or twice daily) ascending doses. In subjects with hematological malignancies (N = 142), ENTO 800 mg twice daily was administered and pharmacokinetic samples were collected on Cycle 1 Day 1 (pre-dose, 1.5 and 4 h post-dose) and subsequent cycles (pre-dose). A nonlinear mixed-effects model was fitted to ENTO plasma concentrations. Covariates screened for influence on ENTO PK were baseline body weight, BMI, BSA, age, creatinine clearance, AST, ALT, bilirubin, sex, race and disease status (HV versus patient). Relationships between model predicted ENTO exposures and early efficacy end points such as tumor size (SPD), overall response rate (ORR) and best overall response (BOR) were evaluated.

Results: A two-compartment model with dose dependent, non-linear absorption and first order elimination described ENTO PK, based on visual predictive check and parameter estimate precision. ENTO PK was unaffected by the baseline covariates evaluated. ENTO exposures (AUC, Cmax and Ctrough) were comparable between HVs and patients (CLL or FL). Over the range of ENTO exposures (~3 to 4-fold range between midpoint of first vs fourth quartile), no association was observed with SPD, ORR or BOR for either CLL or FL population.

Conclusions: ENTO PK is unaffected by demographic, biometric, or disease-relevant covariates. No relevant relationship between exposure and early efficacy in a limited subset of patients was observed, suggesting that ENTO 800 mg BID provided exposures resulting in consistent therapeutic effects.

W-13

A Model-Based Meta-Analysis of Insulin PK-PD in Glucose Clamp Studies of Diabetes Mellitus Type 1 and Non-Diabetic Human Subjects

Eric G. Burroughs[1*], Craig Fancourt[2], Kevin Dykstra[1], Sandra A.G. Visser[2]

[1]qPharmetra, Andover, MA, USA; [2]Merck & Co. Inc., Kenilworth, NJ, USA

Objectives: A model-based meta-analysis (MBMA) of hyperinsulinemic glucose clamp clinical data was conducted to quantitatively characterize differences in standard insulin pharmacokinetics (PK) and glucose metabolism (PD) in Type 1 diabetics (T1DM) compared to non-diabetics (ND).

Methods: A literature search identified 21 clinical study publications examining glucose disposal rates (GDR) under different insulin infusion rates (IIR) and steady-state insulin ([*INS*]) and glucose ([*GLC*]) concentrations among T1DMs, with or without ND control groups (two seminal ND-only studies were included to support ND modeling). The relationship between [INS] and IIR and GDR was described by a steady-state mechanistic PK-PD clamp model [1]. Parameters were estimated by fitting the literature data using nonlinear mixed effects techniques. Models were explored using different random (study) and population effects (ND vs. T1DM). Visual

predictive check simulations ensured central tendencies and variability in the relationships were captured.

Results: The PK model's insulin clearance was saturable, resulting in total clearance declining with increasing [*INS*]. The non-specific clearance mechanism was dominant under high [*INS*] conditions. No population differences in insulin PK were identified. A population difference was estimated for the PD model's maximum insulin-dependent glucose clearance and half-maximal insulin-mediated disposition. Compared to NDs, the [*INS*] required to maintain a given GDR was increased 1.5-fold among T1DMs, and the maximum GDR for a given fixed [*GLC*] target level was reduced 13 % among T1DM subjects. As shown in Figure 1, together these effects result in slightly higher GDR among NDs than in T1DMs, with the difference depending on both [*GLC*] and [*INS*].

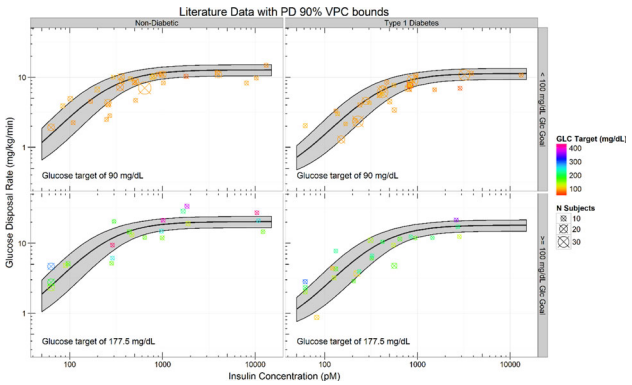

Fig. 1 Visual Predictive Check of GDR vs IIR for Final PD Model. Observed data are grouped into four panels by population type and if the glucose goal was above or below 100 mg/dL; the mean projection is shown as a *black line* bounded by a grey polygon representing the 90 % prediction interval; the size of the symbols are proportional to the relative number of subjects in a particular trial arm while the color of the symbols indicate glucose target levels

Conclusions: The clamp PK-PD model successfully described the relationship between IIR and [*INS*] and between GDR and [*INS*] and [*GLC*] for T1DM and ND populations. Simulations based on the final model were used to plan, and were ultimately in agreement with, a clinical clamp study of T1DM subjects [2].

References:

1. Fancourt et al., ACOP 2015.
2. Kandala et al., ACOP 2015.

W-14

Population Pharmacokinetics of Ethanol in Moderate and Heavy Drinkers

Yu Jiang[1], Nick Holford[2], Daryl J.Murry[1], Timothy L.Brown[3], Gary Milavetz[1*]

[1]College of Pharmacy, University of Iowa, USA, [2]Department of Pharmacology and Clinical Pharmacology, University of Auckland, New Zealand, [3]National Advanced Driving Simulator, Center for Computer Aided Design, University of Iowa, USA

Objectives: To investigate the effect of sex, age, and previous drinking history on ethanol pharmacokinetic parameters with the implementation of a rate dependent extraction model [1], which takes into account the change in hepatic first-pass extraction along with absorption rate and a body composition model that accounts for fat free mass and fat mass [2].

Methods: 108 moderate or heavy drinkers were dosed orally on 2 occasions to achieve a peak blood ethanol concentration of 0.65 g/L or 1.15 g/L using a randomized, crossover design. A total of 6025 breath measurements were obtained and converted into blood alcohol concentration by applying a blood: breath ratio of 2100:1. NONMEM 7.3.0 was used for data analysis. A semi-mechanistic rate dependent extraction model with zero-order input followed by first order absorption was utilized with V allometrically scaled by normal fat mass, V_{max} allometrically scaled by total body weight and portal vein blood flow allometrically scaled by fat free mass. The effects of sex and age (21–34, 38–51, or 55–68 years of age) on V, V_{max}, and K_m; and the effect of drinking status (moderate or heavy drinkers) on V_{max} and K_m were explored. The covariate effect was considered to be statistically significant if the 95 % non-parametric bootstrap confidence interval of the fractional difference did not include 1.

Results: The 95 % bootstrap confidence interval of fractional differences between groups in age, sex and ethanol consumption history all contain 1, indicating none of those covariates have significant effects on any ethanol disposition parameters.

Conclusions: Age and sex were not regarded as significant predictors for ethanol disposition parameters after accounting for body size and composition. The results indicated a 19 % higher V_{max} and 15 % lower K_m for heavy drinkers compared with moderate drinkers, but the difference was not statistically significant.

References:

1. Holford, N.H., Complex PK/PD models–an alcoholic experience. Int J Clin Pharmacol Ther, 1997. 35(10): p. 465–8.
2. Holford, N., et al., The Influence of Body Composition on Ethanol Pharmacokinetics using a Rate Dependent Extraction Model. PAGE, 2015. 24 Abstr 3405 [http://www.page-meeting.org/default.asp?abstract=3405].

W-15

Population Pharmacokinetics and Pharmacodynamics of Blosozumab

Cheng Cai Tang[1], Charles Benson[2], Juliet McColm[3], Adrien Sipos[2], Bruce Mitlak[2], Leijun Hu[2*]

[1]Eli Lilly and Company, Singapore, Republic of Singapore; [2]Eli Lilly and Company, Indianapolis, IN, USA; [3]Eli Lilly and Company, Windlesham, United Kingdom

Objectives: Blosozumab is a humanized monoclonal antibody against sclerostin that is being evaluated as a treatment for osteoporosis. Population modeling was utilized to characterize the pharmacokinetics (PK) of blosozumab and establish pharmacodynamic (PD) exposure–response relationship for bone mineral density (BMD) changes in lumbar spine (LS) and total hip (TH).

Methods: The population PK model used data from three phase 1 studies in healthy postmenopausal (PMP) women (single or repeated intravenous infusions or subcutaneous [SC] injections of blosozumab or placebo) and one phase 2 study in osteoporotic PMP women (4 blosozumab SC regimens or placebo). The exposure–response model was constructed by jointly fitting LS and TH BMDs from the Phase 2 study. Limited covariate exploration was conducted on PK and PD parameters.

Results: Blosozumab PK data were best described by a two-compartment open model with both linear and saturable clearances (CL).

In the final PK model, the linear CL was 8.82 mL/h; volume of distribution was 3.96 L; bioavailability for the 2 SC formulations used was 54 % and 69 %, respectively. These values are typical for monoclonal antibodies. Body weight was found to influence the volumes and saturable CL.
The exposure–response model well described the observed changes in BMD. Briefly, blosozumab exposure was linked to a hypothetical target engagement module which led to LS and TH BMD responses through indirect response relationships. The baseline concentration of procollagen type 1 N propeptide (P1NP) was found to be a significant covariate for the production rate constant of BMD.
Conclusion: The population PK model and the exposure–response model for blosozumab adequately captured the observed PK and BMD data. By clinical trial simulations, these models support selection of appropriate regimens for future development of blosozumab.

W-16

Population Pharmacokinetics and Pharmacodynamics (PK/PD) of AMG 416 in Chronic Kidney Subjects With Chronic Kidney Disease (CKD) and Secondary Hyperparathyroidism (sHPT) Receiving Hemodialysis

Murad Melhem[1*], Per Olsson Gisleskog[2], Justin Wilkins[2], Adimoolam Narayanan[1], Ping Chen[1]

[1]Amgen Inc. [2]SGS Exprimo NV

Objectives: AMG 416 is a novel calcium-sensing receptor (CaSR) activator currently in development for the treatment of sHPT. The objectives of this analysis were to develop a population PK/PD model relating AMG 416 exposure to markers of efficacy (intact PTH, iPTH) and safety (corrected serum calcium, cCa); to evaluate covariate effects on PK/PD parameters; and to perform PK/PD simulations exploring the interplay between treatment and both markers.
Methods: Serum iPTH and cCa concentration–time data were collected from 3 clinical studies following the administration of AMG 416 as single or multiple intravenous doses (2.5 to 60 mg). Population PK/PD modeling of AMG 416 was performed using NONMEM 7.2. A semi-mechanistic model, implementing allosteric activation, was use to describe the relationship between AMG 416, iPTH and cCa (Figure 1). Impact of relevant covariates (weight, sex, race, age, phosphorus, time on dialysis and vitamin D) was evaluated using forward/backward selection. The model performance was evaluated using standard goodness-of-fit plots and prediction-corrected visual predictive checks (pcVPC).
Results: The interaction between AMG 416, iPTH and cCa was well described by the model. Estimates of turnover half-lives of iPTH and cCa were 0.25 h and 21.66 h, respectively. The estimated cooperativity constant was 4.94 confirming allosteric activation effects of AMG 416 on CaSR. The extent of inter-individual variability in model parameters was low to moderate (5–61 %). No covariates were identified as significant predictors of PD variability. pcVPC confirmed the predictive ability of the model. Simulations suggested that at steady-state maximum AMG 416 concentration (72.11 ng/mL), mean CaSR occupancy was increased by approximately 10 %, resulting in mean relative PTH suppression of approximately 60–70 %.
Conclusions: The current model incorporates the major components of the PTH/Ca homeostatic system, and describes the AMG 416 allosteric activation effects of CaSR. Dose adjustment by relevant covariates was deemed unwarranted.

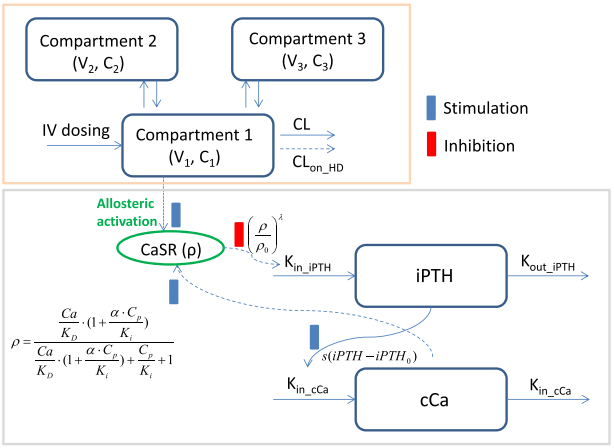

Fig. 1 Semi-mechanistic PK/PD Model Structure. $K_{in,PTH}$ and $K_{out,PTH}$: the zero-order production rate of PTH and the first-order elimination rate constant for iPTH, respectively; ρ0: the Ca/CaSR occupancy at baseline; λ: a constant determining the strength of the effect of changes in ρ on iPTH production; $K_{in,Ca}$ and $K_{out,Ca}$: the zero order production rate of Ca and the first order elimination rate for Ca, respectively; S: the slope relating changes in iPTH from baseline to Ca production; K_i: the equilibrium dissociation constant for AMG 416 at the CaSR; K_D: the equilibrium dissociation constant for Ca at the CaSR; α: the cooperativity constant; C_p: the AMG 416 plasma concentration

W-17

Datasets for Pharmacometric Analyses: Internal Review and Standardization Efforts

Andrijana Radivojevic[1*], Henning Schmidt[2]

[1]Novartis Pharmaceuticals Corporation, One Health Plaza, East Hanover, 07936, NJ, USA, [2]Novartis Pharma AG, Postfach, 4002 Basel, Switzerland

Objectives: The main goal of this work is to standardize the dataset specifications used for pharmacometric analyses, leading to improved efficiency of dataset preparation and assuring consistent quality.
Methods: Extensive review of historical and existing data requests within Novartis Pharmacometrics group has been performed. This included 384 different data requests, spanning the period of years 1999–2015. Inter-modeler variability considering styles, preferences, analysis platforms, modeling methods, disease area specific requirements and more, has been captured. Type of data to be included in the analysis datasets and relevant clinical questions have also been assessed.
Results: The existing generalized dataset described in [1] has been updated to cover at least 95 % of identified needs in a diverse pharmacometric group. Proposed dataset structure is user-friendly, understandable and modeling-platform-independent. It captures elaborate extend of clinical information, and it facilitates project onboarding and takeover. The standalone generalized dataset format becomes fully useful only when it is supported by tools for automatic quality checks and conversion to analysis datasets. Proof-of-concept for the complete solution is implemented in [2].

Conclusions: Underestimation of the time needed for preparation of high quality modeling dataset is a common mistake and lack of data standards and supporting tools could lead to direct implications of reproducibility and auditing of modeling work [3]. Therefore, standardizing dataset format within pharmacometric organization is a pivotal step toward efficient implementation of model-based drug development.

References:

1. H. Schmidt, A. Radivojevic (2014) Enhancing population pharmacokinetic modeling efficiency and quality using an integrated workflow. *J Pharmacokinet Pharmacodynam*. doi 10.1007/s10928-014-9370-4.
2. H. Schmidt (2013) SBPOP Package: Efficient support for model based drug development—from mechanistic models to complex trial simulation. PAGE meeting, Glasgow, UK [http://www.page-meeting.eu/default.asp?abstract=2670], [http://www.sbtoolbox2.org].
3. S. Jönsson, E. N. Jonsson (2007) Timing and efficiency in population pharmacokinetic/pharmacodynamic data analysis projects. Pharmacometrics: The Science of Quantitative Pharmacology. Edited by E. Ette and P. J. Williams, John Wiley & Sons, Inc.

W-18

Pharmacokinetics of Flavopiridol Using Bolus or Hybrid Administration Schedules in the Treatment of Acute Leukemias

Carl LaCerte[1], Vijay Ivaturi[1*], Jacqueline M. Greer[2], Judith E. Karp[2], Michelle A. Rudek[2]

[1]Center for Translational Medicine, University of Maryland Baltimore; [2]The Sidney Kimmel Comprehensive Cancer Center at Johns Hopkins, Baltimore, MD

Objectives: To characterize the pharmacokinetics of total and unbound flavopiridol administered using either a bolus or a hybrid schedule (bolus followed by a 4-h infusion); the latter designed to overcome flavopiridol plasma protein binding [1].
Methods: Data from 129 patients enrolled in a Phase 1 (49 patients/hybrid schedule) and two Phase 2 (48 patients/hybrid schedule; 32 patients/bolus schedule) FLAM studies (sequential flavopiridol, ara-C, and mitoxantrone) were used for modeling. Bolus flavopiridol administration consisted of 3 consecutive days of 1 h IV bolus dosing at 50 mg/m^2. Hybrid flavopiridol administration consisted of 3 consecutive days of 0.5 h IV bolus dosing followed by a 4 h IV infusion with a range of doses explored (mg/m^2 for bolus:infusion): 20:30, 25:35, 30:40, 30:50, 30:60, and 30:70. Standard population PK methods were used to simultaneously fit the total and unbound flavopiridol concentrations from all 3 studies. A full model approach was used to assess the limited covariate information (body surface area, age, and sex) for explanatory ability.
Results: A 2-compartment model for total flavopiridol with mixed proportional and additive residual variability adequately described the typical and individual profiles. The population estimates of CL, V, Q and V2 were 37.8 L/h, 78.7 L, 9.68 L/h and 102 L, respectively. A fraction-unbound parameter to account for unbound flavopiridol was estimated to be 11.2 %. Plasma binding of flavopiridol was found to be linear/unsaturable. No covariates were found to have a clinically important effect on the PK parameters.
Conclusions: The pharmacokinetics of flavopiridol have been adequately characterized across studies, doses, and administration schedules facilitating future work to assess relationships between exposure and response.

References:

1. Byrd JC et al. Blood. 2007;109:399–404.

W-19

A PBPK Model Platform for Nanoparticles Including Lymphatic and Size-Dependent Transport

Colin Phipps[1,*], Andrea Edginton[1]

[1]School of Pharmacy, University of Waterloo, Ontario, Canada

Objectives: One of the benefits of physiologically-based pharmacokinetic (PBPK) models is their ability to perform interspecies extrapolation by parameterizing mechanistic processes with physically meaningful constants. Another benefit is their flexibility to consider various administration routes by adapting a single drug-dependent model. A number of PBPK models have been developed for the distribution of nanoparticles [1–3]; however, they suffer from issues that preclude the utilization of the aforementioned benefits. This work addresses three fundamental areas of nanoparticle PBPK models: (i) convective and mechanistic transvascular transport models, (ii) addition of the lymphatic system, and (iii) size-dependent transport and uptake.
Methods: A comprehensive PBPK model was developed using MATLAB that includes mechanistic transvascular transport terms, uptake by the mononuclear phagocyte system and lymphatic transport in each organ. These processes are size-dependent with size partitioned into discrete bins to facilitate differential equations for each bin. A generic schematic of the processes in a typical compartment is presented in the Figure. Sensitivity analyses were performed to determine the impact of model parameters in various treatment scenarios.

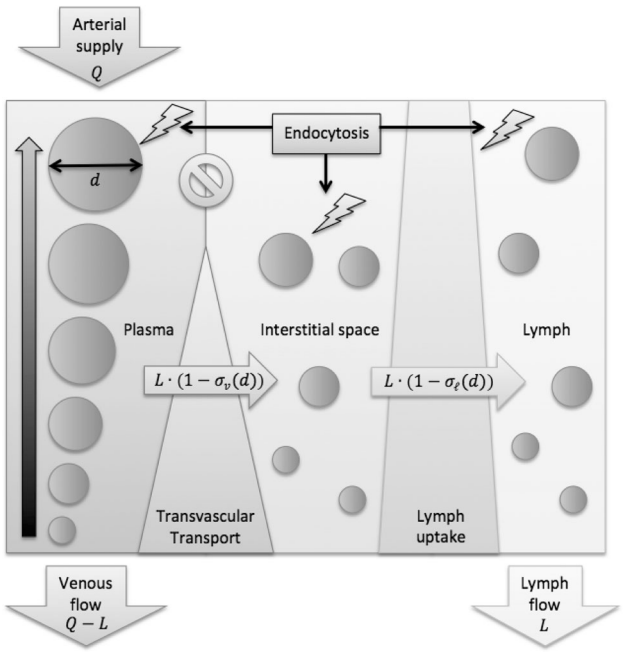

Results: Lymphatic and mechanistic transport terms allowed for the direct estimation of physiologically meaningful parameters (e.g. vascular and lymphatic reflection coefficients, denoted σ_v and σ_ℓ).

The model accommodates cases where lymphatic transport plays a crucial role in disposition, such as subcutaneous administration. Sensitivity analyses demonstrated the relative importance of vascular reflection coefficient estimation to IV administration prediction and lymphatic reflection coefficients to subcutaneous and dermal routes.
Conclusions: It is imperative that the current framework for PBPK models used to predict nanoparticle biodistribution be reassessed so that the existing body of research can be utilized to guide future modeling attempts and nanoparticle development. Utilizing the comprehensive and mechanistic model developed here has yielded translatable results and can be expanded to include targeted delivery and nanoparticle release profiles in future work.

References:

1. Lin Z. et al., Nanotoxicology, 2015(0):1–11.
2. Bachler G. et al., International Journal of Nanomedicine, 2013. 8:3365.
3. Li, D. et al., Nanotoxicology, 2014. 8(sup1):128–137.

W-20

Eslicarbazepine Acetate Drug–Drug Interactions: Characterization Through a Model-Based Population Approach

Sunkaraneni, S[1]; Ludwig EA[2*]; Blum D[1]; Fiedler-KellyJ[2]

[1]Sunovion Pharmaceuticals Inc., Marlborough, MA; [2]Cognigen Corporation, Buffalo, NY

Objectives: A population model-based characterization of drug–drug interactions (DDI) was conducted to assess whether potential interactions of antiepileptic drugs (AEDs) used concomitantly with eslicarbazepine acetate (ESL, Aptiom) to treat partial-onset seizures (POS) had a clinically significant effect on eslicarbazepine (primary active metabolite) pharmacokinetics (PK).
Methods: DDI with AEDs were evaluated in Phase I studies of ESL 1200 mg QD co- administered with lamotrigine, topiramate, phenytoin and carbamazepine. Pooled PK data from three Phase III trials of ESL (400–1200 mg) coadministered with carbamazepine, phenobarbital, phenytoin, levetiracetam, gabapentin, or valproate were also characterized through a population approach. The effects of AEDs on apparent eslicarbazepine clearance (CL/F) and exposure and ESL on CL/F and exposure to other AEDs were evaluated.
Results: In Phase I studies, co-administration of ESL decreased the exposure to lamotrigine (14 %), topiramate (18 %), and carbamazepine (10 %); and increased the exposure to phenytoin (35 %). In the same subjects, lamotrigine, topiramate, carbamazepine, and phenytoin decreased the exposure to eslicarbazepine by 4, 7, 32, and 33 %, respectively. In the population pharmacokinetic analyses, a one-compartment model with first-order absorption and linear elimination described eslicarbazepine pharmacokinetics; for other AEDs, population models were developed to estimate apparent oral clearance. Coadministration of ESL and carbamazepine resulted in decreased exposure to both carbamazepine (4–10 %) and eslicarbazepine (25–34 %). Eslicarbazepine exposure decreased (34 %) in presence of phenobarbital and similar metabolic inducers including phenytoin and primidone. No clinically relevant change in exposure was seen in the remaining AEDs studied (Figure 1).

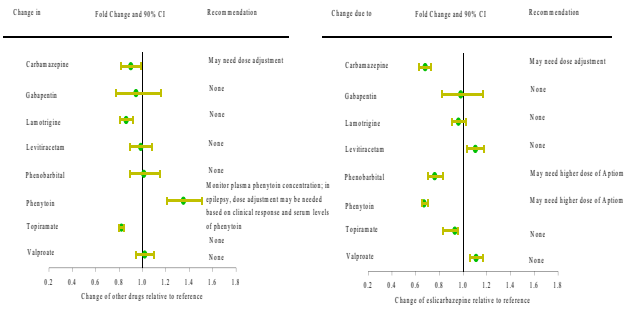

Fig. 1 Potential Impact of ESL on the exposure to Other AEDs (*left panel*) and Potential Impact of Other AEDs on exposure to eslicarbazepine (*right panel*)

Conclusions: In these studies, no clinically relevant DDIs were observed when ESL was co- administered with levetiracetam, gabapentin, lamotrigine, topiramate, phenobarbital, or valproate, therefore, no dose adjustment of these AEDs or ESL is anticipated. In contrast, co- administration of carbamazepine, phenytoin and phenobarbital led to potentially clinically meaningful reductions in eslicarbazepine exposure. The dose of ESL may need to be increased and should be guided by both pharmacokinetic and clinical response considerations. Altered exposure to phenytoin suggests that monitoring of phenytoin plasma concentrations may be warranted.

The results in this abstract have been previously presented in part at the American Academy of Neurology Annual Meeting, April 2011, Honolulu, Hawaii using Phase 3 data from 2 studies.

W-21

Building an Inflammatory Bowel Disease Network, a Systems Pharmacology Approach

Ignacio Gonzalez-Garcia[1,2*], Itziar Irurzun-Arana[1], Leire Ruiz-Cerdá[1], Chuanpu Hu[3], Honghui Zhou[3], An Vermeulen[4], Iñaki F. Trocóniz[1], José David Gómez-Mantilla[1]

[1]Pharmacometrics and Systems Pharmacology. University of Navarra, Pamplona, Spain; [2]Pharmacy and Pharmaceutical Technology Department, University of Valencia. Valencia, Spain; [3]Janssen Research and Development, LLC, Spring House, USA; [4]Janssen Research and Development, a division of Janssen Pharmaceutica NV, Beerse, Belgium

Objectives: Systems pharmacology it is a new tool that allows the study of complex biological systems [1], like immunological response to antigens. Inflammatory Bowel Disease (IBD) is a complex disorder, which evolves through several complicated immunological pathways and is characterized by processes of remission and relapse producing a functional impairment of the gut wall. It includes Crohn Disease (CD) and Ulcerative Colitis (UC) [2]. The objective of the current work was to develop a systems pharmacology model for CD and UC integrating the main known components and reactions as a tool to identify possible therapeutic targets and biomarkers.
Methods: A theoretical disease network was developed using information taken from literature (Figure 1). Boolean functions were designed to link all the components in order to build the network. 5000 simulations were carried out to validate the network.

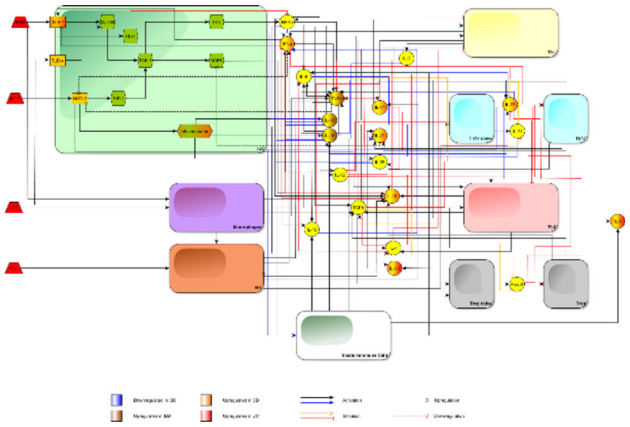

Fig. 1 Theoretical IBD network

Results: The network contains 45 nodes and more than 150 interactions. The network model was able to simulate the gastrointestinal tract state with different underlying alterations. The simulation exercise allowed identification of model elements, whose profiles changed due to the underlying alterations.
Conclusions: A systems pharmacology model was developed integrating the main known pathways in IBD. The model has shown its applicability in identifying altered pathways, which resembled different statuses of the disease, opening up the potential to identify therapeutic targets and biomarkers.

References:

1. van der Graaf PH, Benson N. Systems pharmacology: bridging systems biology and pharmacokinetics-pharmacodynamics (PKPD) in drug discovery and development. Pharm Res 2011 28(7):1460–4.
2. Abraham C, Cho JH. Inflammatory bowel disease. N Engl J Med. 2009;361(21):2066–78.

W-22

Identification and Quantification of Noncompliance Patterns Associated to Specific Clinical Outcomes

Steven Sanche[1], Jun Li[1,2], Fahima Nekka[1,2*]

[1]Faculté de Pharmacie, Université de Montréal, Québec, Canada; [2]Centre de recherches mathématiques, Université de Montréal, Québec, Canada

Background: Lack of adherence to prescribed medication is considered a major problem for outpatient health, which leads to lower treatment efficacy, increase toxic events and resistance to treatment. Clinical evidence indicates that specific therapeutic outcomes are more likely associated to some particular noncompliance patterns. Identification and quantifications of these patterns characteristics and their link to outcomes is of great importance for treatment success.
Objective: Within the particular context of chronic viral drugs, efavirenz for HIV viral counts as an example, we determine major determinants that link noncompliance patterns to clinical outcomes, with a particular emphasis on the resistance selection window (RSW).
Methods: Various noncompliance patterns were simulated using Markov process in order to mimic realistic adherence patterns, recorded by Medication Event Monitoring Systems (MEMS). A population-pharmacokinetic model of efavirenz, known for its relatively low clearance, high potency for susceptible viral strains but a broad resistance selection window, has been used. The probability of therapeutic success or failure of these noncompliance patterns is determined.
Results: Medication clearance, potency and the extent of RSW dictate whether a pill count is sufficient to predict clinical outcomes. For those patients taking 80 % of their pills, the usual criteria of compliance, the probability of plasma concentrations located in RSW varies significantly in terms of noncompliance pattern.
Conclusion: These findings can help clinicians in their decision regarding the importance of monitoring the drug intake of outpatients.

References:

1. Girard, P et al. (1998). A Markov mixed effect regression model for drug compliance. Statistics in Medicine, 17(20), 2313–2333.
2. Li, J., & Nekka, F. (2009). A probabilistic approach for the evaluation of pharmacological effect induced by patient irregular drug intake. Journal of Pharmacokinetics and Pharmacodynamics, 36(3), 221–238.
3. Bangsberg, D. R et al. (2006). Adherence-resistance relationships for protease and non-nucleoside reverse transcriptase inhibitors explained by virological fitness. AIDS (London, England), 20(2), 223–231.

W-23

Simulation from ODE-Based Population PK/PD and Systems Pharmacology Models in R with mrgsolve

Kyle T. Baron[1*] and Marc R. Gastonguay[1]

[1]Metrum Research Group, LLC, Tariffville, CT

Objective: To develop computer software facilitating large-scale simulation from hierarchical, ordinary differential equation (ODE) based models typically employed in drug development.
Methods: Specific software requirements were specified to enable a modern and efficient simulation platform. A C++ interface between R and the ODEPACK solver DLSODA was developed using Rcpp. C++ classes were developed to abstract solver setup, data sets and records, and PK dosing events. S4 classes and methods were created to represent the model in R as an updatable object. The modeler creates a model specification file consisting of R and C++ code that is parsed, compiled, and dynamically loaded into the R session. Input data are passed in and simulated data are returned as R objects, so disk access is never required during the simulation cycle after compiling.
Results:The following software requirements were met:

- NMTRAN-like input data sets
- Bolus, infusion, compartment on/off and reset functionality
- Bioavailability, ALAG, SS, II, ADDL, MTIME
- Multivariate normal random effects simulated using RcppArmadillo
- Compatible with parameter estimation and design packages in R (nlme, saemix, PopED, PFIM)
- Integration with data summary (dplyr) and plotting (ggplot, lattice) packages
- Parallelization with existing R infrastructure (mclapply) or Sun Grid Engine (qapply)
- Compatible with output from many different model estimation platforms
- Easily integrated with Shiny to create model-visualization applications

Benchmark:

- Simulation of 4- and 26-week trials of 1000 patients with daily oral dosing as an indirect response model with 1-compartment PK took 1.35 and 9.01 s (average, 10 replicates), respectively, on MacBookPro 2.4 GHz

Conclusions: mrgsolve is a powerful and efficient tool for simulation from ODE-based PK/PD and systems pharmacology models. The resulting computational efficiency facilitates model exploration and application, both during model development and decision-making phases of a drug development program.

References:

1. A. C. Hindmarsh, "ODEPACK, A Systematized Collection of ODE Solvers", in Scientific Computing, R. S. Stepleman et al. (eds.), North-Holland, Amsterdam, 1983, pp. 55–64.

W-24

Population Pharmacokinetic-Pharmacodynamic Modeling and Simulation of Neutropenia in Patients With Advanced Cancer Treated With Palbociclib

Wan Sun[1*], Diane Wang[1]

[1]Clinical Pharmacology, Pfizer Oncology, Pfizer Inc, San Diego, CA, USA

Objectives: Neutropenia is the most common hematologic toxicity following treatment with palbociclib, a cyclin-dependent kinase (CDK) 4/6 inhibitor approved for metastatic breast cancer. There is a paucity of pharmacokinetic (PK)-pharmacodynamic (PD) modeling studies of neutropenia associated with targeted anticancer drugs, such as CDK4/6 inhibitors. A PK-PD model was developed to describe the time course of absolute neutrophil count (ANC), quantify the exposure–response relationship for neutropenia, and characterize neutropenia associated with palbociclib treatment.
Methods: A semi-mechanistic PK-PD analysis was performed using data from 185 advanced cancer patients receiving palbociclib in 3 clinical trials (NCT00141297; NCT00420056; NCT00721409). A population PK model was developed first to obtain the individual PK parameters that were sequentially used in the PD portion of the model. Plasma concentration was related to the anti-proliferative effect of palbociclib on stem cells through drug-related parameters; maturation of neutrophil in bone marrow was mimicked through a proliferation compartment, 3 transit compartments, and blood circulation compartment using system-related parameters. The effects of covariates including demographic factors and laboratory test variables were evaluated. Different approaches were used to assess model adequacy and predictive capability; model-based simulations were conducted.
Results: The final model adequately described longitudinal ANC with good predictive capability across dose levels and regimens. Gender and baseline albumin level were significant covariates on baseline ANC value. The model suggested correlation of higher palbociclib dose levels associated with lower ANC time profiles; ANC nadir was reached approximately 21 days after initiation of palbociclib treatment (both schedules: 3 weeks on/1 week off [3/1]; 2/1). Model-predicted ANC time profiles suggested that neutropenia associated with palbociclib is rapidly reversible rather than cumulative, with no trend of worsening ANC level observed over multiple cycles (Figure).

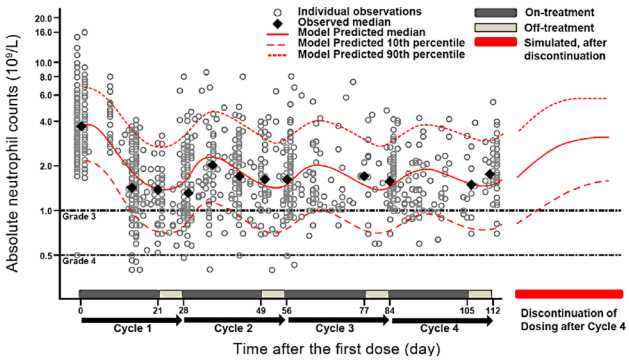

Fig. 1 Observed and model-simulated ANC time profile for patients treated with a starting dose of palbociclib 125 mg (3/1 schedule), with simulation alone for ANC values after discontinuation of dosing. Black dashed lines are reference lines for ANC = 1.0×10^9/L and ANC = 0.5×10^9/L; ANC = absolute neutrophil count

Conclusions: PK-PD modeling analyses support the approved palbociclib dosing and management strategies for the breast cancer indication and aid in predicting ANC and neutropenia incidence in future palbociclib trials with different dosing regimens/combinations and optimizing dosing schedules for future indications.

W-25

Impact of Model Uncertainty on Phase 2 Diabetes Trial Design

Timothy H Waterhouse*, Xiaosu Ma, Jenny Y Chien

Eli Lilly and Company, Indianapolis, IN

Objectives: To evaluate the impact of different levels of model uncertainty (due to limited prior data in patients) on the power of Phase 2 trial designs for treatment of T2DM, and the performance of exposure–response versus dose–response models.
Methods: A population PK/PD model was used to simulate exposure–response relationships for HbA1c and glucose in a hypothetical patient population. Although the true underlying model is assumed to be known (an indirect reponse model, with HbA1c linked to glucose), different levels of uncertainty are simulated as scenarios with varying confidence in the model parameters. The uncertainty in estimates of Emax and EC50, ranging from 0 to 200 % CV, reflect the amount of prior knowledge in patients. Doses for the simulations were selected based on the current parameter estimates. 1000 trial replicates were simulated for each combination of sample size and number of dose levels. Power was calculated for various metrics, including ability to estimate model parameters and the target dose, using both exposure–response and dose–response models. Simulations are visualized using Shiny, an R package.
Results: In general, power increased with sample size and number of dose levels, and decreased with increasing uncertainty. For example, using an exposure–response model for a 5-dose design, the sample size required for at least 80 % power to estimate a target dose whose true typical HbA1c response is within 0.15 % of the desired response was 39/arm for the lowest uncertainty, and 53/arm for the highest uncertainty (Figure 1). Exposure–response models typically provided slightly greater power than dose–response models. When using the linear model, power was significantly lower due to model misspecification.

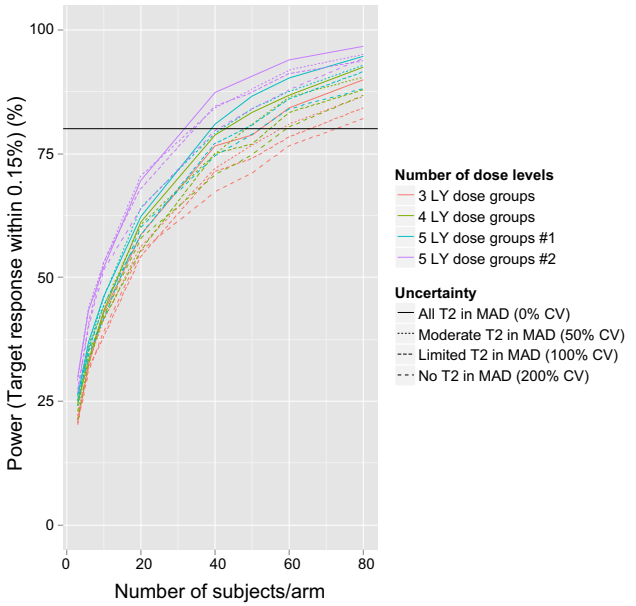

Fig. 1 Power to estimate a target dose whose HbA1c change is truly within 0.15 % of the desired response when using an exposure–response Emax model

Conclusions: Model uncertainty has significant impact on the design of a dose-finding Phase 2 study. Thus, leveraging prior data in T2DM patients may have significant cost-saving benefits. Further, Emax models based on exposure and dose performed comparably, while a simple linear regression was extremely poor, suggesting that power is low when using a model that does not well describe the underlying dose–response relationship.

W-26

Population Pharmacokinetics of a Pangenetic NS5A inhibitor, ABT-530, in HCV infected Patients with and without Cirrhosis

Chih-Wei Lin*, Aksana Kaefer Jones, Wei Liu, Sandeep Dutta

Clinical Pharmacology and Pharmacometrics, AbbVie

Objectives: ABT-530 is a nonstructural protein 5A (NS5A) inhibitor with pangenotypic activity against HCV virus. The purpose of this analysis was to characterize the population pharmacokinetics of ABT-530 in HCV infected subjects.
Methods: Data from 38 HCV infected subjects who received ABT-530 doses ranging from 15 to 400 mg QD (15, 40, 120 (with and without cirrhotics) or 400 mg QD) following 3 day monotherapy was included in the population pharmacokinetic analysis. The model was built using nonlinear mixed-effects modeling in NONMEM 7.3. Based on ABT-530 pharmacokinetic profile, transit compartments were explored to describe the delay in drug absorptions. A gamma density function was used to estimate the number of transit compartments during the model development. A schematic of the model is shown in Figure. Model evaluation and validations were conducted to assess adequacy and robustness.
Results:
Observed ABT-530 pharmacokinetic profiles were well described by a two-compartment disposition model with a delayed absorption. Five transit compartments were estimated to describe the delayed absorption with a mean transit time of 4 h, consistent with estimates from gamma density absorption function (4.6 transit compartments with a mean transit time of 3.6 h) evaluated during model development. The estimated apparent clearance (CL/F) and apparent volume of distribution (V/F) were 300 L/h and 220 L, respectively. The nonlinear pharmacokinetics of ABT-530 was addressed by dose-dependent bioavailability as elimination half-life was similar across doses. Both the observed exposures and the population pharmacokinetic model estimated exposures were similar in cirrhotic and non-cirrhotic subjects. Steady state exposures of ABT-530 are predicted to be achieved by Day 7 with minimal accumulation.
Conclusions: The developed ABT-530 population pharmacokinetic model well characterized the observed ABT-530 exposures in HCV infected patients and can be used in combination with viral response data to support dose selections and inform combination strategies. The gamma density function provided a fast and precise estimation of the number of transit compartments during model development.

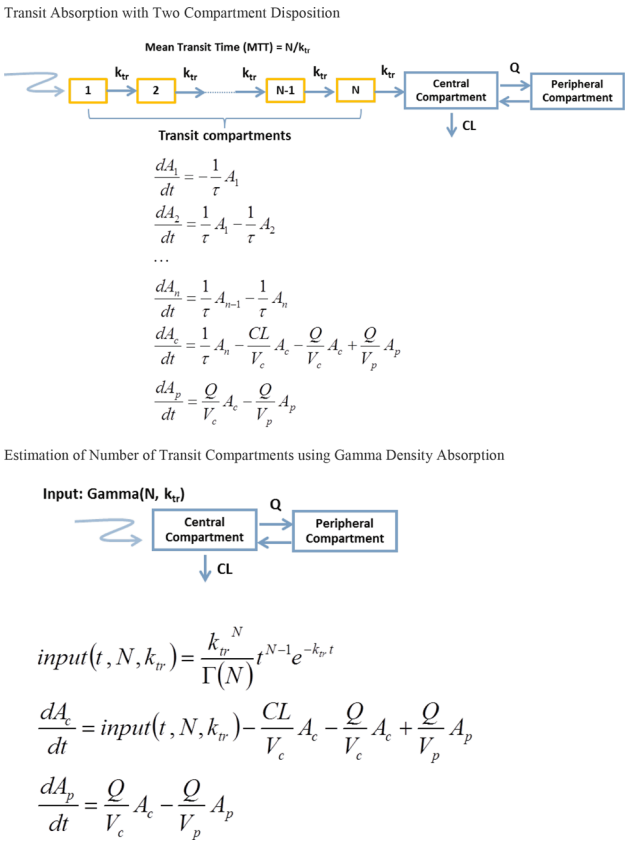

Fig. 1 Schematic of population pharmacokinetic model

W-27

Toward Progressive Reporting of Modeling and Simulation Results—Part 1: Analysis of KIWI^{TM} Metadata

Sébastien Bihorel*, Cynthia Walawander, Jill Fiedler-Kelly, David Fox, Andrew Rokitka, Thaddeus Grasela

Cognigen Corporation, Buffalo, NY

Objective: Typical pharmacometric reports provide comprehensive documentation about data assembly and modeling methods and

results. However, they are costly, time consuming, and do not necessarily serve the dynamic data accretion required during R&D lifecycle. KIWI™, a secure internet-based service providing high throughput NONMEM® processing, is the basis for a progressive reporting process that facilitates the capture of critical information during model development, enables team access to evolving results, and facilitates rapid report assembly. An analysis of KIWI metadata was performed to assess system performance and evaluate its use in facilitating progressive reporting.

Methods: KIWI supports the collection of metadata using a relational database management system, broadly grouped into categories of project management and run-specific information.

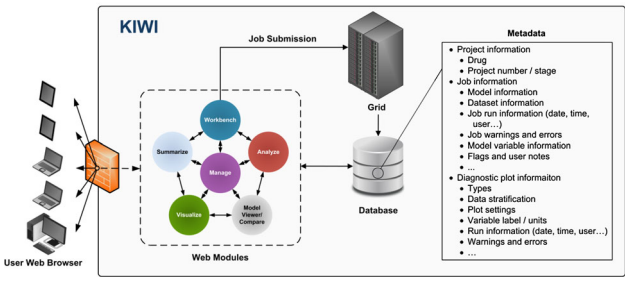

Fig. 1 KIWI work flow. Metadata is automatically captured or manually provided by users in the form of run-specific flags or notes. Analysis of metadata was achieved using SQL queries and R-based post-processing

Results: Simple queries can provide the distribution of project-related metadata metrics, e.g., median percentage of runs per project included in the critical path, or assess correlations between metrics, e.g., project duration versus number of modelers involved. KIWI provides filtering functionality of run metadata, including flags, facilitating the collaborative review of modeling results. Flags are also leveraged to build the critical modeling path and generate run records for regulatory submission. The automated export of validated graphs and preformatted, report-quality tables can save >2 h per run. A retrospective analysis shows a 16 % reduction in project duration since KIWI was introduced to support modeling.

Conclusions: KIWI provides ready access to analysis metadata that can be used to monitor system requirements and analysis status, as well as forecast resource needs for subsequent modeling efforts. Ongoing efforts are directed at leveraging metadata and run connections to automate progressive reporting and further facilitate the preparation of technical reports.

These results have been previously presented and published in the PAGE 2015 conference proceedings as Abstract III-28.

W-28

Linking a Mechanistic Model of Bone Mineral Density to a Time-to-Event Model to Evaluate Effects of Various Therapies on Fracture Risk in Postmenopausal Women with Osteoporosis

Eudy, RJ[1,3*], Gillespie, WR[2], Riggs, MM[2], Gastonguay, MR[1,2,3]

[1]BME Department, University of Connecticut, [2]Metrum Research Group, LLC, and [3]Metrum Institute, Tariffville, Connecticut

Objectives: Predict regional changes in bone mineral density (BMD) in patients with osteoporosis on three classes of osteoporosis drugs by leveraging summary-level data from the literature, using a multiscale systems model of bone metabolism. Also implement a time-to-event (TTE) model of fracture events to evaluate mono- or combination therapy in terms of reducing probability of fracture during long-term (10-year) treatment.

Methods: The BMD model was developed using data from 27 documented clinical trials with teriparatide, denosumab and combination therapy. Parameters were optimized using the R package *minqa* and changes in BMD were simulated using R package *mrgsolve*. The final model was evaluated by sensitivity analysis.

The TTE model was developed using individual-level data from NHANES (2005–2008) database and summary-level BMD data from selected publications (17 trials involving various treatments). The BMD timecourse used by the fracture model was simulated by the BMD model. Candidate models were evaluated by DIC and PPC (posterior predictive check).

Results: Changes in BMD as a result of denosumab, teriparatide or combination therapy were described by ODEs with changes in formation activity (OB compartment) as the input and changes in resorption activity (OC compartment) as the output. The final BMD model structure is $\frac{dBMD}{dx} = k_{in} \cdot \frac{OB^{\gamma}}{OB_0} - \frac{OC^{\delta}}{OC_0} \cdot BMD \cdot k_{out}$, with estimated parameters $\delta = 0.102$ (mean; 95 %CI −0.666 to 0.869) and $k_{out} = 0.000137$ (−0.273 to 0.273), k_{in} solved at steady state and initial conditions, and Υ fixed at original model value. The hazard model took the form

$$h_{ij}(t) = h_{0j}(t)e^{\beta_{BMD,j}\log\left(\frac{BMD_{spine,ij}(t)}{0.8}\right)+\beta_{postMenoAge}\left(postMenoAge_{ij}(t)-20\right)} + \beta_{radFracture}I_{radFracture,ij} + \beta_{BMI}\left(BMI_{ij}-27.1\right),$$

with $h_{0j} = 0.319$(mean; 95 % CI 0.022–0.437), $\beta_{BMD} = -4.80$ (−8.98 to 0.733), $\beta_{postMenoAge} = 0.0267$ (0.013–0.04), $\beta_{radFracture} = 1.05$(0.384;1.83) and $\beta_{BMI} = -0.0104$ (−0.0388 to 6.54E−5).

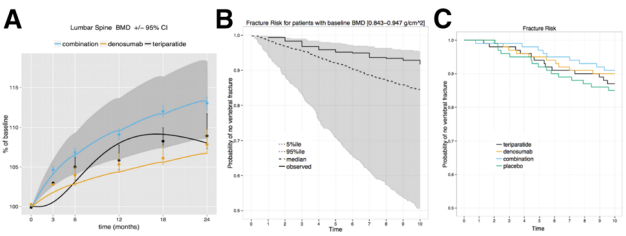

Fig. 1 Model Simulations (A) Simulated BMD as a result of mono (denosumab or teriparatide, 60 mg/6mo and 20mcg/d, respectively) or combination therapy (same dosage as monotherapy arms) resembles clinical BMD data; shading shows changes in estimated parameter values ±20 %. (B) PPC at population level of probability of fracture, using model built from NHANES dataset (C) Simulated probability of event for patients on teriparatide (20mcg/d), denosumab (60 mg/6mo) alone or in combination show estimated relative reduction in fracture risk over a 10-year treatment period

Conclusions: The BMD model parameters were sensitive to perterbations around 20 % of the typical value, and these estimates captured the central tentency within the 95 %CI of the clinical BMD data. The median predictions of fracture occurance by TTE model were also very close to clinical data.

W-29

Development of a Population Pharmacokinetic Model for Vancomycin on an Extracorporeal Membrane Oxygenation (ECMO) Therapy Patient Population

Jason Healy[1,*], Jason Moore[1], Brandi Thoma[1], Michelle Peahota[1], Nicholas Cavarocchi[1], Walter Kraft[1]

[1]Thomas Jefferson University, Philadelphia, PA

Objectives: Vancomycin is a frequently used antibiotic in the treatment of critically ill individuals. However, information detailing pharmacokinetics for patients undergoing extracorporeal membrane oxygenation (ECMO) therapy is relatively sparse. This study looks to develop a population pharmacokinetic model for vancomycin in ECMO patients to identify the presence of meaningful covariates.
Methods: A structural model was developed using non-linear mixed effects modeling (NONMEM VII) on the concentration–time profiles of 14 ECMO patients who received an infusion of 1–2 g of vancomycin over 1–2 h. Vancomycin concentrations were measured 0.5, 1, 2, 4, and 6 h upon completion of the infusion. The model discrimination was based on the objective function value (OFV), the goodness of fit plots, and parameter estimates. A covariate model was developed using the stepwise forward inclusion backwards elimination method ($p < 0.05$).
Results: A two-compartment model with log-normally distributed inter-subject variability and proportional residual error model, was found to better describe vancomycin disposition than a one-compartmental model ($\Delta OFV = -33.0$). The median central volume of distribution (Vc) was 21.3 L in ECMO patients, while the peripheral volume of distribution (Vp) was 24.4 L. The median clearance was 3.96 L/h, while the intercompartmental clearance (Q) was 11.5 L/h. Covariates of weight and creatinine clearance were found to have a significant effect on the central volume of distribution and the clearance, respectively, using a centered linear model ($p < 0.05$).
Conclusions: This study demonstrates the appropriateness of using a two-compartment model to describe the disposition of vancomycin given to ECMO patients.

References:

1. Donadello K, et al. Critical Care. 18(6): 632, 2014.
2. Mulla H & Pooboni S. British Journal of Clinical Pharmacology. 60(3): 265–75, 2005.
3. Purwonugroho TA, et al. The Scientific World Journal. Epub 2012 April 1, 2012.

W-30

Comparison of Laplacian, Quasi-Random Parametric Expectation Maximization (QRPEM) and Non-parametric Methods for Population Analysis of Complex Dynamic System with Non-static BQL Data

Shuhua Hu*, Bob Leary, Kevin Feng, Mike Dunlavey

Certara/Pharsight, Cary, NC

Objectives: To compare the capability of Laplacian and QRPEM engines in Phoenix® NLME™ (Pharsight/Certara) for population analysis of a complex dynamic system with non-static BQL data; and to use the non-parametric adaptive grid (NPAG) engine as a post-processor for parametric runs to detect any serious violation of normality assumption such as bimodality.
Methods: The example used to test the capability of these three methods is a highly nonlinear, multi-scaled and long-term HIV dynamic model [1] with clinical data [1] including treatment interruptions, total CD4+ T-cells and non-static BQL viral load. Both Laplacian and QRPEM engines started with same initial values for fixed and random effects and were implemented in the same machine with same setting. Compared to parametric methods such as Laplacian and QRPEM methods, NPAG makes no assumption on the distribution form of random effects and hence can be used as a post-processor for parametric runs.
Results: We found that QRPEM converged at iteration 110 with 12000 s runtime in which Laplacian estimation just finished two iterations and then stuck at iteration 4. This is not unexpected as QRPEM is based on quasi-random importance sampling approach to compute required integrals and does not use explicit numerical optimization while Laplacian engine involves explicit numerical optimization and requires evaluation of second derivatives for approximation. The Q–Q plots obtained by QRPEM for random effects show that there are discernible divergences from normal distributions for several random effects. Plots of estimated cumulative distribution functions (CDF) obtained by NPAG demonstrate that two of these random effects seem to have bimodal shape distributions (see figure shown below).

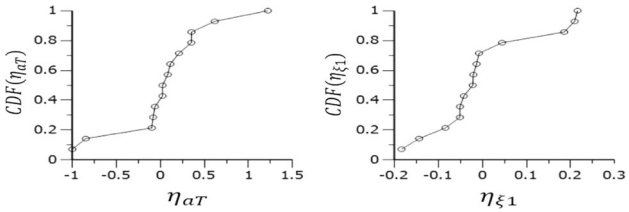

Conclusions: This example demonstrates that for population analysis of a complex dynamic system with complicated data, QRPEM is method of choice and nonparametric engine should be used as a post-processor whenever there is a doubt of the normality assumption.

References:

1. H.T. Banks, et al., Journal of Biological Dynamics, 2 (2008), 357–385.

W-31

Comparison of Model Based and Model Independent Approaches for Handling Data Below the Limit of Quantitation

V.Goti[1*], R.Burns[1], A.Chaturvedula[1,2], E.Ette[3]

[1]Center for Pharmacometrics, Mercer University, Atlanta, GA; [2]GVK Informatics Pvt.Ltd, Hyderabad, India; [3]Anoixis Corporation, Natick, MA

Background: Current literature suggests that model dependent analyses that maximize the likelihood of the data above the limit of quantitation and treat below the limit of quantitation (BQL) data as censored yield the most accurate and precise parameter estimates[1]. A recent publication compared model independent data imputation methods[2], but there are no literature reports of the comparison of model dependent and model independent approaches with regard to estimation efficiency.
Objectives: To compare the efficiency of model independent approaches [conditional multiple imputation (CMI) and fractional conditional single imputation (FCSI)] to model dependent approach [M3 method] for handling BQL data in nonlinear mixed effects models.
Methods: Concentration vs time data were simulated using a two compartment model in NONMEM® (7.2). Simulations were performed according to four scenarios with varying random variability parameters (Table 1). BQL data identified in the simulated datasets

were replaced with imputed values in accordance with the CMI and FCSI methodology. After imputation, model parameters were estimated using first order conditional estimation with interaction in NONMEM® (7.2) and compared with those obtained using the M3 method. Efficiency of each methodology was evaluated by assessing %bias and %absolute error.

Results: The M3 method produced least biased and most precise estimates. With regard to %bias, M3 method showed bias in estimation of between subject variability (BSV) on CL/F for scenarios 1 and 3.Estimation of BSV on Vp/F and BSV on KA were biased for scenarios 1 and 4 respectively. With regard to %absolute error, estimation of BSV on Vp/F, BSV on KA and BSV on Q/F were imprecise for all scenarios. Estimation of Vp/F was imprecise for scenarios 3 and 4.

Conclusions: Likelihood based approach for handling BQL data yielded more efficient parameter estimates than the data imputation methods in a nonlinear mixed effects modeling setting.

Scenario1	BSV = 30 %CV, RUV = 15 %CV	Clearance (CL/F) = 29.5 L/h
Scenario2	BSV = 45 %CV, RUV = 15 %CV	Central Volume of Distribution (Vc/F) = 56.8 L
Scenario3	BSV = 30 %CV, RUV = 25 %CV	Peripheral Volume of Distribution (Vp/F) = 60.1 L
Scenario4	BSV = 45 %CV, RUV = 25 %CV	Absorption rate constant (KA) = 3.46 h^{-1}
		Inter-compartmental Clearance (Q/F) = 11.0 L/h

BSV between subject variability, *RUV* residual unexplained variability

References:

1. S. Beal, JPKPD October 2001, Volume 28, Issue 5, 481–504.
2. Ette et al., Data Imputation, Pharmacometrics the Science of Quantitative Pharmacology, John Wiley and Sons Inc.

W-32

Population PK/PD/Survival Modeling Analysis of Icotinib in Chinese Non-Small Cell Lung Cancer Subjects

Jia Chen, Dongyang Liu, Qian Zhao, Ji Jiang, Pei Hu*

Clinical Pharmacology Research Center, Peking Union Medical College Hospital and Chinese Academy of Medical Sciences, Beijing, China

Objective: Icotinib is an on-market novel anti-cancer to treat non-small cell lung cancer (NSCLC) in China. Up to date, the influence factor affecting PK profile, effect and overall survival in Chinese NSCLC patients and their relationship was not well characterized. In order to make clear on that, a population model was developed to quantitatively describe PK, PD and overall survival in Chinese NSCLC patients.

Methods: Data from patients (n = 122) who received icotinib were used for population PK/PD modeling. Icotinib concentrations were fitted to a one compartment model with one transit compartment to describe the delayed absorption. An exposure–tumor response model of drug effect on tumor growth dynamics incorporated with AUCss was used. Survival model was developed using weibull distribution model and drop-out model was developed using logistic regression model. PK and PD model was constructed using FOCEI method and survival and drop-out model using Laplace method. Covariates were screened using stepwise method and model was validated using visual predictive method (VPC) and bootstrap.

Results: Population PK analysis showed that BMI had an positive effect on V and GGT was a negative influential covariate of CL. PD model found patients with adenocarcinoma had better effect than non-adenocarcinoma while accepted icotinib treatment. Survival model showed AUCss and tumor shrinkage ratio in 4th week could be predictors for the overall survival of patients. Drop-out model showed that patients dropped from icotinib treatment owing to higher exposure.

Conclusion: The population PK/PD/survival model was developed linking exposure, tumor dynamics, and overall survival in Chinses NSCLC patients. The relationship, covariates and predictors were helped to predict clinical outcome in terms of our model following icotinib treatment in NSCLC.

References:

1. Wang HY, et al. Chin Med J(Engl). 2011, 124(13):1933.
2. Shi Y, et al. Lancet oncol. 2013, 14(10): 953–61.
3. Hansson EK, et al. CPT Pharmacometrics Syst Pharmacol. 2013 doi: 10.1038/psp.2013.61.

W-33

Translating Older R Data Manipulation Workflows to the Modern Equivalents

Devin Pastoor[1*], Vijay Ivaturi[1]

[1]Center for Translational Medicine, School of Pharmacy, University of Maryland

Objectives: In the past 2 years, an explosion of new packages have been developed for use in the R ecosystem. These packages build on the new tooling such as leveraging C ++, continuous build systems, and the author's previous experiences to introduce faster, easier to use, and better tested packages well-suited for incorporation into a pharmacometrician's workflow. The objectives of this work were to provide a reference guide to facilitate translation of old scripts to the new equivalents, and provide a set of examples to introduce the capabilities these packages provide.

Methods: Three model datasets and one data assembly challenge were used to demonstrate how the datasets could be manipulated to perform common tasks such as calculation of summary statistics, conversion from long-to-wide format, and preparation for modeling or visualization softwares. Each task was accomplished using base R and older packages such as *plyr* and *reshape2,* then again using their modern counterparts *dplyr*, *tidyr* and *stringr*.

Results: Use of *dplyr*, *tidyr*, and *stringr* provide simpler API's to allow for more readable code, with the added benefit of running up to 100's of time faster than their older counterparts. The packages do not map one-to-one in usage, as the older packages often play many roles (e.g. reshaping and manipulating at the same time), whereas the

modern versions take the approach of each handling one role (e.g. *dplyr* for data manipulation, *tidyr* for reshaping). Given their focus on performing one task well, the new packages can be more quickly updated, better qualified, and more easily understood.

Conclusions: It was demonstrated that a traditional analysis workflow in R using packages such as *reshape2* and *plyr* can be quickly and easily updated to use *dplyr* and *tidyr*. This improves the raw analysis performance, increases code legibility, and improves the overall flow of data through the entire analysis pipeline. The tasks presented are representative of common data manipulation objectives, and the code presented can be easily adapted across a variety of additional situations common in pharmacometrician's workflows.

W-34

Assessment of Exposure–Response (E-R) and Case–Control (C–C) Analyses in Oncology using Simulation Based Approach

Jinzhong Liu[1], Yaning Wang[2] and Liang Zhao[3*]

[1]Indiana University School of Medicine, Indianapolis, IN; [2]DPM/OCP/OTS/CDER, FDA, Silver Spring, MD; [3]DQMM/ORS/OGD/CDER, FDA, Silver Spring, MD

Objectives: Incremental median survival benefit with increasing drug exposure, as obtained by Kaplan–Meier estimation, suggests that increasing drug exposure could result in additional survival benefit for patients with low drug exposure. However, bias could be introduced due to unbalanced distribution of baseline risk factors affecting clinical response. Two ways have been attempted to correct the bias: multivariate Cox modeling and C–C analysis. This study is to evaluate (1) the performance of multivariate Cox modeling for E-R analysis when drug exposure is confounded with other risk factors and (2) the performance of C–C analysis at the presence of confounding risk factors when multivariate Cox modeling is not sufficient to correct the bias.

Methods: Seven true E-R relationship scenarios were created, with ECOG, tumor size at baseline, and drug exposure set as risk factors driving efficacy. For each scenario, 1000 virtual clinical trials were simulated. For each simulated virtual clinical data, multivariate Cox modeling and C–C analysis were conducted. Their performances were evaluated by comparing to the underlying true models. The 7 true E-R relationship scenarios are illustrated in Table 1.

Results: Multivariate Cox modeling can introduce bias for the estimation of E-R relationship, when the underlying model assumes a non-linear drug exposure effect on the hazard function (scenarios 3, 4, 6 and 7). For all investigated scenarios, C–C comparisons between Q1, Q2, Q3, Q4 and their corresponding matched control groups revealed the true underlying E-R relationships.

Conclusions: When drug exposure effect is non-linear, multivariate Cox modeling can introduce bias for drug exposure effect estimation. Even though the bias of drug exposure effect estimation could be addressed by implementing non-linear fit for the Cox model, this method has not been widely applied [1]. C–C analysis can correctly estimate the exposure-effect relationship under all investigated scenarios.

References:

1. Yaning Wang, et al. Clin Pharmacol Ther. Apr 2015. 97(4): 404–410.

Table 1 Performances of multivariate Cox modeling and case–control analysis for seven scenarieos

	Underlying scenario types	True mathematical models	Biased prediction?	
			Multivariate Cox modeling	Case–control analysis
1	Multivariate Cox model	$h(t) = h_0(t) \times \exp(0.7 \times ECOG + 0.07 \times Tumor\ size - 0.012 \times C_{trough})$	No	No
2	Parametric model + linear concentation effect	$h(t) = 0.065 \times \exp(0.7 \times ECOG + 0.07 \times Tumor\ size - 0.012 \times C_{trough})$	No	No
3	Parametric model + non-linear concentation effect (slow saturation)	$h(t) = 0.060 \times \exp\left(0.672 \times ECOG + 0.089 \times Tumor\ size - 0.008 \times \frac{60 \times C_{trough}}{10 + C_{trough}}\right)$	Yes	No
4	Parametric model + non-linear concentation effect (fast saturation)	$h(t) = 0.054 \times \exp\left(0.675 \times ECOG + 0.104 \times Tumor\ size - 0.005 \times \frac{60 \times C_{trough}}{0.1 + C_{trough}}\right)$	Yes	No
5	Parametric model + linear concentation effect + interation term	$h(t) = 0.067 \times \exp(1 \times ECOG - 0.015 \times C_{trough} + 0.0145 \times ECOG \times C_{trough})$	No	No
6	Parametric model + non-linear concentation effect + interation term (slow saturation)	$h(t) = 0.060 \times \exp\left(1.4 \times ECOG - 0.012 \times \frac{60 \times C_{trough}}{10 + C_{trough}} + 0.013 \times ECOG \times C_{trough}\right)$	Yes	No
7	Parametric model + non-linear concentation effect + interation term (fast saturation)	$h(t) = 0.052 \times \exp\left(1.65 \times ECOG - 0.007 \times \frac{60 \times C_{trough}}{0.1 + C_{trough}} + 0.006 \times ECOG \times C_{trough}\right)$	Yes	No

W-35

Survey of Methodologies for Exposure–Response Analysis of Oncology Drugs Approved in FDA from 2010 to 2015

Tong Lu[1], Dan Lu[1], Bert L. Lum[1], Mark Stroh[1], Priya Agarwal[1], Jin Y. Jin[1], Amita Joshi[1*]

[1]Genentech, Inc., South San Francisco, CA

Objectives: Exposure–response (E-R) analysis is extensively used in drug development and regulatory decision-making, and is still a developing field in oncology. This survey will provide an overview and discussion of E-R methodologies used in FDA oncology approvals from 2010 to 2015.
Methods: 41 New Molecular Entity (NME) in oncology approved by FDA in 2010 $\sim$ 2015 were surveyed [1]. Both exposure-efficacy (E-E) and exposure-safety (E-S) analyses were reviewed. Analyses that were not relevant to dose justification, as commented by the reviewers, were excluded from the summary. FDA's methods were chosen when different from sponsors. Results were summarized as pie charts and as table with pros and cons and case examples.
Results: In 41 NMEs, 55 E-E and 49 E-S analyses were performed. Typical E-E analysis included Kaplan–Meier plots & Cox proportional hazard (Cox PH) model for time-to-event data (26 cases), and logistic plot & regression model for binary data (19 cases). For E-S, logistic analysis played the central role (29 cases); time-to-event analysis was also conducted but with much lesser extent (5 cases). The graphical evaluations (box, logistic and Kaplan–Meier plots) when used usually followed by modeling approaches (logistic regression and Cox PH models). Longitudinal plots were observed (1 case each for safety and efficacy) to assess the impact of exposure on time-profile of continuous outcomes. More advanced methodologies were presented for palbociclib, including parametric time-to-event model for PFS and longitudinal PK/PD model for neutrophil count. Additional methodologies not mentioned in FDA reviews but discussed will be longitudinal models for categorical data and case-matching analysis for survival data. These methodologies may be more robust to refine E-R relationship in oncology but need further evaluation.
Conclusions: This presentation summarized the E-R analysis for the recent FDA oncology approvals and outlines other potential useful advanced methodologies. It provides a framework for appropriate application and further advancement of E-R methodology to support dose justification and optimization in oncology.

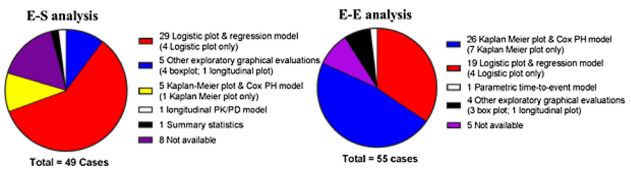

Fig. 1 Summary of the E-R analysis approaches for the 41 drugs reviewed

References:

1. http://www.accessdata.fda.gov/scripts/cder/drugsatfda/. Clinical Pharmacology & Biopharmaceutics Reviews

W-36

Analysis of Exposure–Response Relationships for Cobimetinib in Combination with Vemurafenib

Nageshwar R Budha[1*], Mathilde Marchand[2], Laurent Claret[2], Christine Falcoz[2], Christine Garnett[2], Rene Bruno[2], Nalin Tikoo[1], Ilsung Chang[1], Susan Eng[1], Nicholas Choong[1], Mark Dresser[1], Luna Musib[1], Jin Y Jin[1]

[1]Genentech Inc, South San Francisco, CA, [2]Pharsight Consulting Services

Objectives: Cobimetinib, a potent and highly selective inhibitor of mitogen activated protein kinases, is currently being developed in combination with vemurafenib to treat patients with BRAFV600 mutation-positive melanoma. The aim of these analyses was to explore the exposure–response (E-R) relationships for cobimetinib in combination with vemurafenib in patients with melanoma and solid tumors.
Methods: Data from three clinical studies, MEK4592 g (Phase I, n = 114), NO25395 (Phase Ib, n = 131), and GO28141 (Phase III, n = 495) were used in the analysis. E-R relationships were assessed for efficacy endpoints, progression free survival (PFS) and objective response rate (ORR) and selected safety events. Binary endpoints i.e. proportion of responders and frequencies of safety events were explored by logistic regression. The time-to-event variable PFS was explored by Kaplan–Meier analysis and log rank test p-values by quartiles of exposure. Longitudinal tumor size data were analyzed using simplified tumor growth inhibition model. Concentration-QTc interval analyses were performed using linear mixed effects modeling.
Results: No E-R relationship was observed between PFS and cobimetinib exposure in the cobimetinib plus vemurafenib arm (log rank p = 0.98). Similarly, no E-R relationship was observed for ORR. No clinically significant trends of E-R relationship were observed for safety events following 60 mg QD dose of cobimetinib on a 21/7 schedule in combination with vemurafenib in Study GO28141. No E-R relationship was observed between tumor size ratio metrics and cobimetinib exposure. QTc interval is not related to cobimetinib exposure either as a single agent (MEK4592 g) or in combination with vemurafenib (GO28141).
Conclusions: Overall, results from the E-R analysis suggest no relationship between cobimetinib exposure and efficacy or safety within the exposure range observed at 60 mg QD cobimetinib on a 21/7 schedule and that current cobimetinib dose in combination with vemurafenib for treatment of patients with advanced melanoma with BRAFV600 mutations is optimal.

W-37

Model Based Network Meta-Analysis for Pharmacometrics and Drug-Development: A 3 year Research Collaboration between Pfizer and the University of Bristol

David Mawdsley[1], Meg Bennetts[2], Sofia Dias[1], Martin Boucher[2*], Tony Ades[1], and Nicky J. Welton[1]

[1]School of Social and Community Medicine, University of Bristol; [2]Pharmacometrics, Global Clinical Pharmacology, Pfizer Ltd

Objectives: Network Meta-Analysis (NMA) allows simultaneous comparison of multiple treatments [1], and provides a framework for model comparison and assessment of evidence consistency. Model based meta-analysis MBMA [2] has been used to assess multiple treatment comparisons, however little attention has been given to assessment of consistency [3]. This project aims to integrate the two approaches to allow formal assessment of consistency for MBMA models.
Methods: We illustrate the importance of assessing model fit using a MBMA comparing Naproxen vs placebo for treating pain. The fit and

model predictions are compared for different time-course models. We indicate how the methods can be extended to multiple treatments, using a network of trials of multiple treatments, doses and time-points for osteoarthritis.
Results: We show that parameter estimates are sensitive to choice of model and that ignoring time/dose in a NMA can lead to inconsistent treatment effects, motivating a model-based analysis.
Conclusions: This collaboration offers the potential to combine all the available dose–response and time-course evidence in a model-based network meta-analysis (MBNMA) to compare the relative efficacy of multiple treatments, while allowing model fit and evidence consistency of the whole network to be assessed.

References:

1. Dias, S., Sutton, A. J., Ades, A. E., & Welton, N. J. (2013). Evidence synthesis for decision making 2: a generalized linear modeling framework for pairwise and network meta-analysis of randomized controlled trials. Medical Decision Making: An International Journal of the Society for Medical Decision Making, 33(5), 607–17.
2. Mould, D. R. (2012). Model-based meta-analysis: an important tool for making quantitative decisions during drug development. Clinical Pharmacology and Therapeutics, 92(3), 283–6.
3. Dias, S., Welton, N. J., Caldwell, D. M., & Ades, A. E. (2010). Checking consistency in mixed treatment comparison meta-analysis. Statistics in Medicine, 29(7–8), 932–44.

W-38

Modeling the Neuropsychiatric Inventory (NPI) – Strengths and Weaknesses of a Multidimensional Item Response Theory Approach

Sebastian Ueckert[1*], Peter Lockwood[2], Pam Schwartz[2], Steve Riley[2]

[1]Pharmacometrics Research Group, Department of Pharmaceutical Biosciences, Uppsala University, Uppsala, Sweden; [2]Pfizer Inc, Global Innovative Pharma Business, Clinical Pharmacology, Groton, CT, USA

Objectives: The NPI is a behavior instrument widely used in clinical trials of antidementia agents. It measures the severity and frequency of 12 non-cognitive symptoms of dementia ranging from agitation/aggression to changes in appetite and eating behaviors. From the perspective of the data analysis, this multi-facetted score represents a challenge requiring a balance of clinical complexity and statistical parsimony.
The objectives of this work were to investigate the strengths and weaknesses of a multidimensional item response theory model (MDIRTM) for simultaneous, longitudinal modeling of the NPI frequency and severity outcomes in an Alzheimer's population.
Methods: NPI item frequency and severity scores collected over time from 954 patients receiving a placebo treatment were collated from several Pfizer clinical trials. The patient data was used to build a MDIRTM describing the probability of each frequency and severity score as a function of multiple patient-specific latent variables and item-specific discrimination parameters. The longitudinal evolution of the score was described using a linear disease progression model with latent variable-specific slopes.
Model selection and evaluation were performed using simulation based diagnostics and objective function value (OFV) using NONMEM 7.3 for parameter estimation and R for creation of diagnostics.
Results: Based on OFV, a MDIRTM with three latent variables provided the best description of the data. The three dimensional model accurately reflected the correlations in the data between items, between frequency and severity component as well as over time. Different rates of disease progression were identified for different latent variables.

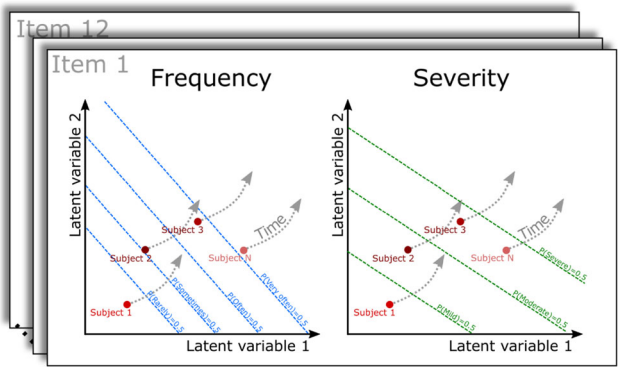

Fig. 1 Schematic representation of a version of the model with subjects moving over time in a hypothetical 2D latent variable space partitioned by item-specific decision boundaries

Conclusions: MDIRTM constitute an attractive approach to describe multifaceted composite scores like the NPI with a minimal set of assumptions. From a practical perspective, model complexity might constitute a hurdle.

W-39

Model-Based Analysis of the Relationship between Pembrolizumab Exposure and Response in Melanoma

Manash S. Chatterjee[1*], David C. Turner[1], David Dong[1], Malidi Ahamadi[1], Julie Stone[1], Dinesh P. De Alwis[1], Anna Kondic[1]

[1]Merck Research Laboratory, Merck & Co., Inc., USA

Objectives: Pembrolizumab is a PD-1 antibody that has shown robust antitumor activity in multiple tumor types. Here we characterized the relationship between exposure to pembrolizumab in serum (i.e. AUC over 6 weeks at steady state) and melanoma antitumor response measured as the sum of the longest dimension of tumor lesions across protocols KEYNOTE-001, KEYNOTE-002 and KEYNOTE-006.
Methods: Pooled data from 1366 subjects treated for melanoma was first graphically analyzed to evaluate changes in tumor size at 24 weeks versus exposure. Logistic regression analysis quantified the relationship between exposure and ORR. Longitudinal tumor size data were next analyzed using a nonlinear mixed effects model. The structural model was parameterized with both first-order tumor growth and shrinkage rates, assuming that only some fraction of lesions was accessible for antitumor effect. Patient- and study-specific factors were explored as covariates to explain variability on model parameters. The influence of pembrolizumab exposure was included as an additional estimated parameter on the modeled tumor shrinkage rate. Due to co-linearity of patient ipilimumab treatment history and dose, independent exposure–response parameters were estimated for the ipilimumab-naive and ipilimumab-experienced subpopulations. Simulations were conducted with final parameter estimates, and for graphical presentation, converted to response categories analogous to RECIST.
Results: Pembrolizumab exposures showed a small and statistically insignificant influence on the final model estimated tumor decay parameter. A covariate search on the base structural model revealed PD-L1 expression and baseline tumor size to have a significant association with estimated rate of tumor size decline, while

ipilimumab treatment history and baseline tumor size were predictive of the fraction of tumor responding. In addition, *BRAF* mutation status was related to the tumor growth rate.
Conclusions: This exposure–response analysis indicates the currently approved 2 mg/kg Q3 W dose is near the maximal response plateau of the exposure–response curve. Baseline tumor size, ipilimumab treatment history, *BRAF* mutation, and PD-L1 expression status are significant predictors of model parameters.

W-40

Development of a Non-Human Primate PK/PD Model of a Monoclonal Antibody for the Treatment of Systemic Lupus Erythematosus

Konstantinos Biliouris[1], David Dai[2], Ivan Nestorov[2], Guangqing Xiao[2], Qin Wang[2], Lawrence J. Lesko[1], Mirjam N. Trame[1*]

[1]Center for Pharmacometrics and Systems Pharmacology, Department of Pharmaceutics, University of Florida, Orlando, FL; [2]Biogen, Cambridge, MA

Objectives: Systemic Lupus Erythematosus (SLE) constitutes an auto-immune disease that affects approximately 1 in 2000 individuals [1]. Although SLE is a widespread disease, only one new treatment has been approved by FDA since 1955 and therefore new, more targeted and effective therapies are needed. The objective of this work was to develop a nonhuman primate (NHP) pharmacokinetic/pharmacodynamic (PK/PD) model for a novel humanized monoclonal antibody (mAb), BIIB059, that targets the blood dendritic cell antigen 2 (BDCA2) on plasmacytoid dendritic cells and is currently under development for SLE treatment [2].
Methods: PK data from 19 cynomolgus monkeys were utilized for the development of the NHP PK model. These data were obtained from 3 different studies including single or multiple dosing, with BIIB059 administered intravenously or subcutaneously. BDAC2 receptor (PD marker) levels from 6 cynomolgus monkeys were used for the development of the NHP PD model, wherein both direct and indirect response models were evaluated. Parameter estimation was conducted in NONMEM 7.3.
Results: A two-compartment PK model with first order elimination was found to best describe the NHP BIIB059 data. BDCA2 levels were best captured using an indirect PD model with stimulation of the dissipation of the response. Despite the limited data availability, the PK/PD model described the data with reasonable accuracy.
Conclusions: A PK/PD model was built that describes the PK/PD profile of BIIB059 in NHP. Various approaches are now being tested [3,4] for scaling the NHP model to humans and will be validated against available PK/PD data from healthy subjects and SLE patients.

References:

1. Bertsias G, Cervera R and Boumpas TD., EULAR textbook on rheumatic diseases, (2012): 476–505.
2. Pellerin A et al., EMBO Molecular Medicine, 7.4 (2015): 464–476.
3. Shi R et al., ASCPT, 2015.
4. Testa B et al., Pharshight Corporation (at http://www.pharsight.com/library/Rosenon2007.pdf).

W-41

Optimal Design for Pediatric Study of a Monoclonal Antibody Exhibiting Nonlinear PK

Liviawati Wu, Edward Lee, Thuy Vu*

Clinical Pharmacology, Modeling and Simulation, Amgen Inc., Thousand Oaks, CA

Objectives: To determine the optimal PK sampling scheme for a pediatric study and to prospectively power the pediatric PK study using precision criteria [1,2].
Methods: Prior population PK analysis of a monoclonal antibody described the target-mediated drug disposition characteristics in the adult population. The disposition parameters of interest for precision determination are clearance [CL], volume of distribution [V], and maximum target concentration [R_{max}], with adjustment for body weight effects on CL and V. PK sampling scheme was optimized using Population Fisher Information Matrix (PFIM)[3]. A realistic weight distribution for subjects aged 6 to 18 years were randomly sampled from the National Health and Nutrition Examination Survey demographic database. Subjects < 60 kg were assumed to receive half of the dose for adults. Six sample size scenarios were tested, (3, 4, 6, 8, 10, or 12 from each age group [6–12 and 12–18 years]). For each scenario, 300 simulated datasets were created and parameters were re-estimated using NONMEM; 95 % CI [confidence interval] of parameters were calculated for each run. Power was defined as the percentage of runs with 95 % CI within 60–140 % of the true parameter values [1,2].
Results: PFIM determined the optimal sampling scheme to be 1, 2, 4, 5, 14, (35–42), (56–63), (70–77), and 84 days postdose. NONMEM simulation and re-estimation results suggested that a minimum sample size of n = 10/age group was necessary to achieve > 80 % power for estimating 95 % CI of CL, V and R_{max} within 60–140 % of the true parameter values.

Design	Nsub = 12			Nsub = 6		
	CL	V	RMAX	CL	V	RMAX
Full	7.8	8.1	8.2	11.0	11.4	11.6
Reduced	7.9	12.2	113.4	11.1	17.4	165.1
Optimized	7.9	8.1	12.2	11.1	11.5	17.2

Numbers are %RSE from PFIM

Full (NCA, $N_{samples}$ = 15): 0.3333, 1, 2, 3, 4, 7, 11, 14, 21, 28, 42, 56, 63, 84, 98 days

Reduces (population analysis, $N_{samples}$ = 9): 1, 3, 4, 7, 14, 28, 42, 63, 84 days

Optimized (population analysis, $N_{samples}$ = 9): 1, 2, 4, 5, 14, 42, 63, 77, 84 days

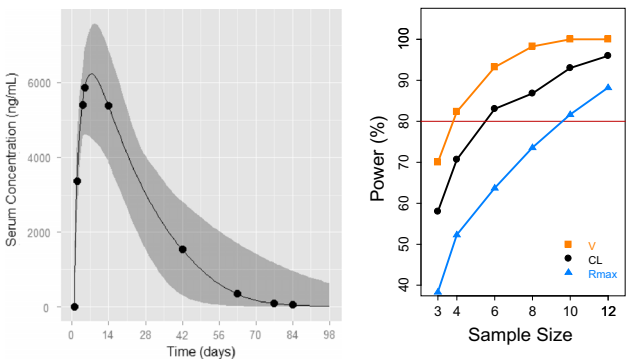

Conclusions: We've demonstrated that for a compound with nonlinear PK, the number of PK samples and pediatric subjects can be

reduced significantly without compromising the standard precision required for the key PK parameters.

References:

1. Wang Y, et al. J Clin Pharmacol. 52(10):1601–1606, 2012.
2. FDA. Guidance for Industry. General Clinical Pharmacology Considerations for Pediatric Studies for Drugs and Biological Products 2014.
3. Bazzoli C, et al. Comput Methods Programs Biomed. 98(1):55–65, 2010.

W-42

Clinical Trial Simulations to Assess the Probability of Revealing Biomarker Dose–Response in Ph1 Trials

Tong Lu[1], Yuying Gao[2], Lichuan Liu[1], Alex Huang[1], Amita Joshi[1], Jin Yan Jin[1*]

[1]Genentech, Inc., South San Francisco, CA; [2]Quantitative Solutions, Menlo Park, CA

Objectives: For rational dose selection of targeted anticancer agents, it is critical to obtain early assessment of clinical activity and target modulation. However, in Ph1 dose escalation, biomarker dose–response (D-R) assessment based on tumor biopsy data is challenging, considering the uncertainty around efficacious dose, small sample size, high inter-subject variability, and high biopsy failure rate. The objective of this work is to assess the power of detecting biomarker D-R relationship by clinical trial simulations.
Methods: 1) Simulation: Based on available biomarker D-R relationship (inhibitory Emax model), 3 scenarios were simulated with ED50 within, below, or above Ph1 dose range. For each scenario, 1000 sets of parameters were generated, incorporating uncertainty and inter-trial variability for ED50 (assume 75 %), and observed variability for baseline E0 (sampling with replacement). The pre- and post-treatment data were simulated for each subject, with 1000 subjects/dose for 6 dose levels. 2) Bootstrapping: for each scenario, 1000 Ph1 trials (n = 9/trial: 3 subjects/dose, 6 dose levels, 50 % failure rate regardless of dose) were generated by resampling from simulated subjects; 1000 sets of bootstrapped parameters were derived by fitting to the Emax model. 3) Evaluation criteria: a) power of detecting D-R relationship (i.e., ED50) was assessed by % of bootstrapped parameters falling into predefined interval ([0.7–1.3]) of true value; b) success rate of achieving certain target inhibition at certain dose.
Results: In this specific case, when ED50 was in the middle of the dose range, the power of detecting true ED50 was decent (49 %) in spite of small sample size and high failure rate; for scenarios where ED50 was below or above the dose range, the powers went down significantly (drop more pronounced when above the range). Simulation also suggested strong likelihood of ED50 underestimation when ED50 was above the dose range.
Conclusions: To inform oncology biomarker strategy, theoretical simulations can be conducted with varying assumptions to assess the probability to reveal the biomarker D-R in Ph1 trial.

References:

1. Overman MJ et al. Use of Research Biopsies in Clinical Trials: Are Risks and Benefits Adequately Discussed? J Clin Oncol. 2013;31(1):17–22.

W-43

Investigating Robustness of Proposed Models to Describe the Novel Mechanism of Atypical Nonlinear Plasma Protein Binding Behavior of Tigecycline

Daniel de Jong, Amelia N. Deitchman, Ravi Shankar Prasad Singh, Hartmut Derendorf*

University of Florida, Department of Pharmaceutics, Gainesville, FL

Objectives: Tigecycline, a broad-spectrum antibiotic, exhibits atypical nonlinear plasma protein binding. Recent investigations have shown that this is likely associated with metal-ion chelation. We aim to determine via sensitivity analysis which mechanism(s) of interactions between protein, metal-ions, and tigecycline are robust in describing given observed experimental results.
Methods: A global sensitivity analysis to evaluate four putative mechanisms with varying interactions between protein, metal ions, and tigecycline (e.g. metal-ion-protein interaction, drug-metal-ion interaction) was performed using the 'sensitivity' package for R (version 3.0.2). Sobol's algorithm was used to compute the first and total order sensitivity indices for model parameters. Unbound concentrations of tigecycline were simulated in the range of 0.001 to 100 μg/mL. Upper and lower parameter boundaries were chosen based on physiologically feasible values. The threshold value for parameter significance for sensitivity indices was set to 0.05.
Results: The results of the sensitivity analysis showed that tigecycline's protein binding parameters (maximum capacity, dissociation constant, and the cooperativity factor) were sensitive parameters in all evaluated models with total order sensitivity indices ranging from approximately 0.2 to 0.5.Whereas, in general, metal-ion parameters had less influence on outcome variability: Parameters involved in metal-ion-drug interaction (indices: 0–0.10), metal-ion-protein interaction (indices: 0.03–0.08) and metal-ion-drug-protein interactions (indices: 0.04–0.1) were found not to be consistently significant drivers for the observed effect.
Conclusions: The metal-ion assisted cooperative binding model most accurately described experimentally observed characteristics. The global sensitivity analysis showed that protein-drug interaction parameters significantly contributed to variability, while metal-ion binding parameters had a less significant influence on outcome variability.

W-44

Binning of Exposures in Survival Analysis for Oncology - A Simulation Study

Matts Kågedal[1*], Shang-Chiung Chen[1], Russ wada[2], Jin Y Jin[1]

[1]Genentech Inc, San Francisco, CA; [2]Quantitative Solutions, Menlo Park, CA

Objectives: To evaluate the impact of binning patients based on exposure by quartiles, tertiles or twotiles on the ability to 1) detect an E-R trend; and 2) compare efficacy in the low exposure treatment bin over control.
Methods: A simulation study was performed assuming a 2-arm oncology trial with n = 100 per arm. Two E-R scenarios were assumed; 1) No E-R trend and a hazard ratio (HR) of 0.67 across all exposure levels. 2) Marked E-R trend where the HR ranged from 1 to 0.4 from low to high exposure. The simulated trials were evaluated using Cox regression after binning exposure by quartiles, tertiles and twotiles. The assessment was based on an 80 % CI (CI_{80}) and the point estimate (HR_{PE}).

Results: In scenario 1 (no E-R trend), the likelihood of correctly identifying a benefit of treatment ($CI_{80} < 1$) at low exposure based on quartiles was 61 %. This was worse than tertiles and twotiles wich had a likelihood of 70 % and 79 % respectively. With quartiles there were more spurious results based on the HR_{PE} with 18 % of the simulations suggesting an ER-trend (HR of high bin lower than the low bin by at least 0.2). When analyzing scenario 2 (no benefit in the lowest quartile and a marked ER relation), the likelihood of showing similarity to control in lowest exposure bin was 0 % based on CI_{80} and 63 % based on the point estimate ($HR_{PE} = 0.8–1.25$), clearly lower compared to tertiles and twotiles. The likelihood of detecting an ER-trend was highest based on quartiles at 91 % based on CI_{80} which was slightly better than tertiles at 89 % and clearly better than twotiles at 85 %.
Conclusions: The proposed clinical trials simulations approach enabled a quantitative evaluation of a key component of the E-R analysis plan. Binning by tertiles appears to provide the best ability to draw correct exposure–response conclusions in the tested oncology trial design.

W-45

A M&S Framework for Exposure–Response Analysis in Oncology: Comparison and Considerations of Multiple Methodologies

Dan Polhamus[1*], Jonathan French[1], Shang-Chiung Chen[2], Bei Wang[2], Chunze Li[2], Dan Lu[2], Sandhya Girish[2], Jin Jin[2], Angelica Quartino[2]

[1]Metrum RG, Tariffville, CT; [2] Genentech, San Francisco, CA

Objectives: There is a need for dose optimization in oncology drug development. Typical M&S framework for this application focuses around exposure–response (ER) analysis with direct or indirect (e.g., via tumor growth inhibition (TGI)) ER for progression free survival (PFS) and overall survival (OS). ER assessments in oncology are frequently confounded by multiple prognostic factors and alternated dosing history, neccessitating multiple methodological considerations. Here, we propose and discuss a M&S framework for ER analysis in oncology with a case example to compare different aspects of multiple direct ER methodologies.
Methods: The direct ER approaches are exemplified using data from an oncology Phase 3 trial with methods including: (1) stratified Kaplan–Meier (KM) estimates by exposure quartiles, (2) Cox proportional hazards (CPH) analysis with covariate adjustment, (3) case matching (CM) to address confounding effects on ER, and (4) parametric survival modeling (PS) for extrapolation to other dosing regimens.
Results: CPH, while allowing direct ER assesment, relies on assumptions about the relationship of covariates with outcome and exposure. Recent publications from FDA reviewers proposed matching methods easing these assumptions [1], but ER assesment is no longer directly addressed as in such approaches as in CPH. A doubly robust ER using CPH within CM on strata of exposure is demonstrated, guarding against either poor matching or model misspecification. In addition to TGI, PS gives another longitudinal approach to evaluate the ER relationship for dose/regimen optimization if deemed desirable based on CPH and/or CM ER.
Conclusions: Universal discussion and adoption of a general ER framework will expedite trial design and analysis. We propose and discuss one possible ER M&S framework that guards against model mispecification, provides a clear strategy for dose optimization if indicated, and to addresses regulatory review questions.

References:

1. Yang J, et al. "The combination of exposure–response and case–control analyses in regulatory decision making". J Clin Pharmacol. 53(2): 2013.

W-46

Leveraging Biomarkers, Clinical Endpoints, and Exposure–Response Modeling and Simulation to Optimize Phase 3 Dose Selection

Mathangi Gopalakrishnan[1*], James Bolognese[2], Jaydeep Bhattacharya[2], Cecilia Fosser[2], Nitin Patel[2]

[1]Center for Translational Medicine, University of Maryland, Baltimore, MD; [2]Cytel Inc, Cambridge, MA

Objective: A key goal of early clinical development programs is to optimize Phase 3 dose selection in order to maximize the benefit-risk of the drug. The main objective of this research is to leverage the relationship between biomarkers, clinical endpoints and exposure response modeling for making go/no-go decisions in early clinical development and improve the selection of target doses.
Methods: A simulation based framework [1] is used to evaluate different early biomarker trial designs to improve Phase 3 dose selection. The early development scenario consists of two biomarker trials namely Ph1b-Proof of Concept (PoC) and Ph1b-Dose finding (DF) followed by a Ph2b DF trial. The biomarker levels (BM1, BM2) are measured on days 1 and 14 during the trials and BM3, measured on day 28, is the early clinical endpoint. A linear relationship is assumed between biomarkers and the Ph2b clinical endpoint, observed after 12 weeks of therapy. The biomarker responses are generated using an additive baseline effect-inhibitory Emax model using area under the curves as the exposure metric with underlying pharmacokinetic (PK) variability. A Bayesian tri-variate normal distribution model is assumed for the 3 biomarkers and posterior probabilities are used to make go/no-go decisions regarding the next stage of the trial and for dose selection. The simulations are carried out using a trial version of CytelSim® software.
Results: Based on two sequences of trial designs (PoC → Ph2b & PoC → Ph1bDF → Ph2b), preliminary results assuming moderate PK variability have indicated that the probability of selecting the correct dose is similar between an exposure based metric and a dose metric.
Conclusions: A Bayesian modeling framework to leverage the relationship between biomarkers, clinical endpoints and PK exposures for early clinical development decision and optimize phase 3 dose selection has been developed and further investigations are underway.

Reference:

1. Musser, Bret et al., Therapeutic Innovation & Regulatory Science, May 2015: 49 (3) : 405–414.

W-47

Pharmacokinetic Modeling of Plasma and Salivary Caffeine Circulation in Infants Receiving Extended Caffeine Therapy for Intermittent Hypoxia Treatment

Xiaoxi Liu[1], Tian Yu[1], Nicole R. Dobson[2], Betty L. McEntire[3], Robert M. Ward[1], Michael G. Spigarelli[1], Carl E. Hunt[4], Catherine MT Sherwin[1*]

[1]Department of Pediatrics, School of Medicine, University of Utah, Salt Lake City, Utah, [2]Pediatrics, Tripler Army Medical Center, Honolulu, HI, [3]American SIDS Institute, Naples, FL, [4]Pediatrics, Uniformed Services University, Bethesda, MD, United States

Objectives: To develop a novel plasma/salivary caffeine recirculation model and explore the potential application of salivary caffeine measurement as a surrogate for caffeine therapeutic monitoring.
Methods: Preterm infants were enrolled in a study evaluating the effects of extended caffeine on intermittent hypoxia. Caffeine was administered orally to patients and paired salivary and plasma samples were taken. Caffeine concentrations in salivary and plasma samples were analyzed by a validated high performance liquid chromatography method. The PK model was developed using NONMEM 7.3.
Results: A total of 29 infants were included with median (5–95th quantiles) gestational age of 28 weeks (25–31 weeks), postnatal age of 7 weeks (3–12 weeks) and body weight of 2100 g (1600–2567 g). Caffeine PK in plasma and saliva was simultaneously described by a three-compartment recirculation model with an additive error model. The final parameter estimates (95 % confidence interval) of plasma clearance (CL1), salivary clearance (CL2), plasma volume of distribution (V1) and salivary volume of distribution (V2) were 0.0159 L/h (0.0137–0.0181 L/h), 0.0058 L/h (0.0054–0.0062 L/h), 0.439 L (0.311–0.567 L), 0.0088 L (0.0022–0.0154 L). The salivary secretion rate (CL3) and caffeine absorption rate (KA) were fixed to 0.006 L/h and 1.48/h, respectively, based on literature data. Current body weight, birth weight, gestational age, postmenstrual age and postnatal age were not significantly correlated with any PK parameters.
Conclusion: Caffeine PK in saliva and plasma was well described by a three-compartment recirculation model. Future studies will utilize this model to investigate the feasibility of using salivary caffeine concentrations to predict plasma caffeine levels.

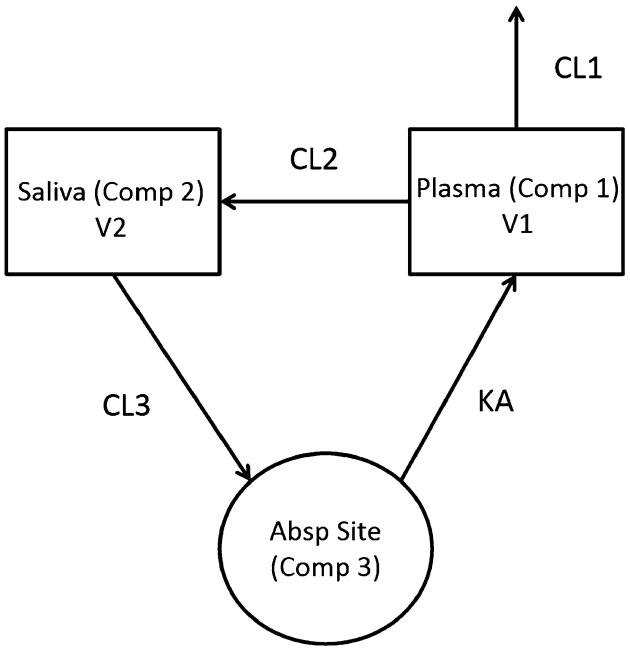

W-48

To antidote or not? Population Pharmacokinetic Modeling and Bayesian Forecasting as a Tool to Predict the Need for Antidote in Acute Acetaminophen Overdose

Julie Desrochers[1*], Wendy Klein-Schwartz [2], Suzanne Doyon[2], Joga Gobburu[1], Mathangi Gopalakrishnan[1]

[1]Center for Translational Medicine, [2]Maryland Poison Center, University of Maryland School of Pharmacy, Baltimore, MD

Objectives: The clinical practice for assessment of acute acetaminophen (APAP) overdoses relies on a single timed plasma acetaminophen concentration (PAC) obtained at least 4 h post ingestion plotted on the Rumack-Matthew nomogram. Case reports of nomogram failure have been reported. The aim of this study was to develop an improved tool for N-acetyl cysteine (NAC) administration decision in acute APAP overdose using population pharmacokinetic (PK) modeling and Bayesian forecasting.
Methods: Retrospective cohort of 228 acute APAP overdoses (at least 2 PK samples/subject) reported to the Maryland Poison Center between June 2010 and April 2014 were used to develop a population PK model using Phoenix NLME 1.3. A one compartment model with first order absorption and linear elimination with uncertainty in patient reported dose was considered with clinically relevant covariates. The validated population PK model was then used to perform Bayesian forecasting of subsequent APAP levels using one or two PAC and evaluated for prediction bias. Bayesian forecasting based NAC administration decision was compared with clinical decision.
Results: Final model included allometric scaling factors on CL and V, use of activated charcoal as a fractional effect on F and CL, and APAP product category as a fractional effect on absorption rate constant. Using one or two PAC as feedback with Bayesian forecasting, the subsequent PAC were predicted with a %ME (Mean error) between 5.4 and 11.7 %. The Bayesian forecasting approach correctly predicted the administration of NAC 90 % of the times and an early decision for NAC administration with a sensitivity of 86 %. (Table 1).

Table 1 Comparision of prediction of administration of NAC to clinical decision of administration of NAC

	Clinical decision	Bayesian forecasting with 1 PAC as feedback	Clinical decision 1st PAC $\leq$ 4 h Bayesian	Bayesian forecasting with 1st PAC $\leq$ 4 h
Yes-NAC	131/228 (57 %)	168/228 (74 %)	36/75 (48 %)	59/75 (79 %)
Correctly made Yes-NAC decision		118/131 (90 %)		31/36 (86 %)
No- NAC	97/228 (43 %)	60/228 (26 %)	39/75 (52 %)	16/75 (21 %)
Correctly made No-NAC decision		47/97 (48 %)		11/39 (28 %)

Conclusions: The applicability of the Bayesian forecasting using one PAC or two PAC for prediction of subsequent APAP levels to make a clinical NAC administration decision has been demonstrated. The improved tool will be further investigated for use in clinical practice.

W-49

Systemization of Logistic Regression Analysis for Pharmacometric Applications

Julie Passarell[1], Caroline Passarell[1], Darcy Hitchcock[1], Jill Fiedler-Kelly[1], Ted Grasela[1]

[1]Cognigen Corporation, Buffalo, NY

Objectives: Efficacy and safety data are oftentimes collected as binary (yes/no) data in clinical trials during drug development. The implementation and growing use of CDISC standards in data collection and categorization of adverse event data using the MedDRA dictionary has facilitated the standard format of clinical trial data collected across the pharmaceutical industry. A commonly-used statistical method for analyzing binary data is logistic regression (LR) analysis. The objective of this work was to develop a system to standardize analysis dataset creation, exploratory data review, and LR analysis procedures for exposure–response analyses of binary endpoint data.
Methods: SAS® software was used to develop a code library to transform source clinical trial data into an analysis-ready dataset for use in exposure–response analyses. A library of SAS® code for the creation of standard exploratory graphs and tables was also developed. A systematic approach to statistical analysis using SAS® PROC LOGISTIC and NONMEM was developed, based on standard methods for model building and discrimination, to facilitate the calculation of standard statistics and production of typical diagnostic plots for model building and evaluation.
Results: The standardized process for dataset creation, exploratory data analysis, and LR was tested on 10 compounds and refined as new variations and additional data checks were identified. This refined process and systematic approach resulted in a greater than 70 % decrease in analyst time required for evaluation of exposure–response relationships for binary endpoints. Other positive benefits of system implementation include a reduction in training time for new pharmacometricians and improved quality and consistency of reporting for LR exposure–response.
Conclusions: Standardization of analysis-ready dataset creation for binary endpoints and the logistic regression analysis process has proven instrumental in generating timely understanding of exposure–response relationships to facilitate model-based decision making under tight timelines and allowing for the evaluation of additional endpoints and synthesis of findings across endpoints.

References:

1. Hosmer DW, Jr, Lemeshow S. Applied Logistic Regression. 2nd ed. New York, NY: John Wiley & Sons; 2000.

W-50

Pharmacokinetic-Pharmacodynamic Analysis of Spectinamide Antibiotic Lee1599 in *Mycobacterium tuberculosis* Infected Mice

Chetan Rathi[1*], Dorababu Madhura[1], Ashit Trivedi[1], Jiuyu Liu[2], Michael Scherman[3], Gregory Robertson[3], Richard Lee[2], Anne Lenaerts[3], Bernd Meibohm[1]

[1]University of Tennessee Health Science Center, [2]St. Jude Children's Research Hospital, [3]Colorado State University

Objectives: Spectinamides are a novel series of spectinomycin analogs for the treatment of tuberculosis. PK/PD characterization of spectinamides in the early drug development stage is critical for its rational dose selection. Here, we have described the characterization of the PK/PD relationship and identification of the main driver for its efficacy based on a dose fractionation study of lead spectinamide Lee1599 in a mouse model of *M.tb* infection.
Methods: The dose fractionation study was conducted in mice as described in Table 1. Dosing was continued for 4 weeks with blood sampling at 0.25 h and 8 h after the last dose, followed by a washout period after which the mice were sacrificed and the lungs removed for measurement of colony forming units (CFU). Drug concentrations in plasma were analyzed with a validated LC–MS/MS method followed by pharmacokinetic analysis using nonlinear mixed effect modeling. Based on the individual posthoc estimates, simulations were performed for each mouse to calculate the PK/PD indices: C_{max}/MIC, AUC_{0-168}/MIC and %T > MIC, assuming a MIC of 1600 ng/ml. The relationship between PK/PD indices and $\log_{10}$ CFU was analyzed using nonlinear regression.
Results: An open two compartment model with linear elimination from the central compartment characterized the plasma concentration–time profile of Lee1599.The average CL, V_c, Q, and V_p was estimated to be 0.318 L/h/kg, 0.286 L/kg, 0.0096 L/h/kg, and 0.349 L/kg. The inter-individual variability in CL was estimated as 24.2 %. An inhibitory sigmoid maximum effect (E_{max}) model was used to describe the relationship between PK/PD indices and $\log_{10}$ CFU. C_{max}/MIC and AUC_{0-168}/MIC correlated well with $\log_{10}$ CFU ($R^2 = 0.522$ and 0.488, respectively), suggesting that the half-maximal inhibitory effect was reached at a C_{max}/MIC of 264 and an AUC_{0-168}/MIC of 1040.
Conclusions: The bactericidal activity of Lee1599 is concentration-dependent and this supports the use of intermittent administration of Lee1599. This information will be the basis for dosage regimen selection in future efficacy studies.

Table 1 Dose fractionation scheme of Lee 1599

Total weekly dose (mg/kg)	2000	1000	500	298.8	200	120	80	50	40	30	20	10
5 × per week (M-F)	20 BID	100 BID	50 BID		20 BID			5 BID				1 BID
5 × per week (M-F)		200 QD	100 QD		40 QD			10 QD				2 QD
3 × per week (M, W, F)				99.6								
QD		40 QD					10 QD					
2 × per week (M, R)							40 QD				10 QD	
1 × per week (M)									40 QD			10 QD

The number of mice in each group ranged from 3 to 5

W-51

Effect of Trial Design on Exposure–Response (E-R) Analyses in Rare Diseases: A Simulation Case Study in Duchenne Muscular Dystrophy (DMD) with the 6-Minute-Walk-Test-Distance (6MWTD) Endpoint

Jeannine Fisher[1*], CJ Godfrey[1], Janelle Hajjar[2], Marc R. Gastonguay[1]

[1]Metrum Research Group, LLC, Tariffville, CT; [2]University of Connecticut, Storrs, CT

Objectives: Drug development challenges in rare diseases such as DMD include small patient populations, large interpatient variability in clinical endpoints, and dose selection with limited dose–response data. A recent FDA Draft Guidance [1] suggests that randomized, placebo controlled trials are preferred but trials using external historical controls may also be useful in establishing evidence of efficacy. Using historical data [2,3], we evaluated the impact of trial designs on quantitative E-R characterization in DMD patients treated with Drug X.
Methods: Individual plasma drug exposures were simulated assuming a population clearance = 20 L/h (20 %CV). Given natural history DMD disease progression, 1-year change from baseline 6MWTD data were simulated with mean = −23.6 meters in boys > 7 years on continuous steroid use[2]. Inter- and intra-individual SD was fixed to 65.9[2] and 4 meters[3], respectively. E-R was modeled using an EMAX relationship. 500 parallel-design trials were simulated with N = 150/trial. Model-based estimates of E-R parameters from each trial were summarized for precision and bias. R3.1.1 and NONMEM® 7.3 were used for data analysis and modeling, respectively.
Results:

DMD E-R summary table

Design	Parameter	Bias* (%)	Precision* (%)
1[#]	EC50	5.0	47.9
	EMAX	4.28	10.6
2[##]	EC50	13.6	42.4
	EMAX	2.60	11.6

[#] Placebo, 0.3- and 9-times EC50; [##] Placebo, 0.3-, 1-, and 9-times EC50; *Median

Conclusions: Even with a reasonable dose-ranging design, the precision of EC50 parameter estimates was consistently poor in DMD trials of this size. Evaluation of alternative designs and analysis methods will be necessary to support dose selection with sufficient precision in DMD and other rare diseases.

References:

1. Guidance For Industry: Duchenne Muscular Dystrophy and Related Dystrophinopathies: Developing Drugs for Treatment. FDA, CDER (2015).
2. Mazzone et al. Neurology,2011;77:250–256.
3. McDonald et al. Muscle & Nerve, 2010;41:500–510.

W-52

Modeling the Impact of Antidrug Antibody Formation on the Pharmacokinetics of a Fully Human Monoclonal Antibody in a Preclinical Rodent Model

Josiah T. Ryman[1*] and Bernd Meibohm[1]

[1]Department of Pharmaceutical Sciences, University of Tennessee Health Science Center, Memphis, TN

Objective: The objective of this study is to assess the time course and extent of ADA formation and its impact on the PK profile after administration of a human monoclonal antibody at differing dose levels and with different immunomodulation strategies in rats.

Methods: A human IgG2 monoclonal antibody (mAb1), without target binding in rats, was dosed at three different levels: 0.01, 50 and 300 mg/kg weekly in Sprague–Dawley rats for 4 weeks. Within each dose level, three immunomodulation strategies were used. One group was administered mAb1 alone. The second group was administered mAb1 and an immunosuppressive regimen of rapamycin (6 mg/kg) at the beginning of the study and tacrolimus (2 mg/kg) weekly. The third group was administered mAb1 and methotrexate (5 mg/kg) in 3 consecutive doses on days 0, 1 and 2. Blood samples were drawn from the tail vein at predetermined time points and analyzed for mAb1 concentrations and the presence of ADA. Population PK modeling of the mAb1 concentrations and ADA effect was performed using nonlinear mixed effects modeling (NONMEM).
Results: mAb1 serum concentrations were best described by a two-compartment model. The formation of ADA increased clearance for mAb1 and ADA signal-to-noise ratio was incorporated into the model using a modifier for clearance of (1 + (ADA*SN)**ANTI), where ADA signals the presence of antidrug antibody in the sample, SN is the signal-to-noise ratio measured in that sample and ANTI is the estimate of the ADA effect on clearance. The point estimates were the following: clearance 0.000433 l/h/kg; absorption rate constant 0.00360 h^{-1}, volume of distribution of the central compartment 0.0866 l/kg, inter-compartmental clearance 0.000100 l/h/kg and effect of ADA on clearance 1.57.
Conclusions: This study and model illustrate the substantial impact of ADA formation on the clearance of therapeutic proteins when compared to animals without an immune response.

W-53

Development of a Mega Population Pharmacokinetic (PK) Model of an Antibody–Drug Conjugate (ADC) Platform

Jian Xu[1*], Leonid Gibiansky[2], Jonathan Squire[1], Xin Wang[1], Sandhya Girish[1], Jin Jin[1]

[1]Genentech, Inc., South San Francisco, CA; [2]QuantPharm LLC, North Potomac, MD

Objectives: ADCs developed using a platform share the same antibody technology: protease-labile linker and potent anti-cancer toxin. The similarity of ADC structures from this platform may result in comparable PK properties. The goal of this analysis was to develop a mega model that simultaneously describes antibody-conjugated toxin data from multiple ADCs in this platform, and assesses differences and similarities of PK parameters among different ADCs.
Methods: Clinical conjugated toxin data of multiple ADCs were obtained from several Phase 1 or 2 studies. Population PK models for each ADC were developed, and then various features of these models were combined in one mega model. A series of mega-models starting from the model that had all compound-specific parameters up to the model that had common parameters for all compounds were developed. Visual predictive checks (VPC) were used to assess ability of the models to predict PK for each ADC. Influences of body weight, gender, and dose on model parameters were evaluated.
Results: A unified model (two-compartment model with parallel time dependent clearance and Michaelis–Menten elimination, clearance and volume increasing with weight, and clearance mildly increasing with dose) described conjugated toxin PK of all ADCs. Michaelis–Menten elimination had only minor effect on PK. Time-dependence of clearance had no effect beyond the first dosing cycle. The model with all parameters except clearance shared by all ADCs provided reasonable conjugated toxin predictions and VPC plots for all ADCs.

This model can be applied in the exposure–response analysis to evaluate key safety events in the future.
Conclusions: A developed population mega-model successfully described conjugated toxin PK of all ADCs. The model will be applied to predict properties of ADCs under development and propose optimal dosing regimens.

M-54

A Dynamic Model-Based Analysis of a Multi-Level Glycemic Clamp Study of Regular Human Insulin in T1DM Subjects

Bhargava Kandala*, Craig Fancourt, Kuenhi Tsai, Marian Iwamoto, Christina Canales, Amy Cheng, Michael Crutchlow, David E. Kelley, Sandra A.G. Visser

Merck & Co., Inc., Kenilworth, NJ USA

Objective: Hyperinsulinemic clamp studies assess non-linear insulin pharmacokinetics (PK) and pharmacodynamics (PD) during steady-state conditions. This investigation aimed to determine if a well-sampled clamp experiment can be used to identify dynamic insulin PK-PD parameters by utilizing the entire clamp study time-course.
Methods: 12 T1DM subjects received infusions of regular human insulin (RHI) and glucose during a 3-period multi-glycemic (200, 75, and 300 mg/dL) 9-h clamp study. During period one, the insulin infusion rate (IIR) was varied to achieve a target glucose infusion rate (GIR) of 5 mg/kg/min. During periods 2–3, IIR was fixed at steady state IIR from period one, and GIR was varied to achieve the set glucose target.
Two dynamic insulin-glucose models were fit using nonlinear mixed effects (NONMEM) to the PK-PD data: (a) a "dynamic" steady-state (DSS) model based on a PK-PD model-based meta-analysis (MBMA) of the T1DM clamp literature [1]; (b) a modified integrated glucose-insulin (IGI) model [2] with insulin secretion removed for T1DM, and peripheral glucose removed for improved fit.
Results: Statistical analysis of (GIR) and glucose revealed that steady-state was achieved during the final 30 min of each 3-h clamp period. The mean steady-state RHI clearance and GIR were in agreement with the literature T1DM model [1]. Comparing the DSS and IGI model fits, both models yielded reasonable and comparable estimates of key insulin and glucose PK-PD parameters.
Conclusions: Both the DSS and IGI models could describe the RHI clamp data well and provided distinct advantages in the quantification of RHI PK-PD. These models provide a modeling platform to analyze and simulate future trials under both clamp and non-steady state conditions in the development of novel insulins.

References:

1. Burroughs et al., ACOP 2015.
2. Silber et al., J Clin Pharmacol 2007; 47:1159–7.

W-55

Development of a Plasma/Dermis Population Pharmacokinetic Model for GSK1940029

John Zhu*, Thomas Wilde, Richard Brigandi

GlaxoSmithKline, King of Prussia, PA

Objectives: Develop a plasma/dermis population pharmacokinetic (PK) model using Phase I data.
Methods: A two-compartment model (1st compartment dermis and 2nd compartment plasma) was developed using NONMEM based on healthy volunteer plasma concentration data from a Phase I study in which subjects received single or multiple daily topical administrations of 0.1–1.0 % (w/w) GSK1940029 gel. Application was to the thighs or back at varying body surface area [BSA] under occluded or non-occluded conditions. Data from an in vitro human abdominal-skin percutaneous absorption experiment was added to the dataset for subjects receiving 1 % gel under non-occluded conditions for simultaneous analysis with the plasma data. The flux determined from the same in vitro experiment was used to back-calculate the amount of dose that could have been absorbed into the systemic circulation. The final plasma/dermal model was evaluated with visual predictive check.
Results: Based on PK results from non-compartmental analysis, the strength of the gel formulation did not affect systemic absorption/exposure at the gel strengths studied (0.1 to 1 %), thus these different gel strengths were assumed to have the same flux. Flux under occluded conditions was assumed to be 5-fold higher than under non-occluded conditions (Hostynek 1997). Under these assumptions, BSA was a limiting factor for systemic absorption with PK exposure approximately proportional to BSA. Load of the gel formulation applied did not affect systemic absorption/exposure at the load studied (between real world use of 1 mg gel/cm^2 and maximum artificial use of 10 mg gel/cm^2). Pharmacokinetic parameters were precisely estimated (relative standard error RSE 7.2–49.8 %). Inter-individual variability (IIV) estimates ranged 52.5–82.2 % for CL, V, and skin tissue unbound f_{ut}. No IIV on R1 (flux) was needed. Residual error was determined for plasma (CV 71.8 %).
Conclusions: A two-compartment plasma/dermis population PK model was developed. The model predicted a free dermis concentration 1.6-fold the human IC50, suggesting a different formulation with higher flux would be needed for efficacy when treating skin conditions.

Reference:

1. Hostynek J, Magee P. 1997. Modelling in vivo human skin absorption. Quant Struct Act Relat 16(6):473–479.

W-56

Getting Clear on Non-Specific Tissue Clearance of mAbs: Insights from PBPK Modeling

Ludivine Fronton[1]*, Hans Peter Grimm[1]

[1]Roche Pharmaceutical Research and Early Development, Pharmaceutical Sciences, Roche Innovation Center Basel

Objectives: Physiologically-based pharmacokinetic (PBPK) modeling is necessary to understand and interpret biodistribution and pharmacological effects of monoclonal antibodies (mAbs) in tissue. However, common biodistribution data of 125-iodine radiolabelled mAbs does not allow to identify quantitatively the tissues involved in the non-specific clearances of mAbs which are important to understand tissue-specific effects of e.g. ADC. The objectives of our work are (i) to extend the PBPK model to describe biodistribution data of mAbs radiolabeled by non-residualizing 125-iodine (125I) and residualizing 111-indium (111In) radionuclides and (ii) to determine non-specific tissue clearances of mAbs with different affinities to FcRn.
Methods: Experimental plasma and tissue data in mice of three non-targeted mAbs with different affinities to FcRn were obtained from literature [2]. For this, the PBPK model from [1] was extended to account for the residence of radiolabels inside cells following their internalization. Simultaneous fitting of data using 125I and 111In was

used to identify the tissue specific clearances of the mAbs. Parameter estimation and simulations were done using standard routines from the MATLAB R2014a package.
Results: The extended PBPK model allowed estimating non-specific intrinsic clearance of tissues. Furthermore, with the variants of mAbs the effect of FcRn binding differences on the clearance pattern was investigated.
Conclusions: Tissues clearances can be discussed in terms of their contribution to the total plasma clearance. Here, "big" and highly perfused tissues/organs are dominant. On the other hand, clearance per unit of organ weight may become important, specially for ADC. It reveals that liver and spleen have the highest values. Manipulation of FcRn binding affinity provides new insight on the extension of FcRn capacity which seems to be homogenous across tissues/organs and on the high clearing capacity of liver and spleen which interpretation can be extended to FcRn dynamics.

References:

1. Fronton L et al. J Pharmacokinet Pharmacodyn, 41(2):87, 2014.
2. Yip V et al. mAbs, 6(3):689, 2014.

W-57

Novel Mechanism-based Population Pharmacokinetic/ Pharmacodynamic Model of Blood Pressure and the Antihypertensive Activity of Fimasartan

Jürgen Bulitta[1*], Soo-Heui Paik[2], Soyoung Shin[3], Cornelia Landersdorfer[4], Tae Hwan Kim[5], Min Gi Kim[5], Seok Won Jeong[6], Rajbharan Yadav[4], Beom Soo Shin[6]

[1]College of Pharmacy, University of Florida, FL; [2]Boryung Pharm. Co., Ltd., Seoul, Korea; [3]Department of Pharmacy, Wonkwang University, Iksan, Korea; [4]Monash Institute of Pharmaceutical Sciences, Monash University, Australia; [5]School of Pharmacy, Sungkyunkwan University, Suwon, Korea; [6]College of Pharmacy, Catholic University of Daegu, Gyeongsan-si, Korea

Objectives: Fimasartan is a novel angiotensin II receptor blocker available in South Korea and Latin America. Our aim was to develop a novel population pharmacokinetic/pharmacodynamic model to describe the time-course of blood pressure and the antihypertensive activity of fimasartan to support human dose selection.
Methods: The population pharmacokinetic/pharmacodynamic model was developed by combining data from two previously published studies that contained no modeling analyses. These datasets included 56 healthy volunteers receiving placebo, a single oral dose of 20 to 480 mg fimasartan, or seven doses of placebo, 120, or 360 mg every 24 h, and 39 patients with mild-to-moderate hypertension receiving placebo, 20, 60, or 180 mg every 24 h for 28 days. Fimasartan plasma concentrations were determined by LC–MS/MS and modelled simultaneously together with all systolic and diastolic blood pressure data. Population modeling was performed in S-ADAPT.
Results: The population pharmacokinetic model accounted for enterohepatic recirculation. Diastolic and systolic blood pressure were described by turnover models whose input rate followed a circadian rhythm. Fimasartan inhibited the input into the diastolic and systolic blood pressure compartments. The maximum extent of inhibition of diastolic blood pressure was 30.7 % in patients and 19.2 % in healthy volunteers. Half-maximal inhibition required 12.9 ng/mL (156 % CV) fimasartan. The coefficients of correlation of the observations vs. individual (population) fits were 0.918 (0.788) for diastolic blood pressure, 0.891 (0.720) for systolic blood pressure, and 0.932 (0.801) for plasma concentrations. Visual predictive checks indicated adequate predictive performance.
Conclusions: The developed population PK/PD model successfully described and predicted the antihypertensive activity of fimasartan in Korean patients and can support optimal dose selection in patients.

W-58

Semi-Mechanistic Population Pharmacokinetic/ Pharmacodynamic Modeling and Covariate Analysis for ISIS GCGRRx (449884), a Second Generation Antisense Oligonucleotide Glucagon Receptor (GCGR) Inhibitor for the Treatment of Type 2 Diabetes Mellitus

Kenneth Luu[1*], Erin Morgan[2], Sanjay Bhanot[2], Richard Geary[2], Yanfeng Wang[1]

[1]Pharmacokinetics and Clinical Pharmacology; [2]Clinical Development, Isis Pharmaceuticals, Carlsbad, CA

Objectives: Perform a model-based analysis to evaluate the pharmacokinetic/pharmacodynamic (PK/PD) results of GCGRRx obtained from a Phase 1 trial in healthy volunteers and a Phase 2 trial in patients with type 2 diabetes mellitus (T2DM).
Methods: The overall model consisted of: 1) a 2-compartment PK model (elimination from the peripheral compartment) and three transit absorption compartments, 2) an indirect response model (peripheral concentration driving the PD) for FPG (fasting plasma glucose) and 3) a semi-mechanistic model linking the relationship between the FPG and HbA1c (hemoglobin A1c) using the RBC lifespan model from Hamren et al. [1] with slight modification. Stepwise covariate models (SCM) were built for each of the three models. Modeling included combined Phase 1 and Phase 2 trial data ($N = 88$ for PK, $N = 86$ for FPG, $N = 49$ for HbA1c). NONMEM 7.2, R 3.1.1 and PSN 3.4 were used for model development and data visualization.
Results: All parameters were estimated with reasonable precision (Table 1). Visual predictive check (VPC) plots indicated that the trend and variability in PK and PD were well captured.
Several baseline covariates (BW, BSA, HbA1c, FPG, Glucagon) were identified as statistically significant on PK and/or PD response as shown in Table 1; however, their clinical relevance needs to be evaluated with additional data.
Conclusion: A comprehensive model was developed for ISIS GCGRRx, capturing the time course of PK and PD (FPG and HbA1c) and population variability. Although clinical relevance is yet to be assessed, inclusion of covariates allowed for improved prediction accuracy. The model was useful for trial simulation especially for dose selection of later clinical studies.

Table 1 Parameter estimates for the PK/PD models

PK model			FPG model			HbA1c model		
Parameter	Estimate (% RSE)	% BSV (% RSE)	Parameter	Estimate (% RSE)	% BSV (% RSE)	Parameter	Estimate (% RSE)	% BSV (% RSE)
$MTT_{absorption}$ (hr)	0.765 (10.7)	55.4 (9.93)	k_{out} (day^{-1})	0.0268 (14.9)	96.3 (36.8)	λ	0.355 (11.7)	12.4 (14.9)
CL_{Periph} (L/h)	65.5 (9.56)	48.9 (16.7)	I_{max}	0.308 (5.10)	25.8 (10.7)	k_{gl} (day^{-1})	0.000168 (20.5)	NE
Q (L/h)	5.56 (11.9)	48.5 (24.4)	IC_{50} (ng/ml)	1.77 (19.5)	91.7 (31.1)	*RBC Lifespan* (day)	135 fix	NE
V_{periph} (L)	49400 (9.09)	52.6 (23.8)	*Baseline FPG* (mg/dL)	147 (1.56)	35.4 (1.67)	k_{inRBC}	1.11 fix	NE
$V_{central}$ (L)	55.0 (6.93)	36.2 (21.0)	*Baseline HbA1c on Baseline FPG*	0.19 (4.28)	NA	*Baseline HbA1c on* λ	0.0445 (19.6)	NA
BW on $V_{central}$	0.019 (8.26)	NA	*Baseline HbA1c on* I_{max}	0.37 (10.9)	NA	*Baseline FPG on* λ	−0.000529 (14.1)	NA
BSA on V_{periph}	0.622 (30.1)	NA	*Baseline BSA on* I_{max}	0.669 (22.0)	NA	*Baseline Glucagon on* λ	0.000771 (43.7)	NA
BSA on CL_{periph}	0.831 (37.4)	NA	*%Residual Error (Proportional)*	9.87 (13.8)	NA	*%Residual Error (Proportional)*	8.44 (11.1)	NE
%Residual Error (Proportional)	36.5 (35.7)	NA						

NE not estimated, NA not applicable, %BSV between-subject variability expressed as a percentage, %RSE relative standard error expressed as percentage, FPG fasting plasma glucose, HbA1c glucosylated hemoclobin, BW body weight, BSA body surface area, MTT mean transit time, Q intercompartmental clearance, V_{periph} peripheral volume, $V_{central}$ central volume, k_{out} rate of FPG disposition, IC_{50} concentration for 50 % inhibition of input rate (k_{in}), λ glucosylation exponent

References:

1. Hamren, B., Bjork, E., Sunzel, M. & Karlsson, M. Models for plasma glucose, HbA1c, and hemoglobin interrelationships in patients with type 2 diabetes following tesaglitazar treatment. Clinical pharmacology and therapeutics 84, 228–35 (2008).

W-59

Cell-Level Model of Pharmacodynamics-Mediated Drug Disposition: Application to Filgrastim (Neupogen)

Liviawati Wu[1], Wojciech Krzyzanski[2], Juan Jose Perez-Ruixo[1,3], John Harrold[1*]

[1]Amgen, Thousand Oaks, CA; [2]SUNY Buffalo, Buffalo, NY; [3]current affilitation: Janssen Research & Development, Beerse, Belgium

Objectives: To develop a mechanistic model capable of describing pharamacodynamics-mediated drug disposition (PDMDD) which is identifiable from typical in vivo PK/PD data.

Methods: A PDMDD model was developed by combining elements from a cell-level model of target interaction [1] with a traditional model of target-mediated drug disposition (TMDD) [2]. Four different indirect response models (IDRs) [3] were used to identify signature responses of the model. The performance of the model was further evaluated using two previously published filgrastim studies involving single (intravenous and subcutaneous) and multiple subcutaneous doses [6,7] in humans. Data included serum filgrastim concentration and absolute neutrophil counts (ANC).

Results: The cell-level PDMDD model accounted for the linear systemic drug clearance, endocytotic internalization and degradation, and loss due to cell elimination. Comparison of the IDRs with PDMDD versus non-PDMDD scenarios indicates a separation of clearance rates which occurs after a single cycle, but this is not observable in vivo (e.g. free drug observations) until multiple cycles of treatment. The model simultaneously explained the neutrophil-mediated disposition of filgrastim, the kinetics of the endogenous G-CSF (eG-CSF), and ANC dynamics, including the rebound effect in ANC due to accumulation eG-CSF in neutropenic patients, thus eliminating the need for a feedback mechanism [4, 5]. Parameter estimates were in the physiological ranges or agreed with similar parameters reported in the literature.

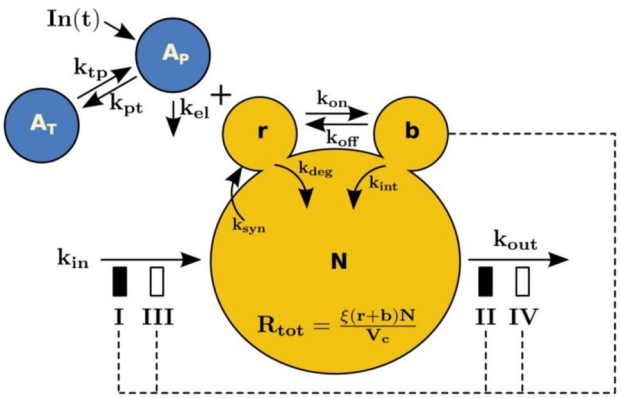

Conclusions: Analysis of the PDMDD model found that multiple dosing data might be required to produce effects in plasma concentration needed to identify model parameters. The PDMDD model reduced to the standard TMDD model in the absence of pharmacological effect on the target. Future applications include chemotherapy induced cytopenias affecting clearance of endogenous hematopoietic growth factors and/or monoclonal antibodies.

References:

1. Sarkar CA. Mol Pharmacol. 2003.
2. Mager DE. JPKPD. 2001.
3. Dayneka NL. J Pharmacokinet Biopharm. 1993.
4. Pastor ML. Pharm Res. 2013.
5. Quartino AL. Pharm Res. 2014.
6. Wang B. JPKPD 2001.
7. Borleffs JC. Clin Ther. 1998.

W-60

Assessment of CYP3A-Mediated Drug–Drug-Interaction Potential for PF-X in Healthy Subjects: A Multiple-Dose Study using Itraconazole

Francois Gaudreault[1*], Martin Bednar[1], Brendon Binneman[1], Danny Chen[1], John Litchfield[1], Christopher Shaffer[1], Li Di[1], Jessica Mancusso[1], Laura Zumpano[1], Noam Epstein[2]

[1]Pfizer Worldwide Research and Development, Cambridge, MA, USA. [2]Pfizer Clinical Research Unit, New Haven, CT, USA

Objectives: The purpose of this study is to characterize the pharmacokinetic profile of PF-X when co-administered with a strong cytochrome P450 3A (CYP3A) inhibitor in healthy volunteers.
Methods: The impact of co-administration of itraconazole, a strong inhibitor of CYP3A, on the pharmacokinetics of PF-X was simulated using SimCYP® assuming that CYP3A accounts for 97 % of the fractional metabolism of PF-X. The model was calibrated using the data obtained from a validated population pharmacokinetic model based on PF-X exposures observed in completed Phase 1 studies. The simulation suggested that PF-X potentially carries a significant risk of CYP3A interaction with both strong [$\geq$ 5-fold increase in exposures (AUC and Cmax)] and moderate ($\geq$ 2 but $<$ 5-fold increase in exposures) CYP3A inhibitors when co-administered at steady-state, warranting the conduct of the present study to confirm the extent of an in vivo drug interaction. This study was an open-label, fixed-sequence study in thirteen healthy adult volunteers assigned to the following sequence:

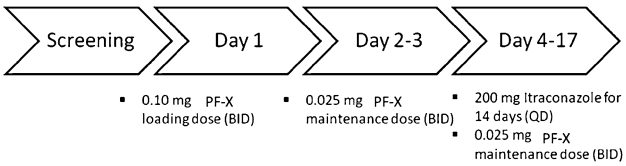

Fig. 1 Study design

Results: The preliminary results (Figure 2) suggest that PF-X does not carry a risk of a CYP3A drug interaction when co-administered with itraconazole, a strong CYP3A inhibitor. The observed plasma exposures of PF-X, itraconazole and its metabolites are within the expected range for testing the study hypothesis.

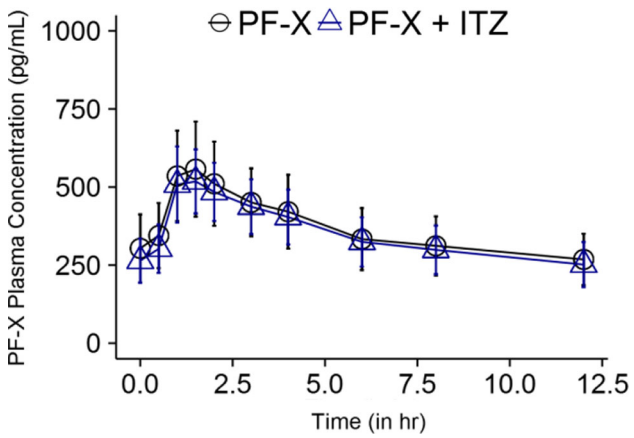

Fig. 2 Time-course of PF-X with and without Itraconaozle

Conclusions: The lack of drug–drug-interaction observed in this study was unexpected based on the in vitro-generated data and the SimCYP® model predictions. This potential discrepency will be further elucidated by additional work characterizing the CYP-dependent fraction metabolized and the potential human clearance pathway(s) for PF-X.

W-61

Minimal Physiologically-Based Pharmacokinetic (mPBPK) Model for a Monoclonal Antibody (mAb) against Interleukin-6 in Mice with Collagen-Induced Arthritis (CIA)

Xi Chen[1], Xiling Jiang[2], William J Jusko[1], Honghui Zhou[2], Weirong Wang[2*]

[1]University at Buffalo, Buffalo, NY; [2]Biologics Clinical Pharmacology, Janssen R&D, Spring House, PA

Objectives: To assess the binding and disposition kinetics of a mAb and its soluble target IL-6 in serum and target tissue sites using mPBPK modeling.
Methods: The concentration profiles of the mAb and free and total IL-6 in serum and joint lavage fluid were obtained in mice with CIA. mPBPK modeling approach was applied to characterize mAb pharmacokinetics and its interplay with IL-6 in serum and joint. A 'ankle (synovial fluid)' compartment was included to describe mAb distribution. Quasi-equilibrium target-mediated drug disposition (TMDD) features were incorporated in serum and 'ankle (synovial fluid)' to delineate the interrelationships between mAb and IL-6. A stepwise modeling strategy was adopted (Figure 1). Model fittings were performed with NONMEM version 7.2.

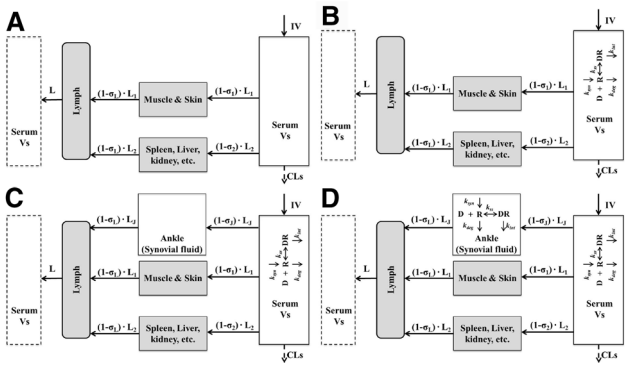

Fig. 1 Scheme of MPBPK models stepwise developed for charecterization of the distribution kinetics of mAb in joint and its interrelationship with IL-6 in both serum and joint

Results: The mPBPK models well described the mAb and IL-6 concentration profiles in serum and joint lavage fluid. Model parameter estimates suggest moderate distribution of mAb to joints (reflection coeffient, $\sigma_{joint} = 0.734$). The baseline IL-6 concentration in serum is approximately 100-fold lower compared with joint (0.0029 and 0.251 pmol/mL). IL-6 exhibits significantly faster turnover rate (k_{deg}) in serum compared with joint (835 and 52.6 day^{-1}). Elimination of mAb-IL-6 complex in serum ($k_{int} = 6.91$ day^{-1}) is similar to that of free mAb. Elimination of mAb-IL-6 complex in joints ($k_{int} = 21.6$ day^{-1}) is similar to the lymph flow rate, suggesting its removal in joints is mostly driven by lymphatic drainage t.
Conclusions: The developed mPBPK models characterized mAb distribution kinetics and its interrelationship with IL-6 in serum and joints. Therapeutic effects of mAbs are determined by their distribution to sites of action, interactions with targets (binding affinity), and properties of target (baseline and turnover rates). This work provides useful insights to better understand these determinants of the exposure–response relationship of mAbs.

References:

1. Cao Y, Jusko WJ (2014) Journal of Pharmacokinetics and Pharmacodynamics 41 (4):375–387.

W-62

Pharmacokinetic and Pharmacokinetic/Pharmacodynamic Modeling to Inform Optimal Dose of Vorapaxar

Ferdous Gheyas[1*], Junghoon Lee[1], Anne Chain[1], Julie Stone[1], Rada Savic[2], Mats Karlsson[3], Mark Pfister[4], and Mark Lovern[4]

[1]Merck & Co; [2]UCSF; [3]Uppsala University; [4]Quantitative Solutions

Objectives: Vorapaxar is a protease-activated receptor-1 (PAR-1) antagonist indicated for the reduction of thrombotic cardiovascular events in patients with a history of myocardial infarction (MI) or with peripheral arterial disease (PAD). During the clinical development of vorapaxar, two of the key program questions were

- What is the optimal dose of vorapaxar?
- Can the same dose be given to all patients?

Population PK and PK/PD models were developed to address these questions.
Methods: A population PK model was developed using data from 12 healthy volunteer (HV) and 4 patient studies. TRAP-induced platelet aggregation (TIPA), a target engagement biomarker, was the PD endpoint in the PK/PD model. TIPA data were available in a subset of studies.
Results: The final population PK model was a 2-compartment model with first-order absorption. Body weight, race, gender, and creatinine clearance had mild to modest effects on vorapaxar exposure. These effects were not clinically relevant.
The PK/PD model was a sigmoid Emax model with an effect compartment. No significant covariate effects were found, except a slight age effect (not clinically relevant) and a substantial study effect on EC50. EC50 was ~5-fold higher for two HV studies compared to that for the patient studies and the other HV studies. This difference could not be explained by demographic or study design/execution factors and was considered indicative of uncertainty in the PK/PD relationship.

The clinical pharmacodynamic target for the prevention of thrombotic events is ≥80 % inhibition in TIPA response. Simulations based on PK and PK/PD models demonstrated that ≥2.5 mg QD dose is required to provide ≥80 % TIPA inhibition in most patients (Figure).

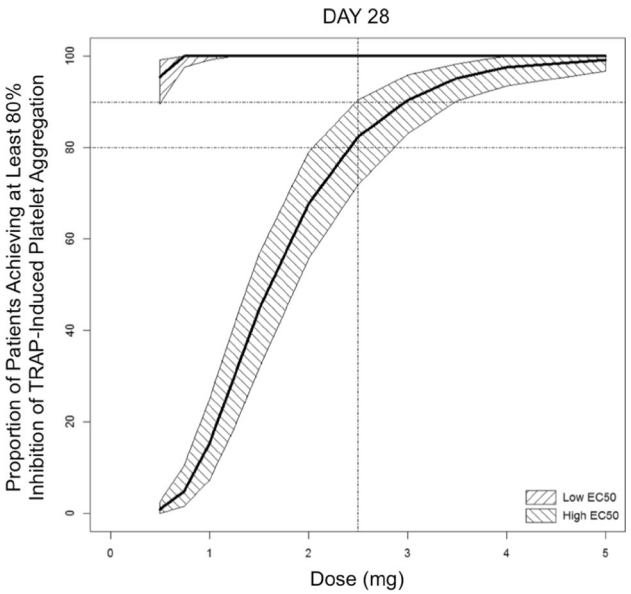

Fig. 1 Simulation results for proportion of patients achieving ≥ 80 % TIPA inhibition

Conclusions: Modeling results suggest that no dose adjustment based on intrinsic factors is needed and all patients who are eligible to take vorapaxar should be given a daily dose of 2.5 mg.

W-63

Development of a Quantitative Systems Pharmacology (QSP) Model of Psoriasis: Overview and Challenges

Loveleena Bansal[1*], Tom Wilde[2], Grace Kang[1], Rebecca Baillie[3], Christina Friedrich[3], Valeriu Damian[2]

[1]Stiefel Discovery and Preclinical Development, GSK, [2]Modeling and Translation Biology, DMPK, GSK, [3]Rosa & Co

Objectives: Psoriasis is a chronic inflammatory skin disease with a complex pathogenesis involving multiple tissues (skin, systemic circulation and lymph node) and immune response spanning a number of cell types such as Th17 cells, macrophages etc. A QSP model of

Psoriasis is being developed to better understand its pathophysiology and to assess the targets/compounds in development within GSK for the treatment of this disease.

Methods: A detailed "PhysioMap" of psoriasis describing its processes and the crosstalk between these processes was developed in collaboration with Rosa & Co. Following this collaboration, ordinary differential equations (ODEs) were added to this map to build a quantitative model of psoriasis. The parameters in this model such as cell turnover rates, production and degradation rates of inflammatory mediators, parameters describing immune regulation by cytokines, or correlations between disease processes and clinical outcomes are being calculated using in vitro, in vivo and patient clinical data from literature.

Results: Significant progress has been made in the development of a QSP model of psoriasis with three main compartments (Figure 1): skin, systemic circulation and lymph node. This model describes the processes related to recruitment of immune cells from lymph nodes and blood to skin, production of inflammatory mediators in skin, activation of keratinocytes as well as correlation of these processes to clinical outcomes. In this poster, we will outline the steps for developing the psoriasis model and addressing the challenges that are typical of QSP models of this scale such as in vitro to in vivo translation of estimated parameters, estimation of cell and cytokine levels in different tissues, and the need for effective literature mining.

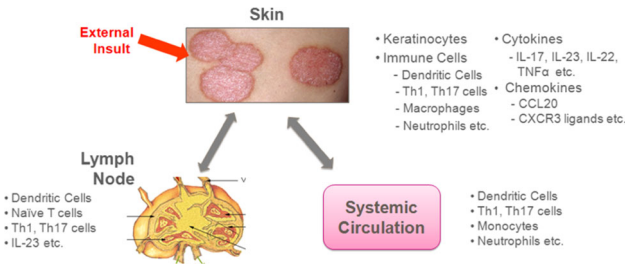

Fig. 1 The main compartments in the psoriasis model and thier components. An external insult initiates the activation of keratinocytes in skin. Also, there is tranfer of immune cells between the skin and lymph node and systemic circulation

Conclusions: QSP modeling allows integration of data from multiple physiological scales and sources to build a quantitative model of disease progression. This model will be crucial in further understanding the pathogenesis of psoriasis, prioritizing novel targets for its treatment and estimating the efficacy of GSK compounds.

W-64

Population Pharmacokinetic and Pharmacodynamic Analyses of Entecavir in Pediatric Subjects

Phyllis Chan[1*], Diane R. Mould[2], Malaz AbuTarif[1], Jessica Wen[3], Mei-Hwei Chang[4], Karan Emerick[5], Laurie Reynolds[1], Richard Bertz[1], Marc Bifano[1]

[1]Bristol-Myers Squibb, Princeton, NJ; [2]Projections Research, Inc., Phoenixville, PA; [3]University of Pennsylvania, Philadelphia, PA, [4]National Taiwan University Hospital, Taipei, Taiwan; [5]University of Connecticut, Hartford, CT

Objectives: Entecavir (ETV) is a guanosine nucleoside analogue with activity against hepatitis B virus (HBV) polymerase and is primarily eliminated by renal clearance. Analysis was conducted to develop a population pharmacokinetic (PPK) and pharmacodynamic (PPD) model in HBV-infected children > 2 years, to investigate subject factors that influence variabilities of entecavir exposures and longitudinal HBV DNA viral load change from baseline, and to confirm and simplify pediatric dose regimens that produce exposures comparable to the known efficacious doses in adults.

Methods: PK and PD data came from two pediatric (n = 121) and three adult (n = 177) studies. Base models were constructed describing structural components and associated between and within subject variability terms. Full model included all pre-specified covariates that were found statistically significant from univariate analysis ($p < 0.005$). Backward elimination retained statistically significant covariate effects in the PPK model ($p < 0.001$). Only two covariates were included in the PPD full model, hence no backward elimination was performed. ETV exposure metrics were simulated using PPK final model for each pediatric age group.

Results: The pediatric PPK was best described using first-order absorption and a 2-compartment disposition model, including weight as an allometric function on all parameters, creatinine clearance on clearance, and ETV dose on inter-compartmental clearance. Individual model-based ETV exposures were within efficacious ranges in adults, and simplified weight-based dosing were simulated. Pediatric PPD was described by a direct effect inhibitory Emax model based on duration of treatment, with ETV exposure (AUCss) as the primary response predictor. Additional covariates were ALT, normalized baseline viral load on the maximum response; and ALT on the time to achieve half-maximal response.

Conclusions: PK and PD data were adequately described by non-linear mixed effects models. Pediatric dosing recommendations for simplified pediatric weight groups were developed.

W-65

Viral Dynamics Modeling of MK-3682 Monotherapy in HCV-infected Patients

Pratik Bhagunde, Matthew L. Rizk, Bill Marshall, Joan Butterton, Wei Gao*

Merck & Co., Inc., Kenilworth, NJ

Objectives: MK-3682 is a nucleoside analog inhibitor of the Hepatitis C Virus (HCV) Nonstructural protein (NS) 5B RNA polymerase. MK-3682 is being developed as one component of an all oral combination treatment regimen for treatment of chronic hepatitis C virus infection. We aim to investigate the antiviral effect of MK-3682 monotherapy in HCV-infected patients using a semi-mechanism based viral dynamics model.

Methods: 24 genotype (GT) 1 and 20 GT 2/3 HCV-infected treatment naïve patients were randomized to receive 4 treatments: placebo or MK-3682 at 50, 150 or 300 mg once daily (QD) for 7 days. Plasma HCV RNA levels were quantified at various time points during 35 days post treatment. A population-based KPD-viral dynamics model was developed to characterize the HCV RNA profiles. MK-3682 dose was administered in the central compartment, which was related to the amount in the effect compartment through first-order kinetics. Viral kinetics were described by a standard viral dynamics model. MK-3682 levels in the effect compartment inhibited virion production.

Results: The KPD viral dynamics model adequately described the viral kinetics profiles in the HCV-infected patients, with the viral dynamics system parameter estimates in good agreement with reported values in the literature. The individual value of the rate constant in the Dose (PK) compartment was comparable to the observed terminal elimination rate of MK-3682 prodrug in plasma. Additionally, a delay introduced by the KPD model was necessary to capture the onset of viral load decline.

Conclusions: The KPD viral dynamics model provides an adequate description of viral response after short-term monotherapy with MK-

3682 in treatment-naïve HCV-infected patients. The KPD model allows for projection of MK-3682 efficacy under various conditions, and potentially can help inform the future probability of success of different formulations in development.

References:

1. Pillai, G., et al. A semi-mechanistic and mechanistic population PK-PD model for biomarker response to Ibandronate, a new bisphosphonate for the treatment of osteoporosis. Br J Clin Pharmacol 2004 (58): 618–31.

W-66

Translational PK-PD-Viral Dynamics (VD) Modeling: An Application in Respiratory Syncytial Virus (RSV) Program

Beesan Tan[1,2*], Virna Schuck[1,3]

[1]Formerly DMPK, AstraZeneca, Waltham, MA; [2]Clinical Pharmacology, Pfizer, Cambridge, MA; [3]Clincial Pharmacology, Novartis, East Hanover, NJ

Objectives: RSV, common cause of lower respiratory tract infections, usually results in self-limiting flu-like signs and symptoms, but can cause serious complications in children, elderly and immune-compromised populations. This work illustrates the application of a translational PK-PD-VD modelling approach in an early phase RSV program, focusing on characterizing the anti-viral activity of benchmark compound RSV604.
Methods: RSV kinetics in human appears to be similar to influenza, with slightly prolonged viral production. A target cell-limited acute VD model with delayed virus production, originally developed for Influenza A infection [1], was fitted to the viral load data in RSV-challenged study [2]. RSV604 anti-viral activity was simulated by linking its PK and in vitro EC_{50} to the VD model. E_{max} model was used to describe the inhibitory effect of the compound on viral production rate. It was assumed that RSV production could be completely inhibited by RSV604. The EC_{50} parameter in this model was fixed to the average of in vitro RSV604 EC_{50} values against common clinical isolates of RSV [3].
Results: The VD model was able to capture the observed RSV viral load in challenged subjects without pharmacological intervention. Simulations demonstrated a larger beneficial effect if treatment is initiated earlier, however, treatment initiated as late as 6 days post infection (dpi) can still offer some benefit. Following 3 days QD dosing of 450 mg RSV604 initiated at 6 dpi, the viral load is predicted to be approximately 1 log (PFU/mL) less than the placebo group.
Conclusion: The integrated PK-PD-VD model can be applied in the early phase RSV program to provide a more integrated comparison of various compounds against the benchmark compound, to guide the selection of the lead compound, and to inform clinical study design e.g. dosing strategy and treatment window.

References:

1. Baccam et al. (2006). J Virol. 80:7590–7599.
2. DeVincenzo et al. (2010). Proc Natl Acad Sci USA.107: 8800–8805.
3. Chapman et al. (2007). Antimicrob. Agents Chemother. 51:3346–3353.

W-67

Application of Model Informed Drug Discovery and Development (MID3) to Gout

Scott Marshall[1*], Soto Elena[1], Barry Weatherley[1], Rujia Xie[2], Liang Li[3], Dick Willke[4], Pinky Dua[1]

[1]Pharmacometrics & Clincial Pharmacology, Pfizer, UK; [2]Pharmacometrics, Pfizer China; [3]Global Health & Value NY US; [4]Peking University/Pfizer PMx Education center

Objectives: A multifaceted MID3 strategy plan was enabled to explore the challenges associated with novel approaches to treatment of hyperuricemia in patients with gout. The links between System Pharmacology (SP) & mechanistic PK/PD and Model Based Meta-Analysis (MBMA) & early Cost Effectiveness (CE) predictions in asset, mechanism and disease level decision making are described (Figure 1).
Methods: A mechanistic PK/PD model was developed based on the SP but simplified and calibrated on internal and literature data [1]. Drug effects on serum Uric Acid (sUA) formation and clearance; and xanthine (Xa) clearance was explored by simulation. A MBMA was conducted on a literature database of monotherapy and combination treatments [2]. Simulations of the population response to treatment were linked to expected reduction in gout flares. An available cost-effectiveness model [3] was utilized to explore impact of treatment changes on CE compared to standard of care (Figure 1).
Results: Predictions from the PK/PD model indicated that titration would be necessary to reduce the expected increase in Urinary Uric Acid (UUA) on day 1 of treatment with a potent URAT-1 inhibitor. A dual inhibitor could better balance urinary and circulating levels of Xa and sUA reducing the need for titration. The MBMA supported the conclusions from the PK/PD (less than additive effect of XOi & URAT-1) and provided links between treatment effects in different populations. The CE indicated that utility in addition to reduction in gout flares would be required in establishing the cost-effectiveness of future gout treatments (Figure 1).

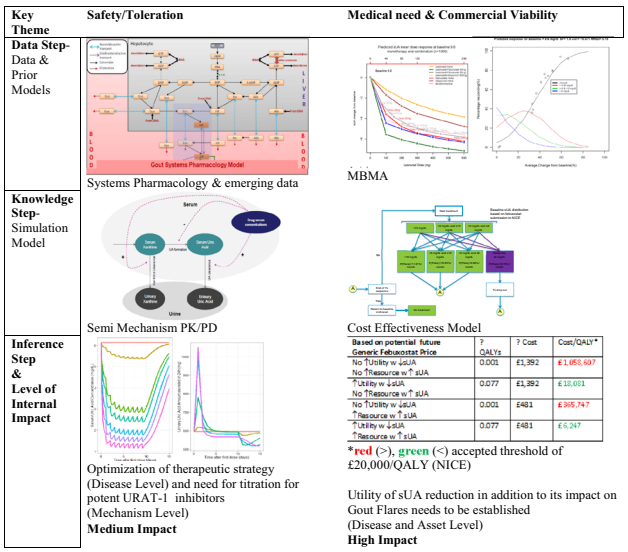

Fig. 1 Key components of MID3 strategic plan and associated "learning and confirming" steps

Conclusions: This work demonstrates how components of the MID3 plan informed asset, mechanism and disease level strategy and decision making in the development of novel therapies for gout. This work also exemplifies some of the concepts outlined in the proposed EFPIA MID3 good practice document [4, 5].

References:

1. Soto etal PAGE 24 (2015) Abstr 3529 www.page-meeting.org/?abstract=3529.
2. Xie etal PAGE 24 (2015) Abstr 3513 www.page-meeting.org/?abstract=3513.
3. NICE technology appraisal guidance [TA164. Published date: December 2008 https://www.nice.org.uk/guidance/ta164.
4. Marshall etal PAGE 23 (2014) Abstr 3299 www.page-meeting.org/?abstract=3299.
5. Milligan etal J Pharmacokinet Pharmacodyn (2014) 41:S7–S101 M-057.

W-68

Nonlinear Pharmacokinetics of Letermovir in Phase 1 Suggest a Role of Induction

M. Prohn[2], D. Zhang[1*], T. Kerbusch[3], W. L. Marshall[1], K. Dykstra[2], C. R. Cho[1]

[1]Merck & Co., Kenilworth NJ, USA, [2]qPharmetra LLC, Cary, NC, USA, [3]Quantitative Solutions B.V., Oss, The Netherlands

Objectives: Letermovir is in Phase 3 development for the prophylaxis of cytomegalovirus (CMV) infection in transplant patients. Letermovir pharmacokinetics (PK) are complex with greater than dose proportional increases in exposure, changes in PK characteristics but limited accumulation upon multiple dosing and large variability in absorption profiles upon oral administration. Previous models were sufficient for informing dose selection for the Phase 3 study, but did not support critical questions such as predicting the impact of drug–drug interactions or sub-populations. The development of an updated population PK model describing all healthy volunteer data will enable support of such critical questions concerning the first 8–15 days of dosing prior to reaching steady state.
Methods: The full dataset included 6730 observations obtained in 8 Phase I studies (219 healthy volunteers) obtained after either single or multiple dose PO or IV administrations of 30–960 mg Letermovir. Modeling was performed using NONMEM 7.3 with stepwise-covariate modeling (SCM, PsN 4.2.0).
Results: The final Phase I model was a 4-compartment model with concentration dependent nonlinear clearance and inter-compartmental clearance, a Savic transit absorption model, and inter-individual variability on key parameters. The model included induction of clearance. After 8–15 days the induction effect reached its steady-state, resulting in an increase of clearance by approximately 12, 12 or 71 % upon multiple PO dosing of 240 or 480 mg (QD) or 720 mg (BID), respectively. No clinically relevant covariates were identified.
Conclusions: The final model describes the complex letermovir PK in healthy volunteers during the first days of dosing prior to steady state. The model enables support of critical questions that may arise concerning the short-term effect of intrinsic and extrinsic factors which may impact PK.

W-69

Physiologically Based Pharmacokinetic Modeling of Renally Cleared Drugs in Children

Wangda Zhou[1*], Trevor Johnson[2], Nidal Al-Huniti[1], Khanh Bui[1], Amy Cheung[3], Maria Learoyd[3], Jianguo Li[1], Hongmei Xu[1], Diansong Zhou[1]

[1]Quantitative Clinical Pharmacology, AstraZeneca, Waltham, MA; [2]Simcyp (A Certara Company), Sheffield, UK; [3]Quantitative Clinical Pharmacology, AstraZeneca, Cambridge, UK

Objectives: To evaluate the physiologically based pharmacokinetic (PBPK) modeling approach in the characterization of pediatric PK for drugs predominantly excreted unchanged via renal clearance.
Methods: Four orally administered drugs: ceftibuten, levocetirizine, pregabalin and sotalol and four intravenously administered drugs: AZ#1, AZ#2, meropenem and vancomycin were selected for PBPK modeling. Simcyp simulator version 14 release 1 was used to conduct all simulations. Full or minimal PBPK models were constructed for these compounds based on physicochemical properties and clinical observations. All models were first validated with clinical PK data in healthy adult volunteers. Following appropriate optimization in adult population, pediatric PK was predicted for each drug across all age groups using Simcyp pediatric module with application of physiological-based ontogeny. The predicted AUC, CL, Cmax, tmax were then compared with available literature or internal pediatric clinical data for each age group.
Results: Pediatric PBPK models reasonably predicted the clearance values in neonates (0–1 month), infants and toddlers (1 month - to 2 years), pre-school (2–6 years) and school-aged children (6–11 years), and adolescents (12–17 years) for both orally and intravenously administered drugs. All the predicted clearance and AUC values are within 1.5-fold of those observed values, except for vancomycin at one age group (pre-school), which is within 2-fold of the observed value.

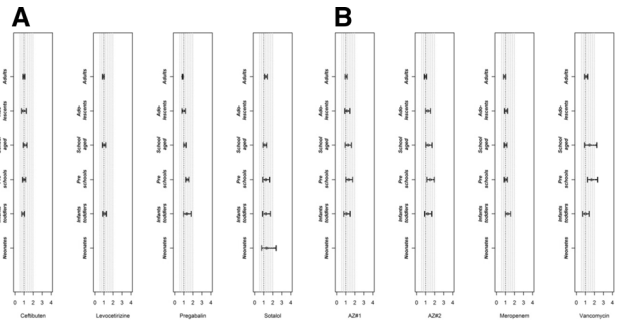

Fig. 1 Comparison between observed and predicted clearance values of **A** orally and **B** intravenously administered drugs. Results are presented as mean ratios (observed/predicted values) in each age group with a 95 % confidence interval

Conclusions: Pediatric PK of drugs primarily eliminated through renal clearance is well predicted using pediatric PBPK models. PBPK modeling with Simcyp adequately characterized renal clearance maturation and could be a powerful tool to guide pediatric clinical trial design of renally cleared drugs.

W-70

Population Pharmacokinetic and Pharmacodynamic Modeling of Ramosetron for the Prophylaxis of Postoperative Nausea and Vomiting

Seong-heon Lee[1*], In-je Kim[2], Seong-wook Jeong[1]

[1]Anesthesiology and Pain Medicine; [2]Molecular Medicine, Chonnam National University, South Korea

Objectives: Ramosetron, one of type 3 serotonin receptor antagonists, is used for the prevention and treatment of postoperative nausea and vomiting (PONV). The main objective of this study was to characterize the population pharmacokinetics and pharmacodynamics of ramosetron in adults.
Methods: Fifty elective surgical patients aged 19–80 years received one of an intravenous bolus dose of ramosetron (0.3 mg, 0.45 mg or 0.6 mg) 30 min before the end of surgery. Plasma concentrations of ramosetron in 462 plasma samples were measured, and the Rhodes Index for Nausea, Vomiting and Retching (RINVR) was assessed until 48 h after the administration of ramosetron as a surrogate measure for the antiemetic effect of ramosetron. Plasma concentrations and RINVR scores were analyzed with NONMEM. Based on the principles of allometry, body weight was incorporated in the base pharmacokinetic model, along with fixed allometric exponents. Covariate analysis was performed by means of a stepwise forward inclusion and backward elimination procedure. The exposure–response relationship was evaluated using the linear and sigmoid E_{max} models.
Results: Pharmacokinetics of ramosetron were best described by a three-compartment mammillary model. Besides the priori-implemented body weight, only age had an effect on metabolic clearance. No other investigated covariates, including sex and other size descriptor (such as LBM) significantly affected the pharmacokinetics of ramosetron. The exposure–response relationship between ramosetron plasma concentration and RINVR score was not reliably described with the linear and sigmoid E_{max} models.
Conclusions: A population pharmacokinetic model of ramosetron in adults was established and it described the data well. However, antiemetic effect of ramosetron was not described by simple pharmacodynamic models. Future modeling should focus on the prolonged effect of ramosetron and the natural extinction of PONV to clarify the exposure–response relationship.

W-71

Use of Pharmacokinetic and Pharmacodynamic Knowledge of Bilastine for the Optimal Design of the First Pediatric Trial

Valvanera Vozmediano[2], John C. Lukas[2*], Mónica Rodríguez[2], Román Valiente[1]

[1]Clinical Research Department, FAES FARMA, S.A, 48940, Spain; [2]Drug Modeling & Consulting, Dynakin, SL, Bilbao, Spain

Background: Bilastine is a non-sedating H_1 antihistamine for the treatment of allergic rhinoconjuntivitis and urticaria. The approved therapeutic dose in adults, supported by its pharmacokinetics and pharmacodynamics (PK/PD), is 20 mg/day via the oral route. Bilastine has favorable characteristics for its use in pediatrics. Currently trials in pediatrics are ongoing to determine the PK and PD and confirm the dose predicted by the model presented here.
Aims: (1) Develop a predictive model of bilastine PK and PD for pediatrics by integrating current knowledge. (2) Use the model for optimal design (bilastine dose, number of patients and sample selection) of a pharmacokinetic study in 2 to 11 years old. (3) Confirm the model predictability in the first recruited children.
Methods: A semi-physiological approach was applied in predicting pediatric PK parameters (age ranges in predictions were 2–6 and 6–11 years). The PD assumed that the H_1 antihistamine effect of bilastine in children is substantially similar to that in adults. The time evolution of the plasma levels and the wheal and flare effects after 5, 10, 20 mg/day bilastine were simulated. Model and study design confirmation was performed with data from the first seven children recruited to ensure that plasma levels were in line with the predictions above.
Results: Simulations indicated an adequate efficacy profile with the dose of 10 mg/day in children from 2 up to 11 years of age. Results from the first recruits confirmed the dose and design, hence trial continuation.
Conclusion: The developed model was successfully used to predict bilastine PK behavior in children using the previously available information in adults. The PK parameters predicted in children were used to aid the selection of an optimal dose and the sampling times for the first pediatric trial, increasing the efficiency of the process.